“Priming” as a novel strategy to enhance chemotherapeutic efficacy

Mould, R.

UNIVERSITY OF WESTMINSTER

“Priming” as a novel strategy to enhance chemotherapeutic efficacy

Rhys Mould

2019

A thesis submitted in partial fulfilment of the requirements of the University of Westminster for the degree of Doctor of Philosophy

Contents

Abstract

Aims

The purpose of this thesis was to examine and quantify the effects of the short-chain fatty acid acetate, a by-product of the microbial fermentation of dietary fibre, on the metabolism of cancer cells, and to test whether acetate can sensitize cells to apoptosis induced by anti-cancer drugs, by a process known as priming.

Methods

To examine the effects of acetate, several markers of metabolism were assayed in 3 cell lines HCT116 (Human colon cancer), MCF7 (Human breast cancer) and the control cell line MCF10 (non-cancerous human breast) following 24-hour acetate treatment in doses ranging from 1-25 mM. Reactive oxygen species and Ca^{2+} were measured with fluorescent spectroscopy. Mitochondrial function was measured using the SeaHorse XF_E Analyser and 2-photon-NADH FLIM. Mitochondrial morphology was assessed with confocal microscopy.

To determine whether acetate could prime cells for death, changes in proliferation were measured with the MTT cell viability assay and levels of apoptosis induction were measured with Annexin-V FITC flow cytometry.

Results

Acetate induced a state of oxidative stress in the HCT116 and MCF7 cancer cell lines, indicated by an average 17.5% significant decrease in mitochondrial basal respiration, increased ROS production (significant 24% average increase across the two cancer cell lines), and increased Ca^{2+} levels (significant 22% average). Whilst ROS and Ca^{2+} were elevated in the non-cancerous cell line, there was no significant change in mitochondrial basal respiration, suggesting that acetate treatment did not cause oxidative stress in healthy cells.

When cancer cells were primed with 10 mM acetate 24 hours prior to treatment with cisplatin, there was an average 1.85-fold increase in apoptosis compared to treatment with the drug by itself. This effect was not observed in the non-cancerous cell line.

Conclusions

Priming has been shown to have the potential to improve the efficacy of pre-existing chemotherapeutic agents. With cancer incidence increasing worldwide, there is a need to improve current treatments without exacerbating side effects and impairing patient quality of life. In this thesis, I show that acetate improves the effectiveness of cisplatin in inducing apoptosis, by selectively inducing oxidative stress in a cancer cell line model. My work highlights a new mechanism for the action of acetate and adds further evidence that priming can be used as a safe, effective method to improve chemotherapeutic treatment.

Acknowledgements

A PhD is often said to be one of the most challenging times in a person's life. For me, it was one of the most educational and enlightening, which I attribute to the people who surrounded and supported me, and to those people I dedicate this thesis.

First, I would like to thank the Research Centre for Optimal Health. Professor Jimmy Bell and Dr Louise Thomas took a chance on me and through their carefully nuanced double act, gave me the direction and space that allowed me to grow as a scientist. I hope that this work provides a worthy reflection of their support. Thanks to Dr Meliz Sahuri-Arisoylu and Dr Aine Henley, who showed great patience teaching me in the lab. Thanks to Dr Jim Parkinson and Dr Alistair Nunn for their helpful proof reading and discussions, Wareed and Amy for the conversations, cakes, and support and GW Pharmaceuticals, for the generous funding that made this endeavour possible.

To my family, whose faith, generosity and understanding allowed me to follow this path.

I would like to thank also my friends for their support and understanding throughout this time, including the members of BANT: Nicola, Amy, Ted, Thomas, and finally Holly Bartley, the Queen of Flow Cytometry.

Declaration of Contributors

The majority of the work in this thesis was performed by the author. Any assistance and collaborations are detailed below:

SeaHorse Glycostress Assay

SeaHorse GlycoStress assays were performed by Dr Meliz Sahuri-Arisoylu. Anaylsis of acquired data was performed by the author.

Gene Expression Analysis

Gene expression assays were performed by Dr Meliz Sahuri-Arisoylu. Anaylsis of acquired data was performed by the author.

2-Photon FLIM

2-Photon Fluorescence Lifetime Imaging Microscopy was carried out in collaboration with Dr Alistair Nunn and Professor Stan Botchway at the Rutherford Appleton Laboratory in Oxford. Analysis of acquired data was performed by the author.

List of Figures

List of Tables

List of Abbreviations

2DG	2-deoxy-D-glucose
2P	2-photon
5FU	5-fluorouracil
Acetyl CoA	Acetyl coenzyme A
ACSS1	Acyl-coenzyme A synthase short-chain family member 1
ACSS2	Acyl-coenzyme A synthase short-chain family member 2
ADP	Adenosine diphosphate
AIF	Apoptosis-inducing factor
ANOVA	Analysis of variation
ANT	Adenosine nucleotide translocator
APAF1	Apoptotic protease activating factor 1
ATP	Adenosine triphosphate
Bad	Bcl-2-associated death promoter
Bak	Bcl-2 homologous antagonist killer
Bax	Bcl-2-associated Protein X
Bcl	B-cell lymphoma
Bcl-2	B-cell lymphoma 2 protein
Bcl-W	Bcl-2-like protein 2
Bcl-XL	B-cell lymphoma-extra-large protein
BH	Bcl-2 sequence homology
Bid	BH3 interacting domain death agonist
Bim	Bcl2-like protein 11
BSA	Bovine serum albumin
Ca^{2+}	Calcium ion
$[Ca^{2+}]_c$	Cytosolic calcium concentration
$[Ca^{2+}]_i$	Intracellular calcium concentration
$[Ca^{2+}]_m$	Mitochondrial calcium concentration
CBD	Cannabidiol
Cl	Chlorine
CoA	Coenzyme A
COSMIC	Catalogue of somatic mutations in cancer
Ct	Cycle threshold
CTR1	Copper transporter 1
Cyt *c*	Cytochrome *c*
DAG	Diacylglycerol
$\Delta\psi_m$	Mitochondrial membrane potential
DCF	2',7' –dichlorofluorescin
DCFDA	2',7' –dichlorofluorescin diacetate
DDP	Diaminedichloroplatinum (Cisplain)
DI	Deionized
DISC	Death inducing signalling complex
D Loop	Displacement loop
DMEM	Dulbecco's modified Eagle's medium
DMF	Dimethylformamide

DNA	Deoxyribonucleic acid
Drp1	Dynamin-related protein 1
ECAR	Extracellular acidification rate
ECCG	Epigallocatechin gallate
ETC	Electron transport chain
FAD/FADH	Flavin adenine dinucleotide
FADD	Fas-associated protein with death domain
FasL	Fas ligand
FasR	Fas receptor
FBS	Foetal bovine serum
FCCP	Carbonyl cyanide-p-trifluoromethoxyphenylhydrazone
FFAR	Free fatty acid receptor
FITC	Fluorescin isothiocyanate
FL	Fluorescence channel (flow cytometry)
FLIM	Fluorescence life time imaging microscopy
FSC	Forward scatter
GPCR	G protein-coupled receptor
GDP	Global domestic product
GLUT1	Glucose transporter 1
GLUT2	Glucose transporter 2
GSH	Glutathione
HAT	Histone acetyltransferase
HDAC	Histone deacetylase
hFis1	Human mitochondrial fission protein 1
HK	Hexokinase
HtrA2/Omi	Serine protease, mitochondrial. Also known as Omi
IAP	Inhibitor of apoptosis
IMM	Inner mitochondrial membrane
IP_3	Inositol trisphosphate
JC-1	5,5′,6,6′-tetrachloro-1,1′,3,3′- tetraethylbenzimidazolylcarbocyanine iodide
LUT	Look up table
LD_{50}	Lethal dose 50% or median lethal dose
MAPK	Mitogen activated protein kinase
Mcl-1	Induced myeloid leukaemia cell differentiation protein
MCU	Mitochondrial calcium uniporter
MEME	Modified essential media Eagle
MFI	Median fluorescence intensity
miRNA	Micro ribonucleic acid
MOMP	Mitochondrial outer membrane permeabilisation
mPTP	Mitochondrial permeability transition pore
mtDNA	Mitochondrial DNA
mTOR	Mechanistic target of rapamycin
MTT	3-(4,5-dimethylthiazol-2-yl)-2,5-diphenyltetrazolium bromide
Na^+	Sodium ion
NAC	N-acetyl-L-cysteine

NAD/NADH	Nicotinamide adenine dinucleotide
NADP/NADPH	Nicotinamide adenine dinucleotide phosphate
NCLX	Na^{+}-Ca^{2+}-Li^{+} exchanger
NF-κB	Nuclear factor kappa-light-chain-enhancer of activated B cells
NO	Nitric oxide
NOX	NADPH oxidase
Noxa	Phorbol-12-myristate-13-acetate-induced protein 1
Nrf2	Nuclear factor (erythrioid-derived 2)-like 2 (also known as NFE2L2)
OCR	Oxygen consumption rate
OMM	Outer mitochondrial membrane
Opa1	Mitochondrial dynamin like GTPase, also known as optic atrophy protein 1
OXPHOS	Oxidative phosphorylation
PBS	Phosphate buffered saline
PCD	Programmed cell death
PI	Propidium iodide
PI3K	Phosphoinositide 3-kinase
PIP_3	Phosphatidylinositol (3,4,5)-trisphosphate
PPP	Pentose phosphate pathway
PS	Phosphatidylserine
PTP	Permeability transition pore
Puma	P53 upregulated modulator of apoptosis
qPCR	Quantitative polymerase chain reaction
RIPA	Radioimmunoprecipitation assay
RN	Regulated necrosis
RNA	Ribonucleic acid
ROS	Reactive oxygen species
RPMI	Roswell Park memorial institute medium
SCFA	Short chain fatty acid
SEM	Standard error of the mean
SLC	Solute carrier family
Smac/DIABLO	Second mitochondria derived activator of caspases/Direct IAP binding protein with low pl
SMCT	Sodium coupled monocarboxylate transporters
SMT	Somatic mutation theory
SSC	Side scatter
TCA	Tricarboxylic acid cycle/Kreb's cycle/citric acid cycle
TCSPC	Time-correlated single proton-counting
TIMP-1	Tissue inhibitor of metalloproteinases
TMRE	Tetramethylrhodamine ethyl ester
TNF-α	Tumour necrosis factor-α
TNFR1	Tumour necrosis factor receptor 1
TRADD	Tumour necrosis factor receptor type 1 associated death domain protein
TRPA1	Transient receptor potential cation channel 1
TRX	Thioredoxin
TP53	Tumour protein 53, commonly referred to as p53

tRNA	Transfer RNA
UCP	Uncoupling proteins
uPA	Urinary-type plasminogen activator
UQ_2/UQH_2	Ubiquinone/ubiquinol
UV	Ultra violet
VDAC	Voltage dependant anion channel
VPA	Valproic acid

1.0 Introduction

1.1 Cancer

Cancer is a group of widespread and potentially fatal diseases characterised by the unregulated proliferation of abnormal cells which, if malignant, have the potential to spread to and proliferate in other parts of the body. The invasive cells can outgrow the surrounding healthy cells and tissue, leading to organ failure and eventually death (World Health Organization, 2017). There are over one hundred different types of cancer, which together accounted for 8.8 million deaths globally in 2015, making it one of the leading causes of death worldwide (World Health Organization, 2018). The risk of cancer increases with age (Cancer Research UK, 2018), and the rate of cancer incidence worldwide is increasing, particularly in developing countries, as a result of aging populations and the rising prevalence of cancer-associated lifestyle choices, such as smoking, alcohol consumption, diet, physical inactivity (Jemal et al., 2011), and obesity (Flegal et al., 2013). Although a predisposition to cancer can be inherited, it is estimated that lifestyle and environmental factors account for 90-95% of all cancer cases (Anand et al., 2008). The total economic impact of cancer, as a consequence of premature death and disability, was estimated to be $1.6 trillion in 2010, equating to over 1.5% of the World's Global Domestic Product (GDP) (Livestrong and American Cancer Society, 2010).

The term cancer refers to the disease state wherein the mechanisms that regulate cell growth, division, and death fail, resulting in the accumulation of abnormal cells known as a tumour or neoplasm (Bertram, 2000). Cancerous tumours are malignant, meaning they have the potential to spread from their site of origin to other parts of the body; a process called metastasis (National Cancer Institute, 2015). Tumours that do not spread are considered benign and often can be removed by surgery. Although there is a smaller chance of metastasis, benign tumours can still pose risk to the patient by compressing surrounding tissue, causing nerve damage (Giglio and Gilbert, 2010) and ischemia (Noje et al., 2009).

In addition, benign tumours have the potential to become malignant if left untreated (Clark, 1991).

Historically, the development and growth of a tumour was considered to be driven by mutations or changes in the level of expression of genes that regulate the division or removal of cells, broadly categorised into oncogenes or tumour suppressor genes (Croce, 2008) (Figure 1). Oncogenes encode proteins that control the proliferation or removal of cells. In cancer, these are often mutated or expressed at high levels. In contrast, tumour suppressor genes govern a wider range of cellular processes that protect against cancer, such as cell cycle control, protein turnover, and DNA (deoxyribonucleic acid) damage repair (Sherr, 2004). In cancer, these genes are under-expressed or express mutated, disabled proteins. Currently, the Catalogue of Somatic Mutations in Cancer (COSMIC) database lists 719 genes for which mutations in are causally implicated in cancer (Futreal et al., 2004). In addition to oncogenes and tumour suppressor genes, microRNA (micro ribonucleic acid, or miRNA) genes, which code for small, non-coding RNAs, are also implicated in tumorigenesis and resistance to treatment (Fadejeva et al., 2017). miRNAs have roles in the regulation of gene expression and as such, dysregulated expression of miRNAs can in turn affect the expression of oncogenes or tumour suppressor genes (Peng and Croce, 2016). A mutation in a single oncogene or tumour suppressor is not usually sufficient to cause cancer alone; rather, mutations accumulate as a result of other mutations. For example, a mutation in a gene that repairs damaged or mutated DNA can lead to the propagation of more faulty genes, and in a chain reaction-like system, a cell can accumulate an increasing number of mutations, and so become more resistant to the machinery regulating normal cell proliferation (Merlo et al., 2006). With sufficient growth and mutations, tumour cells can penetrate into the circulatory system and spread to other tissues – a process known as metastasis. Once a tumour has metastasised, the patient's prognosis becomes substantially worse (Jiang et al., 2015).

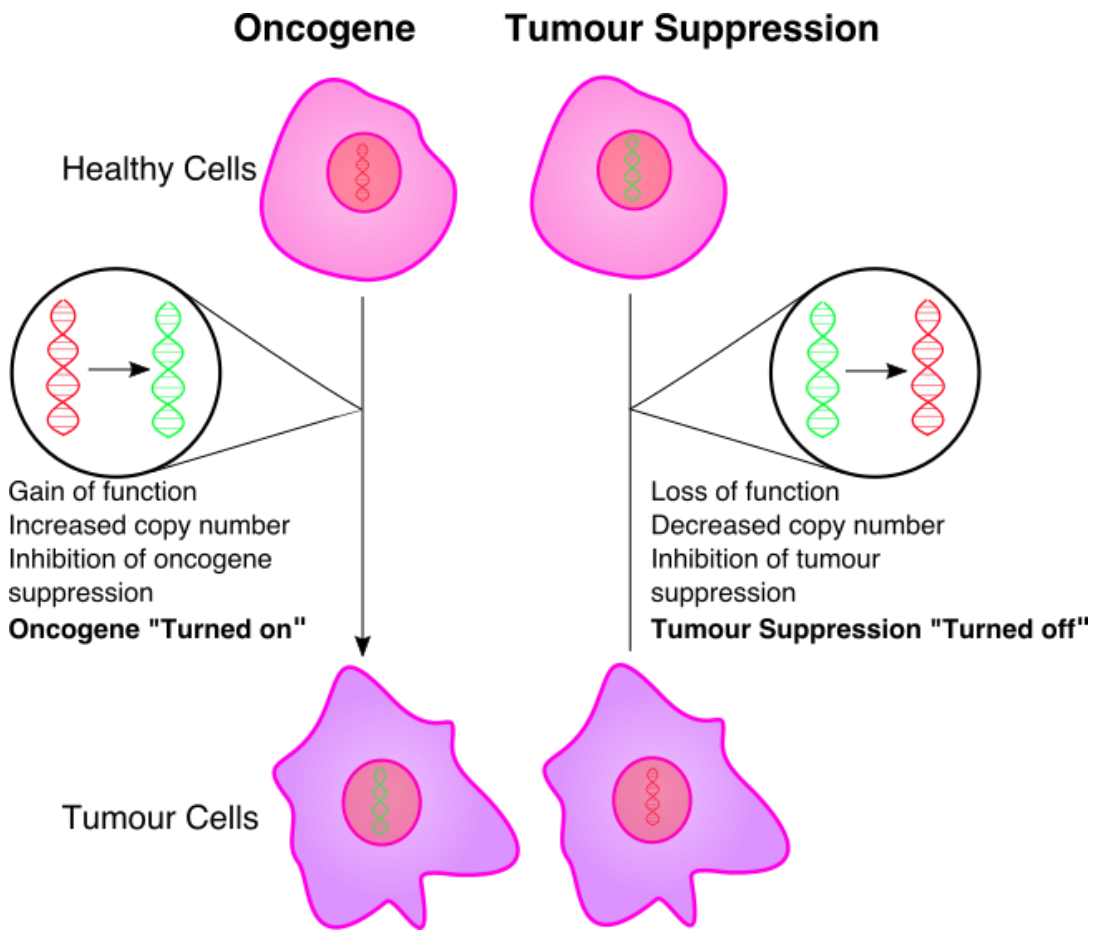

Figure 1 | **Oncogenes and Tumour Suppressors: Mechanisms of Carcinogenesis**. On the left, activation of oncogenes results in rapid cellular proliferation. On the right, deactivation of tumour suppressor genes removes the regulation of proliferation.

More recently, evidence indicates that cancer may rather be primarily a disease of metabolic disorder, and that genomic instability is a consequence of an initial metabolic disturbance rather than the cause of it (Seyfried et al., 2014). This remains a provocative viewpoint in cancer research, as the somatic mutation theory (SMT) of cancer origin, as it became known, was near universally accepted and drove cancer research for decades (Soto and Sonnenschein, 2004). Nevertheless, inconsistences in SMT led scientists to question the theory, including early experiments which showed that combining the cytoplasm of a non-cancerous cell with the nucleus from a tumour cell led to reduced tumourgenicity (Israel and Schaeffer, 1987), and more recent experiments that showed that transfer of normal mitochondria into tumour cells inhibited proliferation and increased drug sensitivity (Elliott et al., 2012). Whilst there remain arguments against tumorigenesis being driven solely by metabolism, such as in immune cells

that adopt different metabolic phenotypes in response to antigens yet rarely form tumours (Altman and Dang, 2012), the increasing recognition of cancer as a metabolic disease provides exciting implications for the future of cancer treatments (Coller, 2014).

1.2 | Cancer Cell Metabolism

1.2.1 | The Hallmarks of Cancer

The hundreds of oncogenes or tumour suppressor genes, not counting genes for which altered levels of expression or epigenetic changes are linked to cancer (Futreal et al., 2004), creates a large number of possible genotypes which generates enormous heterogeneity and complexity, even within similar types of cancer, which has significant clinical implications (Marusyk and Polyak, 2011). Despite this, cancers have been generally observed to share several key characteristics, which became known as the “Hallmarks of Cancer” (Hanahan and Weinberg, 2000) (Figure 2).

In 2011, these original hallmarks were revised to include genomic instability, inflammation, evasion of the immune system, and the reprogramming of energy metabolism, necessary to fuel the “limitless replicative potential” of cancer cells (Hanahan and Weinberg, 2011).

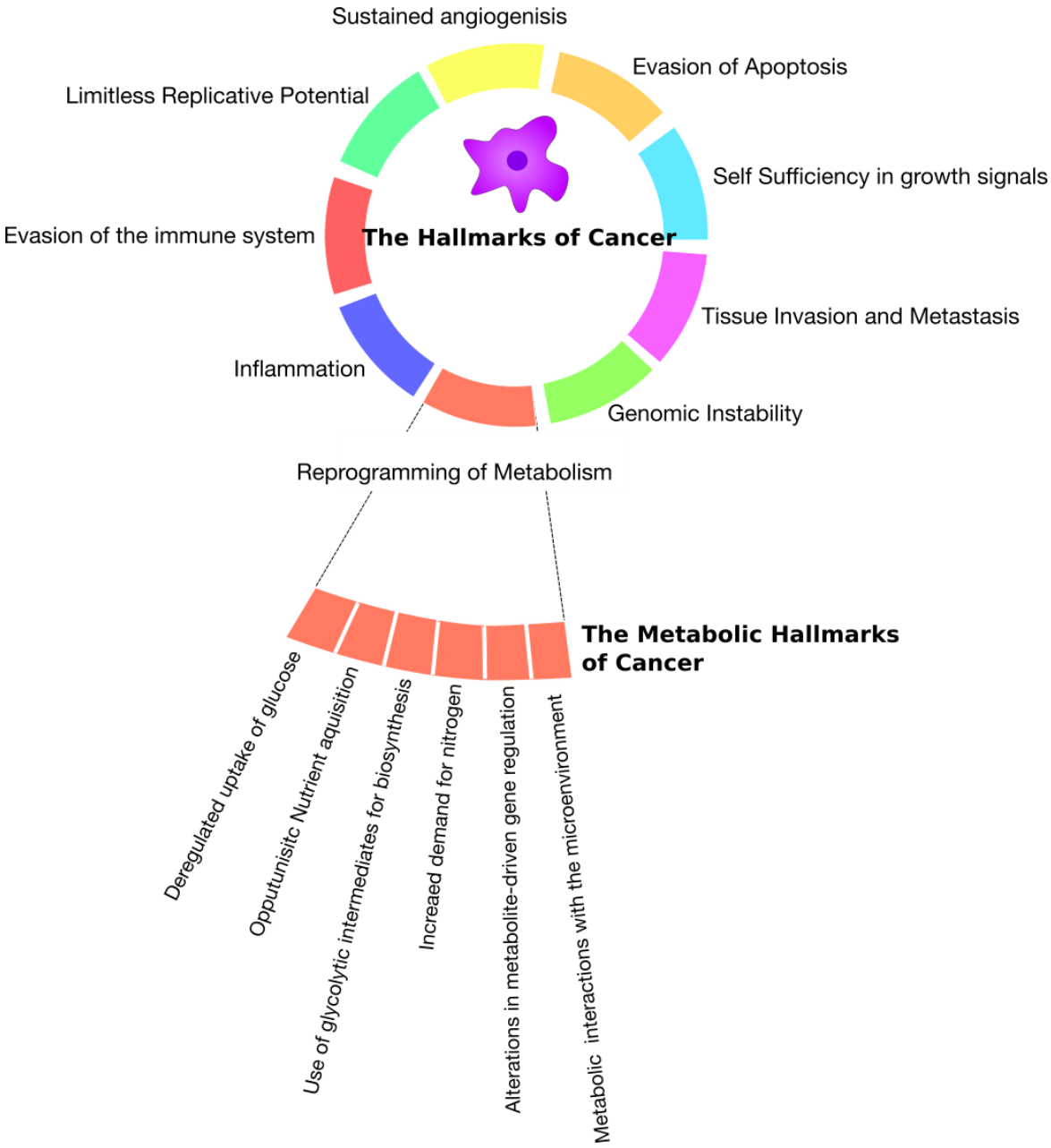

Figure 2 | The Hallmarks of Cancer. In spite of the complex genetic variety of cancer, Hanahan and Weinberg proposed 9 characteristics that are observed in all cancer cells. Later, Pavlova and Thompson proposed a further 6 metabolic features that are generally conserved in cancer cells

1.2.2 The Metabolic Hallmarks of Cancer

The accelerated rate of proliferation in cancer creates new metabolic demands of the cell: to ensure survival in stressful nutrient depleted conditions, and to support the enhanced energetic and biosynthetic needs of rapid growth (De Berardinis and Chandel, 2016). To meet these demands, cancer cell metabolism is often altered relative to healthy cells. Some of these alterations are sufficiently well-conserved across different types of cancer that the reprogramming of cellular metabolism is considered a hallmark of cancer.

One of the first and most well-known changes that was identified was the shift in energy production from oxidative phosphorylation (OXPHOS) to the anaerobic process of glycolysis despite the presence of adequate oxygen, known as the Warburg Effect (Warburg, 1956). A decrease in oxygen dependence can confer a proliferative advantage to cancerous cells; allowing cells to migrate and thrive further from the oxygen-rich environment around blood vessels (Hsu and Sabatini, 2008). Substrates that would normally be consumed in OXPHOS and the tricarboxylic acid (TCA) cycle are diverted into catabolic processes that produce fatty acids, essential for rapid cellular proliferation.

Metabolic changes in cancer cells are now a substantial field of research itself. Progressing from Hanahan & Weinberg's Hallmarks paper, Pavlova and Thompson went on to describe six additional hallmarks of cancer metabolism (Figure 2) (Pavlova and Thompson, 2016):

1.) Deregulated uptake of glucose and amino acids
2.) Use of opportunistic modes of nutrient acquisition
3.) Use of glycolysis/TCA cycle intermediates for biosynthesis
4.) Increased demand for nitrogen
5.) Alterations in metabolite-driven gene regulation
6.) Metabolic interactions with the microenvironment

Common deregulated mechanisms include the excessive activation of phosphoinositide 3-kinase (PI3K), which through the protein kinase (Akt) and mechanistic target of rapamycin (mTOR) signalling pathways can enhance

glucose uptake into the cell via the glucose transporter 1 (GLUT1), and inhibit the entry of metabolites into the TCA Cycle, thus conferring increased cellular dependence on glycolysis (Courtnay et al., 2015), or increased gain of function of *MYC*, a gene encoding a transcription factor, c-MYC, which amplifies the expression of genes that promote cellular growth and proliferation (Stine et al., 2015). Tumour protein p53 (*TP53*), which encodes p53 is another notable example; primarily associated with roles in DNA repair, cell cycle arrest and apoptosis, loss of p53 has also been associated with increased glycolysis (Kruiswijk et al., 2015).

1.3 | The Mitochondria & Their Role in Cancer

Otto Warburg attributed his observation that cancer cells seemed to ferment glucose despite the presence of oxygen to defects in mitochondrial respiration, since OXPHOS occurs in the mitochondria. Nowadays, it is generally accepted that far from being defective, mitochondria in fact play key multifunctional roles in tumorigenesis and cancer cell progression (Zong et al., 2016). This is further demonstrated by the observation that removing mitochondrial DNA from a cell delays tumour growth (Tan et al., 2015). Furthermore, cancer cells that rely more on glycolysis still retain fully functional mitochondria (Zu and Guppy, 2004).

Mitochondria are double-membrane bound organelles with integral roles in cell metabolism – through the TCA cycle and OXPHOS they supply the majority of a cell's energy, and are also vital in a number of essential cellular functions, including various signalling, biosynthetic, and cell death pathways. In cancer, mutations in mitochondrial genes perturb the bioenergetics and biosynthetic states to support the altered requirements of the cells (Brandon et al., 2006). As such, the mitochondria are essential for cancer cell growth, proliferation and survival (Wallace, 2015). The following sections describe the key functions of mitochondria, and how impaired or modified function can contribute not only to the growth of cancer, but also to an extremely varied range of pathophysiologies.

1.3.1 | Mitochondrial Morphology & Dynamics

The mitochondrial membranes consist of an outer mitochondrial membrane (OMM) facing the cytosol, and the inner mitochondria membrane (IMM) encasing the mitochondria's inner space; the matrix. The IMM is folded into protrusions called cristae, increasing the surface area for the biochemical processes, such as OXPHOS, that occur within or across it.

Classically depicted as discrete, tubular structures, typically between 0.75 and 3 μM in diameter, mitochondria are in fact dynamic structures that can fuse into long, elongated networks, split into smaller, singular structures and move along microtubular networks, depending on the cell's energetic requirements (Senft and Ronai, 2016). Mitochondrial fusion and fission are tightly controlled processes, regulated by a number of proteins including the cytosolic dynamin related protein (Drp1) (Smirnova et al., 2001), human mitochondrial fission protein 1 (hFis1) (Yoon et al., 2003) and the mitochondrial dynamin-like GTPase (Opa1) (Meeusen et al., 2006). Fusion of mitochondria into elongated networks is associated with increased ATP production (Youle and van der Bliek, 2012), and has also been seen to act as a mitochondrial repair mechanism, with healthy mitochondria fusing to damaged ones and removing the damaged parts (Youle and van der Bliek, 2012). Fission of mitochondria into a more fragmented state on the other hand has been identified as an early pre-requisite step in programmed cell death (PCD) (Suen et al., 2008) and has also been identified as a quality control mechanism – allowing unrepairable mitochondria to be "teased apart" from the rest of the network, and then targeted for lysosomal degradation in a process known as mitophagy (See section 1.3.2) (Higuchi-Sanabria et al., 2018). The proteins that regulate fusion or fission events have themselves been shown to have key roles in programmed cell death; the down regulation of Drp1 and hFis1; mitochondrial fission proteins, induce a resistance to apoptosis, whilst down regulation of Opa1, which regulates fusion, enhances sensitivity to apoptosis (Lee et al., 2004).

1.3.2 | Autophagy, Mitophagy, & Mitochondrial Biogenesis

Autophagy describes the regulated destruction of cellular components. This process is utilized by cells to remove unnecessary or dysfunctional organelles, or to promote survival in conditions of starvation to maintain cellular energy levels via a process akin to recycling (Mizushima and Komatsu, 2011). Since the removal of malfunctioning organelles is essential for healthy cellular function, autophagy has a key role in preventing a range of diseases. Impaired or excessive autophagy is linked neurodegenerative disease, cardiac disease, infection, and cancer (Levine and Klionsky, 2004).

Being at the centre of cellular metabolism and energy production, the selective degradation of mitochondria, known as mitophagy, is of specific interest to researchers, particularly with respect to its role in disease. The accumulation of damaged mitochondria as a consequence of impaired mitophagy can lead to Parkinson's Disease (Narendra et al., 2009) and is implicated in ageing (Shi et al., 2017), with the pathogenesis of both being tied to increased oxidative stress, decreased Ca^{2+} buffering, and loss of ATP.

The biogenesis of mitochondria is essential to maintaining healthy cellular homeostasis. The removal of superfluous mitochondria and production of additional mitochondria is dictated largely by the energetic demands of the cell. The synthesis of mitochondria is therefore considered a stress response to counteract decreases in ATP production (Lee and Wei, 2005). Biogenesis, like mitophagy, is a highly regulated and complex process (Poyton and McEwen, 1996). The mitochondria, possessing its own DNA, must replicate, transcribe and translate it's genome in coordination with mitochondrial genes within the nucleus and direct these proteins to the appropriate space to form the mitochondria.

Mitophagy and mitochondrial biogenesis are regulated by communication between the mitochondria and nucleus, which contains genes for both mitochondrial genesis and autophagy regulation. The communication is referred to as mitochondrial retrograde (mitochondria to nucleus) or anterograde (nucleus to mitochondria) signalling. In both pathways, signals between mitochondria and nucleus effect changes in nuclear gene transcription in order to reconfigure cellular

metabolism based on cellular demands or mitochondrial health (Liu and Butow, 2006; Ng et al., 2014).

1.3.3 | Mitochondrial DNA

The mitochondria contains its own DNA; a circular genome of 16,569 base pairs. In addition to ribosomal RNAs and transfer RNAs (tRNAs), 13 polypeptides are encoded, which make up some of the complexes of the electron transport chain (ETC) (described in section 1.5.1) (Anderson et al., 1981). Aside from its circular structure, mitochondrial DNA (mtDNA) possesses several features that differentiate it from nuclear DNA. It contains no introns, but rather a single non-coding region called the displacement loop (D-Loop) (Lee and John, 2015). The function of the D-loop has yet to be fully resolved, but researchers have identified a protein, ATAD3p, as having a high affinity for the D-loop, which when silenced resulted in the disruption of the structure of mitochondrial nucleoids, suggesting the D-loop plays a role in maintaining mtDNA organisation and structure (He et al., 2007).

Despite its small size compared to the nuclear genome, the essential functions regulated by the mitochondria mean that mutations that occur in mtDNA can manifest in a range of diseases in many different tissues with a wide variety of clinical features, including diabetes, hearing loss, infantile encephalopathy (Taylor and Turnbull, 2005) and tumour formation (Gasparre et al., 2008). Indeed, mtDNA mutations have been detected in a large percentage of cancers, yet whilst mutations that occur in coding regions have the potential to disrupt the cell's energy production and redox state, most have been found to occur in the control region of the genome, which would suggest that it is unlikely mtDNA mutations drive tumour growth (Kirches, 2017). The role of mtDNA in tumour development is further complicated as each cell contains multiple mitochondria each with their own copies of mtDNA, meaning wild type and mutant mtDNA can co-exist within a cell in a state called heteroplasmy. Thus, the biological impact of mtDNA mutations depends on the proportion of mitochondria within a cell containing mutated mtDNA compared to mitochondria with no mutations (Chatterjee et al.,

2006). The overall copy number of mitochondria has been observed to be decreased in cancer relative to normal cells, correlated in some types with reduced expression of respiratory genes. On the other hand, tumours with high mtDNA content, which may confer increased mitochondrial dependence, may present a vulnerability to mitochondria targeted therapies (Reznik et al., 2016).

1.3.4 | Mitochondrial Metabolism

The mitochondria are primarily associated with the production of the cell's energy-rich substrate, adenosine triphosphate (ATP), through the aerobic pathway of OXPHOS. Embedded on the inner membrane of the mitochondria are a series of 5 protein complexes which make up the ETC, which catalyse a series of redox reactions, transferring electrons from high-energy donors to acceptors (See Table 1). The energy released in these reactions is used to generate a transmembrane proton gradient across the inner mitochondrial membrane, which drives the production of ATP from the final complex in the chain, ATP synthase. The final electron acceptor in the process is oxygen, making the process aerobic. OXPHOS is described in more detail in Table 1 and Figure 3.

COMPLEX	NAME	REACTION
I	NADH Dehydrogenase	Transfer of electrons from NADH to ubiqunone (UQ) to form ubiquinol (UQH_2)
II	Succinate Dehydrogenase	Transfer for electrons from succinate to ubiqunone (UQ) to form ubiquinol (UQH_2)
III	Cytochrome bc1	Electrons from the quinone pool are transferred to cytochrome *c*
IV	Cytochrome *c* oxidase	Electrons from reduced cytochrome *c* are transferred to molecular oxygen to produce water
V	ATP Synthase	Produces ATP

Table 1 | **Complexes of the Electron Transport Chain**. Imbedded in the inner mitochondrial membrane, Complexes I through IV pump protons derived from metabolic intermediates into the mitochondrial matrix. The proton gradient drives the production of ATP through Complex V.

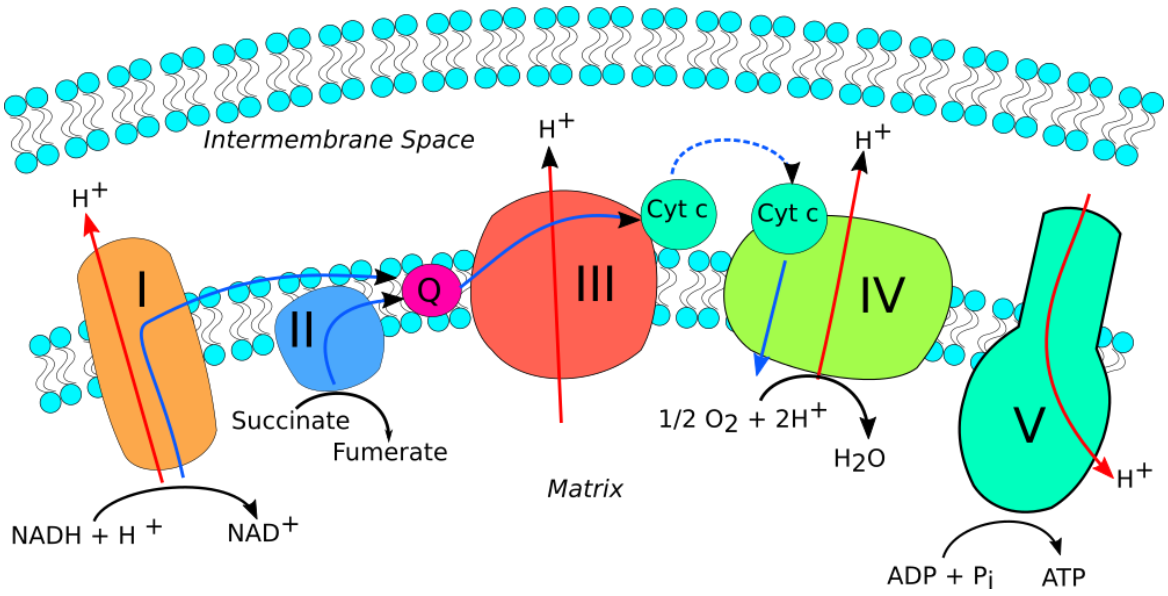

Figure 3 | **The Electron Transport Chain.** Through Complexes I-IV, metabolic intermediates are reduced to produce high energy electrons (blue arrows), which push protons (red arrows) across the inner mitochondrial membrane, generating an electrochemical gradient between the intermembrane Space and the Matrix. This gradient drives the production of ATP from Complex V, also known as ATP Synthase.

OXPHOS occurs on and across the inner membrane of the mitochondria. In the matrix another energy releasing pathway occurs: the TCA Cycle, also known as the citric acid cycle or Kreb's cycle. The TCA cycle starts with acetate, in the form of acetyl coenzyme A (Acetyl CoA), produced from sugar, fat, and protein catabolism, and ends with the production of carbon dioxide and the electron carriers flavin adenine dinucleotide ($FADH_2$) and nicotinamide adenine dinucleotide (NADH), which shuttle the high-energy electrons, derived from the catabolism of the sugars, fats, and amino acids, to the ETC (Nelson and Cox, 2008). The cycle is illustrated fully in Figure 4.

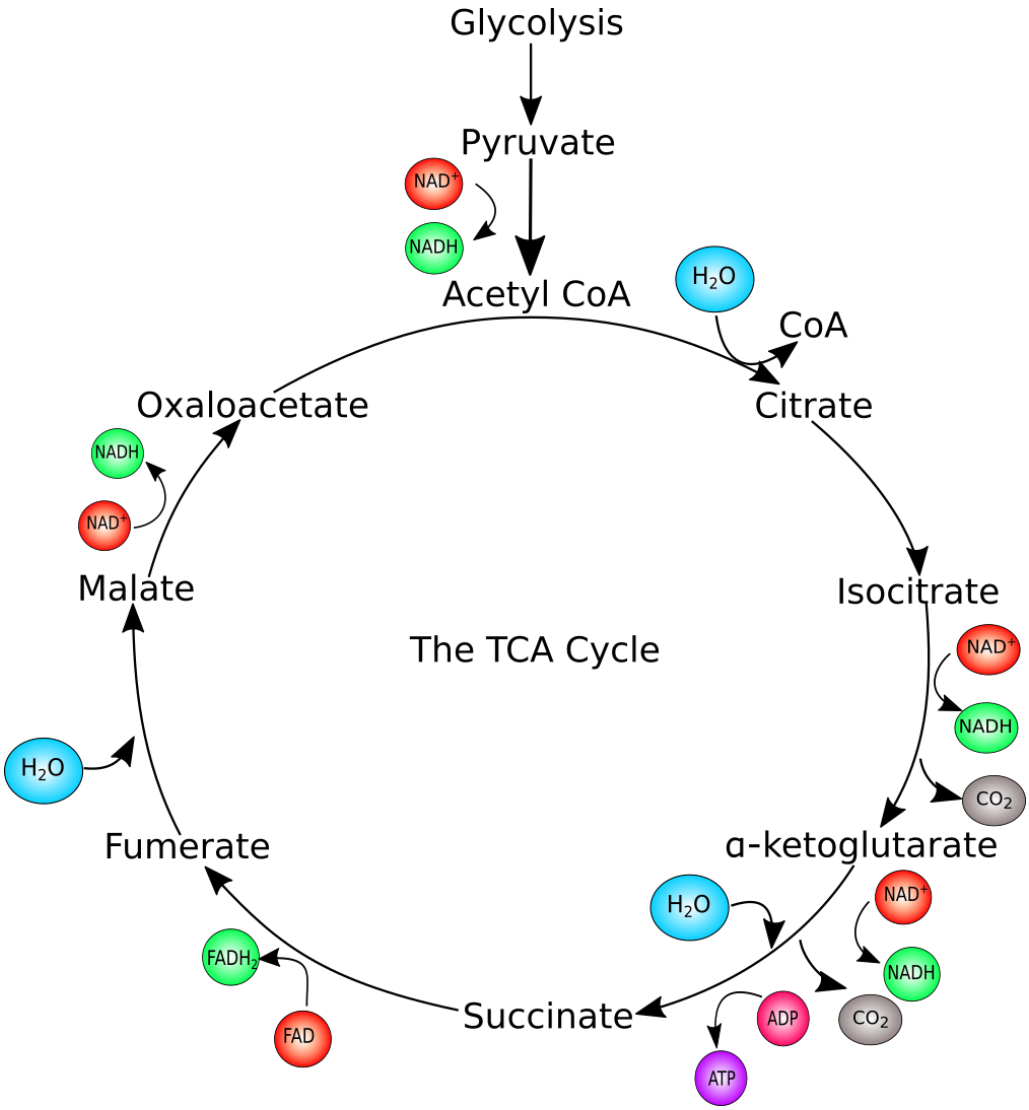

Figure 4 | The Tricarboxylic Acid (TCA) Cycle. The TCA cycle is a series of reactions that produces CO_2, ATP, NADH and FADH, starting with the oxidation of acetyl CoA. As well as producing energy itself in the form of ATP, NADH and FADH are used in the electron transport chain to generate energy though oxidative phosphorylation.

1.3.5 | The Mitochondria and the Production of Reactive Oxygen Species

Reactive oxygen species (ROS) describes a number of highly reactive chemicals, all of which originate from molecular oxygen (O_2) (Table 2). ROS are a natural by-product of mitochondrial respiration, in particular from Complexes I and III in the ETC (Holmström and Finkel, 2014). Members of the ROS family, such as hydroxyl radicals and superoxide anions, are extremely reactive and can cause DNA and RNA damage, excess oxidation of amino acids, and deactivation of enzymes if levels are allowed to accumulate – a state known as oxidative stress (Sosa et al., 2013).

SPECIES	SOURCE	ACTION
Superoxide $O_2{\cdot}^-$	Complex I,III	Reacts with compounds with double bonds (e.g. Fe-S proteins)
Hydrogen Peroxide (H_2O_2)	SOD-catalysed Dismutation of $O_2{\cdot}^-$	Oxidises proteins. Forms OH·
Hydroxyl Radical (OH·)	Reduction of H_2O_2	Extremely reactive with all biomolecules

Table 2 | **The Reactive Oxygen Species** produced from mitochondrial respiration, with the mode of action of each. Hydrogen peroxide and the hydroxyl radical are not directly produced by the mitochondria, but are rather produced as side effects of the removal of the superoxide anion.

To prevent oxidative stress, ROS levels are regulated by a cell's antioxidant defences, which includes enzymes such as catalase and superoxide dismutase (SOD), which catalyse the decomposition of hydrogen peroxide into water and oxygen and the conversion of the superoxide radical into oxygen (Birben et al., 2012). Owing to their reactive and destructive properties (see Table 2), for a long time ROS had been perceived as largely toxic and harmful, associated with a variety of diseases including asthma, hypertension, and retinopathy (Auten and Davis, 2009). The increased incidence of cancer at older age has been attributed to elevated ROS, for example through a decline in ROS clearing enzyme-activity

at older age (Van Remmen et al., 2003). Oxidative stress was also considered to be a major cause of aging: numerous studies have demonstrated that ROS accumulates in an organism as it ages, and that reducing oxidative damage extends the lifespan of model organisms. This became known as the free radical theory of aging (Beckman and Ames, 1998). This theory, and the overall consensus that ROS are largely deleterious to organisms, is being increasingly challenged by more recent research which identifies ROS as vital molecules for a number of essential cell signalling pathways (Gladyshev, 2014). For example, deletion of *sod-2*, encoding the antioxidant protein SOD, extended the lifespan of the model organism *Caenorhabditis elegans* (Van Raamsdonk and Hekimi, 2009). Examples of ROS-dependent signalling pathways include the nuclear factor kappa-light-chain-enhancer of activated B cells (NF-κB) pathway, which is implicated in a number of cellular processes including cell adhesion and differentiation, and the mitogen activated protein kinase (MAPK) pathway, crucial in cell growth and cell death (Jixiang Zhang et al., 2016). Furthermore, ROS production and removal affects the balance of oxidation and reduction reactions in a cell, known as the cell's redox state. Interestingly, the redox state of the cell fluctuates during the cell cycle, which led researchers to propose the production of ROS, controlling the redox state, can regulate cellular proliferation (Sarsour et al., 2009). Direct ROS/redox regulation of a number of cell-cycle proteins, including p21 and cyclin D1, has been observed *in vitro* (Fitzgerald et al., 2015; Lim et al., 2008).

1.3.5.1 | ROS and Cancer

In cancer cells the levels of ROS can be increased, enhancing the metabolic rate of the pathways described above, particularly those involved in cellular proliferation (Sullivan and Chandel, 2014). At the same time, cancer cells also increase their anti-oxidant capacity to protect against oxidative stress and cell death (Reczek and Chandel, 2018) (See Figure 5). For example, the transient receptor potential cation channel 1 (TRPA1), over-expressed in cancer, is activated by ROS, leading to the influx of Ca^{2+} which serves to upregulate Ca^{2+} dependent anti-apoptotic survival pathways (Takahashi et al., 2018).

Changes in the redox state of cancer cells are inextricably linked to hallmark changes in cellular metabolism. Intermediates from glycolysis, elevated in cancer cells, are funnelled into pathways such as the pentose phosphate pathway (PPP), which produces ribose-5 phosphate, a precursor to nucleotide synthesis as well as nicotinamide adenine dinucleotide phosphate (NADPH), a molecule involved in ROS removal (Described in more detail in Section 1.3.8) (Panieri and Santoro, 2016).

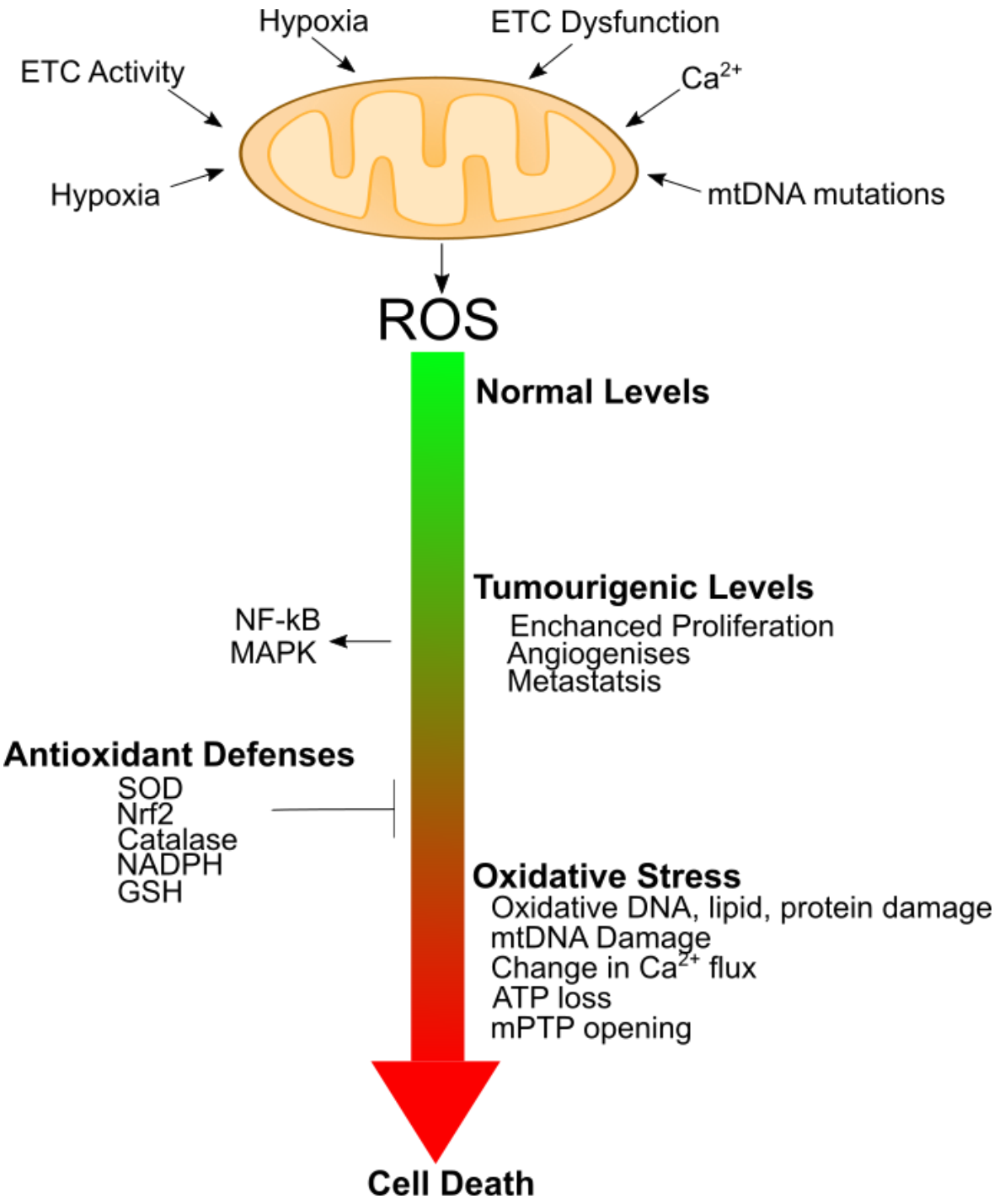

Figure 5 | ROS in Cancer: A Double-Edged Sword. Elevated ROS in cancerous cells, produced primarily by the electron transport chain within the mitochondria, can promote tumorigenesis. If ROS levels continue to rise, it can cause oxidative stress which can lead to cell death. To prevent this, cancer cells can increase antioxidant defences.

1.3.6 | Mitochondria and Calcium Signalling

Calcium ions (Ca^{2+}) are of vital importance in the physiology of cells. Ubiquitous in cellular signalling pathways, Ca^{2+} can interact directly in processes such as apoptosis, protein conformation and localisation, or indirectly as a second messenger in almost all receptor-based signalling pathways (Clapham, 2007). The calcium based signalling mechanism is based on changes in the amplitude, frequency, duration, and localization of cytosolic calcium ($[Ca^{2+}]_c$). Such spatiotemporal changes arise from the entry of Ca^{2+} into the cell from the extracellular matrix, or the release of Ca^{2+} from various intracellular stores, notably the mitochondria, as well as the endoplasmic reticulum and the Golgi apparatus (Contreras et al., 2010). Thus, by acting as Ca^{2+} buffers for the cytosol, these organelles play key roles in cellular signalling.

Ca^{2+} freely diffuses through the outer mitochondrial membrane, primarily through the voltage dependent anion channel (VDAC), a large, weakly selectively anion channel, abundant on the OMM. VDAC can assume open or closed conformations, a feature which plays a key role in the regulation of apoptosis (Rizzuto et al., 2010). Transport across the inner membrane into the matrix is driven by the electrochemical gradient generated across the membrane by the ETC through ion channels – notably the mitochondrial calcium uniporter (MCU) (Kirichok et al., 2004). Efflux out of the mitochondria is mainly attributed to the Na^{+}-Ca^{2+}-Li^{+} exchanger (NCLX). As will be described in sections 1.3.6.1 and 1.3.6.2, mitochondrial Ca^{2+} ($[Ca^{2+}]_m$) flux is key in vital cell processes such as energy metabolism and cell death. Therefore, disruptions to the mitochondrial Ca^{2+} transport machinery can manifest in a variety of pathologies, such as tumorigenesis and oxidative stress (Marchi and Pinton, 2014). The entire picture of Ca^{2+} transport has yet to be fully realised, highlighted by studies in MCU deficient mice, which although exhibited an impaired ability to perform “strenuous work”, unexpectedly showed no alteration in basal metabolism rates (Pan et al., 2013), suggesting the activity of other Ca^{2+} influx transporters can be enhanced to maintain a level of Ca^{2+} homeostasis (Marchi and Pinton, 2014).

1.3.6.1 | Mitochondrial Ca^{2+} and Metabolism

Aside from maintaining $[Ca^{2+}]_c$ homeostasis, mitochondrial Ca^{2+} affects the rates of mitochondrial respiration through the allosteric activation of a number of mitochondrial enzymes, including pyruvate dehydrogenase, the activation of which increases NADH supply and thus ATP production, and ATP synthase (Complex V), increasing the output of ATP (Griffiths and Rutter, 2009). This general upregulation of the mitochondrial metabolic machinery by Ca^{2+} provides the cell a signalling pathway to modify ATP production to meet energetic demand (Bianchi et al., 2004).

1.3.6.2 | Mitochondrial Ca^{2+} and Cell Death

It is now well established that mitochondria play key role in the regulation and initiation of apoptosis and other forms of cell death (Martinou and Youle, 2011), the minutiae of which are discussed in Section 1.6. An initial step in mitochondrial-regulated cell death is the formation of the permeability transition pore (PTP) on the outer membrane of the mitochondria. This perforation of the membrane releases pro-apoptotic factors such as cytochrome *c* or apoptosis inducing factor (AIF) into the cytosol, which then go on to activate the apoptotic machinery (Orrenius et al., 2015). The opening of these pores is enhanced by the sustained mitochondrial accumulation of Ca^{2+} (also known as Ca^{2+} overload) (Lemasters et al., 2009). Further to this, the subsequent depolarization of mitochondria caused by Ca^{2+} overload in a particular sub-cellular region initiates a wave of further mitochondrial Ca^{2+} uptake and depolarization, propagating an apoptosis-initiating signal across the whole cell (Pacher and Hajnóczky, 2001).

1.3.7 | The Interplay Between Mitochondrial Ca^{2+}, ROS, and Morphology

There exists a complex interaction between the signalling molecule, Ca^{2+} and the by-products of mitochondrial respiration, ROS (Figure 6). For example, mitochondrial Ca^{2+} overload can also lead to enhanced generation of ROS (Kowaltowski et al., 1998). The mechanisms of this production are not yet fully understood. It has been suggested that Ca^{2+} causes a conformational change in Complex I, and can indirectly inhibit Complex III through the production of nitric oxide (NO), both mechanisms inducing ROS production (Feissner et al., 2009) Additionally, the increase in the mitochondrial respiratory rate driven by $[Ca^{2+}]_m$ leads to a subsequent increase in ROS production. Increases in mitochondrial Ca^{2+} concentration ($[Ca^{2+}]_m$) or ROS can enhance the concentration of the other, creating a positive feedback loop that, if not broken by the mitochondria's anti-oxidant defences or by mitochondrial Ca^{2+} efflux channels, can lead to a state of oxidative stress or cell death by apoptosis (Feissner et al., 2009).

Ca^{2+} is also suspected to have a role in regulating mitochondrial dynamics; it has been shown that increases in $[Ca^{2+}]_c$ inhibit mitochondrial movement and can cause changes in morphology from an elongated to a more rounded shape (Szabadkai et al., 2006). This relationship is thought to be mediated by interactions between Ca^{2+} and the proteins that regulate mitochondrial morphology such as Drp1 and hFis1 for fission, and Mfb1 and Opa1 for fusion (Jeyaraju et al., 2009). The extent of the mitochondrial network and the distribution of mitochondria in general has a profound effect on the mitochondrial-based Ca^{2+} signalling. For example; fragmentation of the mitochondrial network has been shown to inhibit the Ca^{2+} propagation described in Section 1.3.5.2 (Szabadkai et al., 2006).

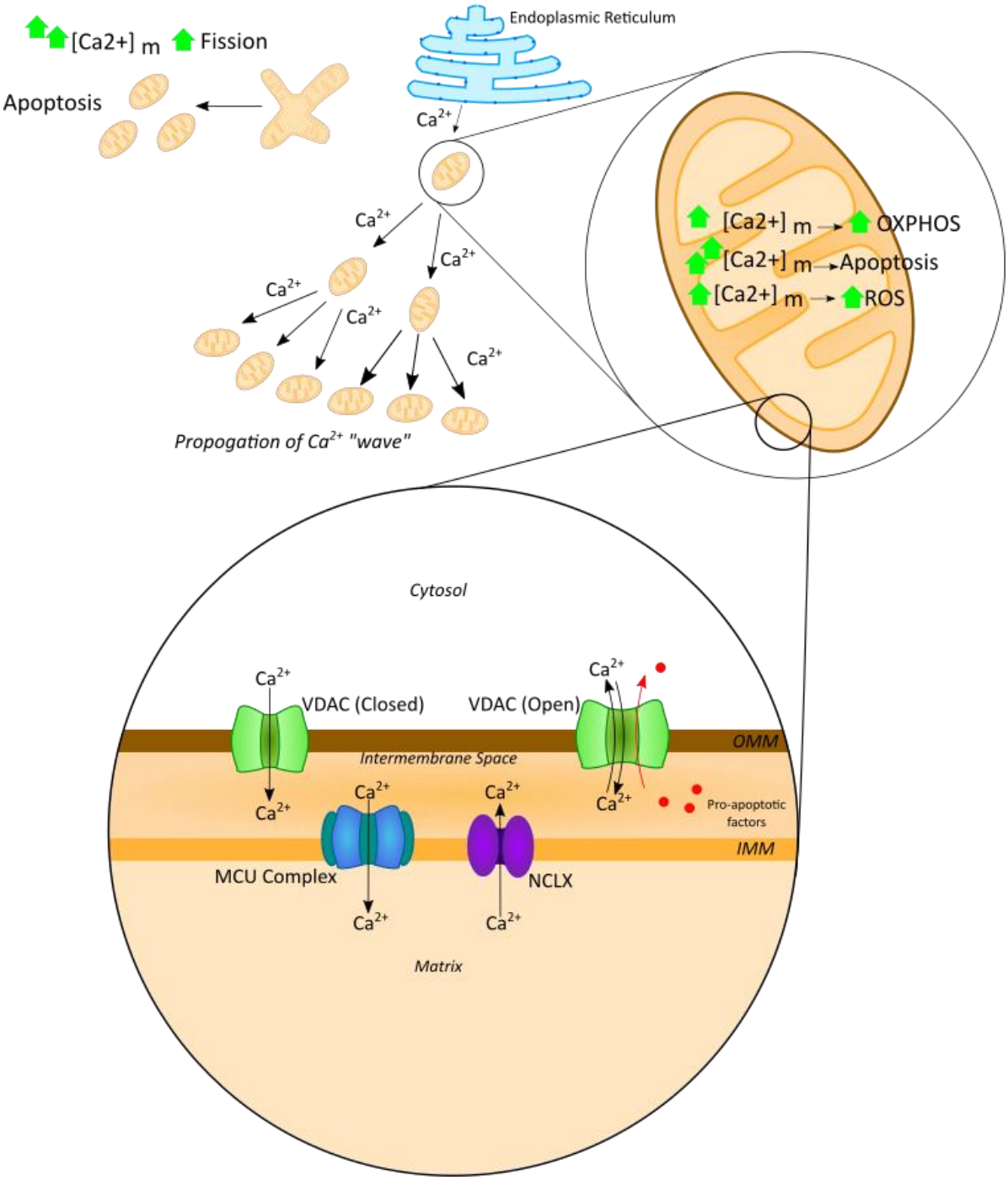

Figure 6 | Calcium Interactions with the Media. Calcium is taken up by the mitochondria from areas of high $[Ca^{2+}]_c$, such as those in proximity to the endoplasmic reticulum. Ca^{2+} moves passively across the outer mitochondrial membrane via VDAC. From the intermembrane space, Ca^{2+} is moved into the mitochondrial matrix through the MCU complex, and is removed via NCLX. Increases in $[Ca^{2+}]_m$ stimulate increased OXPHOS rates and ROS production. Sustained high $[Ca^{2+}]_m$ can result in mitochondrial fission and the opening of mPTP (including VDAC), both of which can lead to apoptosis. Increases in $[Ca^{2+}]_m$ can trigger the enhanced uptake of Ca^{2+} in neighbouring mitochondria, allowing the propagation of a Ca^{2+} signalling "wave" across the cell.

1.3.8 | NADH Metabolism

The pyridine nucleotides, nicotinamide adenine dinucleotide (NAD) and nicotinamide adenine dinucleotide phosphate (NADP) are two molecules which, as electron carriers, play important roles in cellular redox chemistry. NAD exists in oxidised (NAD+) and reduced (NADH) forms. The redox chemistry of NAD links the major energy producing pathways in the cell: the conversion of pyruvate into acetyl CoA in glycolysis yields NADH, which can transfer electrons to NADH dehydrogenase, also known as Complex I, in the mitochondrial ETC. The resulting NAD+ can then be reduced in the TCA cycle, allowing the cycle of NAD+ to NADH to perpetuate (Blacker and Duchen, 2016).

Whilst NAD/NADH primarily acts as an electron donor in these energy-producing or catabolic pathways, NADP/NADPH has a somewhat counter-role, regulating antioxidant defences that protect the cell from oxidative stress, caused by the production of ROS as a side-effect of OXPHOS. Two such antioxidant systems, glutathione and thioredoxin, act as a first line of defence against the accumulation of hydrogen peroxide (H_2O_2), which itself is produced by the neutralisation of superoxide, another reactive species. In these systems, enzymes catalyse the reduction of H_2O_2 into water through the oxidation of glutathione (GSH) and thioredoxin (TRX) respectively. Glutathione reductase and thioredoxin reductase then restore GSH and TRX back to their reduced forms, the electrons for which are provided by NADPH (Blacker and Duchen, 2016). In a stark contrast to this anti-oxidant activity, NADPH also has a role in the “intentional” production of the ROS superoxide through NADPH oxidase enzymes (known as NOXs), particularly in neutrophils, as part of the immune response (Geiszt, 2006; Lambeth, 2004).

1.4 | Targeting Cancer Metabolism

The alterations in metabolism, as described in the previous sections, whilst proving advantageous for cancer cell proliferation, can potentially present a target for treatments. For example, targeting glycolysis through the inhibition of the glucose transporter 2 (GLUT2) (Wu et al., 2009) or the glycolytic pathway enzyme hexokinase (Maschek et al., 2004) were shown to induce apoptosis in cancer cells or to enhance the efficacy of anti-cancer drugs. Reversal of the Warburg Effect has also shown potential as a novel treatment: in glioblastoma, increased oxygen consumption conferred to a decrease in proliferation (Poteet et al., 2013), and in melanoma cell lines, a “reversal of the metabolic switch” by inhibiting glycolysis led to cell cycle arrest and enhanced sensitivity to apoptosis (Bettum et al., 2015). Metformin, a complex I inhibitor commonly used to treat the metabolic disorder type 2 diabetes has been found to have additional anticancer properties in diabetic patients by inhibiting the mTOR signalling pathway (Zi et al., 2018). Furthermore, enhancing mitochondrial ROS production has been used to improve sensitivity to anticancer drugs (Yun et al., 2015). Manipulating the cell’s ability to remove dysfunctional mitochondria by targeting autophagy and mitophagy is also being investigated as a novel target (Mathew et al., 2007).

1.5 | Cancer Chemotherapy

Historically, the treatment of cancer uses a single or a combination of 3 treatment approaches: surgery, radiotherapy, and chemotherapy (Cancer Research UK, 2017). Other approaches, such as hormone therapy (Vorobiof, 2016) or immunotherapy (Vorobiof, 2016) are being developed and improved continuously. Whilst surgery and radiotherapy are effective at removing solid, localised tumours from the body, chemotherapy is often used in conjunction with these approaches to improve their effectiveness, or as the primary course of treatment for non-solid cancers such as leukaemia, or to treat cancers that have spread from their site of origin (NHS, 2017).

Early chemotherapeutic drugs originated from the research of chemical weapons, such as mustard gas, to treat cancers (Goodman et al. 1946). Although modern chemotherapy has since moved towards a more regulated, targeted approach, in many cases the primary mode of action for a wide range of anti-cancer drugs is targeting the rapid proliferation of cancer cells; one of the 6 hallmarks of cancer. As a consequence, healthy cells with a naturally high rate of proliferation, such as those found in hair roots or in the lining of the gut, are also affected, meaning that chemotherapy is often accompanied by a number of often severe side effects (American Cancer Society, 2016).

1.5.1 | Types of Chemotherapy

The end result of most chemotherapeutic drugs is cell death by apoptosis, although the route through which this process is triggered varies enormously between the vast number of drugs available. Table 3 summarises the major categories of chemotherapy with some examples, highlighting the variation in drug mechanism. Section 1.5.2 then discusses the mode of action of cisplatin, selected as a model of chemotherapy in this study in closer detail.

CATERGORY	MECHANISM	EXAMPLES
Alkylating Agents	Akylation of DNA, triggering cell death through DNA damage	Cisplatin, cyclophosphamide, oxaliplatin
Tyrosine Kinase Inhibitors	Inhibition of unregulated phosphorylation (Gaumann et al., 2016)	Dasatinib, Erlotinib
Topoisomerase Inhibitors	Inhibition of DNA repair and transcription cancers (Xu and Her, 2015)	Camptothecin, doxorubicin
Antimetabolite	Inhibition of metabolic pathways	5FU, Methotrexate

Table 3 | **Types of Chemotherapy Drugs**. Despite the large number of commercially available chemotherapy drugs, many share common underlying mechanisms and are often grouped into categories. This table, whilst not exhaustive, highlights some common drugs and their mechanisms. Different types of chemotherapy drugs are often used in combination, which is referred to as combination therapy. 5FU: 5-florouracil

1.5.2 | Cisplatin

Diaminedichloridoplatinum (DDP), also known as cisplatin, is one of the most widely used and potent anti-cancer drugs available (Siddik, 2003). As an alkylating agent, its primary mode of action is through the damage of a cell's DNA, inducing apoptosis (Figure 7). Cisplatin is thought to enter cells through passive diffusion, although the membrane-bound copper transporter I (CTR1, involved in copper homeostasis) and copper-extruding P-Type ATPases have also been implicated as contributing elements (Lin et al., 2002).

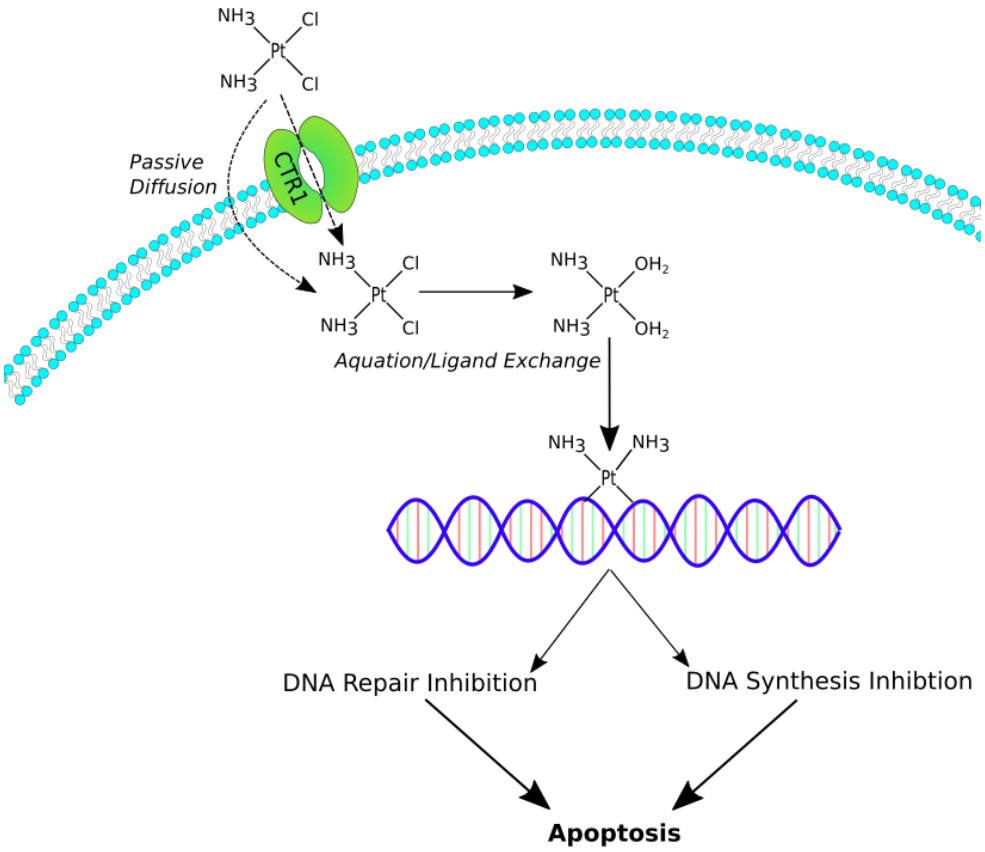

Figure 7 | Mechanisms of Cisplatin. Cisplatin enters the cell through passive diffusion or facilitated by CTR1. Inside the cell, the complex is activated through aquation. The activated complex binds to and distorts the DNA double helix. When the cell fails to repair the resulting lesion, apoptosis is initiated.

Once inside the cell, cisplatin is hydrolysed to produce mono or di-aqua complexes (aquation). Water displaces one or both Cl ions as a consequence of the difference in chloride concentrations between the blood stream and cytosol. These “activated” complexes can react with the nucleophilic centres on guanosine and adenosine – the purine bases of DNA. These reactions can result in the formation of a “cross-bridge” between adjacent or inter-strand guanine residues. This cross-linking is thought to account for the majority of cisplatin’s cytotoxicity, as the resulting distortion of the DNA helix triggers the DNA repair process, which upon failure initiates apoptosis (Dilruba and Kalayda, 2016).

1.5.2.1 | *Cisplatin Cytotoxicity & ROS*

The use of many chemotherapeutic agents, including cisplatin, is limited by the damaging side effects they induce. Among these is the enhanced production of mitochondrial reactive oxygen species (Marullo et al., 2013). Cisplatin has been shown to accumulate in the mitochondria and to bind to mitochondrial DNA (mtDNA). Unlike nuclear DNA, mtDNA lacks any excision repair mechanism, which results in inhibition of protein synthesis. In turn, this leads to a drop in levels of proteins associated with the ETC, and therefore a subsequent deterioration in metabolic function and an increase in ROS production (Choi et al., 2015).

1.5.3 | Chemotherapeutic Drug Resistance & Recurrence

Much like bacteria becoming resistant to antibiotics, cancer can develop resistance to drugs, which has an impact on the treatment of patients as well as the research and development of new anti-cancer agents. In a recent review, Housman et al. outline several categories of mechanisms by which cancer can exhibit resistance. These include drug efflux, DNA damage repair, cell death inhibition, drug target alterations, drug inactivation, and epigenetics, all of which can operate independently or in combination (Housman et al., 2014). Drug resistance often arises following initial treatment with chemotherapy. This development comes from the heterogeneity of a tumour cell population: although a

majority of cells are killed following the initial treatment, a small, resistant population can survive and remain undetected, and eventually form a new tumour which is now resistant to therapy (Cree and Charlton, 2017). Despite a wealth of statistics and data regarding cancer incidence and survival, data regarding recurrence is surprisingly sparse. In a study of 1000 patients diagnosed with breast cancer, Walkington et al. found that 21.4% of patients developed recurrent disease within 10 years following initial treatment (Walkington et al., 2012). The risk of recurrence also has a marked effect on a patient's psychological well-being. In a study of 752 patients, Baker et al. found that over half (68.1%) feared that the disease would return (Baker et al., 2005).

1.5.4 | Chemotherapy Side Effects

Cancer chemotherapy is often accompanied by numerous side effects, including hair loss, nausea, pain, fatigue (Carelle et al., 2002), and a range of psychological effects, such as distress, anxiety and depression (Pandey et al., 2006). The combination of these side effects can have a severe impact on a patient's daily activities, sexual life, and employment, leading to a significant decrease in the quality of both their and their family's lives (Lorusso et al., 2017). The extent and severity of these side effects and their perception by the public is such that it is not unheard of for patients to seek alternative, holistic treatments or to decline treatment altogether. Notably, in some cases patients are reported to decline conventional treatments if they feel that the loss of quality of life is not worth what is perceived as a slight increase in survival chance (Frenkel, 2013). Further to this, Robb et al. reported almost all participants surveyed in a study perceived chemotherapy as "horrible" and the treatment being "almost as bad" as the cancer itself (Robb et al., 2014). The balance between developing drugs quickly whilst limiting exposure to toxic side effects remains a significant challenge in cancer drug development.

With cancer remaining one of the biggest causes of mortality worldwide, it presents a considerable target for researchers and pharmaceutical developers, although this interest and its considerable expenditure does not seem to translate

into success for the patient - one study found that between 2009 to 2013, over half (57%) of European Medicines Agency-approved oncology drugs entered the market without clear evidence that they improved patient survival or quality of life (Davis et al., 2017). Thus, it is clear that there is still a pressing need to improve the effectiveness of modern chemotherapy, and translate clinical trial success into improved outcomes for patients.

1.6 | The Mechanisms of Chemotherapy – Apoptosis

There are hundreds of chemotherapy drugs currently available on the market. Most can be characterised and grouped according to their molecular targets or mechanisms, as briefly detailed in section 1.5. Despite these differences, the end result is that the drugs kill cancer cells by initiating a form of programmed cell death called apoptosis.

Apoptosis is a mechanism for the removal of cells that are no longer required or damaged cells that pose a threat to the organism. Cells undergoing apoptosis display a number of distinct morphological changes: DNA fragmentation, cell shrinkage (pyknosis), membrane “blebbing”: which describes the separation of the cell into fragments called apoptotic bodies, and finally the translocation of the lipid phosphotidylserine from the inner leaflet of the cell membrane to the outside, which signals neighbouring cells and nearby macrophages to phagocytise the cell (Portt et al., 2011).

Apoptosis is triggered by one of two pathways; intrinsic: wherein apoptosis is triggered in response to cellular stresses, and extrinsic: triggered by signals external to the cell (see Figure 8). Both pathways converge on a single “execution” pathway: a series of intracellular proteolytic cascading reactions, mediated by a group of proteases called caspases. The caspases are a family of endoproteases that have a variety of roles in cellular signalling, inflammation, proliferation and regeneration, and cell fate determination and differentiation (Shalini et al., 2014). The caspases are numbered by function: caspases 2, 9, 8 and 10 are known as the initiator caspases, which activate the executioner caspases 3, 6 and 7, which

breakdown other proteins, or activate other enzymes that result in the controlled destruction of the cell (McIlwain et al., 2015).

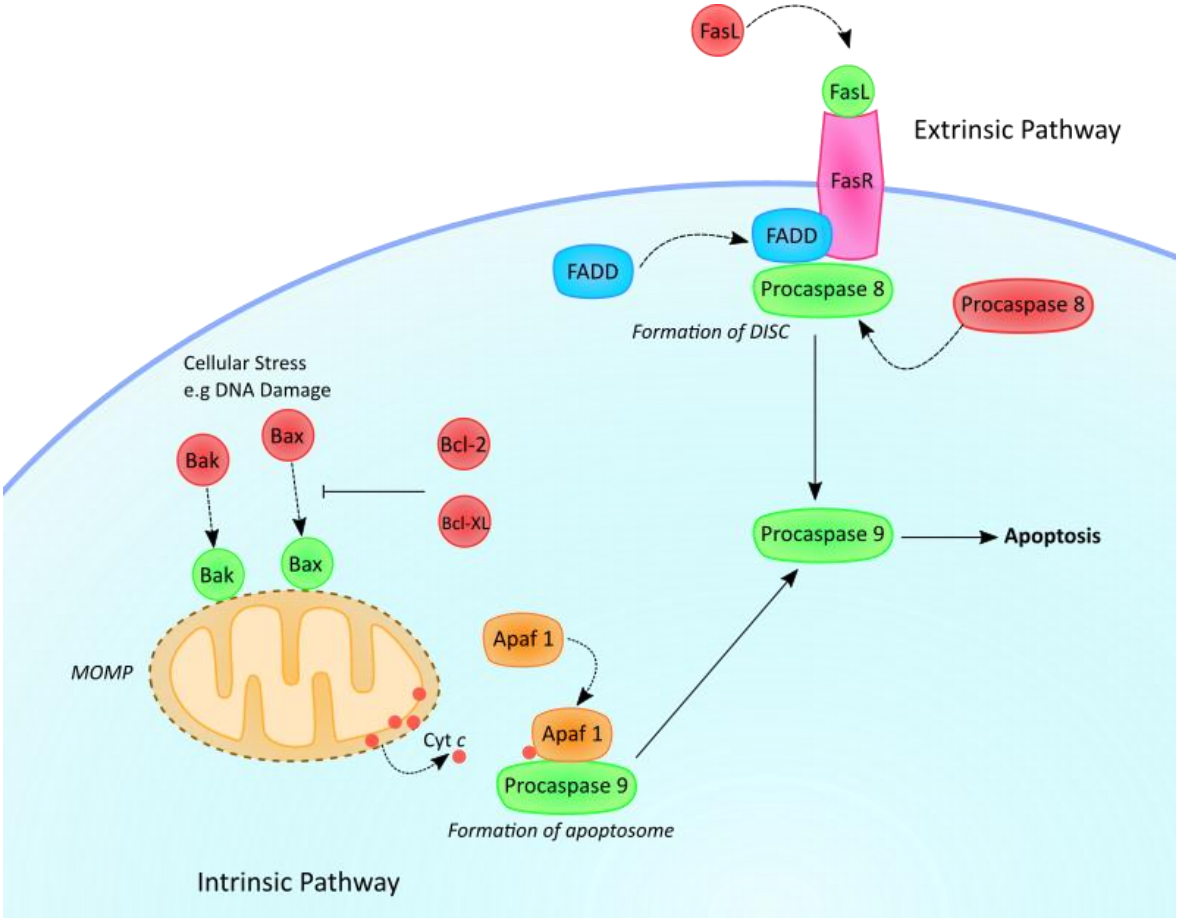

Figure 8 | **Mechanisms of Apoptosis.** Simplified schematics of the intrinsic (left) and extrinsic (right) apoptotic pathways. In the intrinsic pathway, cellular stresses activate pro-apoptotic proteins such as Bax and Bak to initiate mitochondria outer membrane permeabilisation (MOMP). Pro-apoptotic factors (such as cytochrome *c*) leak from within the mitochondria into the cytosol, where they associate with other factors such as apoptotic protease activating factor 1 (Apaf1) to activate the caspase proteins and trigger the execution phase of apoptosis. In the extrinsic pathway, the binding of death ligands (such as TNF-α or FasL) to transmembrane death receptors results in the formation of the DISC complex, which triggers the activation of the caspase cascade.

1.6.1 | Extrinsic Apoptosis

The extrinsic apoptosis pathway is initiated by factors external to the cell. Spanning the membrane of the cell are protein receptors called the death receptors, members of the large tumour necrosis factor family of genes. Interactions between death ligands and their corresponding death receptors transmit a signal from the surface of the cell to the intracellular apoptosis machinery. The best understood mechanisms are the interactions between tumour necrosis factor-α (TNF-α) and tumour necrosis factor receptor 1 (TNFR1) (Chen and Goeddel, 2002), and between Fas ligand (FasL) and Fas receptor (FasR) (Wajant, 2002). In these pathways, the interaction between ligand and receptor recruits cytoplasmic proteins: tumour necrosis factor receptor type 1 associated death domain protein (TRADD) for the TNF-α/TNFR1 interaction and Fas-associated protein with death domain (FADD) for the FasL/FasR interaction. The adapter proteins in turn associate with procaspase 8, forming the death inducing signalling complex (DISC), which activates procaspase 8, triggering the execution pathway of apoptosis (Elmore, 2007) (Figure 8).

1.6.2 | Intrinsic Apoptosis

The intrinsic pathway of apoptosis can occur in response to both negative and positive signals. Negative signals involve the absence of compounds that usually prevent or block apoptosis, whereas examples of positive signals include UV radiation, oxidative stress, and viral infection. The pathway is regulated in the mitochondria by the B cell CLL/lymphoma (Bcl-2) family of proteins; a large group containing both pro- and anti-apoptotic proteins (Green and Llambi, 2015). Activation of the pro-apoptotic members in response to cellular stress is thought to induce a translocation of the proteins from the cytosol to the OMM, where oligomerization interactions form a pore through which apoptosis-inducing factors such as cytochrome *c*, second mitochondria derived activator of caspases/direct IAP binding protein with low pl (Smac/DIABLO), mitochondrial serine protease (HtrA2/Omi), apoptosis-inducing factor (AIF), and endonuclease G can escape into

the cytosol, triggering the caspase cascade and thus the execution pathway to the cell's death (Ouyang et al., 2012) (Figure 8). The regulation and mechanism of this pathway is described in more detail in Section 1.6.3.

1.6.3 | Regulation of Apoptosis

Vital for both cell survival and cell death, apoptosis is a carefully regulated pathway. In a healthy system, apoptosis clears old or damaged cells and has roles in shaping the embryo during development (Haanen and Vermes, 1996). However, excessive apoptosis can cause atrophy and is implicit in neurodegenerative disorders such as Parkinson's disease (da Costa and Checler, 2010) and Alzheimer's disease (Nikolaev et al., 2009). Insufficient apoptosis, or an insensitivity to apoptotic triggers, is a characteristic hallmark of cancer (Fernald and Kurokawa, 2013).

1.6.3.1 | The Bcl-2 Family – Regulators of Apoptosis

The intrinsic pathway of apoptosis is governed by the Bcl-2 family of proteins. Their primary area of function is on the OMM, where they control and regulate the initiation of mitochondrial outer membrane permeabilisation (MOMP) (Kale et al., 2018).

There are three distinct subgroups in the Bcl-2 family, defined by both their role in the apoptotic pathway and the number of Bcl-2 sequence homology (BH) domains they possess (Kale et al., 2018): the pro-survival group containing BH 1-3 domains, the pro-apoptotic effector group containing BH 1-4 domains, and pro-apoptotic activator group with only the BH3 domain (See Table 4). Bcl-2-associated protein X (Bax) and Bcl-2 homologous antagonist killer (Bak) are pro-apoptotic. Upon activation, these BH 1-4 containing proteins are thought to oligomerize to form pores in the mitochondria, as part of the MOMP process, although the exact mechanism is subject to some debate (Kroemer et al., 2007). In a review on the inconsistencies in the current MOMP models, Zamzami & Kroemer

point out that Bax activation can also result in the formation of ion-permeable channels in the IMM, which does not result in the loss of matrix proteins (Zamzami and Kroemer, 2003), suggesting that there could be missing pieces in the MOMP pore complex puzzle, which is further discussed in Section 1.6.4. Performing the opposing function are the pro-survival, BH-1-3 containing proteins, including Bcl-2, induced myeloid leukaemia cell differentiation protein (Mcl-1), B-cell lymphoma-extra-large protein (Bcl-XL) and Bcl-2-like protein 2 (Bcl-W). These proteins inhibit their pro-apoptotic counterparts, repressing MOMP. Finally, the third subgroup of the Bcl-2 family consists of the BH3 only proteins (containing one region of Bcl-2 sequence homology), which are also pro-apoptotic, but unable to initiate MOMP alone. Members of this class include BH3 interacting domain death agonist (Bid), Bcl2-like protein 11 (Bim), Bcl-2-associated death promoter (Bad), P53 upregulated modulator of apoptosis (Puma) and phorbol-12-myristate-13-acetate-induced protein 1 (Noxa). These proteins are regulated in response to a variety of cellular stresses such as DNA damage (Chipuk et al., 2010).

NAME	DOMAINS	ROLE
Bcl-2, Bcl-XL, Bcl-w, Mcl1	BH1-3	Pro-survival
Bax, Bak	BH1-4	Pro-apoptotic effectors
Bim, Bid, PUMA, Bad, Hrk, Bik, NOXA	BH3 Only	Pro-apoptotic activators/sensitisers

Table 4 |The Bcl-2 Family of Proteins. The Bcl-2 family regulate cell death through interactions with the mitochondrial membrane or with each other. These interactions are dictated by the BH domains they possess.

1.6.4 | Models of MOMP

The full mechanism of MOMP has yet to be universally agreed upon, but it is generally thought that it involves the opening or the formation of the mitochondrial permeability transition pore (mPTP). The composition of the mPTP is again subject to much debate, although the central motif is conserved: the release of pro-apoptotic factors from the mitochondria into the cytosol (Suh et al., 2013).

The oligomerization of Bax and/or Bak to create a pore through the OMM, described in Section 1.6.2, makes up just one of a number of currently proposed models (Figure 9). In several of these models VDAC, introduced in Section 1.3.6, is a common denominator. Located on the OMM, it serves as a gateway for the entry and exit of mitochondrial metabolites (Shoshan-Barmatz et al., 2010). In one model, Bax interacts directly with VDAC to create a larger pore in the membrane to allow intramembrane apoptotic factors to escape (Shore, 2009). Another, almost in direct contrast, suggests that Bid interacts with VDAC to close the channel, disrupting mitochondrial ATP/ADP exchange which then causes membrane permeablisation through a yet unidentified, alternative mechanism (Rostovtseva et al., 2005). Another model proposes the rupture of the OMM altogether, caused by a change in the concentration of solutes in the mitochondrial matrix, which in turn drives water into the mitochondria, causing it to swell which eventually perturbs the OMM. The entry of these low-molecular weight solutes is believed to occur through the mPTP, which in this model is thought to consist of VDAC on the OMM, adenine nucleotide translocator (ANT) on the IMM, and cyclophilin D in the matrix, although its exact composition is again not yet fully determined (Garrido et al., 2006). Some studies however suggest that VDAC is not essential to MOMP at all. For example, experiments have shown that mitochondria lacking all isoforms of VDAC (VDAC1, 2 and 3) remain able to undergo the permeability transition, as well as Ca^{2+} and oxidative stress-induced cell death (Baines et al., 2007).

VDAC plays an additional role in cancer metabolism: protecting cancer cells against apoptosis and contributing to the Warburg effect through binding to hexokinase (HK). In glycolysis, HK catalyses the ATP-dependent conversion of

glucose to glucose-6-phosphate. The binding of HK to VDAC serves multiple purposes that provide a proliferative advantage to cancer cells; by anchoring HK to the mitochondria, HK is allowed direct access to mitochondrial ATP, allowing for increased enzymatic turnover and thus the high glycolytic flux associated with the Warburg effect. HK also competes with the pro-apoptotic Bcl-2 proteins for VDAC binding, inhibiting the initiation of apoptosis (Shoshan-Barmatz et al., 2015).

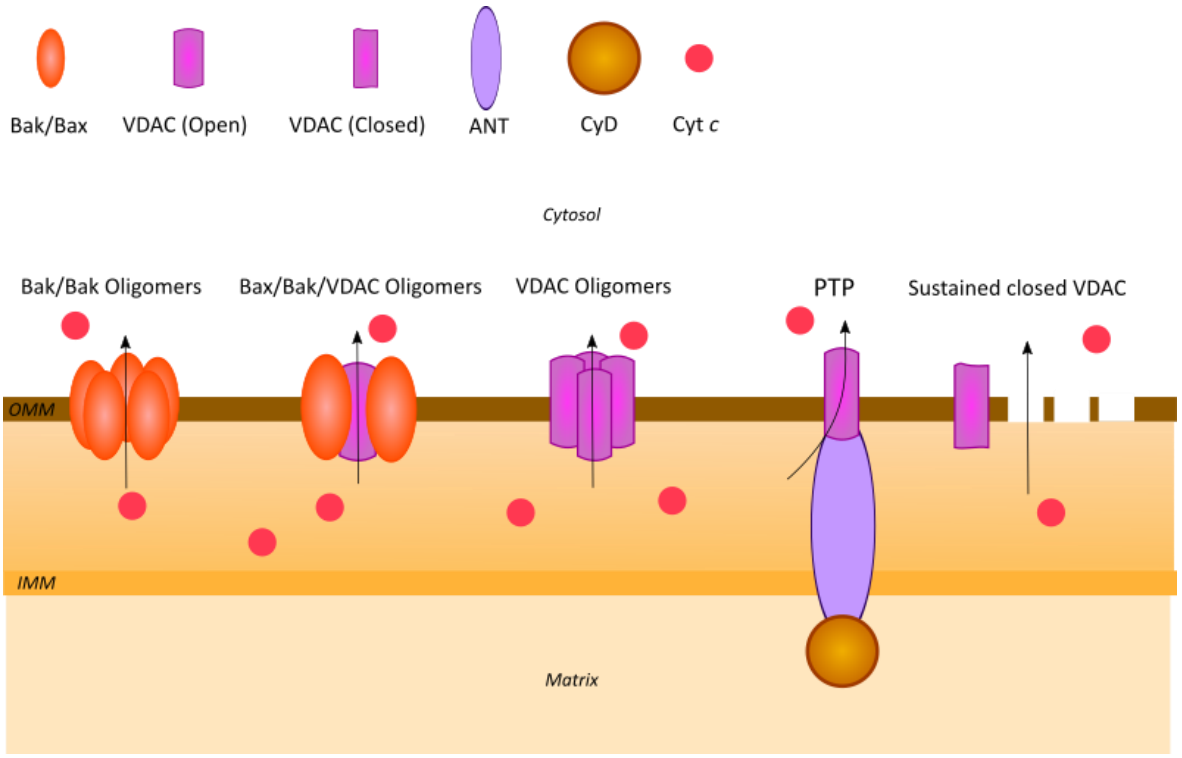

Figure 9 | **Mechanisms of MOMP**. From left to right: Bax and/or Bak, proapoptotic members of the Bcl-2 family, oligomerise into a channel on the outer mitochondrial membrane (OMM). Bak/Bak are also thought to interact with VDAC on the OMM to create a larger channel. Influx of low molecular weight solutes thorough the permeability transition pore (PTP) can cause the mitochondria to take on water, driven by osmotic force. This swelling can lead to the rupture of the OMM. Finally, sustained closure of VDAC can disrupt ATP/ADP exchange between the mitochondria and the cytosol – which causes the release of cyt *c* through an as-of-yet unidentified pore.

1.7 | Priming

Chonghaile et al. showed that a cell's clinical response to chemotherapeutic drugs is dictated by an intrinsic sensitivity to initiate apoptosis (Chonghaile et al., 2011). The group referred to this as "mitochondrial priming", whereby the more "primed" a cell's mitochondria are, the more sensitive they are to apoptotic triggers. This was tested by introducing BH3-linked peptides derived from pro-apoptotic Bcl-2 proteins to tumour cells from patients with a range of different types of cancer. The experiment measured the response to these peptides, and found the cancers that were more "primed" exhibited a greater response to chemotherapeutic treatments (Chonghaile et al., 2011).

If it is possible to manipulate a cell's apoptotic threshold, priming could represent a strategy to improve current chemotherapy regimens, potentially leading to lower dosages and reducing side effects experienced by patients. There have been a large number of studies on natural and synthetic products which appear to have a chemosensitising effect, with some examples highlighted in Table 5. Yang et al. found that the plant polyphenol gossypol increased the sensitivity of colonic cancer cell lines to the anti-cancer drug 5-Fluorouracil (5-FU) through the downregulation of thymidylate synthase, cyclin D1 and the mTOR signalling pathways (Yang et al., 2015). Work from Sharma et al. demonstrated that treating head and neck cancer cell lines with the flavonol quercetin sensitised the cells to the induction of apoptosis by the anti-cancer drug cisplatin (Sharma et al., 2005). Other examples include curcumin (Kumar et al., 2016), the dietary triterpene lupeol (Liu et al., 2016) and even low doses of gamma-rays (Caney et al., 1999). The "sleep hormone" melatonin has been described to possess a priming effect, the mechanism for which lies within alterations to mitochondrial metabolism (Proietti et al., 2017). A final prominent example is cannabidiol (CBD), a non-psychoactive constituent of marijuana. Priming with CBD prior to treatment with cisplatin was found to enhance cell death compared to treatment with cisplatin alone. This priming effect was attributed to elevated ROS, Ca^{2+}, and changes in gene expression, including *VDAC*, *p53* and *Nrf2* (Henley, 2015). The table represents only a handful of examples; the area of research is rapidly expanding, as illustrated in Figure 10.

PRIMING /COMBINATION AGENT	DRUG	CANCER	MECHANISM	REFERENCE
Lupeol (Combination)	5-Fu	Gastric	Up regulation of Bax Up regulation of p53 Down regulation Bcl-2 Down regulation survivin	(Liu et al. 2016)
Cucurbitacin B (Primed)	Cisplatin	Ovarian	Gluthanione depletion Increase in ROS Decrease in Dyrk1B Decrease in pERK1/2 Decrease in pSTAT3	(El-Senduny et al. 2015)
Quercetin (Primed)	Cisplatin	Head and Neck	Decrease in Bcl-2, Bcl-XL Increase in ROS	(Sharma et al. 2005)
Gossypol (Combination)	5-Fu	Colon	Down regulation of thymidylate synthase Inhibition of mTOR signalling pathway Cyclin D1 inhibition	(Yang et al. 2015)
Triptolide (Combination)	Doxorubicin	Breast	Inhibits MDM2 expression	(Xiong et al. 2016)
Epigallocatechin-3-gallate (Combination)	Cisplatin	Lung	Inhibition of DNA Methyltransferase Methylation decreased/expression increased of GAS1, TIMP4, ICAM1, WISP2	(Zhang et al. 2015)
Saikosaponin-a and –d (Combination)	Cisplatin	Cervical	Induction of ROS Decrease in z-VAD Decrease in butylated hydroxyanisole Decrease N-acetyl-L-cysteine	(Wang et al. 2010)
Sildosin (α1A-adrenergic blocker) (Combination)	Gemcitabine	Prostate	ELK1 Inactivation	(Kawahara et al. 2016)
Unimolecular micelles (Combination)	Doxorubicin	Breast	Enhanced drug delivery	(Wang et al. 2016)
Reserveratrol (Combination)	2-DG	Neuroblastoma	Reduction of GRP78, GRP94 Decrease in AKT phosphorylation	(Graham et al., 2016)
Cannabidiol (Primed)	Cisplatin	Breast	Increased ROS Increased calcium levels Increased proton leak Increased VDAC1 expression	(Henley, 2016)

Table 5 |"Priming" in the Literature. Whilst not exhaustive, this table highlights the use of natural products as priming or combination treatments for different types of cancer.

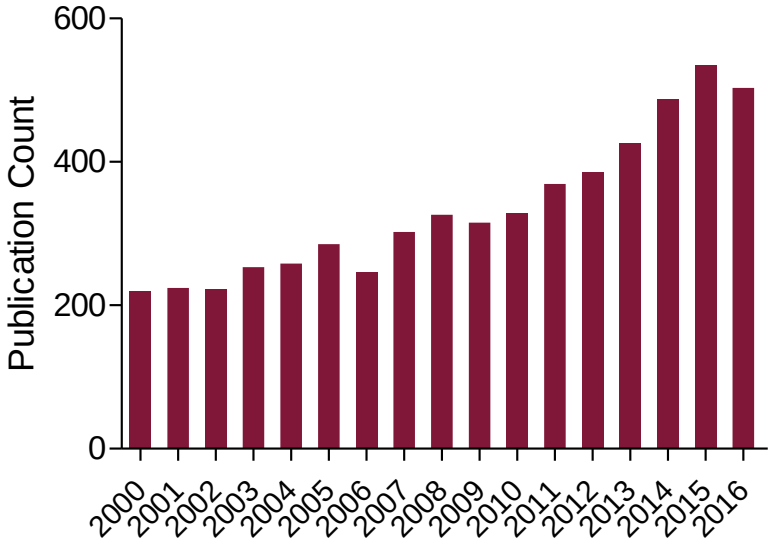

Figure 10 | Chemosensitisation on PubMed. Increase in the number of "chemosensitivity" publications from PubMed

1.8 | Short-Chain Fatty Acids as Potential Priming Agents

Bingham et al. in 2003 revisited the much-debated theory that the consumption of dietary fibre protects against the development of colorectal cancer (Burkitt, 1971; Shankar and Lanza, 1991; Trock et al., 1990). In a large scale observational study they confirmed that dietary fibre was inversely correlated to the incidence of colon cancer and concluded that in populations with a low intake of fibre, doubling the intake could reduce the risk of colorectal cancer by up to 40% (Bingham et al., 2003). Dietary fibre is indigestible to humans and is instead fermented in the digestive tract by the resident microbiota. The impact of the microbiota on human health is a rapidly growing field of research, and its influence has been observed in metabolism (Hansen et al., 2015; Mardinoglu et al., 2015) the immune response (Zhang et al., 2015), and behaviour (Desbonnet et al., 2014; Kelly et al., 2016). In the context of dietary fibre, the observed protective effect against cancer has been attributed to the production of a group of metabolic molecules called the short chain fatty acids (SCFAs) (Gill et al., 2018; Schug et al., 2016; Wong et al., 2006).

SCFAs are organic fatty acids with an aliphatic tail of 2-6 carbons, although typically refers to acetate (2 carbons, C2), propionate (C3) and butyrate (C4) (Figure 11). They are produced in in the lumen of the colon by the fermentation of indigestible fibre by the gut microbiota, in particular anaerobic bacteroides, bifidobacteria, eubacteria, streptococci, and lactobacilli (Layden et al., 2012), in an approximate ratio of 60:20:20 acetate: propionate: butyrate (Morrison and Preston, 2016). As a group, they are reported to be a source of energy in the colon, and to have regulatory roles in glucose, fatty acid, and cholesterol metabolism, appetite and immune regulation, and tumour prevention (den Besten et al., 2013).

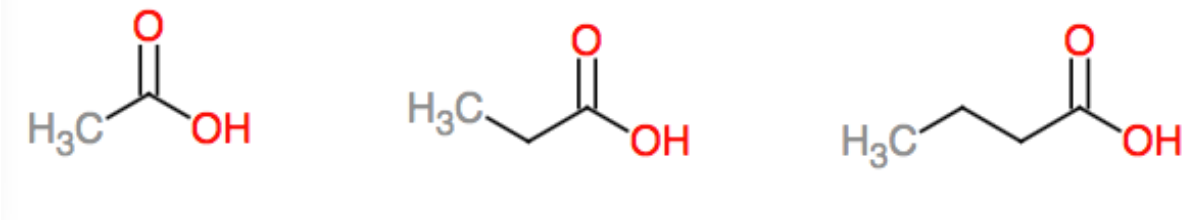

Figure 11 | Chemical Structures of the SCFAs: acetate (left), propionate (middle) and butyrate (right)

1.8.1 | Butyrate

Butyrate is the primary energy source for colonic epithelial cells and has roles in cell proliferation and differentiation (Perego et al., 2018). Primarily found in the colon, butyrate's well defined activity as a histone deacetylase (HDAC) inhibitor (Ho et al., 2017) has earned it special interest from researchers, being implicated in suppressing colonic inflammation (Zimmerman et al., 2012), the induction of apoptosis (Maruyama et al., 2012) and autophagy (Jintao Zhang et al., 2016) in cancer cells. Butyrate has also been shown to stimulate peptide-YY production in enteroendocrine cells, a hormone that is thought to regulate appetite, an effect again attributed to butyrate's HDAC inhibitory activity (Larraufie et al., 2018). Butyrate has also been implicated in regulation of the immune system (Corrêa-Oliveira et al., 2016) through the control of regulatory T cells (Smith et al., 2013) and macrophages (Chang et al., 2014).

1.8.2 | Propionate

Propionate is primarily absorbed by the liver, although its metabolic fate and function is not well understood and subject to conflicting reports in humans at present due to a lack of data from human studies. For example, propionate has been shown to be both an inhibitor of and a substrate for gluconeogenesis (Wong et al., 2006). However, like its counterparts acetate and butyrate, there is evidence that propionate has beneficial health effects. In particular, it has been shown that propionate can protect against obesity through stimulation of gut hormones (Lin et al., 2012), and that long term propionate delivery to the colon prevents increases in body weight and can decrease fat accretion (Chambers et al., 2015). Propionate has also been shown to reduce plasma cholesterol levels though the downregulation of several genes involved in cholesterol synthesis (Alvaro et al., 2008).

1.8.3 | Acetate

Acetate, as well as being the SCFA produced in the largest quantities, has the unique position as a progenitor in a large variety of metabolic pathways (Figure 11). The use of acetate in metabolism is almost universally conserved and can be traced back to the origins of life (Pandey et al., 2018). Prokaryotes, such as those belonging to proteobacteria and cyanobacteria, are known to assimilate acetate to replenish metabolites for the TCA cycle (Tang et al., 2011), while lower eukaryotes, such as slime moulds, incorporate acetate into lipid biosynthesis (Davidoff and Korn, 1963). In humans, whilst the majority of exogenous acetate is a by-product of fibre digestion by gut microbiota, it can also enter the body directly via the diet, and can be produced through the hydrolysis of acetyl-CoA and oxidation of alcohols in the liver, as well as the deacetylation of histones and hydrolysis of acetylated metabolites (Schug et al., 2016). The primary fate of acetate – its conversion into acetyl CoA – means acetate is incorporated into a broad range of metabolic pathways, which can be broadly categorised as energy production, the regulation of protein expression, and the biosynthesis of fatty acids

and sterols. These are described in greater depth in the Sections that follow and illustrated in Figure 12.

1.8.3.1 | Acetate Transport

The mechanisms by which acetate and the other SCFAs are taken up by cells, especially cancer cells, have yet to be fully resolved. In the acidic environment of the large intestine, acetic acid, a weak acid, is present predominately in the anionic form, acetate, to which the cell membrane is impermeable. Thus, the majority of exogenous acetate and other SCFAs must enter the cell through an active transport mechanism, of which 3 have been identified so far (Schug et al., 2016). In the first, acetate transport is bound to the export of bicarbonate ions in the colon. In the second, acetate (and the other SCFA) transport is mediated by sodium coupled monocarboxylate transporters (SMCTs), such as *SLC5A8* (Miyauchi et al., 2004). Finally in the third, the transport of SCFAs is coupled with H^+ through the monocarboxylate protein (Kirat and Kato, 2006).

1.8.3.2 | Acetate Metabolism

Inside the cell, the primary fate of acetate is the conversion to acetyl CoA, catalysed by 2 enzymes: the mitochondria-bound acetyl-CoA synthetase short-chain family member 1 (ACSS1) and the nuclear-cytosolic localized associate acetyl-CoA synthetase short-chain family member 2 (ACSS2) (Fujino et al., 2001; Luong et al., 2000). Acetyl CoA has a unique position as a “central” metabolite, siting at the centre of a number of anabolic pathways. In the mitochondria, acetyl CoA has roles in ketone body synthesis, protein acetylation, and is a source of carbon for the TCA cycle. In the cytosol, ACSS2-derived acetyl CoA is involved in fatty acid synthesis, protein acetylation, and steroid synthesis (Pietrocola et al., 2015). These pathways, particularly fatty acid synthesis, make acetyl CoA a compound of special interest in cancer metabolism owing to the increased demand of cellular components for rapid proliferation. This is highlighted by the

expression of *ACSS2* in many cancer cell lines (Comerford et al. 2014). The incorporation of acetate into the TCA cycle is also of importance to cancer cell metabolism; as the switch from OXPHOS to glycolysis consumes and depletes glucose from the tumour microenvironment, acetate-derived acetyl-CoA becomes an alternative choice to maintain energy homeostasis (Keenan and Chi, 2015).

1.8.3.3 | Acetate Signalling

On the surface of the cell, acetate and the other SCFAs act as ligands to a series of g-protein coupled protein receptors (GPCRs) known as the free fatty Acid receptors (FFARs), of which there are 4 known variants: FFAR1, FFAR2, FFAR3 and FFAR4, also known as GPR40, GPR43, GPR41, and GPR42 respectively (Schug et al., 2016). Of the 4, only FFAR2 and FFAR3 bind to and are activated by the SCFAs (Brown et al., 2003); FFAR1 and FFAR4 are known to bind medium to long-chain fatty acids (C6-C18) (Miyamoto et al., 2016). The affinity and expression of the two SCFA-binding receptors varies.

FFAR2 is expressed in enteroendocrine cells, and binds acetate and propionate > butyrate in order of affinity.

FFAR3 is expressed more broadly; in adipose tissue, in the intestine, and in the peripheral nervous system, and binds propionate > butyrate > acetate in order of affinity (Miyamoto et al., 2016).

Binding of acetate to FFAR2, as is the case in typical ligand-GPCR interactions, is known to cause an increase in intracellular Ca^{2+}. The physiological effects of such interactions are broad and tissue dependent, making FFAR2 a potential target in the therapy of a number of malignancies. In pancreatic β-cells, FFAR2 interactions have been shown to have a role in insulin production and interestingly, expression is altered in insulin resistance (Priyadarshini et al., 2015). In adipocytes, FFAR2 binding has been implicated in leptin production, which has roles in appetite regulation (Ichimura et al., 2009). Through their interactions with the FFAR family, the SCFAs have also been shown to influence immune cell

function, including the production of cytokines, the induction of chemotaxis and the differentiation of immune cells (Corrêa-Oliveira et al., 2016).

There have been relatively few studies on the role of the FFAR family in cancer. One study implicates FFAR2 in the carcinogenesis of gallbladder cancer (Hatanaka et al., 2010) whilst another showed that SCFA exert an antitumorigenic effect through FFAR2 interactions, which was found to be lost in colon cancer cell lines (Y. Tang et al., 2011). Such conflicting reports could indicate that the role FFARs play in cancer is largely tissue and expression-dependant.

1.8.3.4 | Acetate and Genetic Regulation

Acetate has been shown to modulate genetic expression through two mechanisms: increased acetylation of DNA and inhibition of histone deacetylation. The histones are proteins that act as spools for DNA strands, condensing and packaging DNA into tight structures called nucleosomes. This condensed state is associated with decreased gene expression, prohibiting the access of the genetic transcription machinery (Bannister and Kouzarides, 2011). Acetylation of histones, catalysed by histone acetyltransferases (HATs) relax the condensed structure, allowing for increased gene expression, whereas deacetylation, catalysed by histone deacetlyases (HDACs) performs the opposite action (Kuo and Allis, 1998). Acetyl CoA is utilized as a substrate for protein acetylation, and so through the increased levels of ACSS-derived acetyl CoA, acetate supplementation can affect the expression of many different genes (Soliman and Rosenberger, 2011). Furthermore, acetate supplementation has been shown to suppress HDAC expression directly, a role associated with its anti-proliferative effect in cancer (Brody et al., 2017).

1.8.3.5 | Acetate and its Role in Cancer

The evidence presented thus far suggests that acetate has opposing effects in cancerous cells. On one hand, acetate is a key substrate to support the

biosynthetic and energetic needs of a rapidly proliferating tumour, and on the other, demonstrates anti-tumorigenic properties through signalling or epigenetic pathways. Further to this, some studies also implicate acetate in directly inducing apoptosis in a number of cell types (Emenaker et al., 2001; Marques et al., 2013; Oliveira et al., 2015). These conflicting reports may be as a result of the many ways acetate can enter the cell and affect various signalling and metabolic pathways, demonstrating the complexity of the interactions between acetate and the cell.

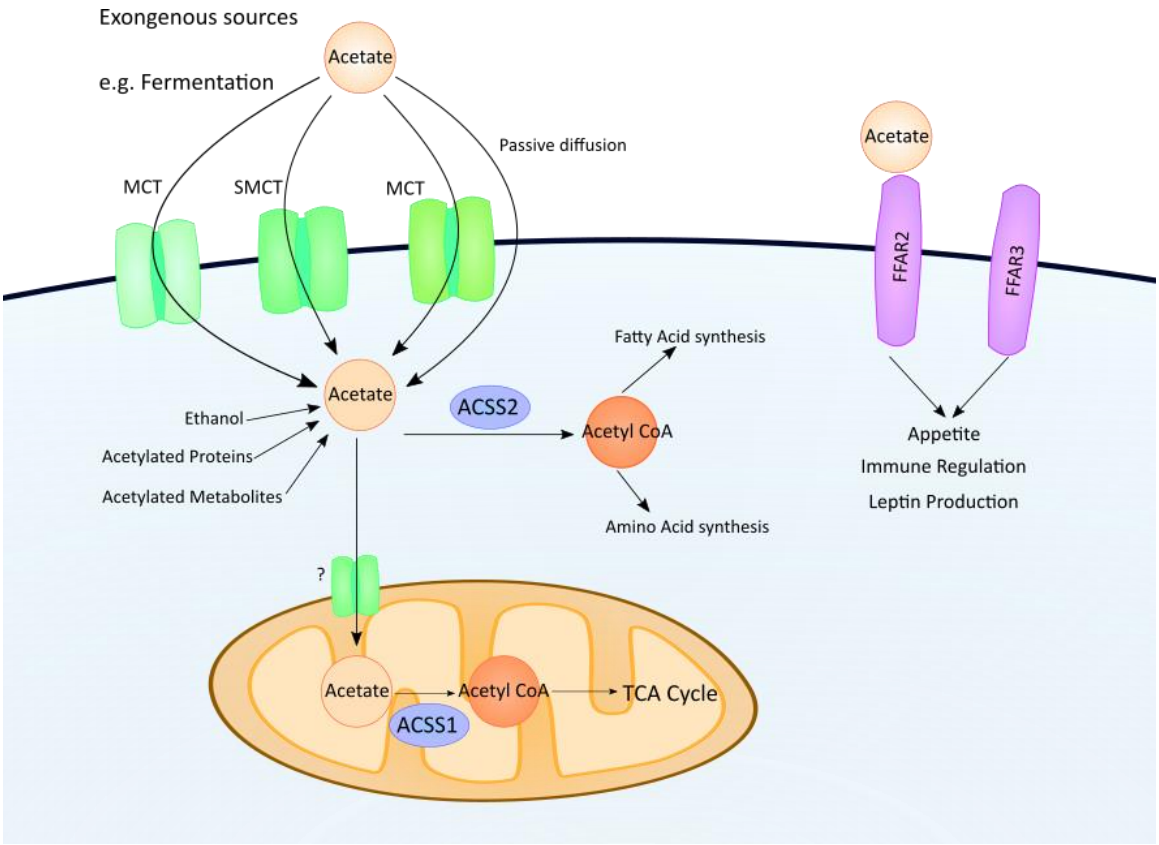

Figure 12| The Metabolic Fates of Acetate. Acetate can enter the cell via various active transporters, or through passive diffusion in acidic environments. Inside, cytosolic acetate is converted to acetyl CoA via ACSS2, which then feeds into a range of catabolic pathways. In the mitochondria, the conversion of acetate to acetyl CoA is catalysed by ACSS1, which then enters the tricarboxylic acid cycle. In addition, acetate can interact with FFAR2 or FFAR3 on the surface of the cell, trigging signals that modulate various metabolic pathways, such as appetite regulation, immune cell regulation, and the production of leptin.

1.9 | Aims

Whilst advances in the knowledge of cancer have led to improvements in the effectiveness of treatment; side effects and the risk of deadly recurrence still present significant problems for those diagnosed. However, recent renewed interest in the cell's mitochondria and how these organelles play a vital role in supporting cancer cell metabolism may provide an opportunity to exploit these organelles to further refine the effectiveness of treatment. Stressing the mitochondria may provide a mechanism to improve a cancer cell's proximity to drug-induced apoptosis – to prime cancer cells for death. Although numerous methods exist to stress cells, the difficulty in finding a suitable agent parallels the challenges in cancer chemotherapy – targeting cancer cells whilst avoiding or limiting cytotoxicity to healthy cells.

With the recent interest in the SCFAs, I have identified a potential priming agent in acetate, the shortest of the SCFAs. As a group, the SCFAs, natural by-products of diet, have been documented to have roles in prevention of colorectal cancer, and preliminary work by my group, has shown that acetate exhibits anti-proliferative effects on cancer cells *in vitro*, whilst having no significant effect on non-cancerous cell lines (Henley, 2015; Sahuri Arisoylu and Bell, 2016). To take these findings forward, the aim of this project was to investigate the potential of acetate as a priming agent. To address this aim, the project attempted to answer 2 broad questions:

1.) How does acetate affect cells?
2.) Can acetate prime cancer cells for death?

As described, acetate has wide-ranging effects on cells. This study was designed to clarify the effects acetate has on cancer cells, with a particular focus on mitochondrial metabolism, as not only are the mitochondria central to chemotherapy-induced apoptosis, but the documented effects of SCFAs on mitochondria are relatively sparse. To this end I measured several key markers of mitochondrial stress, including ROS, Ca^{2+}, morphology, and respiration, and investigated the effect of acetate on overall cell viability and induction of apoptosis. Following this, I investigated the effect that priming – the treatment of cells with

acetate prior to treatment with an anticancer drug – has on apoptosis and cell viability compared to simultaneous treatment with the drug and acetate, and to drug treatment alone.

To answer the questions set out I have selected 2 cancer lines: HCT116 (human colon cancer) and MCF7 (human breast cancer), and a non-cancerous cell line MCF10A (“healthy” breast tissue), as controlled, replicable models to identify the effects of acetate. The selection of cancer cell lines allows me to study the effects of acetate in both tissues that model areas close to and away from the site of acetate production (colon and breast respectively). In addition, MCF7 was used in previous work which examined mitochondrial priming with cannabidiol (CBD) prior to treatment with cisplatin, which has provided a starting point in designing the protocols used for this project (Henley, 2015). Finally, MCF10A, the non-cancerous cell line, was used to ensure that any priming effects caused by acetate are confined to cancer lines.

1.10 | Hypothesis

Priming with acetate enhances cisplatin-induced cell death in cancer cells.

2.0 | Materials & Methods

2.1 | Cell Lines

2.1.1 | HCT116

HCT116 is an adherent, human epithelial cancer cell line derived from colorectal carcinoma (Brattain et al., 1981). HCT116 cells were cultured in Roswell Park Memorial Institute medium (RPMI-1640) (Thermoscientific, UK), supplemented with 10% fetal bovine serum (FBS) (Sigma, UK), 1% l-glutamine (Thermoscientific, UK) and 1% penicillin/streptomycin (Thermoscientific, UK). HCT116 cells were a gift from Dr N. Navaratnam (Medical Research Council, Clinical Sciences Centre).

2.1.2 | MCF7

MCF7 is an adherent, human epithelial cancer cell line derived from a metastatic mammary adenocarcinoma (Soule et al., 1973). MCF7 cells were cultured in Minimum Essential Media (MEM) (Sigma, UK), supplemented with 10% FBS, 1% l-glutamine and 1% penicillin/streptomycin. MCF7 cells were a gift from Dr. N. Haiji (Imperial College London).

2.1.3 | MCF10A

MCF10A is an adherent, human epithelial non-cancerous breast cell line derived from fibrocystic mammary tissue. Non-cancerous, MCF10A was found to exhibit spontaneous immortality after culture in low-calcium media (Soule et al., 1990). MCF10A cells were cultured in a mixture of Dulbecco's Modified Eagle's Media and Ham's F12 nutrient mix (DMEM:F12) (Life Sciences, UK), supplemented with 5% horse serum (Sigma, UK), 1% penicillin/streptomycin, 20 ng/mL epidermal growth factor (Sigma, UK), 0.5 mg/mL hydrocortisone (Sigma,

UK), 100 ng/mL cholera toxin (Sigma, UK) and 10 µg/mL insulin (Sigma, UK). MCF10A cells were a gift from Dr. N. Haiji (Imperial College London).

2.2 | Cell Culture

All work with cell lines was carried out in a laminar flow hood with aseptic technique. Cells were grown in sterile T75 or T175 flasks, stored in a humidified 37°C 5% CO_2 incubator, and passaged at around 80% confluency, based on visual inspection. For passage, media was removed from cells, and washed with sterile phosphate-buffered saline (PBS). Cells were then detached from the surface of the flask by incubating with 1-2 mL TrypLE (ThermoFisher, UK) or trypsin (Sigma, UK) for MCF10A cells for 7 mins. Following detachment, cells were resuspended in fresh media and diluted into new flasks. Cells were only used for experimentation between passage 5 and 25, and periodically tested for mycoplasma infection using the PlasmoTest Mycoplasma Detection Kit (InvivoGen, UK). For seeding cells for experimentation, cells were detached as described above, counted using a haemocytometer, and added to wells with the appropriate volume of media for the plate being used (100 µL total for 96 well plates and initial SeaHorse 24 well plate seeding, 2000 µL for 6 well plates).

2.3 | Reagents

Sodium acetate (Sigma, UK) was dissolved in autoclaved deionized (DI) water to make stock concentrations of 1 M and 100 mM. Acetate was diluted to working concentrations on the day of the experiment in fresh media. DDP (Cisplatin) (Sigma, UK) was dissolved in dimethylformamide (DMF) (Sigma, UK) to a stock concentration of 10 mM. DDP was diluted for experimentation on the day of the experiment in fresh media.

2.4 | Cell Viability

Cell viability was assessed using the 3-(4,5-dimethylthiazol-2-yl)-2,5-diphenyltetrazolium bromide (MTT) assay kit (Sigma, UK). The assay is based on the conversion of MTT (yellow) to formazan (purple) by NADPH-dependent reductases in the cell (Mosmann, 1983). Cells were seeded onto 96 well plates at $3x10^4$ cells per well. The assay was performed as per manufacturer's recommendations. Following treatment, cells were washed with PBS and media was replaced with phenol red-free media. 10 µL MTT solution was then added to each well, and incubated at 37°C 5% CO_2 for 3 hours. Media was removed, and resultant crystals dissolved in 100 µL MTT solvent. Plates were shaken for 5 mins. Viability was then quantified by UV-Vis spectrometry with a microplate reader (SPECTROstar Nano, BMG Labtech, Germany). Absorbance at 690 nm was subtracted from absorbance at 570 nm. Cell viability presented as percentage of the untreated negative control.

2.5 | Bradford Protein Assay

The Bradford Assay, a simple colorimetric assay for total protein quantification, was used to quantify cell number following treatment.

Following completion of the assay, each well was washed twice with ice cold PBS. Cells were then lysed with ice cold radioimmunoprecipitation assay (RIPA) buffer (Sigma, UK) for 15 minutes on a shaker. Each well was then scraped using sterile cell scrapers, and its contents transferred to individual Eppendorf tubes, which were cooled on ice. Tubes were then centrifuged at 16,100 g for 15 mins at 4°C. The supernatant was removed and placed into a new set of tubes. 5 µL of each sample was added to the wells of a 96-well plate in triplicate. 200 µl Bradford Reagent (BioRad, UK) was then added to each well, and absorbance at 595 nm was quantified with a plate reader. A series of protein standards (Bovine serum albumin (BSA), BioRad, UK) was used to create a standard curve to allow quantification of the unknown samples via linear regression.

2.6 | Detection and Quantification of Apoptosis in Response to Acetate Treatment

The induction of apoptosis was measured using the Annexin V-FITC/propidium iodide (PI) staining kit (Abcam, US) via flow cytometry. The assay is based on the translocation of the phospholipid phosphatidylserine (PS) from the inner to outer surface of the cellular membrane during apoptosis. Annexin V, a protein with high affinity for PS, allows for detection of this event when conjugated to a fluorophore, in this case fluorescein isothiocyanate (FITC). PI is a membrane impermeable stain which fluoresces when bound to DNA, allowing for the distinction between late and early apoptosis, as well as necrotic events (Schutte et al., 1998). Each cell line was seeded on 6 well plates at densities of $1.5x10^5$ cells per well and treated with media or 10 mM acetate for 24 hours. The assay was performed as per manufacturer's instructions. Following treatment, cells were washed once with PBS, detached with 200 µL TrypLE, resuspended in 800 µL fresh media, and centrifuged at 1000 g for 5 mins. The resultant pellet was then resuspended in 500 µL supplied binding buffer. Cells were then stained with 5 µL Annexin-FITC and/or 5 µL PI for 5 minutes before analysis with flow cytometry (Cyan ADP, DaktoCytomation).

Cells were gated on software (Summit 4.3, DaktoCytomation) to manually exclude cellular debris using a plot of forward scatter (FSC) vs side Scatter (SSC). Fluorescence of an unstained control was used to set voltage and gain of fluorescence channel 1 (FL1, green, for Annexin V-FITC) and fluorescence channel 2 (FL2, red, for PI) so the background signal was within the 1^{st} log decade. To correct the spectral overlap of the emission spectra of the 2 fluorophores, single stained controls were set up to allow for manual compensation. Stains were considered correctly compensated when the median fluorescent intensity (MFI) in each quadrant for missing stain was equal to or within 1. The percentage of events in the 4 quadrants (see Table 4) of the FITC log vs PI log dot plot was recorded.

ANNEXIN V-FITC	PI	QUADRANT	CLASSIFICATION
-	-	1 (Lower left)	Healthy
+	**-**	**2 (Lower Right)**	**Early Apoptotic**
+	**+**	**3 (Upper Right)**	**Late Apoptotic**
-	+	4 (Upper left)	Necrotic

Table 6|Interpretation of Annexin V-FITC Assay Data. Classification of flow cytometry events based on the combination of signal intensities, interpreted by their location on the dot plot produced. The percentage of events in quadrants 2 and 3 (in bold) were combined to produce total apoptotic events.

2.7 | Detection and Quantification of Autophagy

Autophagy was detected using the Autophagy Detection Kit from Abcam (ab139484, Abcam, UK). The kit utilizes a propriety fluorescent probe to stain autophagic lysosomes and vacuoles. Cells were seeded on 6 well plates at densities of $1.5x10^5$ cells per well. Following treatment, cells were washed with PBS and harvested with TrypLE. After being quenched with media, cells were centrifuged at 1000 g for 5 mins. The resulting pellets were resuspended in 250 µL phenol-red free media, to which 250 µL green detection regent was added. Samples were incubated for 30 mins at 37°C 5% CO_2. Following incubation, cells were centrifuged at 1000 g for 5 mins. Pellets were then resuspended in 1X supplied Assay buffer, and analysed via flow cytometry. Cells were gated manually on software (Summit 4.3) to exclude debris or cellular aggregates using a plot of FSC vs SSC. Data was collected in FL1 and the MFI recorded.

2.8 | SeaHorse MitoStress Assay

Changes in mitochondrial respiration were monitored using the SeaHorse XF_e24 Flux Analyser (Agilent, USA) to carry out the SeaHorse MitoStress Assay according to manufacturer specifications. $3.0x10^4$ cells per well were seeded on supplied SeaHorse 24 well plates. Cells were initially seeded in 100 µL media, to followed by a further 150 µL media was added once the cells had adhered (3-4 hours, based on visual inspection). Cells were then treated with 10 mM acetate or media for 24 hours (working volume of 500 µL per well). Supplied SeaHorse Media (Aglient, USA) was supplemented with glucose and sodium pyruvate to final concentrations of 1 g/L and 1 mM respectively, adjusted to pH 7.4 and filter sterilised before use. Following treatment, cells were washed twice with SeaHorse media and incubated for 1 hour at 37°C with no CO_2.

The assay itself consists of the measurement of the oxygen consumption rate (OCR) in real time prior to and after the injection of 3 known mitochondria-affecting drugs to obtain the parameters described in Table 7:

1.) **Oligomycin** (Sigma, UK), an ATP Synthase inhibitor which allows quantification of OCR dedicated to ATP production.
2.) **Carbonyl cyanide-p-trifluoromethoxyphenylhydrazone (FCCP)** (Sigma, UK), an uncoupling agent which allows measurements of a cell's maximum respiration rate.
3.) **Antimycin A** (Sigma, UK) and **rotenone** (Sigma, UK), Complex I and II inhibitors which allow the determination of the basal rate of respiration. The combination of drugs also allows the calculation of the OCR associated with proton leak, non-mitochondrial respiration, and spare respiratory capacity (Table 7).

Drug concentrations were optimised individually for each cell line to ensure oligomycin and FCCP injections were causing the maximum decrease and increase in OCR. The data was acquired in cycles as follows: Mix: 3 mins, Wait: 2 mins, Measure: 3 mins, as per the manufacturer's instructions. Three Mix/Wait/Measure cycles were performed at the start of the assay, and after each injection. A typical MitoStress assay output is shown in Figure 13.

PARAMETER	RATE MEASUREMENT EQUATION
Non-Mitochondrial Respiration	Minimum rate measurement after Rotenone/antimycin injection
Basal Respiration	(Last rate measurement before injection of oligomycin)-(Non-Mitochondrial respiration rate)
Maximal Respiration	(Maximum rate measurement after FCCP injection)-(Non-mitochondrial respiration)
Proton Leak	(Minimum rate measurement after oligomycin injection) - (Non-mitochondrial respiration)
ATP Production	(Last rate measurement before injection of oligomycin)-(Minimum rate measurement after oligomycin injection)
Spare Respiratory Capacity	(Maximal Respiration)-(Basal respiration)

Table 7 | Interpretation of SeaHorse MitoStress Assay Data. Description of mitochondrial respiration parameter calculations, as performed by the MitoStress Test Report Generator.

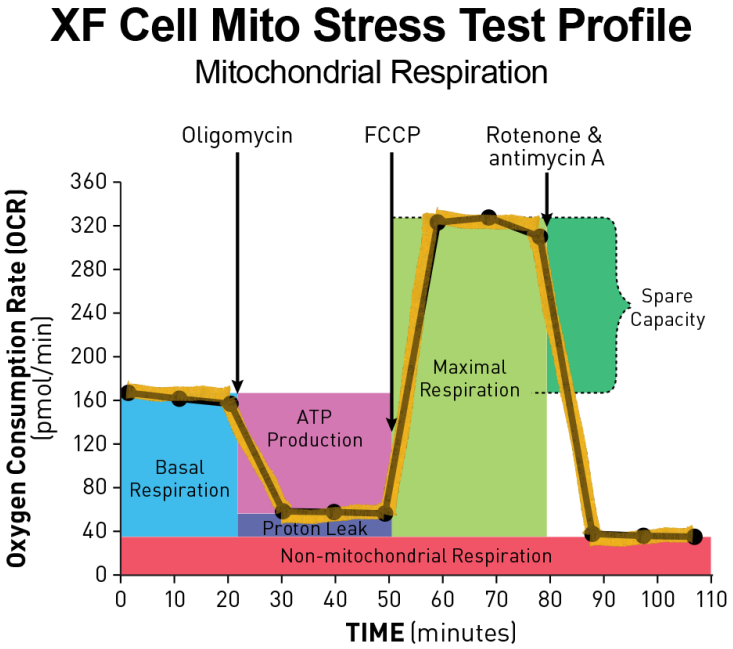

Figure 13 | The SeaHorse MitoStress Assay. Schematic showing a typical SeaHorse MitoStress Assay profile, and how the OCR levels can be interpreted in response to the injection of Oligomycin, FCCP, and Rotenone & antimycin A. Image from Agilent

2.9 | Detection & Quantification of Cellular ROS.

The 2',7'–dichlorofluorescin diacetate (DCFDA) assay was used to detect changes in the levels of ROS. The presence of ROS in the cell converts DCFDA into the highly fluorescent compound 2',7'–dichlorofluorescin (DCF) (Keston and Brandt, 1965; LeBel et al., 1992). Cells were seeded on black-walled 96 well plates at $2.5x10^4$ cells per well. Following treatment, cells were washed with PBS and incubated with 20 µM DCFDA (Sigma, UK) at 37°C 5% CO_2 in the dark for 45 mins. The contents of the well were aspirated from the cells, and replaced with 100 µL PBS per well. Fluorescence induced by ROS was quantified by fluorescence spectroscopy (Excitation 485 nm, Emission 535 nm) (FLUOstar Optima, BMG Labtech, Germany).

2.10 | Detection and Quantification of Intracellular Ca^{2+}

The Fluo-4 Direct Calcium Assay (Invitrogen, UK) was used to detect changes in total intracellular Ca^{2+} levels (Gee et al., 2000). Cells were seeded on black-walled 96 well plates at $2.5x10^4$ cells per well. The assay was performed according to manufacturer's specifications (Invitrogen, 2011). Following treatment, 100 µL 2X Fluo-4 Direct calcium assay reagent was added to each well. Cells were then incubated for 30 mins at 37°C 5% CO_2 in the dark. Changes in Ca^{2+} were then quantified by fluorescence spectroscopy (Excitation 494 nm, Emission 516 nm) (FLUOstar Optima, BMG Labtech, Germany).

2.11 | Observation & Quantification of Mitochondrial Morphology.

2.11.1 | Observation of Mitochondrial Morphology by Confocal Microscopy

The MitoTracker Deep Red stain was used to observe and quantity changes in mitochondrial morphology. Cells were seeded on 6 well plates at $1.5x10^5$ cells per well. Following treatment, cells were washed once with PBS and stained with 100 nM MitoTracker Deep Red (Thermofisher, UK) for 30 mins at 37°C 5% CO_2 in phenol red-free media. The Lecia SP2 (Leica Microsystems, Germany) was used to obtain images, using a HCZ APO L 63X 0.90 NA objective lens. After gain and offset adjustments, cells were observed with a 2X digital zoom at 2048x2048 formats, 8X line averaging. Three images in different regions of the well were collected per treatment condition.

2.11.2 | Analysis of MitoTracker Deep Red Images

The Yeast_Mitomap/MitoLOC plugin for FIJI (Fiji Is just ImageJ, version 1.6) was used to analyse mitochondrial images from confocal microscopy (available from http://www.gurdon.cam.ac.uk/stafflinks/downloadspublic/imaging-plugins). The plugin defines mitochondria in a region of interest manually drawn by the user (Figure 14) and calculates the number of mitochondria, volume, area and six shape descriptors including; “compactness”, “distribution isotropy”, “isoperimetric quotient”, and “sphericity”, as calculated by Vowinckel et al. (Vowinckel et al., 2015). To select cells for analysis, viable cells visible in each image were assigned a number. Three numbers in the range were selected at random using the Microsoft Excel formula =RANDBETWEEN(1,x), where x is the total number of mitochondria in the image. The average measurements of all mitochondria in each analysed cell were recorded.

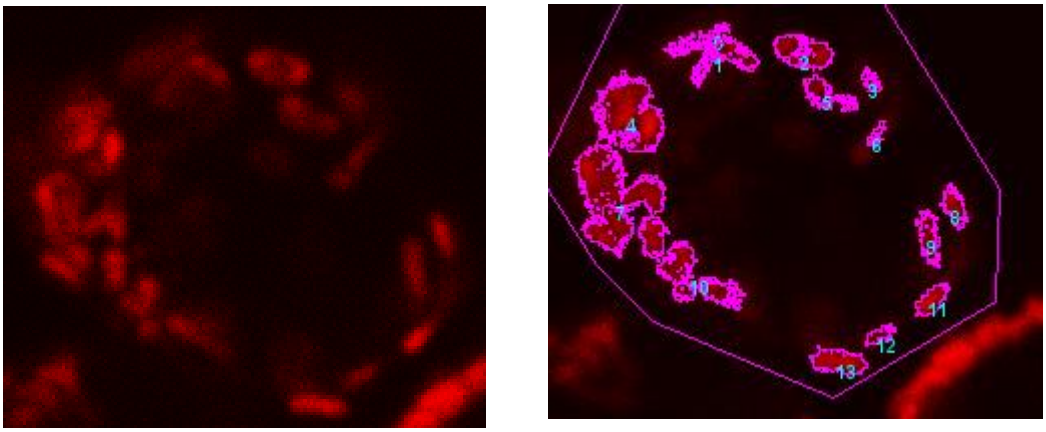

Figure 14 | **The MitoLOC Plugin for ImageJ.** Example images illustrating how the Yeast_Mitomap/MitoLOC FIJI plugin can be used analyse mitochondrial morphology. The left image is a typical image acquired following MitoTracker treatment. On the right, a region of interest is drawn around the cell (purple line). MitoLOC then counts and measures the mitochondria, indicated by the pink outlines with numbering

2.11.3 | Flow Cytometric Quantification of Mitochondrial Morphology

As an alternative method to quantify mitochondrial morphology, MitoTracker Deep Red stained cells were analysed by flow cytometry. This approach was used by Tailor et al. to investigate the effects of butyrate on mitochondrial mass (Tailor et al., 2014), based on protocols developed by Tal et al. (Tal et al., 2009). Cells were grown in 6 well plates and treated with media or 10 mM acetate for 24 hours. On the day of the assay, cells were washed once with PBS and stained with 100 nM MitoTracker Deep Red for 30 mins at 37°C 5% CO_2. Cells were then washed with PBS, detached and harvested, before being resuspended in 500 μL PBS. Cells were then analysed by flow cytometry (Cyan ADP, Beckman Coulter, USA), measuring signal intensity in FL2 (MitoTracker Deep Red).

2.12 | Cell Cycle Analysis

Changes in cell cycle stage were measured with PI staining and flow cytometry (Krishan, 1975). Cells were seeded on 6 well plates at $2.0x10^5$ cells per well. Following treatment, cells were washed with PBS and detached with TrypLE. Cells were then harvested, centrifuged at 1000 g for 5 min, washed with PBS, and

centrifuged again at 1000 g for 5 mins. Pellets were then resuspended in 300 µL ice cold PBS, followed by the drop-wise addition of 700 µL ice cold 100% ethanol. Samples were incubated at -20°C for at least 2 hours. Following incubation, samples were centrifuged at 2000 g for 5 mins, and resuspended in 500 µL fluorescence-activated cell sorting (FACS) buffer. Cells were pelleted once more, and to each pellet, 50 µL 100 µg/mL RNAase was added, followed by 450 µL of 50 µg/mL PI solution. Samples were incubated in the dark for 15 mins at room temperature. Following this incubation, cell cycle stage was observed by flow cytometry measuring signal intensity in FL2. Debris and cellular aggregates were manually excluded using plots of FSC vs SSC. Doublets (single events that actually consist of 2 particles) in cell cycle analysis can produce false positives and so were manually excluded using a plot of FSC-A vs pulse width.

2.13 | Quantitative Real-Time Polymerase Chain Reaction Analysis

For gene expression quantification, quantitative real time-polymerase chain reaction (qRT-PCR) was carried out. Cells were seeded in individual T75 flasks at densities of $5x10^6$ cells per flask. Following treatment, messenger ribonucleic acid ((RNA)(mRNA)) was isolated from the treated cells using the Qiagen RNeasy kit (Qiagen, UK). The kit was used as instructed and the samples were quantitated to 1 µg/µL using the NanoDrop 1000 (ThermoScientific, UK) to normalise RNA amount. Complementary deoxyribonucleic acid (cDNA) synthesis was carried out according to the Thermoscript™ RT-PCR Systems protocol (Invitrogen, UK) using the oligo(dT)20 primer method with an incubation at 50°C for 60 minutes. The reaction was terminated by incubating at 85 °C for 5 minutes. qPCR was carried out in accordance to TaqMan® Universal Master Mix II, no UNG (uracil-DNA glycosylases) for primers in Table 8. The 96 well plate was placed in a preheated Applied Biosystems 7500 Fast Real-Time PCR System instrument and run at a cycling program of 50°C for 2 minutes, 95°C for 2 minutes, 45 cycles of 95°C for 15 seconds followed by 56°C for 30 seconds, then a dissociation confirmation step. Any samples that read < 0.1 cycle threshold (Ct) were removed for quality control purposes. Results were calculated using the ΔΔCt method as described by

Bookout et al. (Bookout et al., 2006). Samples were normalised to the constitutively expressed β-actin.

GENE	ASSAY ID
Voltage Dependent Anion Channel 1 *(VDAC1)*	Hs01631624_gH
P53	Hs01034249_m1
Nrf2	Hs00232352_m1
Acetyl-coenzyme A synthetase short-chain 1 *(ACSS1)*	Hs00287264_m1
Acetyl-coenzyme A synthetase short-chain 2 (*ACSS2)*	Hs00218766_m1
β-Actin	Hs01060665_g1

Table 8 | Taqman Probes Used In Gene Expression Analysis.

2.14 | SeaHorse GlycoStress Test

The short term effects of acetate on glycolysis were measured using the SeaHorse GlycoStress Test (Aglient, UK) on the SeaHorse XF_e24 Flux Analyser (Agilent, USA). Cells were initially seeded in 100 µL media at densities of $3.0x10^4$ cells per well, to which a further 150 µL media was added once the cells had adhered (3-4 hours, based on visual inspection). Supplied SeaHorse Base Media (Aglient, USA) was supplemented with 1% l-glutamine, adjusted to pH 7.4 and filter sterilised before use. Following treatment, cells were washed twice with SeaHorse media and incubated for 1 hour at 37°C with no CO_2. The assay itself consists of the measurement of the extracellular acidification rate (ECAR) in real time prior to and after the injection of 3 known metabolic drugs to obtain the parameters described in Table 9 (See Figure 15);

1.) **Glucose** (Sigma, UK), triggering a glycolytic response as cells utilize the injected glucose (Final concentration: 10 mM)
2.) **Oligomycin** (Sigma, UK), an ATP Synthase inhibitor, inhibiting oxidative phosphorylation, shifting the cell's energy production to glycolysis and revealing the cells maximum glycolytic capacity. (Final concentrations: 2 µg/mL in MCF10A, 1 µg/mL in HCT116 and MCF7)
3.) **2-deoxy-glucose** (2-DG) (Sigma, UK), which inhibits glycolysis through competitive binding to glucose hexokinase, the first enzyme in the glycolytic pathway (Final concentration: 50 mM).

Seeding densities and drug concentrations were optimised individually for each cell line. The data was acquired in cycles as follows: Mix: 3 mins, Wait: 2 mins, Measure: 3 mins, as per the manufacturer's instructions. 3 Mix/Wait/Measure cycles were performed at the start of the assay, and after each injection. To measure the short-term effects of acetate, either media or acetate was injected to a final concentration of 10 mM prior to glucose in the glycostress test.

PARAMETER	RATE MEASUREMENT EQUATION
Glycolysis	(Maximum rate measurement before oligomycin injection)-(Last reate measurement before glucose injection)
Glycolytic Capacity	(Maximum rate measurement after oligomycin injection)-(Last rate measurement before glucose injection).
Glycolytic Reserve	(Glycolytic Capacity)-(Glycolysis)
Non-Glycolytic Acidifcation	Last rate measurement prior to glucose injection

Table 9 | Interpretation of SeaHorse GlycoStress Assay Data. Description of glycolytic parameter calculations, as performed by the GlyoStress Test Report Generator.

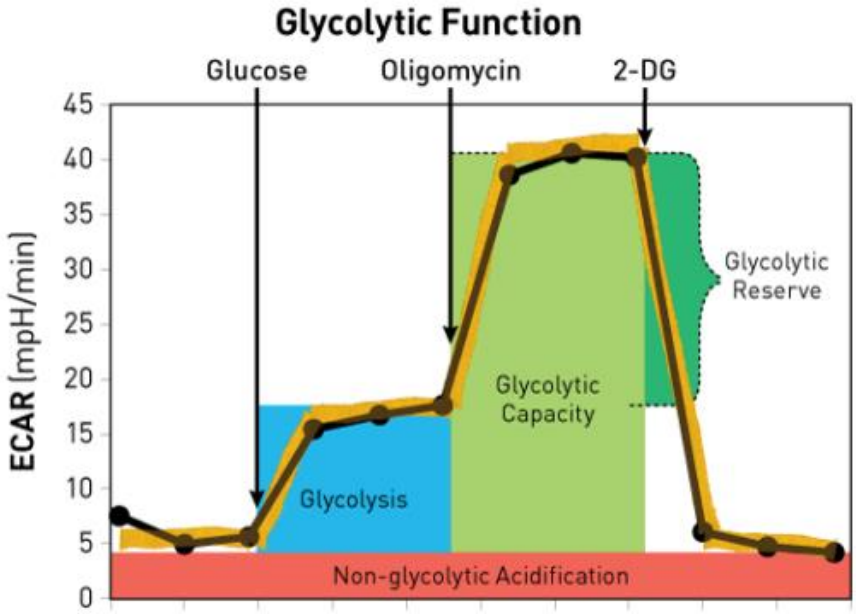

Figure 15 | **The SeaHorse GlycoStress Assay**. Schematic showing a typical SeaHorse GlycoStress Assay profile, and how the ECAR levels can be interpreted in response to the injection of glucose, oligomycin, and 2-DG. Image from Agilent

2.15 | Acute OXPHOS Measurements

The short term effects of acetate on OXPHOS were measured using the SeaHorse XF_e24 Flux Analyser (Agilent, USA). Cells were initially seeded in 100 µL media at densities of $3.0x10^4$ cells per well, to which a further 150 µL media was added once the cells had adhered (3-4 hours, based on visual inspection). Supplied SeaHorse Media (Aglient, USA) was supplemented with glucose and sodium pyruvate to final concentrations of 1 g/L and 1 mM respectively, adjusted to pH 7.4 and filter sterilised before use. Following treatment, cells were washed twice with SeaHorse media and incubated for 1 hour at 37°C with no CO_2. OCR was then measured over the course of 12 hours. To investigate the effect of acetate, acetate (to a final concentration of 10 mM) or media (as a control) was injected following a basal measurement period of 16 minutes.

2.16 | Acute Intracellular Ca^{2+} Measurements

The short term effects of acetate on intracellular Ca^{2+} levels were measured with the Fluo4 Direct Calcium Probe (Invitrogen, UK, see section 2.9) using the BMG NOVOstar fluorescence plate reader (BMG Labtech, Germany). HCT116 ($2.5x10^4$ cells per well), MCF7 and MCF10A ($3.0x10^4$ cells per well) cells were seeded on 96 well black plates and allowed to adhere overnight. Media was then removed from cells, and replaced with 50 µL Opti-MEM reduced serum media (ThermoFisher, UK) (Based on work by Miletta et al. observing the effects of butyrate on intracellular Ca^{2+} (Miletta et al., 2014)) and incubated for 1 hour at 37°C 5% CO_2. Following incubation, 50 µL 2X Fluo-4 Direct calcium assay reagent was added to each well, and incubated in the dark for 30 minutes at 37°C 5% CO_2. Changes in Ca^{2+} were then quantified by fluorescence spectroscopy (Excitation 494 nm, Emission 516 nm). Baseline fluorescence was measured for 8 seconds at 1.46 second intervals. At 15 seconds, 11 µL PBS (control) or 100 mM acetate (final concentration: 10 mM) was injected into relevant wells, and fluorescence recorded for a further 42.6 seconds at 1.46 second intervals.

2.17 | Priming Treatment Protocols

For “priming” treatments, cells were treated for 24 hours with 1, 5 or 10 mM acetate, followed by 24 hour treatment with 100 µM DDP after washing with PBS. In DDP only treatments, cells were treated with fresh media for 24 hours, followed by 24 hour treatment with 100 µM DDP. In “Combination” treatments, cells were treated with fresh media for 24 hours, followed by 24 hour treatment with 10 mM acetate and 100 µM DDP administered simultaneously (See Table 10). Vehicle consisted of a 1% v/v solution of DMF in complete media.

	UNTREATED CONTROL	DDP ONLY	ACETATE PRIMED	COMBINATION
DAY 1	Media/Vehicle	Media/Vehicle	1,5 or 10 mM Acetate	Media/Vehicle
DAY 2	Media/Vehicle	100 µM DDP	100 µM DDP	10 mM Acetate + 100 µM DDP

Table 10 | **Treatment protocols for priming experiments.**

2.18 | Cell Viability in Response to Priming

The MTT Assay (See Section 2.4) was used to measure cell viability in response to priming treatments. Cells were seeded at $3.0x10^4$ cells per well on 96 well plates and treated as per Section 2.17. The MTT assay was then performed as per Section 2.4.

2.19 | Induction of Apoptosis in Response to Priming

The Annexin V-FITC PI assay (See Section 2.6) was used to measure apoptosis induction in response to priming treatments. Cells were seeded at $1.5x10^5$ cells on 6 well plates and treated as per Section 2.17. The Annexin V-FITC PI assay was then performed as per Section 2.6.

2.20 | 2-Photon Fluorescence Lifetime Imaging Microscopy

2-Photon Fluorescence Lifetime Imaging Microscopy (2P-FLIM) was used to image and quantify NADH lifetime decay as a measure of cellular and mitochondrial metabolism. This work was carried out in collaboration with Professor Stan Botchway at the Rutherford Appleton Laboratory, Harwell. The background and merits of this technique are described in detail in Section 5. MCF7 cells were seeded in individual ibidi dishes at densities of 1.2-1.5x10^5 cells per dish. Cells were treated with DMSO, 10 mM acetate, or 25 mM acetate for 24 hours. Before imaging, cells were allowed 15 mins to acclimatise to room temp.

FLIM images were obtained as follows: 2 photon (690 nm) wavelength light was generated by a mode-locked titanium sapphire laser (Coherent Laser Co), producing 180 fs pulses at 75 MHz. This laser was pumped by a solid state continuous wave 532 nm laser. Images were collected through a water immersion 60 X 1.2 numerical aperture objective on a modified Nikon TE2000-U confocal microscope. Emission was collected with an external fast microchannel plate PMT (R3809-U, Hamamastu, Japan), linked to a time correlated single photon counting (TCSPC) module (SPC830, Becker and Hickl, Germany). Lifetime calculations and image analysis were performed on SPCimage analysis software (Becker and Hickl, Germany).

2.21 | Statistical Analysis

All statistical analyses were performed on GraphPad Prism 5.04 (San Diego, USA). Differences between 2 means were analysed by Student's Unpaired T Test. Means were considered significantly different when p <0.05. Differences between groups (>2) of means were analysed by One-Way ANOVA, followed by Tukey's Multiple Comparison Test to investigate specific pair-wise differences. Differences between all means in an experiment were considered significantly different when p <0.05. Differences between individual means in an experiment were considered significantly different when adjusted p <0.05. Calculations of concentration in samples were interpolated from a standard curve using a linear regression.

3.0 | The Effects of Acetate on Cells

The objective of this chapter was to determine the effect, if any, acetate had on the selected cell lines. In Section 1.8.3 it was noted that whilst the effects of the SCFAs as a group on cells being broadly documented, the effects of acetate alone remains relatively unstudied, particularly with regard to its effect on the cell's mitochondria. Furthermore, published studies on acetate and mitochondria usually pertain to acetate as a product of cellular catabolism, rather than exogenous sources of acetate, e.g. following the consumption of dietary fibre.

The effect of SCFAs as a group on apoptosis has been previously investigated, but with the majority of the work focused on either combinations of SCFAs, or on butyrate alone. Jan et al. reported that "propionibacterial SCFA" induces apoptosis in HT29 and CaCo2 cell lines, although the work did not report the effects of acetate alone, as the authors used mixes of propionate and acetate with ratios ranging from 2.5:1 and 2.9:1 propionate: acetate (Jan et al., 2002). Marques et al. observed that acetate induces apoptosis in HCT-15 and RKO colorectal cancer (CRC) cell lines, but at much higher concentrations than used in this study (70 and 110 mM) (Marques et al., 2013). In another study, Comalada et al. noted that out of the 3 main SCFA (acetate, propionate and butyrate), butyrate alone induces cell death (Comalada et al., 2006).

The effect of the SCFA on cellular metabolism trends toward investigations into diet and the inflammatory response, and again predominately focus on butyrate. For example, increases in Ca^{2+} have been observed after treatment with 5 mM butyrate in rat pituitary cells (Miletta et al., 2014) and after treatment with 1 mM acetate or propionate in L cells (a component of the entereoendocrine system) (Tolhurst et al., 2012). Increased production of ROS has also been reported in bone marrow neutrophils in response to treatment with 1-30 mM acetate (Maslowski et al., 2009).

The concentrations of acetate used in this study were selected based on a combination of existing literature reporting SCFA concentrations in the body as well as concentrations of acetate used both in existing publications and preliminary studies. In the literature, there are a wide variety of reported SCFA concentrations, which all depend on from where the sample is taken and how long after a meal. Louis et al. state that in the colon, the SCFA have a combined concentration that varies from 50-150 mM, in a ratio of 3:1:1 acetate: propionate: butyrate, putting acetate at concentration of 30 – 90 mM (Louis et al., 2014). In circulation, acetate has been reported at concentrations of 0.258-0.268 mM in the portal vein, 0.115-0.220 mM in the hepatic vein, and 0.07-0.173 mM in the peripheral circulation (Bloemen et al., 2009; Cummings et al., 1987). Studies investigating the effect of acetate on cancer *in vivo* use concentrations ranging from 6.13 mM (Brody et al., 2017), to 140 mM (Marques et al., 2013). To keep within physiological ranges, and to be consistent with doses used on other studies, it was therefore decided to use doses ranging from 1-25 mM in this project, with a particular focus on 10 mM, which would become the dose used to “prime” cells.

The objectives in this chapter were therefore as follows:

1. Investigate the effects of the SCFA acetate on cell viability and programmed cell death
2. Investigate the effect of the SCFA acetate on cell metabolism.

3.1 | The Effects of Acetate on Cell Viability

The MTT cell viability assay was used to investigate the effect a range of acetate concentrations had on cell viability (Figure 16).

In each cell line tested, acetate had no significant effect on cellular viability at any dose compared to the untreated control.

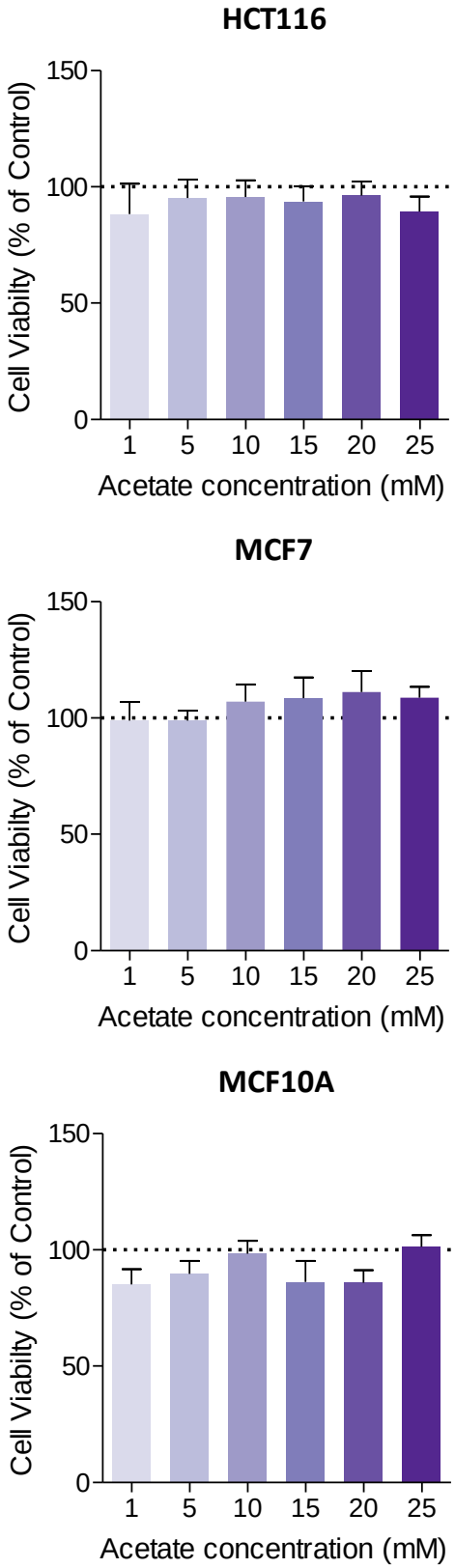

Figure 16 | The Effect of Acetate on Cell Viability. Bars represent mean ±SEM cellular viability as a percentage of the untreated control (dashed horizontal line) from *n* = 5 individual experiments. Differences between treatment and control analysed with unpaired t-test. No asterisk means no statistically significant difference.

3.2 | The Effects of Acetate on Total Cellular Protein Content

The Bradford Assay was used to determine the total protein content of cells treated with acetate for 24 hours (Figure 17).

In HCT116 cells, 25 mM acetate treatment caused a significant decrease in protein content compared to the untreated control (76.66 ± 5.52% of the control, $p = 0.005$). Lower doses of acetate (20 – 1 mM) had no significant effect on protein content.

In MCF7 cells treated with 5 mM acetate, protein content was significantly increased relative to the untreated control (117.30 ± 5.43% ($p = 0.024$). All other doses of acetate had no significant effect on protein content.

In MCF10A cells, acetate treatment had no significant effect on total protein content compared to the untreated control at any dose.

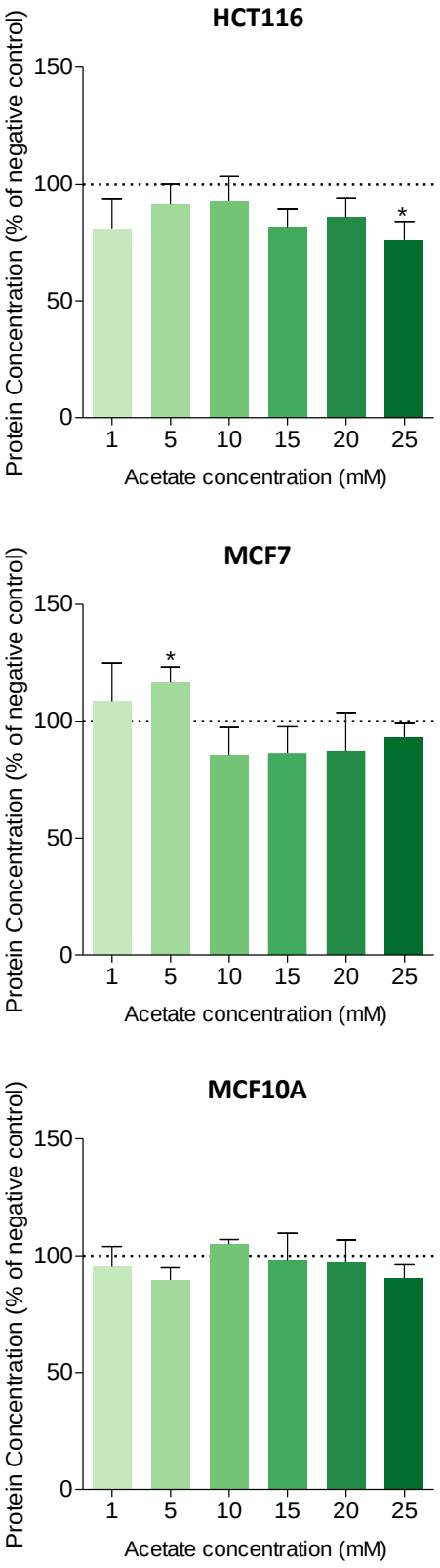

Figure 17 | The Effect of Acetate on Total Protein Content. Bars represent mean ± SEM total protein content as a percentage of the untreated control (dashed horizontal line), from n = 5 individual experiments. Differences between treatment and control analysed with unpaired t-test. * indicates significance (p <0.05) with respect to the negative control. No asterisk means no statistically significant difference.

3.3 | The Effect of Acetate on Apoptosis

To further determine the effect of acetate on cellular health, the Annexin V-FTIC assay was used to investigate to effect of acetate on apoptosis induction compared to an untreated control (Figure 18).

In each cell line tested, 24-hour treatment with 10 mM acetate had no significant effect on the number of apoptotic events compared to the untreated control.

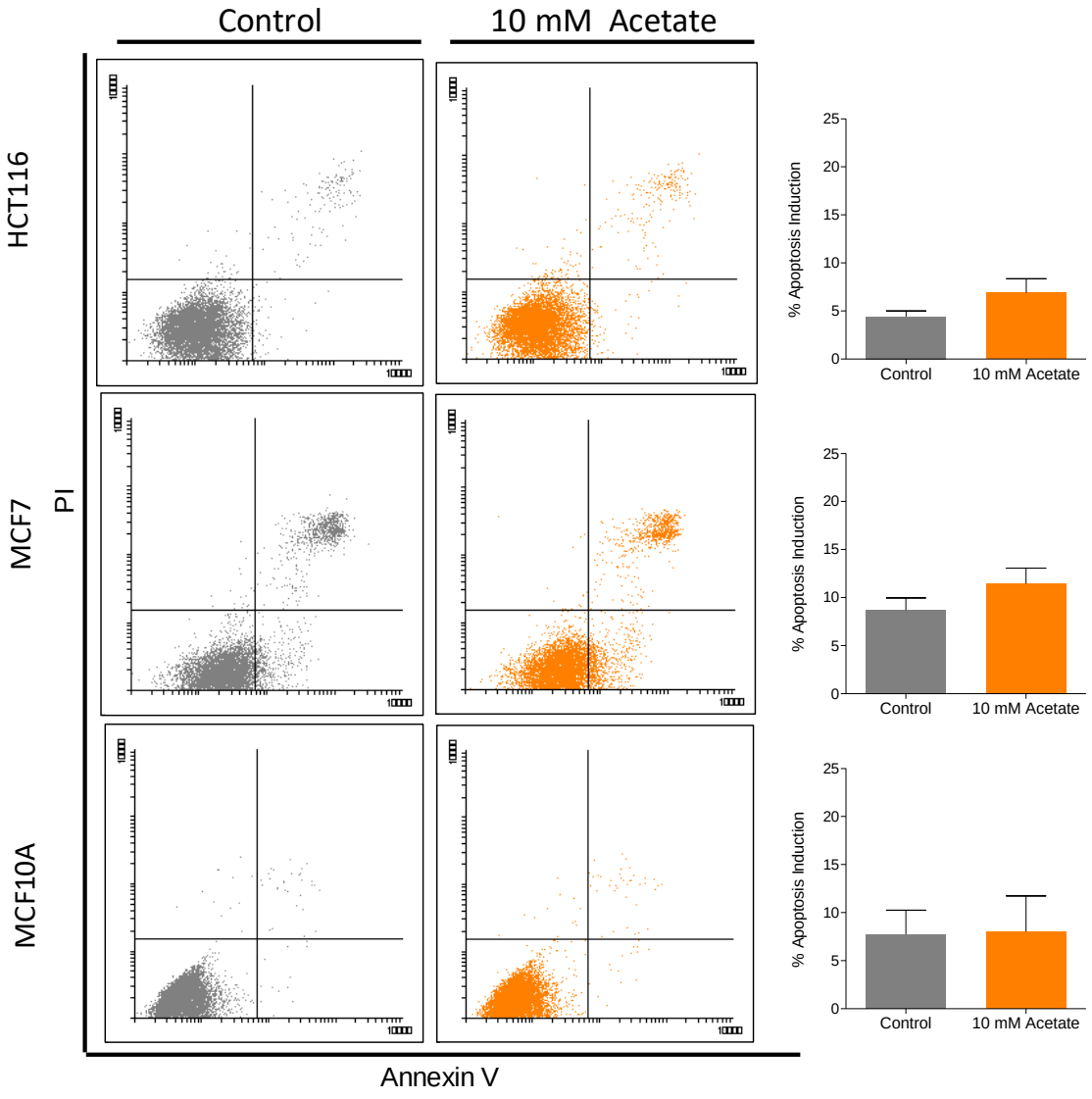

Figure 18 | The Effect of Acetate on Apoptosis. Bivariate dot plots (Representative) show cells/events plotted as function of Annexin V intensity (x-axis) and PI intensity (y-axis) MFI. Events in bottom right and top right quadrants were considered apoptotic. Bars represent mean percentage of total apoptotic events ± SEM from *n* = 5 individual experiments. Differences between control and acetate treatments analysed with Unpaired Student's t-test. No asterisk means not statistically significant.

3.4 | The Effect of Acetate on Autophagy Induction

The effect of acetate compared to an untreated control on autophagy induction was measured via flow cytometry (Figure 19). In HCT116 and MCF7 cells, 24-hour treatment with 10 or 25 mM acetate had no significant effect on autophagy induction compared to the untreated control.

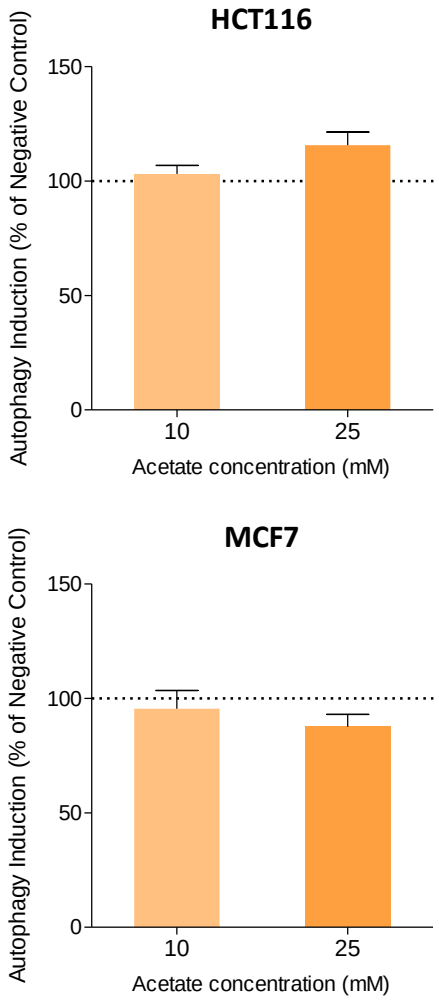

Figure 19 | The Effect of Acetate on Autophagy. Bars represented mean autophagy induction as a percentage of the untreated control ±SEM of *n* = 3 individual experiments. Differences between treatment and control analysed with unpaired t-test. * indicates significance (p <0.05) with respect to the negative control. No asterisk means no statistically significant difference.

3.5 | The Effects of Acetate on Mitochondrial Respiration.

The SeaHorse MitoStress Assay was used to investigate whether acetate affected mitochondrial function. When treated with 10 mM acetate for 24 hours, HCT116 and MCF7 cell lines showed a general reduction in oxygen consumption rate (OCR) compared to the untreated control, whilst in the control cell line MCF10A, OCR appeared relatively unaffected (Figures 20 and 21).

In HCT116, 24-hour treatment with 10 mM acetate significantly decreased basal respiration (79.63 ± 1.36% of the control, $p = 0.039$), maximum respiration (79.10 ± 7.08% of the control, $p = 0.042$) and ATP production (79.71 ± 7.33% of the control, $p = 0.039$) compared to the untreated control. OCR associated with proton leak trended towards a decrease compared to the control, but did not reach significance. (79.01 ± 8.25% of the control, $p = 0.052$). Acetate treatment had no significant effect on the remaining parameters: spare capacity and non-mitochondrial respiration.

In MCF7 cells, treatment with acetate caused a significant decrease in maximal respiration (79.34 ± 3.83% of the control, $p = 0.002$) and spare respiratory capacity (69.52 ± 7.96% of the control, $p = 0.013$) relative to the control. Acetate treatment had no significant effect on basal respiration, ATP production, proton leak, and non-mitochondrial respiration.

In MCF10A cells, acetate treatment had no significant effect on any mitochondrial function parameter compared to the untreated control.

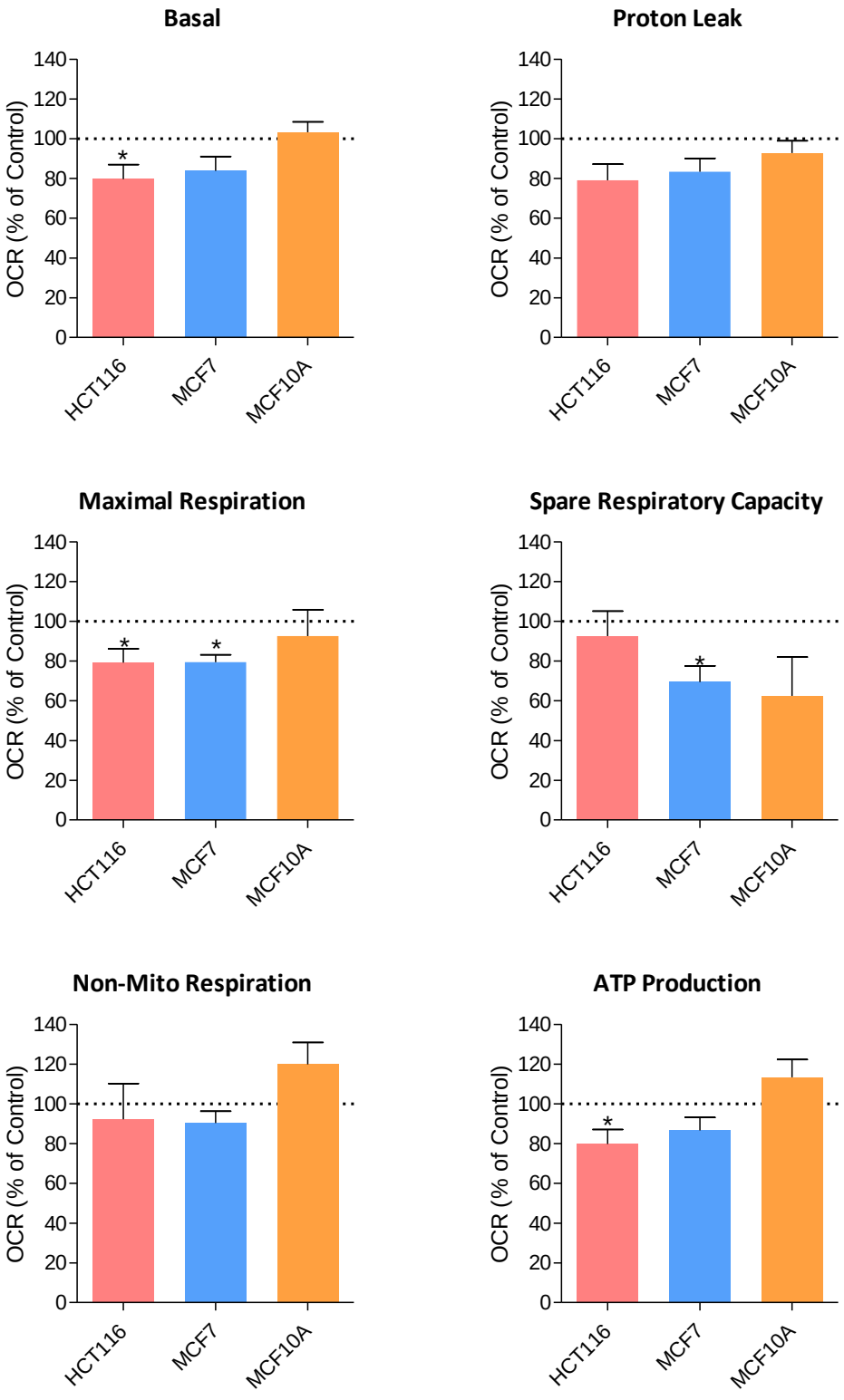

Figure 20 | **The Effect of Acetate on Mitochondrial Respiration**. Bar graphs show the individual parameters of the MitoStress test, presented as the mean percentage of the negative control ±SEM of *n* = 3 independent experiments in each cell line. Differences between treatment and control analysed with unpaired t-test. * indicates significance (p <0.05) with respect to the negative control. No asterisk means no statistically significant difference.

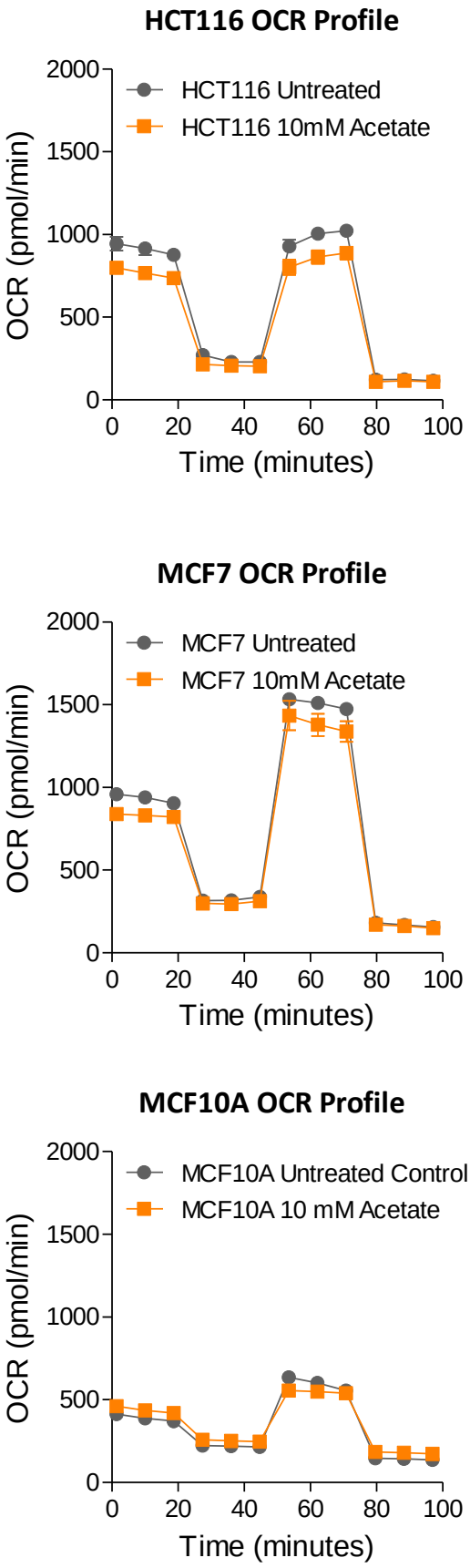

Figure 21 | The Effect of Acetate on Mitochondrial Respiration: MitoStress OCR Proflies. (Representative) show change in OCR over course of the MitoStress Assay.

3.6 | The Effect of Acetate on the Production of ROS.

The effect of 24-hour acetate treatment on the production of ROS was measured using the DCFDA Assay via fluorescence spectroscopy (Figure 22). In all cell lines, acetate induced an increase in ROS levels.

In HCT116 cells, 1-20 mM acetate treatments induced a significant increase in ROS, with 10 mM, the priming dose, causing a 137% ± 11.82 p = 0.029 increase compared to the untreated control. Treatment with 25 mM acetate had no significant effect on ROS levels compared to the control (p = 0.119).

In MCF7 and MCF10A cells, treatment with acetate caused a dose dependent increase in ROS production. In MCF7, ROS levels in treatments 10 mM (114% ± 4.54 of the control, p = 0.040) and above were significantly higher than the untreated control. In MCF10A, ROS levels in all doses of acetate were significantly higher than the control, with 10 mM, the dose used in priming experiments, causing an increase of 121.3% ± 3.79 (p = 0.030) of the untreated control.

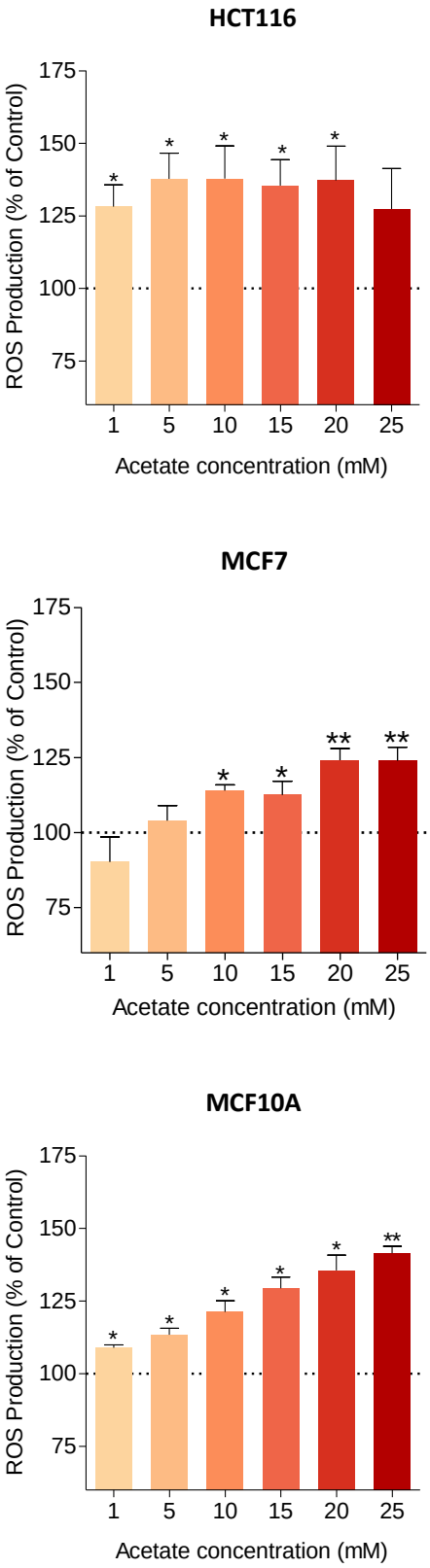

Figure 22 | The Effect of Acetate on Reactive Oxygen Species. Bars represent mean ±SEM ROS levels as a percentage of the untreated control (dashed horizontal line), from *n* = 5 individual experiments. Differences between treatment and control analysed with unpaired T-test. Significance compared to the untreated control indicated by * = $p < 0.05$, ** $p < 0.01$. No asterisk means not statistically significant.

3.7 | The Effect of Acetate on Intracellular Ca^{2+}

The effect of 24-hour acetate treatment on intracellular calcium was measured using the Fluo-4 Direct assay via fluorescence spectroscopy (Figure 23). In all cell lines tested, acetate caused a dose-dependent increase in Ca^{2+} compared to the untreated controls, with doses of 5 mM and above causing significant increases compared to the untreated control. In 10 mM treatments, the dose used in priming experiments, Ca^{2+} levels were increased to 124.4 ± 2.44% (p = 0.002) of the control in HCT116, 117.5 ± 2.51% (p = 0.006) in MCF7 cells, and 126.0 ± 1.38% (p = 0.003) in MCF10A cells.

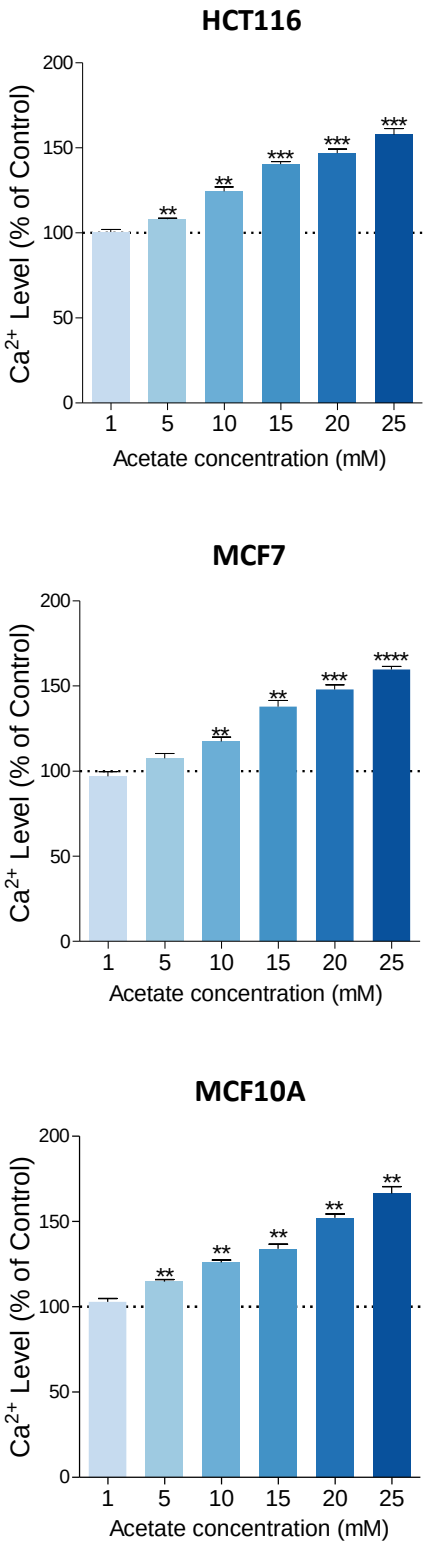

Figure 23 | The Effect of Acetate on Intracellular Calcium. Bars represent mean ±SEM Ca^{2+} levels of each treatment group as percentage of the untreated control (dashed horizontal line), from *n* = 4 individual experiments. Differences between treatment and control analysed with unpaired T-test. Significance compared to the untreated control indicated by * = $p < 0.05$, ** $p < 0.01$, *** $p < 0.001$, **** $p < 0.0001$. No asterisk means not statistically significant.

3.8 | The Effect of Acetate on Mitochondrial Morphology

Mitochondrial imaging of HCT116 and MCF7 cells using MitoTracker Deep Red via confocal microscopy demonstrated a clear change in mitochondria morphology (Figure 24). In HCT116 cells, the mitochondria were smaller and more fragmented in cells treated with 10 mM acetate compared to the untreated control. In MCF7 cells treated with acetate, the mitochondria appeared less numerous but larger and more intense, which may suggest swelling. In MCF10A, there was no discernible difference between the negative control and 10 mM acetate-treated cells.

The MitoLOC plugin for ImageJ/FIJI was used to quantify changes in the mitochondrial morphology from the obtained images (Figures 25, 26 and 27).

In HCT116 cells, treatment with 10 mM acetate caused a significant decrease in the average number of mitochondria per cell (17.73 ± 1.34 vs 21.78 ± 1.34, p = 0.017). There was no significant change in average surface area of mitochondria per cell and in the average total mitochondrial area in cells treated with acetate compared to untreated cells.

In MCF7 cells, the average number of mitochondria per cell was also significantly lower in acetate treated cells (20.84 ± 1.381 vs 26.82 ± 1.925, p = 0.013). The average area of mitochondria and the average total mitochondria in acetate-treated cells were not significantly different compared to untreated cells.

In MCF10A cells, the average number of mitochondria per cell trended towards an increase in acetate treated cells but did not reach statistical significance (43.81 ± 2.457 vs 35.74 ± 3.658, p = 0.0674). The average of area of individual mitochondria was significantly decreased by acetate treatment (2138 ± 157.6 vs 2806 ± 250.5, p = 0.0305), whilst the average total mitochondrial area per cell was not significantly different compared to untreated cells.

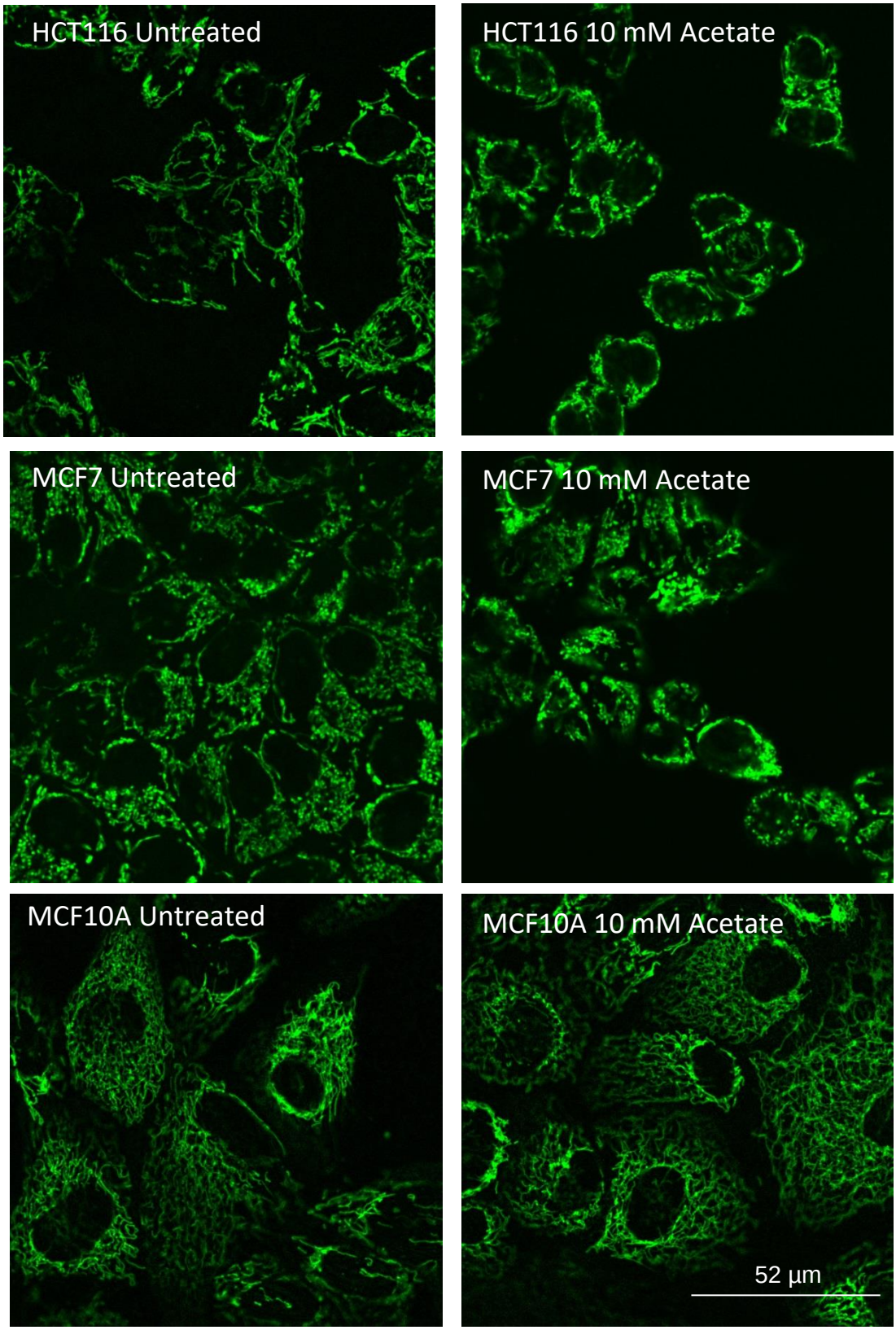
HCT116 Untreated
HCT116 10 mM Acetate
MCF7 Untreated
MCF7 10 mM Acetate
MCF10A Untreated
MCF10A 10 mM Acetate
52 µm

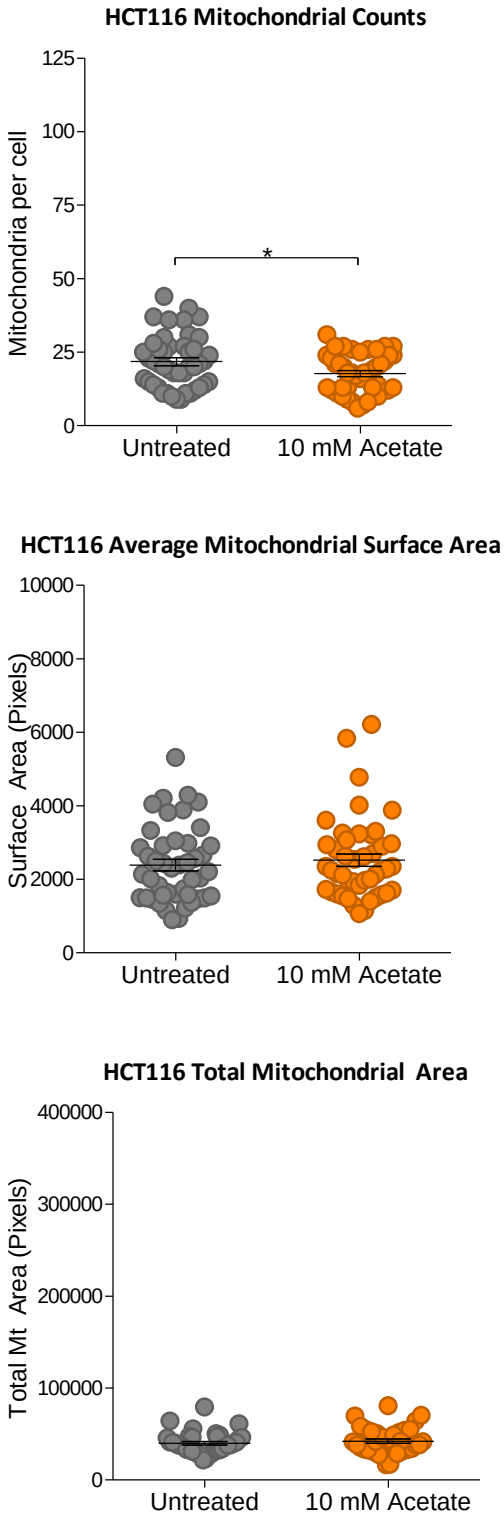

Figure 25 |The Effect of acetate on HCT116 Mitochondrial Morphology – MitoLOC. Images were quantified by the analysis of MitoTracker Deep Red stained cells by the ImageJ plugin, MitoLOC**.** Cells were treated with media (grey) or 10 mM acetate (orange) for 24 hours. Individual points indicate the number of mitochondria per cell, average mitochondrial area per cell, and total mitochondrial area per cell. 5 cells were analysed per image. 3 images were captured for each condition, in n = 5 individual experiments, to give a total of 75 analysed. Differences between treated and control analysed with Unpaired Student's T-test. * indicates significant (p <0.05) difference between means. No asterisk means not statistically significant.

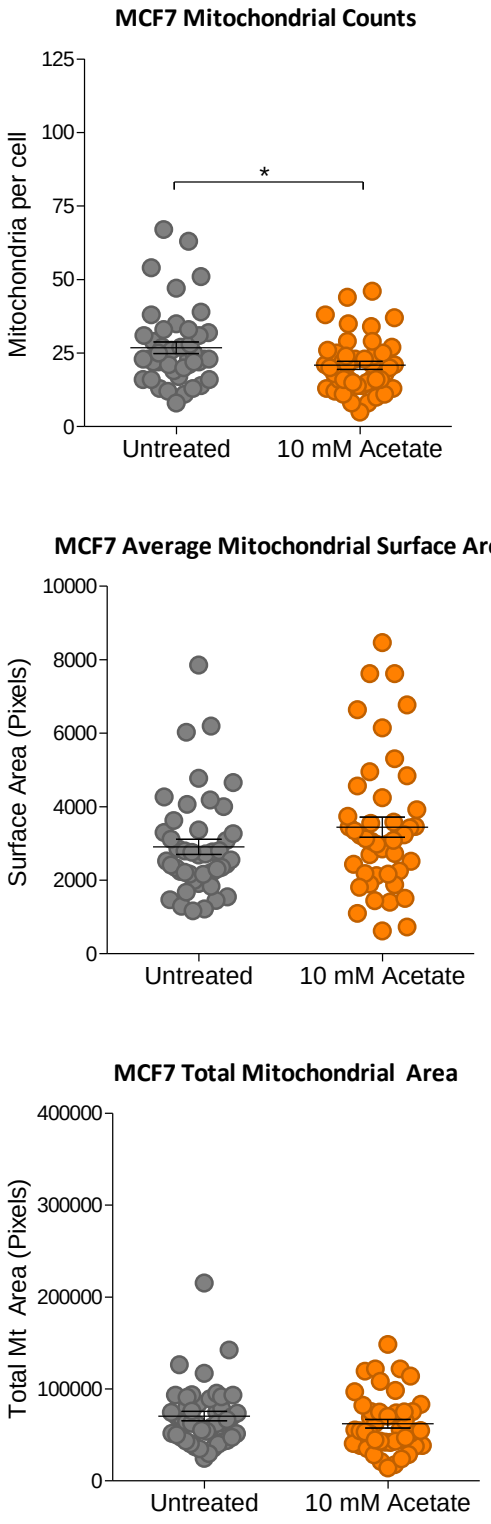

Figure 26 | The Effect of acetate on MCF7 Mitochondrial Morphology – MitoLOC. Images were quantified by the analysis of MitoTracker Deep Red stained cells by the ImageJ plugin, MitoLOC**.** Cells were treated with media (grey) or 10 mM acetate (orange) for 24 hours. Individual points indicate the number of mitochondria per cell, average mitochondrial area per cell, and total mitochondrial area per cell. 5 cells were analysed per image. 3 images were captured for each condition, in n = 5 individual experiments, to give a total of 75 analysed. Differences between treated and control analysed with Unpaired Student's T-test. * indicates significant (p <0.05) difference between means. No asterisk means not statistically significant.

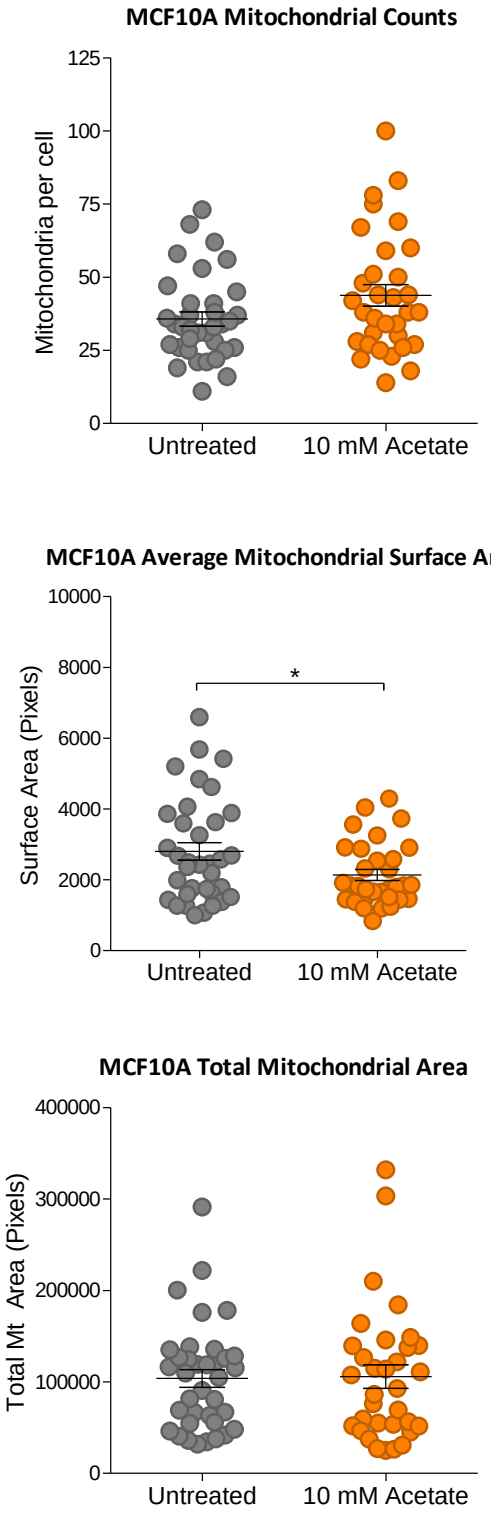

Figure 27 | The Effect of acetate on MCF10A Mitochondrial Morphology – MitoLOC. Images were quantified by the analysis of MitoTracker Deep Red stained cells by the ImageJ plugin, MitoLOC**.** Cells were treated with media (grey) or 10 mM acetate (orange) for 24 hours. Individual points indicate the number of mitochondria per cell, average mitochondrial area per cell, and total mitochondrial area per cell. 5 cells were analysed per image. 3 images were captured for each condition, in *n* = 5 individual experiments, to give a total of 75 analysed. Differences between treated and control analysed with Unpaired Student's T-test. * indicates significant (p <0.05) difference between means. No asterisk means not statistically significant.

Flow Cytometry was used as an additional method to quantify the observed changes in morphology (Figure 28). In each cell line, the higher 25 mM acetate dose induced an increase in fluorescence intensity compared to the untreated control.

In HCT116 cells, 10 mM acetate treatment had no significant effect on MitoTracker intensity. 25 mM treatment significantly increased intensity to 139.7 ± 16.75% of the control (p = 0.0178).

In MCF7 cells, 10 mM acetate had no significant effect on MitoTracker intensity. 25 mM treatment significantly increased intensity to 125.0 ± 7.307 % of the control (p = 0.026).

In MCF10A cells, 10 mM acetate had no significant effect on MitoTracker intensity. 25 mM treatment significantly increased intensity to 117.6 ± 3.123 % of the control (p = 0.0111).

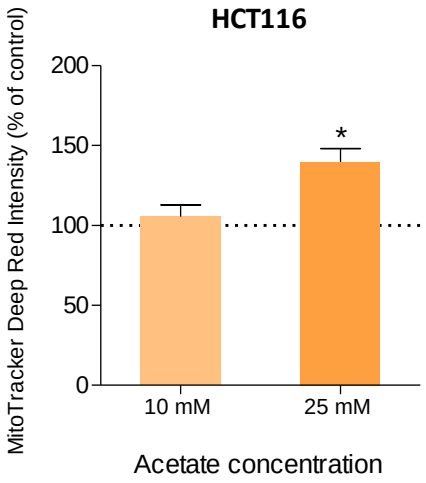

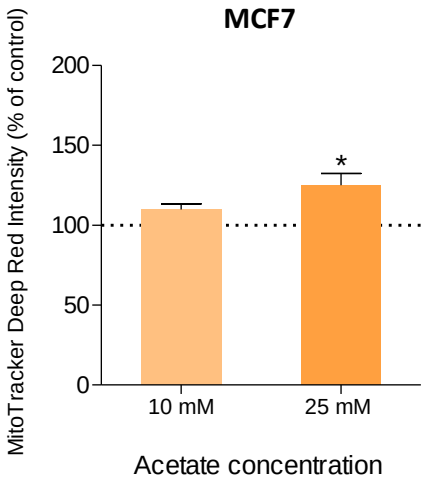

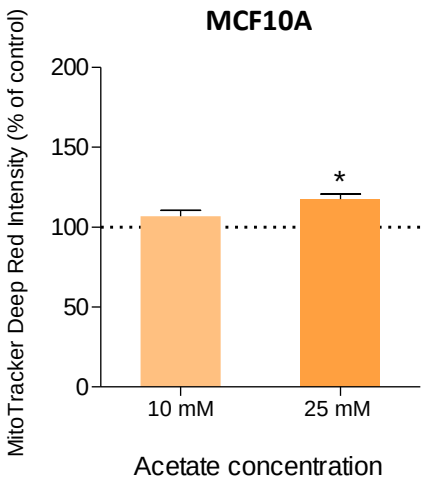

Figure 28 |The Effect of Acetate on Mitochondrial Morphology – Flow Cytometry. Morphology was quantified by changes in MitoTracker Deep Red Intensity**.** HCT116, MCF7, and MCF10A cells were treated with media or acetate for 24 hours. Data presented as mean changes in signal intensity of *n* = 4-7 individual experiments, compared to an untreated control ±SEM. Differences between treated and control analysed with Unpaired Student's T-test. * indicates significant (p <0.05) difference between means. No asterisk means not statistically

3.9 | The Effect of Acetate on Gene Expression

The effect of 24-hour 10 mM acetate treatment on the expression of *ACSS1*, *ACSS2*, *VDAC1*, *P53*, and *NRF2* was measured using qPCR (Figure 29).

In acetate-treated HCT116 cells, the expression of *P53* and *NRF2* was significantly decreased compared to the untreated control (0.64 ± 0.04 fold decrease $p = 0.014$ and 0.81 ± 0.003 fold decrease $p = 0.0004$ respectively). The expression of *ACSS2* and *VDAC1* were unaffected by acetate treatment. *ACSS1* was not expressed in HCT116 cells.

In MCF7 cells, acetate treatment significantly increased the expression of *ACSS2* compared to untreated cells (1.15 ± 0.02 fold increase $p = 0.002$). The expression of *VDAC1*, *P53, ACSS1* and *NRF2* in acetate-treated cells were not significantly different compared to the control.

In MCF10A cells, acetate treatment significantly increased the expression of *ACSS2* and *VDAC1* (1.27 ± 0.04 ($p = 0.021$) and 1.18 ± 0.03 ($p = 0.032$) fold increases respectively). The expression of *ACSS1*, *P53* and *NRF2* were unaffected by acetate treatment.

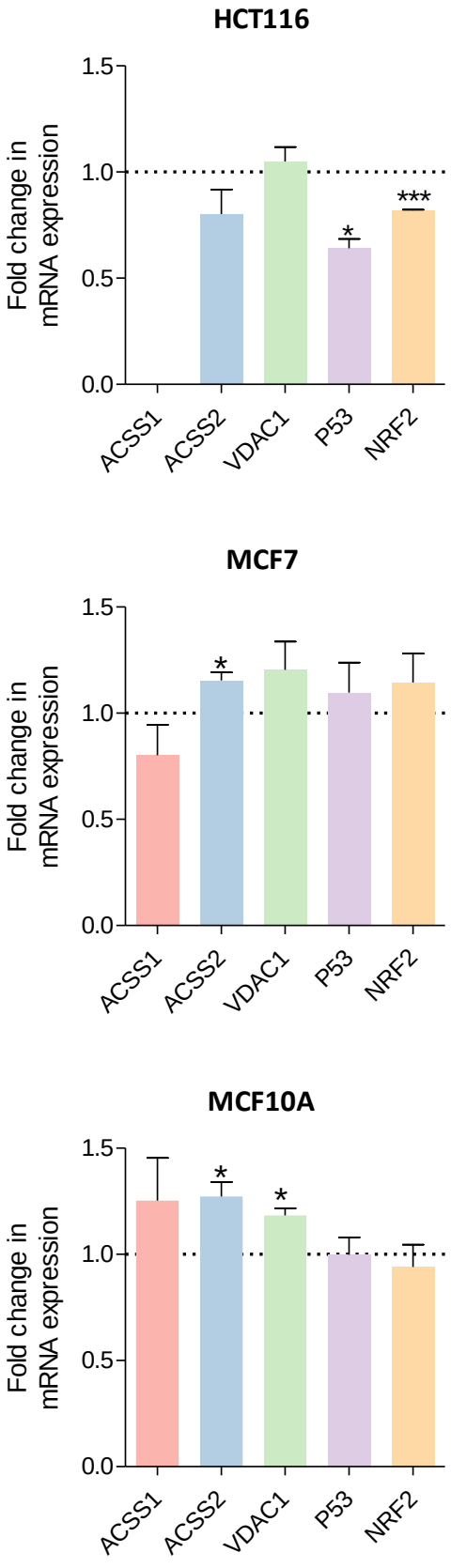

Figure 29 | **The Effect of Acetate on Gene Expression**. Bars represent mean fold change in mRNA expression compared to the untreated control (dashed horizontal line), from *n* = 3-4 individual experiments. Differences between treatment and control analysed with unpaired T-test. Significance compared to the untreated control indicated by * = $p < 0.05$, *** $p < 0.001$. No asterisk means not statistically significant.

3.10 | The Effect of Acetate on the Cell Cycle

The effect of 24-hour acetate treatment on cell cycle state was measured using PI flow cytometry (Figure 30).

In this experiment, only HCT116 cells were tested due to difficulties with the other cell lines forming aggregates and causing blockages in the flow cytometer (discussed in more detail in Section 3.14.7). In HCT116 cells, 25 mM acetate treatment induced a significant decrease in the number of cells in the G_0-G_1 phase compared to the untreated control (mean decrease of 11.89 ± 4.88% p = 0.029). There was no significant change in S phase population between any treatment groups. 10 mM and 25 mM acetate treatments induced a significant dose dependent increase in cells in the G_2-M phase (mean increases of 6.31 ± 2.69% p = 0.033 and 13.26 ± 3.95% p = 0.004 respectively).

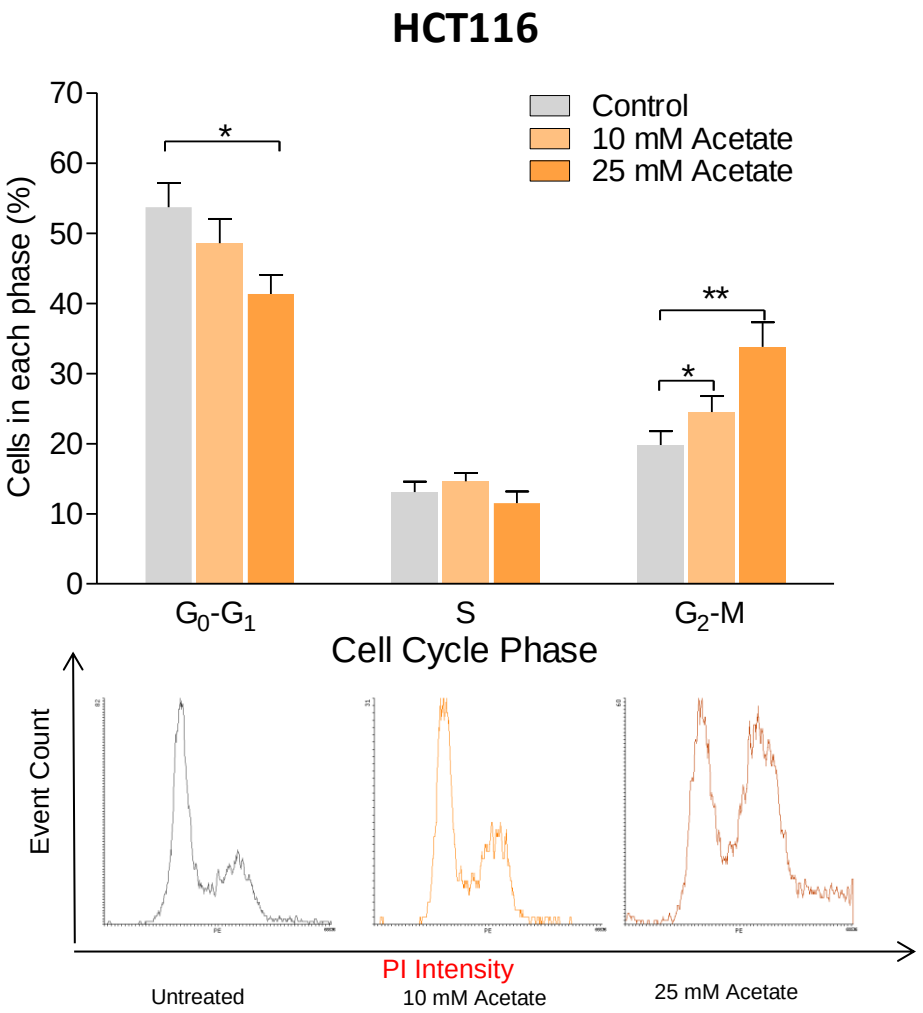

Figure 30 | **The Effect of Acetate on the Cell Cycle**. Bar charts (top) show the mean populations (as a percent of total cell count) ±SEM in the 3 major cell cycle phases: G_0-G_1, S and G_2-M. Differences between treatment group and untreated control analysed with student's t test. Significance compared to the untreated control indicated by * = $p < 0.05$, ** = $p < 0.01$. $n = 8$. Histograms below represent typical univariate histogram plot intensity of PI (FL2) against event count.

3.11 | The Effect of Acute Acetate Treatment on Mitochondrial Function

The short-term effects of acetate on mitochondrial function were measured using the SeaHorse XF_e24 analyser (Figure 31). In each cell line, injection of acetate to a final concentration of 10 mM induced an immediate increase in OCR which continued to increase over the course of the assay.

After 12 hours, OCR in HCT116 cells was significantly increased to 129.6 ± 5.90% of the control (p = 0.0074). In MCF7 and MCF10A, acetate injection had no significant effect on OCR recorded after 12 hours.

Correspondingly, the injection of acetate into each cell type caused an immediate decrease in ECAR, which was sustained over the course of the assay. After 12 hours, ECAR was significantly reduced in each cell line: 81.31 ± 2.14% of the control in HCT116 (p = 0.0009), 82.60 ± 2.19% of the control in MCF7 (p = 0.0014), and 86.83 ± 1.31% of the control in MCF10A (p = 0.0005).

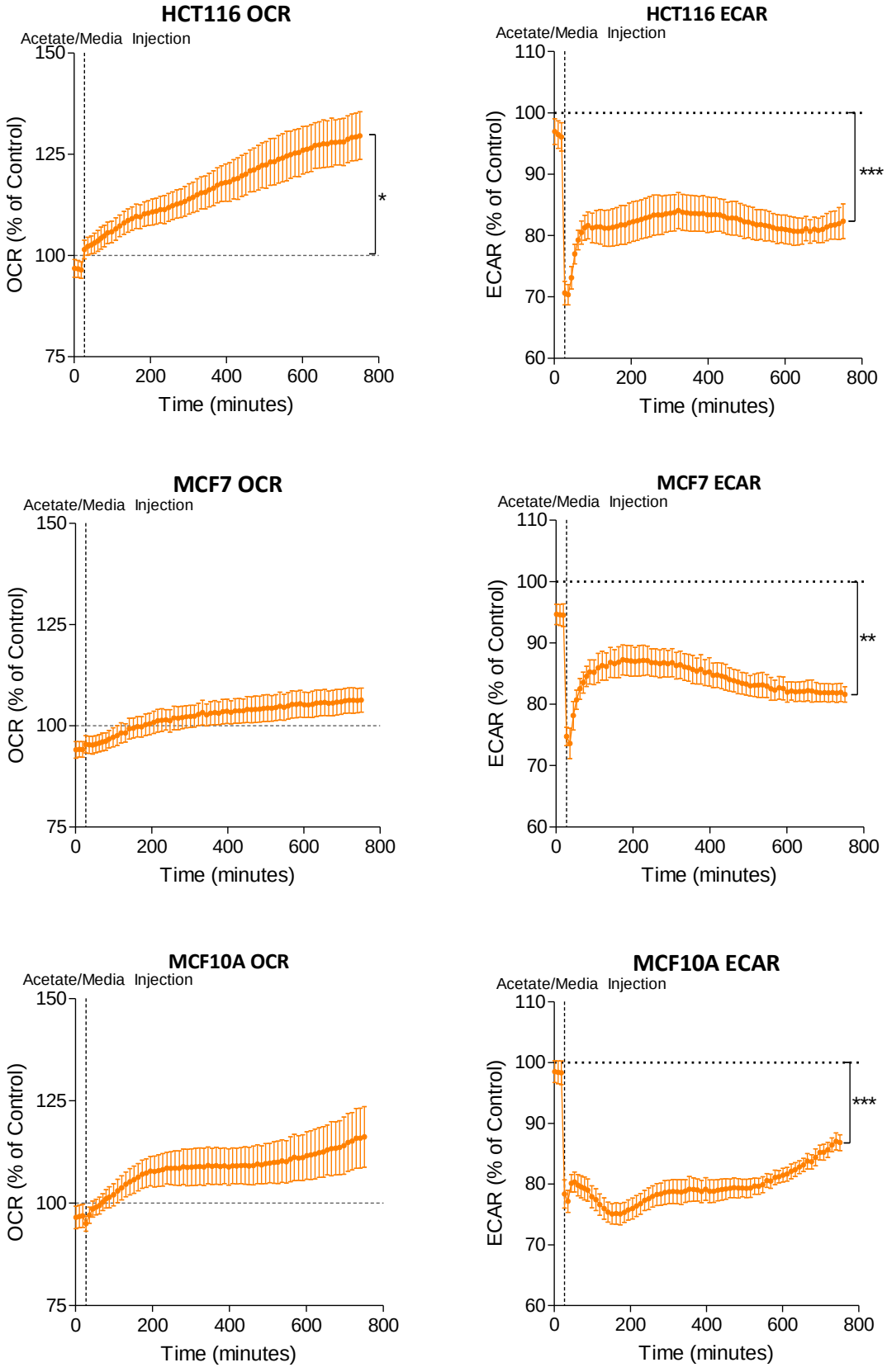

Figure 31 | **The Effect of Acute Acetate Treatment on Mitochondrial Respiration**. Lines represent mean OCR (left) or ECAR (right) change compared to the untreated control (dashed horizontal line) before and after the injection of acetate (dashed vertical line), from n = 5 individual experiments. Differences between treatment and control at the end of the assay analysed with unpaired T-test. Significance compared to the untreated control indicated by * = $p < 0.05$, ** = $p < 0.01$, *** $p < 0.001$. No asterisk means not statistically significant.

3.12 | The Effect of Acute Acetate Treatment on Glycolysis

The short-term effects of acetate on glycolysis were measured with the SeaHorse GlycoStress Assay using the SeaHorse XF_e24 Analyser (Figures 32 and 33).

In HCT116 cells, acetate injection caused a significant decrease in glycolysis (77.28 ± 4.05% of the control p = 0.003), glycolytic capacity (77.26 ± 4.38% of the control p = 0.003), and non-glycolytic acidification (92.86 ± 2.20% of the control p = 0.023). Glycolytic reserve trended towards a decrease in acetate treated cells, but this change was not statistically significant (73.32 ± 11.07% of the control p = 0.061).

Acetate treatment also caused a significant decrease in glycolysis in MCF7 cells (68.76 ± 5.56% of the control p = 0.003). Glycolytic capacity and non-glycolytic acidification remained unchanged following acetate injection. Glycolytic Reserve was significantly increased by acetate treatment (125.60 ± 9.33% of the control p = 0.041).

Acetate treatment had no significant effect on any of the measured glycolytic parameters compared to the untreated control.

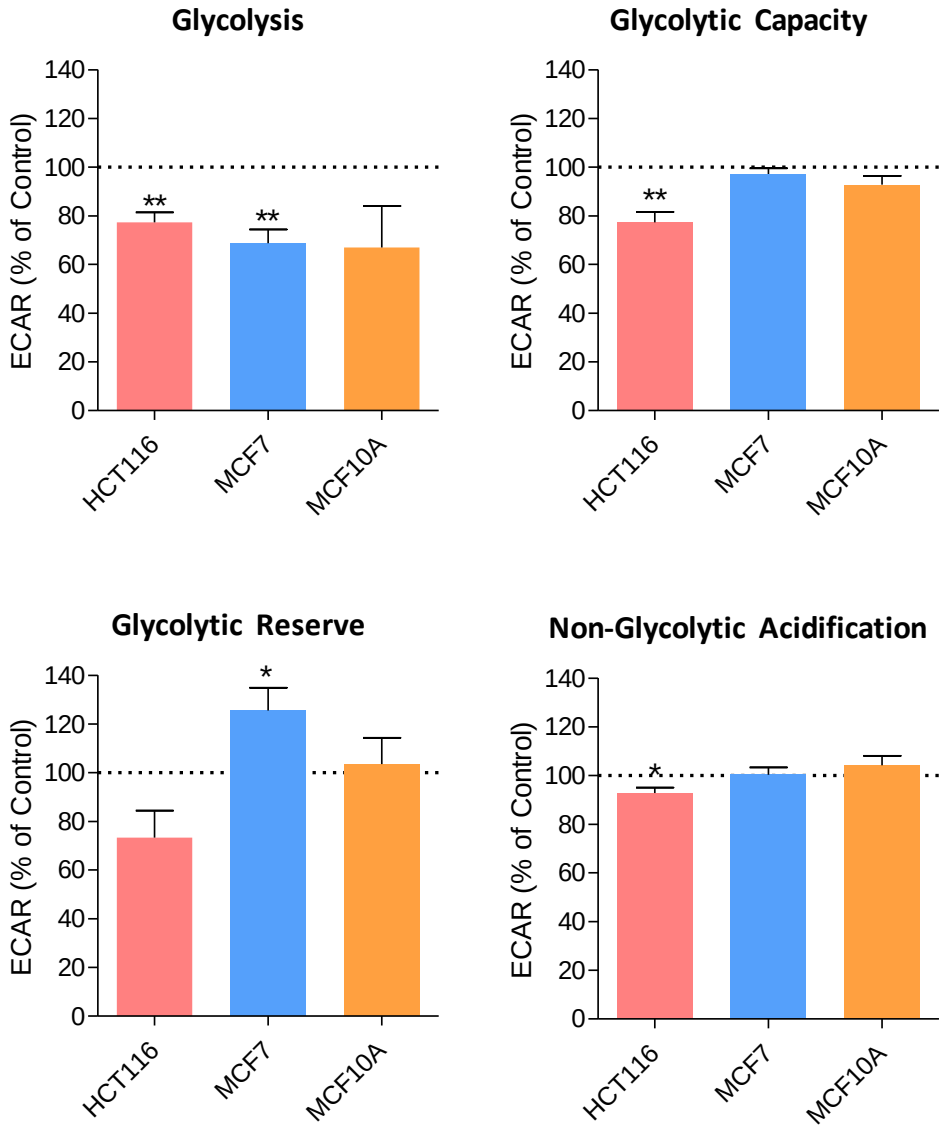

Figure 32 | **The Effect of Acute Acetate Treatment on Glycolysis**. Bar graphs show the individual parameters of the GlycoStress test, presented as the mean percentage of the negative control ±SEM from *n*= 6 independent experiments. Significance compared to the untreated control indicated by * = $p < 0.05$, ** = $p < 0.01$, *** $p < 0.001$. No asterisk means not statistically significant.

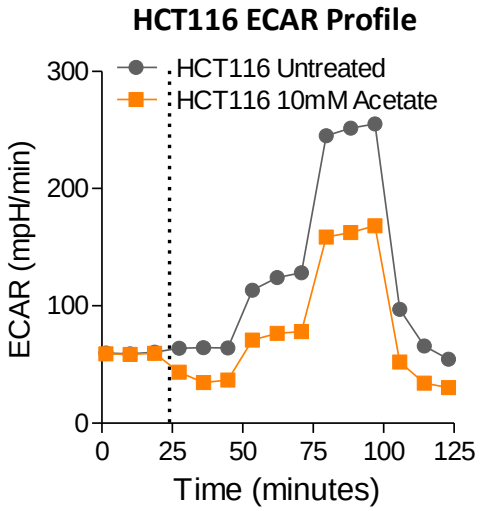

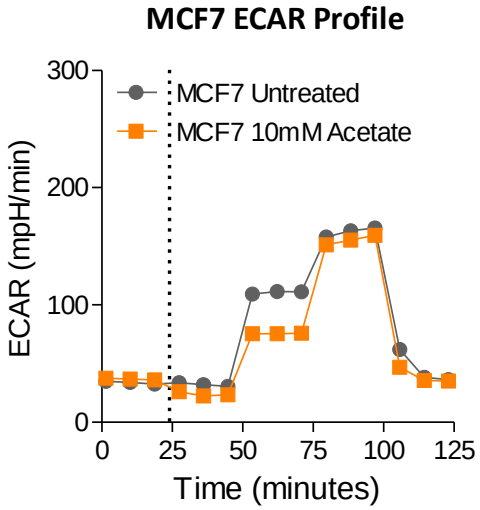

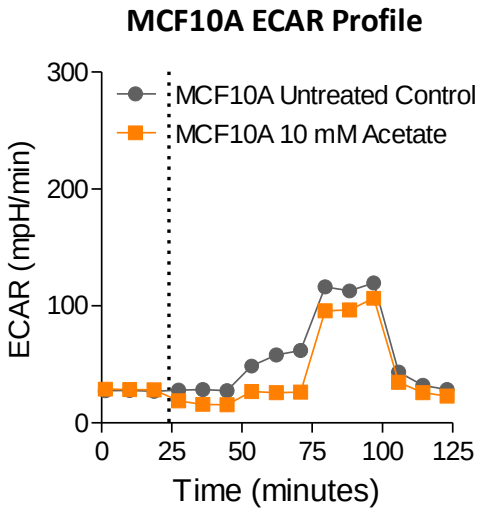

Figure 33 | The Effect of Acute Acetate Treatment on Glycolysis – GlycoStress ECAR Profiles. Lines show change in ECAR over course of the Assay following the injection of media (grey) or acetate (orange), as indicated the by dashed vertical line.

3.13 | The Effect of Acute Acetate Treatment on Intracellular Ca^{2+}

The short term effects of acetate on intracellular Ca^{2+} ($[Ca^{2+}]_i$) were monitored by observing the changes in Fluo4 Direct fluorescence prior to and following the injection of acetate using the BMG NOVOStar fluorescence plate reader (Figure 34).

In HCT116 cells, injection of acetate caused an immediate increase in $[Ca^{2+}]_i$, reaching a peak at 32.06 seconds of 113.90 ± 4.42% of the control that was significantly higher than the control (p = 0.027). $[Ca^{2+}]_i$ levels then dropped to 108.60 ± 3.88% of the control by the end of the measurement period, which was not significantly higher than the control.

In MCF7 cells, injection of acetate did not cause an immediate increase in $[Ca^{2+}]_i$, but rather caused a smaller, yet sustained increase over the course of the measurement period. At the end of the assay, $[Ca^{2+}]_i$ had increased to 102.2 ± 1.30% of the control, which was significantly higher than the control (p = 0.019).

In MCF10A cells, injection of acetate caused a trend towards an immediate increase in $[Ca^{2+}]_i$, reaching a peak at 26.22 seconds of 108.20 ± 3.52% of the control, yet was not statistically significant (p = 0.067). $[Ca^{2+}]_i$ levels then dropped to 104.00 ± 1.84% of the control by the end of the measurement period, which was not significantly higher than the control.

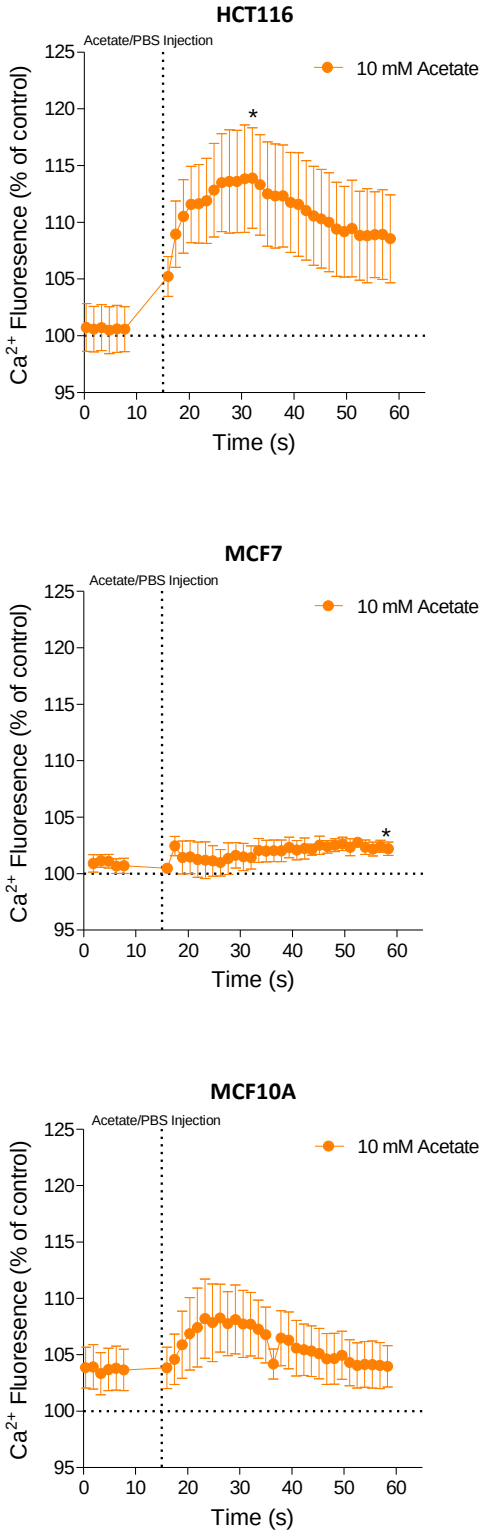

Figure 34 | The Effect of Acute Acetate Treatment on Intracellular Calcium. Orange data points mean represent $[Ca^{2+}]_i$ fluorescence as a percentage of PBS treated cells (dashed horizontal line) ± SEM of n = 5-6 individual experiments. Dashed vertical line indicates the time point at which acetate or PBS was injected into well. Differences in fluorescence between treatment and control at the peak and at the end of the assay were analysed with unpaired T-test. Significance compared to the untreated control indicated by * = $p < 0.05$. No asterisk means not statistically significant.

3.14 | Discussion

3.14.1 | The Effects of Acetate on Cell Viability and Apoptosis

In the first part of this study I assesed what effect that a range of acetate doses had on cell viability. The objective was two-fold: to answer whether acetate alone could affect cell viabilty or induce apoptosis, and to determine if this affect was limited to cancer cells.

Data gathered from the MTT viability assay suggests that 1-25 mM acetate treatment had no significant effect on the viability of both the cancerous and non-cancerous cell lines after 24 hours.

The results of an MTT assay can be considered ambiguous; as the conversion of MTT to formazan is catalysed by NADPH oxireductases (Berridge and Tan, 1993), changes in observed cell viabilty could correspond to changes in metabolic activity, cellular proflieration, or cell death, any of which can lead to a decrease in total enzymatic activity and result in changes in formazan production (Riss TL, Moravec RA, Niles AL, 2013; Wang et al., 2010). I therefore used another test, the Bradford assay, to quantify the total protein content in a population of cells following treatment with acetate and confirm the observations from the MTT assay. Results from the Bradford assay showed that each concentration of acetate tested had no significant effects on cell population in terms of protein content, corroborating the MTT results with one exception: HCT116 cells treated with 25 mM acetate, in which there was a significant decrease in protein content. In the MTT assay, HCT116 viabilty appeared to be reduced following 25 mM acetate treatment, but the difference was not signifcant compared to the untreated control. It may be possible that 25 mM acetate is sufficicent to induce cell death alone, but further work is needed to confirm this.

Finally, results of the Annexin V apoptosis assay confirmed that 10 mM acetate treatment does not induce significantly more apoptosis compared with the untreated control in any cell line. The combination of results from each assay provides strong evidence that the concentrations of acetate used in this study are not sufficient to kill cells alone, a finding that aligns with literature which reports

that lower concentrations of acetate (1-20 mM) have little to no effect on proliferation or apoptosis (Comalada et al., 2006). Marques et al. found that higher concentrations (70-220 mM) caused significant decreases in viability in HCT-15 and RKO colorectal cancer cell lines, which may support the observation in this study that 25 mM treatment decreased total protein content in HCT116 cells (Marques et al., 2013).

The effect of acetate on cell viability and apoptosis is shown in this study to be muted compared to literature investigating propionate and butyrate. Butyrate in particular is consistently shown to have the strongest effect on viability and apoptosis, for example being shown to induce apoptosis in HT29 colorectal cancer cells at concentrations of 5 mM (Wang et al., 2009). In an earlier study, Hague et al. found that a 4 day treatment with 4 mM butyrate caused significant decreases in cell number in a range of adenoma and carcinoma cell lines, as did treatment with 4-10 mM propionate, whilst effects from acetate treatment were only seen at concentrations of 40 – 80 mM (Hague et al., 1995). Furthermore, Hinnebush et al. found that growth inhibition of HT29 and HCT116 colorectal cancer cells was highest following butyrate treatment, followed by propionate and then acetate. Whilst this and other studies may seem to indicate that the effect size on apoptosis or viability increases with increasing SCFA length, the group went on to show that the effect is reduced with SCFAs longer than butyrate, with caproate (C6) having an effect on cells similar in magnitude to acetate. Why butyrate has the strongest effect has yet to be explained; Hinnebusch, attributing the apoptotic effect of the SCFA to histone acetylation, speculated that butyrate may have a greater affinity for certain HDAC isozymes, but conceded that further work is needed to further elucidate this mechanism (Hinnebusch et al., 2002).

By comparison, the effects of the SCFA on viability the of cell types other than colorectal are not as widely investigated in existing literature, which may be because the colon is the site of SCFA production and thus where they are found in highest concentrations. Yonezawa et al. detected the expression of SCFA receptors in MCF7 and subsequently found that the SCFAs, including acetate, increased cellular Ca^{2+} and phosphorylated proteins including heat shock protein 27 and p38. However, the group did not investigate any effect on cellular health (Yonezawa et al., 2007).

3.14.2 | The Effects of Acetate on Mitochondrial Respiration

The SeaHorse MitoStress assay provides a high-throughput means of quantifying the consumption of oxygen as a measure of mitochondrial function. Decreases in mitochondrial function could suggest potential modulation of mitochondrial function, switches in metabolic phenotyping, or general mitochondrial stress (Dranka et al., 2011). Inhibition of OXPHOS has been investigated as an apoptosis-inducing mechanism in anti-cancer drugs, such as staurosporine and taurol, which have been shown to trigger apoptosis in an OXPHOS-dependent manner, inducing mitogenesis and an accompanying increase in ROS production (Yadav et al., 2015). Additionally, “reversing the Warburg effect”, by increasing oxygen consumption, has also been shown to inhibit glioblastoma growth both *in vitro* and *in vivo* (Poteet et al., 2013). Decreased OXPHOS as a result of mitochondrial damage or remodelling would also be consistent with mitochondrial changes observed in the intrinsic pathway of apoptosis (Cosentino and García-sáez, 2014). Targeting OXPHOS in this manner has been demonstrated to be effective in other drugs or molecules, such as epigallocatechin-3-gallate (ECCG), which was shown to target complexes I, II and ATP Synthase within the ETC (Valenti et al., 2013) and Elesclomol, which supresses OXPHOS via down-regulation or suppression of a number of proteins, including Complex I (Barbi de Moura et al., 2012).

In the cancerous cell lines HCT116 and MCF7, treatment with acetate caused a general decrease in mitochondrial function. This effect was strongest in HCT116, in which basal, maximal and ATP production-associated oxygen consumption rates were significantly decreased, whereas MCF7 by comparison experienced decreased maximal respiration rates only. Additionally, acetate treatment of MCF7 cells caused a significant decrease in spare respiratory capacity, which, as measure of the ability of the mitochondria to respond the increased energy demand (Brand and Nicholls, 2011), may indicate mitochondrial dysfunction, as the capacity to respond to stress is diminished. Interestingly, proton leak – the dissipation of the proton gradient across the inner mitochondrial membrane that is not attributable to ATP production, trended towards a decrease in both cancer cell lines. Proton leak can be categorised into basal, which is cell

type specific, and inducible, regulated by proteins such as the adenine nucleotide translocator (ANT) and the uncoupling proteins (UCPs). Inducible proton leak has an important role in brown adipose tissue in heat production (Jastroch et al., 2010), but can also be an indication of mitochondrial damage. Considering the observed decrease in other mitochondrial function parameters tested, one might expect to have seen an increase in proton leak following acetate treatment. This result, whilst it did not reach statistical significance (p = 0.052 in HCT116 and p = 0.069 in MCF7) warrants further investigation – which could include measuring mitochondrial membrane potential. An interesting consideration is that inducible proton leak has a role in removing ROS, so an inhibition in the mitochondria's ability to expel ROS could contribute to oxidative stress (Roland et al., 2011). Alternatively, the decrease in proton leak may simply arise as a result of the overall decrease in OCR relative to the untreated control. The final MitoStress parameter, non-mitochondrial respiration, is unaffected in both cancer cell lines, which confirms that changes in OCR are a direct result of changes to the mitochondria, and not mediated through changes in other oxygen-consuming processes in the cell, such as NADPH oxidase activity (Brand and Nicholls, 2011). Interestingly, acetate treatment did not appear to have any effect on the mitochondrial function of the non-cancerous MCF10A cells, which at this stage could suggest that acetate has no effect on MCF10A cells, or that any effect may not be sufficient to modulate mitochondrial function.

3.14.3 | The Effects of Acetate on ROS

The decreased mitochondrial function could be an indication that acetate induces oxidative stress in cancer cells. To investigate this further, I measured a key marker of mitochondrial stress: ROS.

The production of ROS is a well-established indicator of cellular stress (Cadenas and Davies, 2000). Primarily produced from the mitochondria as a by-product of oxidative phosphorylation, increasing ROS levels has been identified as the mechanism in a number chemosensitisation studies using natural products, such as the sensitization of cells to DDP-induced cell death by saikosaponins,

curcubitacin B (El-Senduny et al., 2015) and *Boswellia ovalifoliolata* (Thummuri et al., 2014). Thus, the intentional induction of ROS is being increasingly identified as a new approach in cancer therapy (Zou et al., 2017).

ROS levels in acetate-treated cell lines were analysed via the DCFDA microplate assay. I found that ROS levels were increased following 24 hour treatment with 1-25 mM acetate in all cell lines. In MCF7 and MCF10A, this effect followed a strong dose-dependent pattern. In the cancer cell lines, the increased levels of ROS could provide an explanation for the observed decrease in mitochondrial function: being in close proximity to the site of ROS production, mtDNA is particularly sensitive to ROS-induced damage and therefore can result in decreased mitochondrial function (Shokolenko et al., 2009). Furthermore, ROS is known to inactivate and degrade mitochondrial proteins such as NADH dehydrogenase and NADH oxidase, again leading to inhibited function (Cadenas and Davies, 2000). ROS levels were also increased in the non-cancerous MCF10A cells in which acetate, based on SeaHorse results described in Section 3.14.2, had no impact on mitochondrial function. An explanation for this may be rooted in intrinsic differences in cancer cell metabolism: basal ROS levels are elevated in cancer cells to drive signalling pathways associated with promoting cellular proliferation (See Section 1.3.5). Thus ROS acts as double-edge sword to cancer cells, as it also renders them sensitive to further augmentations in ROS levels (Schumacker, 2006). Therefore, whilst acetate may be inducing stress in MCF10A cells, it would not appear to be sufficient to damage the mitochondria and induce a state of oxidative stress.

The DCFDA assay is one of the most widely used probes to measure ROS (Eruslanov and Kusmartsev, 2010), yet there are several caveats to its use that should be considered: chief among these is the complex intracellular chemistry of DCDFA, which means it can be oxidised by non-ROS species such as cytochrome *c* (Kalyanaraman et al., 2012). Therefore, to strengthen and expand these experiments, future work could include the use of MitoSOX, a mitochondria-specific probe for the superoxide anion. Not only does this probe provide a direct measurement of ROS (Robinson et al., 2008), targeting the mitochondria can also strengthen arguments that acetate is inducing mitochondrial stress.

3.14.4 The Effects of Acetate on Intracellular Ca^{2+}

Interactions between the mitochondria and intracellular Ca^{2+} ($[Ca^{2+}]_i$) can provide a mechanistic link between changes in mitochondrial metabolism, increases in ROS production, and potentially, sensitivity to apoptosis initiation. Because of the relationship between ROS, and Ca^{2+} (described in section 1.3.7), I expected to see an increase in $[Ca^{2+}]_i$ to accompany the increased levels in ROS, which would further demonstrate that acetate induces oxidative stress. In this study, I found that 24 hour 10 mM acetate treatment increased levels of $[Ca^{2+}]_i$ in a dose-dependent manner.

It is important, however, to consider here the nature of the increased $[Ca^{2+}]_i$ signal in this study, and how changes in signal can be interpreted. The Fluo-4 stain used in this study is not targetable to specific organelles; the esterases that hydrolyse the dye are primarily (but not exclusively) localized in the cytoplasm, meaning an increase in Fluo-4 signal could correspond to increased $[Ca^{2+}]$ anywhere in the cell (Contreras et al., 2010). Total cellular Ca^{2+} can be considered to have two sources: entry from the outside the cell or release from internal stores, such as the ER or mitochondria (Contreras et al., 2010). Therefore, at this stage I cannot exclude the possibility that an increase in signal could be a consequence of Ca^{2+} entry from either source. However, in a review of commonly used Ca^{2+} stains, Thomas et al. found that following immediately following loading, Fluo-4 initially displays a uniform cytoplasmic signal, accompanied by a more intense, yet uniform signal in the nucleus. Interestingly, after a 30 minute incubation at 37ºC, images revealed a marked mitochondrial/ER accumulation (Figure 35) (Thomas et al., 2000). As this 30 minute, 37ºC incubation was used in the protocols in this study, the observed increased $[Ca^{2+}]$ signal following acetate treatment may attributable to increased Ca^{2+} in the intracellular stores, including the mitochondria.

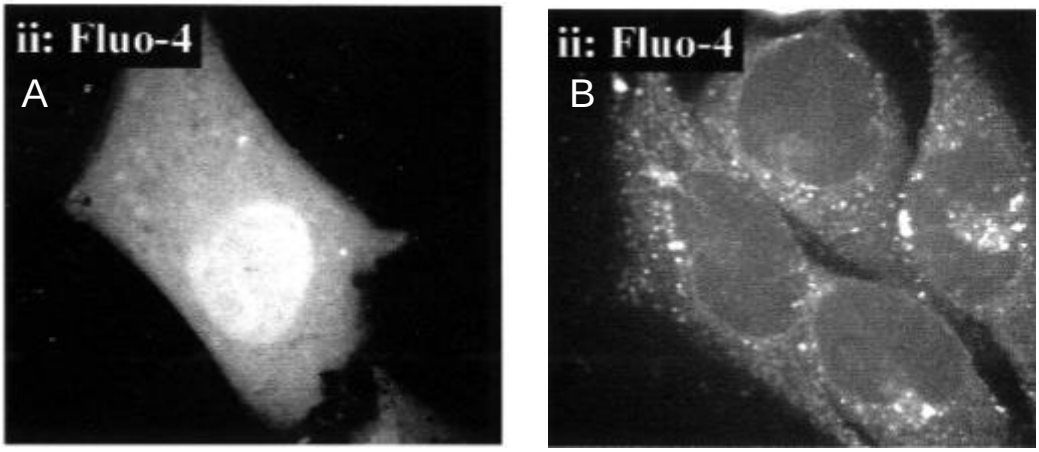

Figure 35 | Mitochondrial Accumulation of the Fluo-4 Calcium Dye. Loading HeLa cells with 1 µM Fluo-4 initially shows a uniform distribution in the cytosol, with a more intense, yet uniform distribution in the nucleus (A). After 30 minutes incubation at 37°C, Fluo-4 shows marked mitochondrial/ER accumulation (B) Images taken from Thomas et al., 2000.

The sustained increased of Ca^{2+} in the mitochondria ($[Ca^{2+}]_m$), known as calcium overload, is known to cause oxidative stress and is considered an important contributor to mitochondrial ROS production, generating ROS through a number of mechanisms. Such pathways include the indirect stimulation of OXPHOS through TCA cycle activation, resulting in a boost in OXPHOS substrate synthesis (e.g. NADH and FADH) (Feissner et al., 2009), nitric oxide production (Peng and Jou, 2010), and Ca^{2+}-mediated opening of the mitochondrial permeability transition pore (mPTP). In the latter mechanism, cytochrome *c* escape through the mPTP is thought to inhibit electron transfer between complex III and IV in the ETC (See Section 1.3.4, Figure 3 and Table 1), with the subsequent ETC dysfunction resulting in increased ROS production (Peng and Jou, 2010). Although Ca^{2+} is widely known to be essential to the process, the mechanism by which $[Ca^{2+}]_m$ triggers mPTP opening remains poorly understood, in part due to the yet-unresolved composition of the mPTP (Wong et al., 2012).

Although now not generally considered an essential component of the mPTP (Kwong and Molkentin, 2015), voltage-dependent anion channels (VDACs), are important regulators of $[Ca^{2+}]_m$ and may also play a role in acetate-induced changes in $[Ca^{2+}]_m$. Interactions with VDAC have been identified as the mechanisms by which CBD causes changes in $[Ca^{2+}]_m$; inhibition of VDAC1 by the

cannabinoid CBD has been shown to induce apoptosis in BV-2 murine microglial cells (Rimmerman et al., 2013), and prime breast cancer cell lines for DDP-induced cell death via decreased expression of the *VDAC1* gene (Henley, 2015). The effect of acetate on VDAC expression will be discussed in more detail in Section 3.14.8.

Another molecule implicated in the mPTP is the adenine nucleotide translocator (ANT), the presence of which is more conserved in proposed models of the mPTP compared to VDAC (Kwong and Molkentin, 2015). ANT sits on the IMM and exchanges OXPHOS-produced ATP for ADP. Because of its role in supplying the ETC with ADP, ANT activity is essential for maintaining OXPHOS activity. ANT is also thought to act as a mitochondrial uncoupler – mediating proton leak across the mitochondria membrane and decreasing mitochondria membrane potential ($\Delta\psi_m$). As ROS production increases with $\Delta\psi_m$, ANT and other uncoupling proteins are thought to play a role in protecting the mitochondria against oxidative damage (Kim et al., 2010). ANT (specifically the ANT2 isoform) may have a role in supporting cancer cell metabolism, as it has been found when OXPHOS activity is impaired, ANT can supply the mitochondria with glycolytically-produced ATP into the mitochondria, maintaining mitochondrial integrity and thereby promoting cellular survival (Chevrollier et al., 2011). Targeting ANT may therefore may present an important target in promoting cancer cell death or increasing sensitivity to apoptotic treatments. Interestingly, work by Jan et al. suggested ANT has a role in how the SCFAs induce apoptosis, as inhibition of ANT removed the apoptotic effect of mixed acetate/propionate treatment in HT29, HeLa, and Caco2 cancer cell lines (Jan et al., 2002). In addition, valproic acid (VPA, a branched SCFA that like acetate, propionate, and butyrate has HDAC inhibitory activity), regulated expression of ANT (specifically, ANT4), which the authors speculate may contribute to the observed VPA-induced $[Ca^{2+}]_m$. overload (Ji et al., 2015). Thus, it may be useful to observe how acetate affects ANT expression, particularly in light of my data showing acetate to have a significant effect on mitochondrial metabolism.

Mitochondrial calcium overload is also known to affect changes in mitochondrial morphology, such as swelling or fragmentation of the mitochondrial

network, both of which are early steps in apoptosis initiation (Giorgi et al., 2012), which is examined in Section 3.8 and discussed in Section 3.14.5.

The role of Ca^{2+} in apoptosis and oxidative stress makes it an attractive target in cancer therapy; changes in Ca^{2+} following treatment are well documented in many chemosensitisation and chemopreventative studies, such as in melatonin (Dai et al., 2002), resveratrol (Sareen et al., 2007) and curcumin (Xu et al., 2015a). Based on the above discussion, it may be possible that the state of oxidative stress, characterised by increased ROS and decreased mitochondrial function, may be a result acetate-induced calcium overload.

To confirm this, the short-term effects of acetate on Ca^{2+} should be investigated. Butyrate, the longest of the SCFA, has been found to increase $[Ca^{2+}]_i$ immediately following treatment, which the authors attributed to interactions with the g-coupled protein receptors FFAR2 and FFAR3 (Miletta et al., 2014). Since acetate is also known to interact with FFAR2 and FFAR3, (Schug et al., 2016), I would propose that through similar interactions, the elevated ROS shown in this study is a result of acetate-induced $[Ca^{2+}]_i$ increase. This is tested in Section 3.14.8.

Crucial to the hypothesis that oxidative stress is induced by acetate mediated mitochondrial Ca^{2+} overload is that the observed increased in Ca^{2+} fluorescence is caused by increased mitochondrial Ca^{2+}. Therefore, despite Thomas et al. demonstrating Fluo-4 may accumulate in the mitochondria and/or ER, it is essential that future work should include the use of mitochondrial-specific Ca^{2+} probes, such as Rhod2 (ThermoFisher, UK) (Fonteriz et al., 2010).

3.14.5 | The Effects of Acetate on Mitochondrial Morphology

To further understand the observed changes in mitochondrial function described in Section 3.14.2, the mitochondria of 24 hour 10 mM acetate or media-treated cells were observed using the MitoTracker DeepRed stain via confocal microscopy (figure 20). From visual observations, the mitochondria of cells treated with 10 mM acetate for 24 hours seemed to reduce in length (more apparent in

HCT116 cells) or swell (more apparent in MCF7 cells) compared to their untreated counterparts. SCFA-induced swelling has been observed following acetate and propionate treatment of isolated mitochondria, which implied that bacterially-produced SCFA induced-apoptosis was mediated by the mitochondria (Jan et al., 2002). The morphology of MCF10A mitochondria, despite the cell line following similar dose-dependent increases in ROS and Ca^{2+} as the cancer cell lines, appeared unaffected by acetate treatment.

In order to quantify these subjective changes, images were analysed using the MitoLOC plugin for ImageJ. My analysis found that the number of mitochondria per cell was significantly decreased in both HCT116 and MCF7 cells compared to untreated cells. However, there were no changes in the average area of individual mitochondria or the average total mitochondrial area per cell. In contrast, acetate treatment of MCF10A cells caused a significant decrease in average mitochondria area, whilst having no significant effect on the number of mitochondria per cell. In Table 11, I suggest possible criteria for identifying mitochondrial fusion, fission, or mitophagy.

	Mitochondrial Count	**Average mitochondrial area**	**Total mitochondrial area**
Fusion	Decreased	Increased	No change
Fission	Increased	Decreased	No change
Mitophagy	Decreased	No change	Decreased

Table 11 | Interpretation of MitoLOC Data. The three parameters measured in the MitoLOC image analysis, and what changes in each could mean in terms of mitochondrial dynamics.

The data from HCT116 and MCF7 cells would therefore suggest that acetate is not inducing fusion, fission or mitophagy. Fewer mitochondria per cell is however consistent with the decreased function observed in Section 3.14.2. Acetate may induce fission in MCF10A cells, as there is a trend towards increased mitochondrial number per cell following acetate treatment ($p = 0.06$).

Fission of mitochondria is a pre-requisite step in apoptosis, and is also associated with oxidative stress (Frank et al., 2012) (As described in Section

1.3.1). This observation is therefore contrary to results from this study which indicate that acetate treatment is not sufficient to induce oxidative stress in MCF10A cells. One plausible explanation could be that the apparent acetate-induced fission in MCF10A is a pre-requisite step for the removal of damaged mitophagy, preparing to clear damaged mitochondria in order to mitigate a state of oxidative stress. This response has been observed following ROS accumulation (Frank et al., 2012), which is also observed in MCF10A cells in this study following ROS treatment.

Overall, whilst acetate does induce significant effects in mitochondrial size and number it is unclear exactly what these changes mean in terms of fission, fusion and mitophagy. It is therefore crucial for future work to include investigations into the detection of mitophagy, for which several techniques are available, including flow cytometry of MitoTracker-labelled cells in combination with mitophagic and lysosomal inhibitors (Mauro-lizcano et al., 2015), using fluorescence microscopy to monitor localization of mitochondrial markers to autophagic machinery markers (Dolman et al., 2013) or western blot for mitochondrial proteins (Ding and Yin, 2012), which were unfortunately not possible in this study due to financial constraints.

Additionally, mitochondria are highly dynamic structures, and can move at along cytoskeleton networks at speeds of up to 5 µm per second (Zheng et al., 2010), and fusion and fission events have been shown to occur at a rate of approximately 1 event per minute per cell in *Dictyostelium discoideum* (Woods et al., 2016). Therefore, with mitochondria in constant state of flux, single images may not represent the full extent of the effect of acetate on mitochondria dynamics. Future work should include time lapse images to assess changes in dynamics and morphology. This was not possible in current study, as the microscope used did not have an incubated stage and had to operate at a relatively high power to obtain images, which may photo bleach the stain or affect the cells.

Another point to consider is the impact of acetate-induced increase in Ca^{2+} on mitochondrial morphology. Increased $[Ca^{2+}]_m$ overload is associated in particular with increased fission (Kaddour-Djebbar et al., 2010). Based on the

increased levels of Ca^{2+} following acetate treatment, one might therefore expect to see mitochondrial fission in all three cell lines. However, Ca^{2+} overload-induced fission is also associated with apoptosis (Kaddour-Djebbar et al., 2010), which was not observed following acetate treatment in this study. Therefore, the increase in Ca^{2+} caused by acetate treatment may not be of a sufficient level to induce apoptotic-associated mitochondrial fission.

It should be noted that the analysis of the mitochondrial images has several weaknesses. Firstly, the MitoLoc plugin was developed for super-resolution images; Vowinckel et al. used a 100X objective, whereas due to the setup of the Leica SP2, 63X was the highest magnification available to me at the University of Westminster for live cell imaging. Secondly, MitoLOC was developed using *Saccharomyces cerevisiae*, which contain fewer mitochondria than human cells, making isolation of individual mitochondria far easier. The combination of these factors is most apparent when analysing MCF10A cells, which contain large numbers of highly interwoven mitochondrial networks, which the MitoLoc plugin often counted to be a single, enormous mitochondrion. Nevertheless, the data provided is still useful for detecting and quantifying large-scale changes in mitochondrial morphology, as long as care is taken to account for these limitations.

In order to overcome some of these shortcomings, flow cytometry was also with the goal of quantifying the intensity of MitoTracker Deep Red in untreated and acetate-treated cells, based on work by Tailor et al. Tailor suggested that a decrease in MitoTracker Deep Red signal was an indicator of increased mitochondrial fusion, and found that treatment with butyrate, the longest of the SCFA, resulted in a dose-dependent decrease in what was described as “Active Mitochondrial Mass” – and thus increased mitochondrial fusion (Tailor et al., 2014). The results obtained for HCT116 and MCF7 cells indicated that there was no change in signal intensity following treatment with 10 mM acetate, but do show significant increases following 25 mM acetate treatment. This is somewhat contradictory to the image analysis, as one might expect a decrease in intensity if there are fewer mitochondria than in the control.

This result may be explained by the fact that uptake of the MitoTracker Deep Red stain is mitochondrial potential-dependent, and so factors affecting

mitochondrial membrane potential could affect the staining intensity (Xiao et al., 2016). Therefore mitochondria sufficiently damaged by oxidative stress may not be visible.

Overall, the combination of image analysis and flow cytometry data would suggest that acetate has a limited effect on mitochondrial shape. However, the significant decrease in mitochondrial number per cell in cancer cells, combined with decreased function and elevated ROS and Ca^{2+}, could indicate mitochondria are being damaged, and subsequently removed by autophagy.

3.14.6 | The Effects of Acetate on Autophagy

Autophagy is the process by which cells maintain homeostatsis through the controlled degradation and recycling of cells or celluar components. Levels of autophagy are generally thought to increase under condititions of stress to ensure cellular survival. Autophagy and apotosis are interwined – excessive autophagy can result in apoptosis, but autophagy has also been considered a response to limit apoptosis. This relationship is further complicated in cancer: genes promoting autophagy are often found to be under expressed in cancer, yet it is considered an essential process to support proliferation and survival in the stressful condtions of the tumour microenvironment (Mathew et al., 2007). Based on this, one may expect acetate to increase autophagic actvity as a response to the observed acetate-induced oxidative stress. This has been reported with propionate and butyrate treatments (Tang et al., 2010). Additionally, the significant decrease in mitochondrial number observed in response to acetate treatment may be a result of mitochondrial degradation, known as mitophagy. However, in this study acetate was observed to have no signficant effect on autophagy induction in any cell line. Although this may not align with effects of other SCFAs, a lack of autophagy may improve the potential of acetate as a priming agent, as autophagy is known to mediate and protect against apoptosis (Yonekawa and Thorburn, 2013). Furthermore, because of its role in cancer as an alternative fuel, acetate may alleviate the conditions of nutrient starvation needed to trigger autophagy. Whilst literature investigating the effects of acetate on autophagy is sparse, accumlation

of acetate in the cell by blocking its conversion into acetyl CoA has been shown to reduce autophagy in yeast and drosphillia (Eisenberg et al., 2014). More work is required to fully explore the effects of acetate on autophagy, espescially as there is no one “gold standard” autophagy test. Therefore, it is recommended to combine multiple techniques such as immunobloting for autophagic markers such as LC3 and p62, or the imaging of autophagic structures such as lysosomes (Zhang et al., 2016).

3.14.7 | The Effects of Acetate on the Cell Cycle

The unrestrained proliferation of cancer cells is often a consequence of cell cycle dysregulation (Collins et al., 1997), a series of events and checkpoints leading up to the division of a cell. These are four major events within a cell cycle: G_1, duplication of cellular contents, S: the duplication of cellular DNA, G_2: checking the duplicated DNA for errors, and Mitosis (M); the division of the cell into two. Targeting the cycle has been a popular target in cancer chemotherapy (Schwartz and Shah, 2005). Not only does inhibition of the cell cycle prevent proliferation, it can also induce or sensitize cells to apoptosis (Vermeulen et al., 2003). The results from my experiments show that acetate induces a dose-dependent increase in G_2-M arrest in HCT116 cells. Manipulating the G_2-M checkpoint, both by bypassing it altogether and arresting cells at that stage, has been shown to lead to increased sensitivity to apoptosis (DiPaola 2002). The G_2-M checkpoint acts as a protective stop-gap, providing a cell time to repair damage to its DNA before apoptosis is triggered. This suggests that bypassing the checkpoint could increase the effectiveness of DNA-damaging drugs, and indeed agents that inhibit G_2 checkpoint regulating enzymes have been found to be effective at increasing the cytotoxicity of chemotherapeutic drugs (Jackson et al., 2000). In contrast, arrest at G_2-M has also been identified to improve apoptotic response, for example combination treatment with the anticancer drug doxorubicin and silibinin, an active ingredient found in milk thistle extract, was found to substantially increase the population of cells in the G_2-M phase, which resulted in greater induction of apoptosis compared to each agent alone (Tyagi et al., 2002). G_2-M arrest has also been identified in butyrate, and, to a lesser extent, propionate (Matthews et al.,

2007). However, the authors of this study reflect that the effects of the SCFA on the cell cycle may be cell-type dependent, as butyrate treatment has been identified to induce G_0/G_1 arrest in lymphoma cells, although the end result was still the induction of apoptosis (Duan et al., 2005).

Therefore in this study it would have been interesting to compare the effects of acetate on each different cell line. However, only HCT116 cells were able to be analysed, due to both MCF7 and MCF10A fixing into clumps which blocked the flow cytometer. This could be a result of combination of the specific flow cytometer having a narrow probe, or difficulty in preparing single cell suspensions following ethanol fixation. It is therefore imperative that future work includes repeating this assay on MCF7 and MCF10A cells. In addition, further work is needed to identify if the observed G_2-M arrest is linked to the acetate-induced effects on the mitochondria.

Also interesting to consider is the relationship between the cell cycle and ROS. In Section 1.3.5.1 it is discussed that by modulating the redox state of the cell, ROS production can effectively regulate the cell cycle. Since ROS is elevated in HCT116 following acetate treatment, it may be possible that the observed G_2-M arrest is caused by ROS production. Such a mechanism has been identified in cardamonin, an extract of the cardamom spice. In that study, it was reported that the cardamonin-induced G_2-M arrested was caused by increased expression of cyclin D1 and p21, an effect that was reversed using the ROS inhibitor n-acetyl-L-cysteine (NAC) (Li et al., 2017). Similar mechanisms have been identified in other natural products, such as in human osteosarcoma cells treated with erianin, an extract of the Chinese orchid *Dendrobium chrystoxum* (Wang et al., 2016) and in lung adenocarcinoma cells treated with curcubatin B, a triterpenoid found in many plants (Guo et al., 2014). As was found in cardamonin, the G_2-M arrest effect of erianin and curcubatin B was inhibited by treatment with NAC. Therefore, additional experiments should include studies of the effect of NAC following acetate treatment, to determine whether the observed G_2-M arrest is ROS-dependent.

3.14.8 | The Effects of Acetate on Gene Expression

It is well documented that the SCFAs can alter gene expression (Astakhova et al., 2016). To further examine these effects in a metabolic context, I measured the expression of genes related to acetate metabolism, namely *ACSS1* and *ACSS2*, *as* well genes involved in the regulation of mitochondrial processes that have so far been examined; *VDAC1* for the regulation of mitochondrial Ca^{2+}, *Nrf2* for the regulation of the cell's defences against oxidative stress, and *p53*, which regulates the cell cycle and apoptosis.

3.14.8.1 | The Effect of Acetate on ACSS1 and ACSS2 Expression

The proteins ACSS1, localised to the mitochondria, and ACSS2, localised to the cytosol, catalyse the conversion of acetate into acetyl CoA – the primary metabolic fate of acetate (Schug et al., 2016). Changes in the expression of both genes are well documented in cancer, with the silencing of both being associated with decreased cancer cell viability (Yun et al., 2009) and reduced tumour formation in mice models (Comerford et al., 2014). The increased expression of *ACSS2* in particular is linked to an aggressive cancer phenotype, thought to be as a consequence of the increased carbon contribution of acetate into biosynthetic and energetic pathways in cancer cells (Lakhter et al., 2016). In my study, acetate treatment caused an increase in *ACSS1* in MCF7, and a decrease in MCF10A – although neither change was statistically significant compared to the untreated controls. ACSS1 was not expressed in HCT116. ACSS2 expression on the other hand was significantly higher in MCF7 and MCF10A. Even though higher expression of ACSS2 is linked to tumour survival, increased expression has been observed as a response to metabolic stress (Schug et al., 2015), and so this increase in expression could be a response to acetate induced stress.

3.14.8.2 | *The Effect of Acetate on VDAC1 Expression*

The *VDAC1* gene encodes the VDAC1 channel on the OMM, which enables the exchange of metabolites, notably ATP and Ca^{2+}, between the mitochondria and cytosol. This key function in metabolism has led to VDAC being described as a “governor” of mitochondrial function and metabolism (Lemasters et al., 2012). As such, the levels of expression of *VDAC* are of particular interest to scientists with respect to a variety of disease states, such as Parkinson’s and cancer (Camara et al., 2017). In cells treated with acetate, there was a trend towards increased expression of *VDAC1* in each cell line; although only in MCF10A cells did this increased expression reach statistical significance compared to untreated cells. Increased expression of *VDAC1* has been linked to increased mitochondrial permeability and apoptosis (Liu et al., 2011), as well as enhanced sensitivity to DNA cross-linking agents such as cisplatin (Sharaf El Dein et al., 2012). Increased intracellular Ca^{2+} has been shown to upregulate *VDAC1* expression (Weisthal et al., 2014) – and as acetate treatment is shown to induce increased intracellular Ca^{2+}, this provides a plausible explanation for the observed increased expression in VDAC1. VDAC is also known to have anti-apoptotic roles; binding by HK has been shown to protect against Bak/Bak-induced apoptosis. This role however is determined by HK expression, which was not measured in this study.

3.14.8.3 | *The Effect of Acetate on Nrf2 Expression*

Nrf2 encodes a transcription factor that regulates the expression of a number of antioxidant proteins as part of the cell’s response against oxidative stress. Under normal conditions, *Nrf2* is broadly expressed, but its activity is suppressed by Kelch like-ECH-associated protein 1 (KEAP1) and Cullin 3 which together rapidly turnover Nrf2 via ubiquination, which marks proteins for degradation via the proteasome. Oxidative stress disrupts the structure of Cullin 3, disrupting the ubiquitination pathway and allowing Nrf2 to accumulate in the cytosol. Nrf2 then translocates to the nucleus, where it associates with a family of proteins called the small Maf proteins. These dimers then bind to antioxidant

response elements on DNA, upstream of a variety of antioxidant genes, inducing their transcription (Qiang, 2013; Yamamoto et al., 2008). In the present study, *Nrf2* expression was significantly decreased in acetate treated HCT116 cells, whilst expression in MCF7 and MCF10A were unaffected by acetate treatment. The reduced expression may explain the greater ROS response and decrease in mitochondrial respiration in HCT116 cells compared to MCF7 and MCF10A following acetate treatment, as *Nrf2* KO cells demonstrate impaired mitochondrial function, diminished mitochondrial membrane potential, and elevated levels of ROS (Holmstrom et al., 2013). This effect is particularly interesting with respect to priming, since inhibiting *Nrf2* expression has been identified as a means to sensitise bile duct cancer cells to cisplatin induced cell death (Sompakdee et al., 2018).

3.14.8.4 | The Effect of Acetate on p53 Expression

p53 encodes what is perhaps the most well-known tumour suppressor protein, tumour protein 53. It's role in the suppression of cancer progression is well documented, as it affects various mechanisms including cell cycle arrest, activation of DNA repair, and the initiation of apoptosis should DNA repair fail (Ozaki and Nakagawara, 2011). p53 has also been shown to directly regulate apoptosis by localising to the mitochondria-ER interface following stress, facilitating movement of Ca^{2+} from the ER into the mitochondria, causing mitochondria Ca^{2+} overload and subsequent apoptosis (Giorgi et al., 2015).

In HCT116, *p53* expression was significantly reduced by treatment with acetate. Expression levels were unaffected by acetate in MCF7 and MCF10A cells. The loss of p53 in HCT116 in this context is somewhat surprising considering the well-defined role of *p53* in cancer cells; loss of p53 function is observed in more than half of human cancers (Ozaki and Nakagawara, 2011). However, the observed decrease in p53 expression may contribute to the state of oxidative stress induced by acetate treatment in HCT116 cells, as it is also shown to play an antioxidant role. Sablina et al. observed that siRNA inhibition of *p53* caused an elevation of intracellular ROS (Sablina et al., 2009). Additionally, the

role of p53 in DNA repair and protection against DNA damage may contribute to resistance to DNA targeting drugs (such as cisplatin), and so a reduction in expression could confer a state of chemosensitivity (Ferreira et al., 1999).

3.14.8.5 | Conclusions on the Effect of Acetate on Gene Expression

Despite consistent responses across cell lines in metabolic markers such as viability, ROS and Ca^{2+}, the effect that acetate had on the expression of the genes studied appeared to follow no apparent cohesive pattern. This discrepancy may be as a result of acetate's role as a HDAC inhibitor (Brody et al., 2017; Soliman and Rosenberger, 2011). Described in Section 1.8.3.4, HDACs are a class of enzyme that catalyse the removal of acetyl groups from histones, causing DNA to wrap more tightly around them, restricting the access of the transcription machinery and thus inhibiting gene expression (Barneda-Zahonero and Parra, 2012). By inhibiting these enzymes, acetate can affect gene expression by modulating the binding of transcription factors and other regulatory proteins to DNA. Thus, acetate could be affecting the expression of a large number of genes beyond the scope of what was investigated in this thesis, and with no one particular gene targeted over another. The non-specificity of HDAC inhibition is clear in the development of HDAC inhibitors as drugs, which are shown in clinical trials to exhibit broad side effects. It is therefore crucial to discover the exact roles of individual HDACs in different types of cancer (Chen et al., 2015).

It is also interesting to note that the despite the varying effects of acetate on gene expression, the overall effect of acetate on cellular metabolism was consistent across the three cell lines. This may indicate the oxidative stress induced by acetate can be accentuated through different epigenetic mechanisms across the different cell types. To address these points, future work should examine the effects of acetate on a much wider range of genes, by employing techniques such as DNA microarray analysis.

Finally, it is important to recall that changes in gene expression may not always correlate to changes in protein expression or even protein activity. Therefore, this section of work can be verified by protein quantification, not included in this study due to time restraints.

3.14.9 | The Effects of Short Term Acetate Treatment on Mitochondrial Function and Intracellular Ca^{2+}

The focus of my work thus far has explored the effects of acetate 24 hours following treatment. *In vivo*, exogenous SCFA treatment has been shown to be metabolised within 60 minutes in mice (Ge et al., 2008), so to provide a clearer mechanistic picture as to how acetate induces oxidative stress 24 hours after treatment, I studied the effect of acetate in a shorter time period. Using the SeaHorse, I found that the injection of acetate caused an immediate increase in mitochondrial respiration, which was sustained across the total 12 hours of the assay, which is in contrast to the observations that mitochondrial respiration is decreased 24 hours following acetate treatment. The increase after 12 hours was statistically significant only in HCT116 cells, although similar trends were observed MCF7 and MCF10A cells. The increase in OCR was accompanied by an immediate drop in ECAR, again sustained over the 12 hours of measurement, and this decrease was significantly lower than the control in each cell line. This would suggest that acetate is inducing an immediate increase in OXPHOS and subsequent decrease in glycolysis. This suspected change in glycolysis was investigated in more detail using the SeaHorse GlycoStress test, which confirmed a significant decrease in glycolysis in each cell line. As with OCR, the effect was most pronounced in in HCT116 cells, in which decreases in glycolytic capacity (a measure of the cell's capacity to respond to the energetic demand of stress) and glycolytic reserve (a measure of the cell's ability to utilize glycolysis beyond the basal rate) were observed.

The next step was to investigate how acetate is causing this immediate change in mitochondrial function. One of the mechanisms that has been discussed in this study is the interaction between calcium signalling and oxidative phosphorylation.

As mentioned in Section 1.8.3.3, acetate acts as a ligand for the g-coupled protein receptors FFAR2 and FFAR3, displaying the greater affinity for FFAR2 (Brown et al., 2003). FFAR2 Is coupled to both G_Q and $G_{i/o}$ signalling pathways. The binding of a ligand to a g-coupled protein that is coupled to the G_q pathway results in the cleavage of phosphatidylinositol 4,5-biphopshate (PIP_2) into

diacylglycerol (DAG) and inositol 1,4,5-triphosphate (IP_3). IP_3 interacts with the Ca^{2+} channels on the endoplasmic reticulum, triggering the release of Ca^{2+} into the cytosol, increasing intracellular Ca^{2+} (Berridge, 1993). I therefore hypothesised that acetate treatment would induce an acute increase in intracellular Ca^{2+}. This has been reported following treatment with butyrate by Miletta et al., who also demonstrated that silencing *FFAR2* and *FFAR3* inhibited the butyrate-induced increase in intracellular Ca^{2+} (Miletta et al., 2014). The rapid increase in Ca^{2+} was observed in HCT116 and MCF10A cells, and although an increase was seen in MCF7, the effect size was small and may warrant further study. It is known that Ca^{2+} can increase the rate of OXPHOS (Hajnóczky et al., 1995; Hawkins et al., 2007), which has been observed in this project in response to acetate treatment. Interestingly, MCF7, which displayed the smallest Ca^{2+} response to acetate treatment, also displayed the smallest change in OCR. These results would indicate that acetate treatment causes an increase in mitochondrial respiration via FFAR2 and FFAR3 mediated Ca^{2+} release. Future work to test this hypothesis should include the knockdown of *FFAR2* and *FFAR3* to examine whether this blunts the Ca^{2+} response to acetate treatment.

3.15 | A Summary of the Effects of Acetate

The results of this chapter are briefly summarised in Table 12, which shows that 24-hour acetate treatment has a similar effect on cancer and non-cancer cell lines, save for two important distinctions. 24-hour treatment had no effect on non-cancerous mitochondrial respiration and no effect on the number of mitochondria per cell (although the average mitochondrial mass per cell was decreased). Acute acetate treatment also appeared to have no significant effects on the non-cancerous cell line.

	Cancerous Cells	Non-Cancerous Cells
MEASURE	**ACUTE TREAMENT**	
Mitochondrial Respiration	Increased[1]	No significant effect
Glycolysis	Decreased	No significant effect
Intracellular Ca^{2+}	Increased	No significant effect
	24 HOURS POST ACETATE TREATMENT	
Cell Viability	No significant effect	No significant effect
Apoptosis	No significant effect	No significant effect
Mitochondrial Respiration	Decreased	No significant effect
Reactive Oxygen Species	Increased	Increased
Intracellular Ca^{2+}	Increased	Increased
Mitochondrial Number	Decreased	No significant effect
Mitochondrial Area	No significant effect	Decreased

[1] In HCT116 and not MCF7

Table 12 | **Summary of the Effects of Acetate**. Cancerous cells: HCT116 and MCF7. Non-cancerous cells: MCF10A. Results were only considered decreased or increased if they were significantly different to their respective controls. Results that were not significantly different are labelled "no effect". Gene expression analysis (for which results were cell-type dependent) and results for experiments that did not include all 3 cell lines are omitted for clarity

The results would indicate whilst acetate treatment does not induce cell death in any of the cell lines studied here, it causes a state of oxidative stress (decreased mitochondrial function) in the cancerous cell lines through a specific mitochondrial pathway (increased ROS, Ca^{2+} and decreased mitochondrial number). Even though similar pathways were affected in the non-cancerous cell line, the effects did not seem to be sufficiently robust to induce a state of oxidative stress. The consequences of these differences, and what it means for acetate as a priming agent, are discussed in Section 6.

The evidence gathered in this section strongly suggests that acetate interacts with the mitochondria of the cell. The observed decreases in respiration, changes in ROS, Ca^{2+}, mitochondrial morphology and gene expression can all be linked by opening of the mPTP, leading to a decrease in mitochondrial membrane potential ($\Delta\psi_m$). Sustained loss of $\Delta\psi_m$ is a key step in the initiation of apoptosis and can be associated the observed with decreases in OXPHOS, increases in ROS and Ca^{2+} and changes in morphology (Zorova et al., 2018). Inducing decreased $\Delta\psi_m$ has been identified as the mechanism by which many molecules can sensitise cancer cells to drug-induced cell death, including curcumin (Xu et al., 2015), ursolic acid (Wu et al., 2016), and neferine (Sivalingam et al., 2017). In future, the effect of acetate on $\Delta\psi_m$ should be investigated both 24 hours after and immediately following treatment, which would serve to predict the potential of acetate as a priming agent. Based on findings from this section and as well as existing chemosensitisiation/priming literature, I would expect acetate to induce significant $\Delta\psi_m$ loss. Several methods are available to measure changes in $\Delta\psi_m$, including the (5,5′,6,6′-tetrachloro-1,1′,3,3′-tetraethylbenzimidazolylcarbocyanine iodide stain (known as JC-1), or the tetramethylrhodamine ethyl ester (TMRE) stain (Perry et al., 2011).

4.0 | Priming With Acetate

The effectiveness of chemotherapeutic drugs is often hampered by cytotoxic side effects. The rising incidence in cancer (National Cancer Institute, 2018) means that there is a need to develop methods of improving the efficiency of drugs, new and existing, whilst limiting the side effects experienced by patients. Priming, introduced in Section 1.7, is being investigated as a novel technique to improve drug efficacy, by manipulating the sensitivity of cancer cell mitochondria to apoptotic triggers (Chonghaile et al., 2011; Reed, 2011). Priming cells with natural products known to have anti-cancerous properties has been successfully demonstrated with compounds such as CBD (Henley, 2015) and curcumin (Zou et al., 2018). In this section, I investigate the use of acetate, a SCFA, as priming agent. Acetate is well documented to have chemopreventative effects both *in vitro* and *in vivo* (Brody et al., 2017). This, in combination with its availability from diet and circulation make it an attractive target as a priming agent.

To test this, I treated HCT116, MCF7 and MCF10A cells with acetate prior to, and in combination with, the widely used chemotherapeutic drug, cisplatin (DDP), the mode of action of which is well established (Section 1.5.1.2). In Section 3, I observed that treatment with 10 mM acetate induced a number of effects consistent with a state of cellular and mitochondrial stress, including enhanced ROS production, increased levels of intracellular Ca^{2+}, decreased mitochondrial function and alterations in mitochondrial morphology. A heightened level of stress can mean a cell is more likely to initiate apoptosis when faced with a second stress, in this case, the addition of DDP.

The priming protocol, including times between priming agent treatment and DDP treatment (see Section 2.13), and concentrations of DDP, was based of published priming work (Henley, 2015), as well as the elevated mitochondria stress markers seen at 24 hours following acetate treatment in Section 3. In this section of the study I compared 3 treatment protocols (see also Table 10, Section 2.17):

1.) **Priming**: 24 hour acetate treatment followed by 24 hour DDP treatment
2.) **DDP alone**: 24 hour control treatment followed by 24 hour DDP treatment
3.) **Combination**: 24 hour media treatment followed by 24 hour acetate and DDP treatment

In this chapter, the objective was as follows:

- To determine that if pre-treatment (priming) with acetate enhances the induction of cell death compared to treatment with drug alone.

4.1 | Effects of Priming with Acetate on Cellular Viability

The effects that priming, cominbation treatments, and DDP alone treatment had on HCT116, MCF7, and MCF10A cell viability compared to the untreated control were analysed by the MTT Viability assay (Figure 36).

In HCT116, all treatments caused a signifcant decrease in cellular viabilty compared to the untreated control. Priming with 10 mM acetate caused a significant decrease in cellular viabilty compared to treatment with 100 µM DDP (50.03 ± 2.65% vs 75.64 ± 3.60%, p = 0.001). 1 and 5 mM acetate priming treatments had so signifcant effect on viabilty compared to DDP treatment. Addiotnally Combination treatment had no significant effect on viabilty to compared to DDP treatment.

In MCF7, there was again a significant decrease in cell viabilty compared to the untreated control for all treatment groups. 1, 5 and 10 mM acetate-primed treatments all showed a significant, dose-dependant decrease in cell viablity compared to DDP treatment (1 mM acetate primed: 68.39 ± 3.88% p = 0.032, 5 mM acetate primed: 67.36 ± 2.34% p = 0.021 and 10 mM acetate primed: 60.74 ± 2.28% p = 0.001 vs DDP: 85.17 ± 2.83%). The combination treatment had no signifcant effect on vialbilty compared to DDP treatment alone.

In the control cell line MCF10A, all treatments showed a signifcant decrease in cell viabilty compared to the untreated control. 1, 5 and 10 mM acetate priming treatments had no signifcant effect on cellular viability compared to DDP treatment alone.

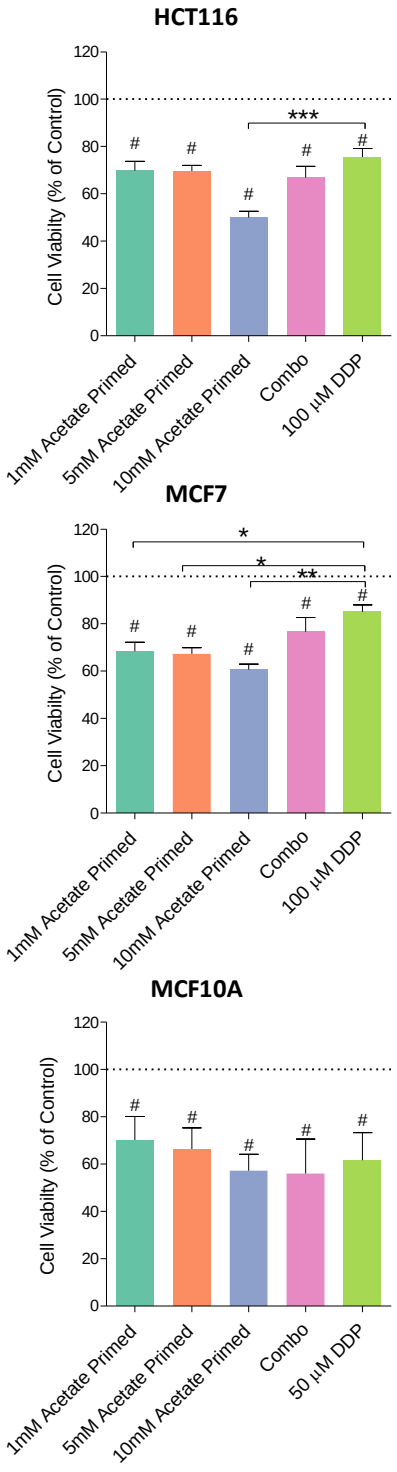

Figure 36 | The Effect of Priming with Acetate on Cell Viability. Bars represent mean cellular viability as percentage of the negative control (100%, indicated as horizontal dashed line) ±SEM of at least *n* = 5 independent experiments. Differences between treatment groups and untreated control analysed via Unpaired Students T-Test. # indicates significant (p <0.05) decrease in viability compared to negative control. Differences in the mean cell viabilities between treatment groups assessed via 1-way ANOVA followed by Tukey's Multiple Comparison Test * indicates significant difference in viability between indicated treatments (* p <0.05, ** p <0.001, ***p <0.0001).

4.2 | Effects of Priming with Acetate on Apoptosis

To investigate whether priming with acetate sensitises cells to DDP-induced cell death, the Annexin-V PI assay was used to measure apoptosis (Figure 37). In HCT116, priming with 10 mM acetate caused significant increases in apoptosis compared to DDP treatment alone (24.13 ± 4.53% vs 10.96 ± 0.769%, $p = 0.038$).

In MCF7, priming with 10 mM acetate also caused a significant increase in apoptosis induction compared to DDP treatment (44.94 ± 3.22% vs 34.84 ± 1.38%, $p = 0.028$)

In the control cell line MCF10A, priming with acetate had no significant effect on apoptosis induction compared to DDP treatment alone.

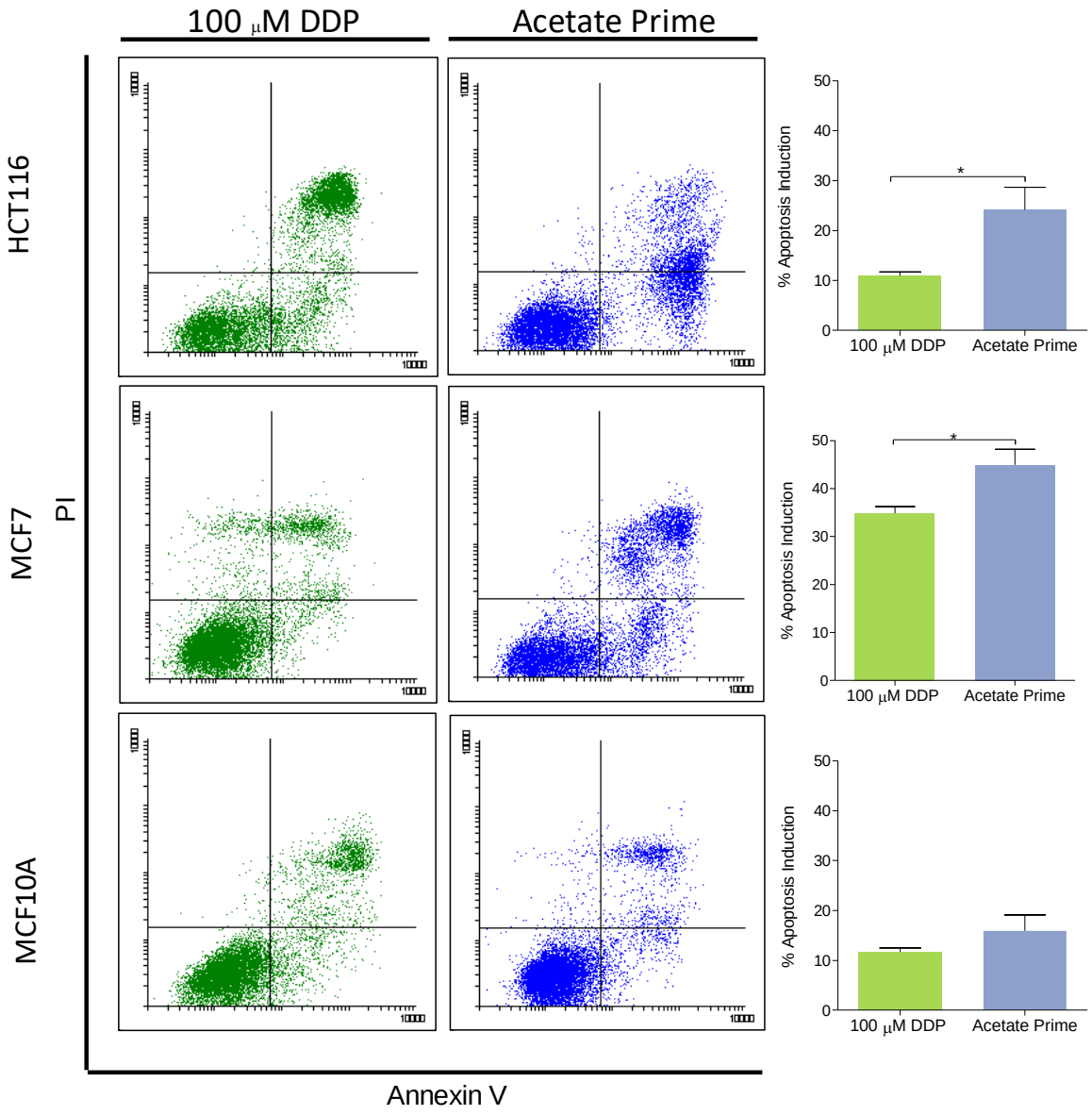

Figure 37 | The Effect of Priming with Acetate on Apoptosis. Bivariate dot plots (Representative) show cells/events plotted as function of Annexin V and PI MFI. Events in bottom right and top right quadrants were considered apoptotic. Bars represent mean percentage of total apoptotic events ±SEM from *n* = 5 individual experiments. Differences between priming and DDP-treated analysed with Unpaired Student's T-test. * indicates significant (p <0.05) difference between means. No asterisk means not statistically significant.

4.3 The Effect of Priming on Mitochondrial Function

Next, I analysed the effect of priming with acetate on mitochondrial function using the MitoStress Assay on the SeaHorse XF_e24 Flux Analyser. Only HCT116 cells were analysed (Figures 38 and 39) due to DDP treatment cells to detach from the surface of the SeaHorse plates. This is discussed in more detail in Section 4.4.2.

Priming with acetate and treatment with DDP both caused a large decrease in the basal respiration, which was significant compared to the untreated control in DDP treated cells (16.47 ± 8.22% of the control p = 0.009) and trending towards significance in primed cells (33.09 ± 18.31% of the control p = 0.067). The difference between primed and DDP-treated cells was not significantly different.

For the maximal rate of respiration, DDP treatment caused a large decrease in OCR compared to the untreated control (32.15 ± 15.44% of the control p = 0.0481). Priming appeared to have no significant effect on maximal respiration. The difference between primed and DDP-treated cells was not significantly different p = 0.531).

For ATP-associated OCR, rates were significantly decreased in DDP treated cells (17.27 ± 7.89% of the control p = 0.009), but not primed cells). The difference between primed and DDP-treated cells was not significantly different.

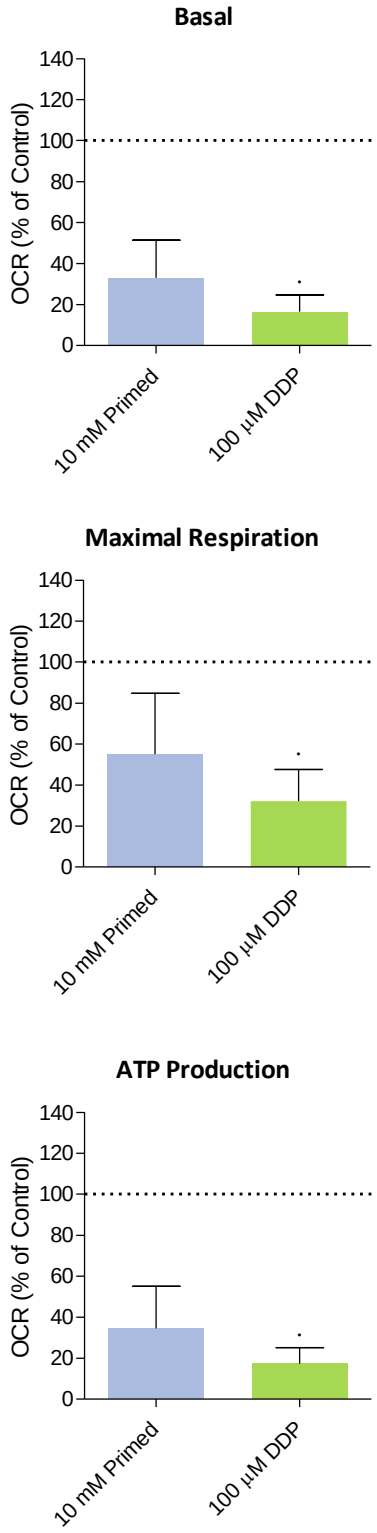

Figure 38 |The Effect of Priming with Acetate on Mitochondrial Respiration. Bar graphs show the individual parameters of the MitoStress test of HCT116 cells, presented as the mean percentage of the negative control ±SEM of *n* = 3 independent experiments. · indicates significance (p <0.05) with regards to the negative control. * indicates significance between primed and DDP treated cell. No · or * means no significant difference.

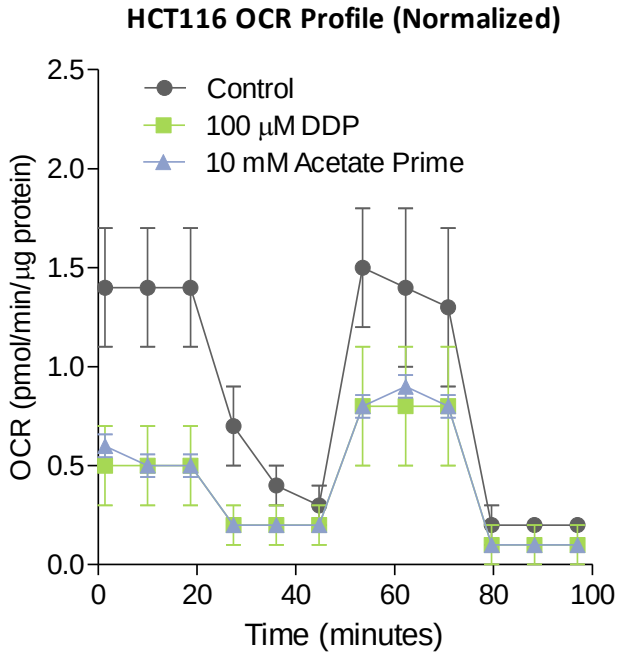

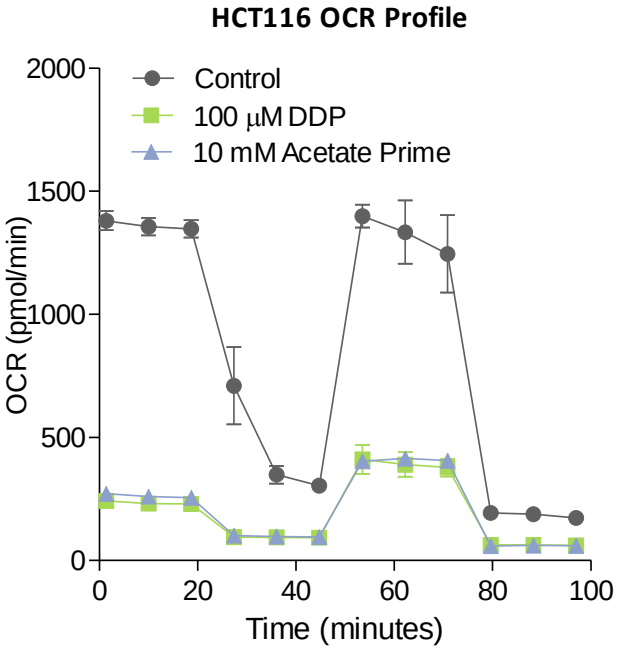

Figure 39 | The Effect of Priming with Acetate on Mitochondrial Respiration - OCR Profiles. (Representative) show change in HCT116 OCR over course of the MitoStress Assay. **A:** Data OCR normalized to protein content, measured via Bradford Assay**. B:** Unadjusted OCR data

4.4 | Discussion

4.4.1 | The Effects of Acetate Priming on Cell Viability and Apoptosis

Results from Chapter 3 present demonstrated that acetate treatments alone can modulate the function of cancer cell mitochondria, whilst having no effect on cell viabilty or the induction of cell death. The next stage in the project was therefore to investigate if these effects translate into increased sensitivity to apoptosis: does acetate prime cells for death?

As with the investgation into the effects of acetate on viabilty and apotosis induction, the MTT assay was used to screen for a priming effect, followed by confirmation using the Annexin V flow cytometry assay. The results indicate that cancer cells undergo signficantly enhanced levels of apoptosis when primed with aceate compared to DDP treatment alone. Furthermore, this effect was not observed in the non-cancerous MCF10A cell line. Addtionally, the sensitization effect is not observed when acetate and DDP are added to cells simultaneously (combination treatments). These findings provide clear evidence that acetate, 24 hours after treatment, is capable of sensitising cancer cells for death. From this, combined with data gathered on the health of acetate-treated mitochondria, it can be concluded that the observed sensitization to apoptosis is caused by priming the mitochondria of cancer cells to death.

This is the first time a SCFA has been demonstrated to enhance the sensitivity of cancer cells to drug-induced cell death. Future work should investigate whether propionate and butyrate exhibit a similar effect to acetate – indeed, one might predict a stronger effect given that propionate and butyrate have been shown to initiate apoptosis alone (See Section 1.8 and 3.3), although this may complicate their potential as priming agents, as they may affect non-cancerous cell viability. Acetate joins a growing list of naturally occur molecules that have potential as priming agents (See Section 1.7, Table 5). It is interesting to consider the mechanisms by which these other priming agents induce chemosensitisation. Quercetin, a flavonoid found in many plants and foods, was found to induce apoptosis via inhibition of the pro-survival Akt pathway, as well as

through the down regulation of superoxide dismustase, which leading to accumulation of ROS, resulting in increased sensitivity of cancer cells to DDP treatment (Sharma et al. 2005). El-Senduny et al. found cucurbitacin B, another compound found in plants, to induce sensitivity to DDP treatment in ovarian cancer cells through G2/M arrest and again, increased ROS production (El-Senduny et al., 2015). Finally, cannabinol (CBD) was shown by Henley to induce chemosensitvity of breast cancer cells to DDP treatment through modulation of mitochondrial function, including changes in ROS and Ca^{2+} (Henley, 2015). The mechanisms of each of these natural products draw parallels to the effects of acetate treatment observed in this study, namely; the induction of oxidative stress through elevated ROS levels. Acetate however stands out in such comparisons to other priming agents as in this thesis, I have shown that it can sensitise different types of cancer cell line to death, an observation which highlights the potential of acetate to improve the treatment of different cancers.

A significant limitation in this section was the effect of DDP on MCF10A cells; in the MTT viability assay, the amount of cell death induced by DDP reduced the viability of cells below the detectable limit of the plate reader, and so the concentration of DDP used for this cell line in this part of the study had to be reduced to 50 µM. This was not a limitation on the Annexin V-FITC assay, which used larger seeding densities and is also more sensitive. To prevent this issue, dose response assays should have been carried out to determine a median lethal dose (LD_{50}) to determine the appropriate concentration of DDP to use for individual cell lines.

4.4.2 | The effects of Priming on Mitochondrial Function

By observing mitochondrial function following priming treatments, I set out to investigate whether there was any difference in mitochondrial function between cells that had been primed with acetate and those that were treated with DDP alone. When normalized to protein content, both primed and DDP-treated cells exhibited a significant decrease in mitochondrial function compared to untreated cells, consistent with what would be expected in a population of cells undergoing or having undergone apoptosis (Lomeli et al., 2017). There was no significant difference in the mitochondrial function between primed and DDP-treated cells, despite treatment with acetate alone being shown in this study to significantly alter mitochondrial function (See Section 3.5). I would attribute this to the significant cell death induced by DDP; which I speculate would mask any effect priming had different from DDP treatment alone. The level of cell death also posed experimental problems, apparent in the large variation in response to treatment observed in this Section. Accurate OCR data is dependent on an evenly distributed monolayer of cells (Aglient, 2017), and although the Bradford Assay was used to correct for changes in cell population, it was difficult to ensure an even monolayer, as cells undergoing apoptosis are likely to detach. These issues made it difficult to obtain meaningful data for MCF7 and MCF10A, which often detached and failed to provide data within the detection limits of the SeaHorse analyser.

Based on these findings and the experienced difficulties, it was decided not to look further at the metabolism of cells following priming, as any observations would be dominated by DDP-induced apoptosis in both experimental conditions. This is further apparent in Figure 40, which shows the stark contrast in mitochondrial morphology between untreated and DDP-treated cells. Furthermore, as the aim of this study was to determine if and how acetate primes cells for death and so studying cells was considered unnecessary to achieve this aim.

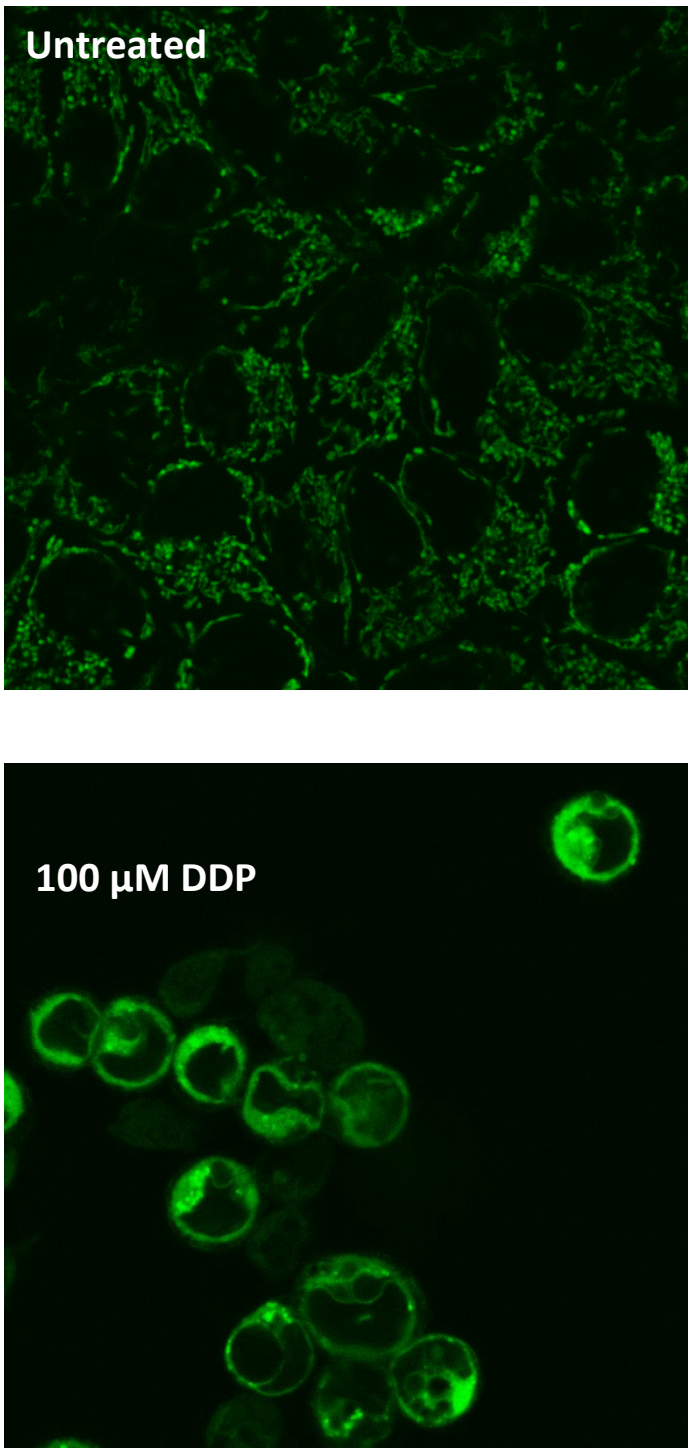

Figure 40 | The Effect of DDP on Mitochondrial Morphology. Cells in images labelled untreated received media for 24 hours. Cells in images labelled 100 µM DDP were treated with 100 µM DDP for 24 hours. For clarity, a green LUT was applied and brightness was adjusted with ImageJ's "Auto" settings.

5.0 | 2P FLIM of NADH as a Measure of Cellular Metabolism

5.1 | 2-Photon Microscopy

The pools of cellular NADH and NADPH regulate the balance between driving energy production and maintaining antioxidant defences. In particular, NADH/NAD^+ links the TCA cycle to the production of ATP in oxidative phosphorylation (Blacker and Duchen, 2016). Thus, levels of NADH/NAD^+ can provide information regarding the metabolic state of the cell (See Section 1.3.8 for more detail). NADH is fluorescent, whilst its oxidised counterpart, NAD^+ is not and therefore the intensity of NADH fluorescence can provide meaningful information as to the metabolic state of a cell without the need for an external probe (Sanchez et al., 2018). However, the absorption maxima for NADH is 340 nm, in the UV region of the electromagnetic spectrum, and so exposure of cells to light of this wavelength is phototoxic. UV can damage cells in a number of ways; the most well-known being the damage to cellular DNA: UV light initiates a fusion reaction between thymine molecules. If this damage is too extensive for the DNA repair systems to fix, p53 will direct the cell to apoptosis (Hoeijmakers, 2009). Additionally, absorption of UV light by chromophores in skin cells can generate ROS (de Jager et al., 2017), which as discussed in Section 1.3.5 are harmful at high concentrations. To circumvent this problem, 2-Photon Microscopy can image cells with lower energy light of a higher wavelength (Vergen et al., 2012). In a 2 photon (2P) system, molecules in the ground state are excited by simultaneous stimulation by 2 photons, providing sufficient energy to move a molecule to its excited state with longer wavelengths (Figure 41).

There are a number of additional advantages that 2P microscopy provides compared to single photon systems (also Figure 41). The probability that a molecule will absorb 2 photons simultaneously increases with excitation intensity; meaning 2P fluorescence is much higher where the laser is focused. This is means 2P microscopy has small excitation volume, reducing out-of-focus noise

(Svoboda and Yasuda, 2006). Additionally, the longer wavelengths used in 2P microscopy, approaching the infrared, make it ideal for imaging thicker specimens, as light in this region is scattered less than visible light used in conventional microscopy (Blacker and Duchen, 2016). Despite these advantages, 2P microscopy has a lower spatial resolution compared to single-photon, as resolution of a microscope is inversely proportional to the wavelength of light used. Thus, a 2P system, using an excitation wavelength twice of that used in a single photon setup will have approximately half the resolution (Diaspro et al., 2006).

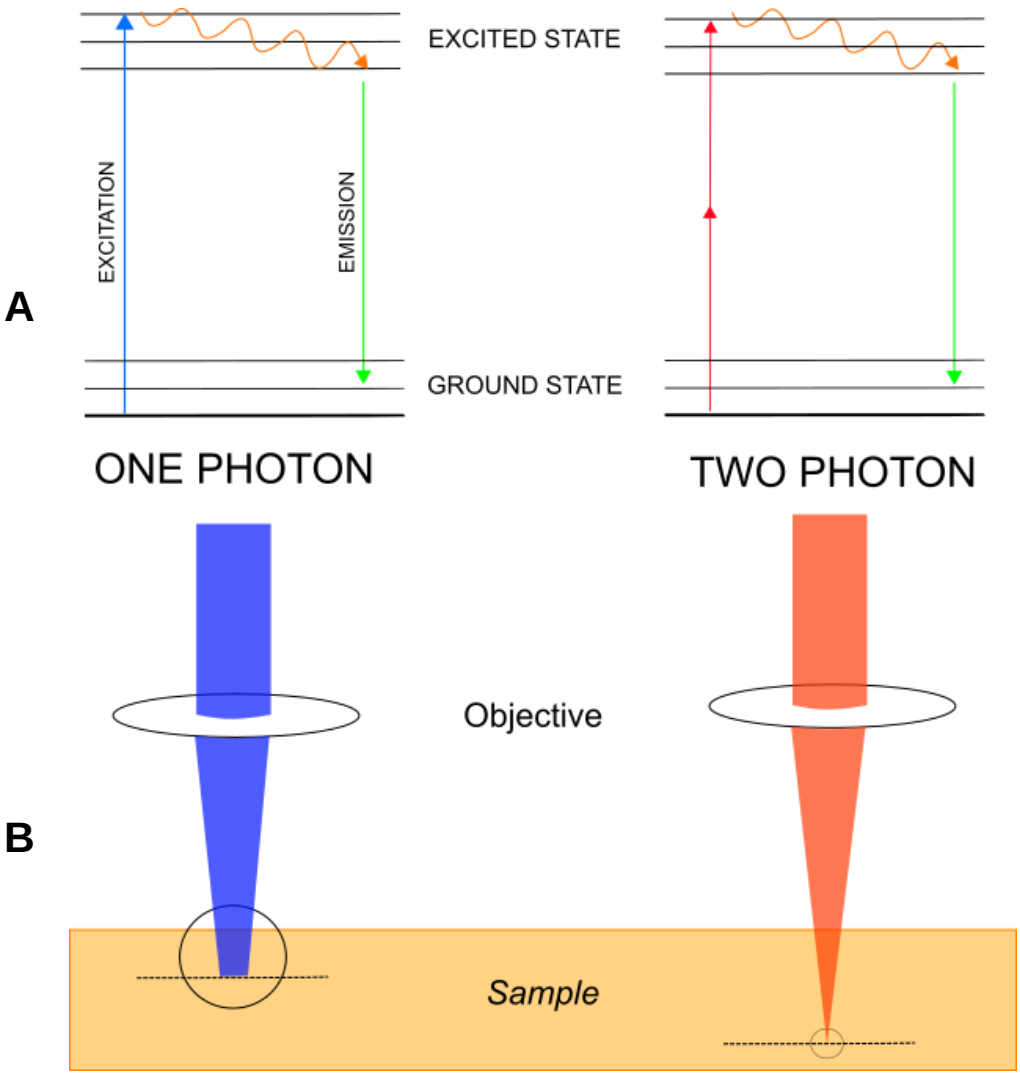

Figure 41 | **The Principles and Advantages of 2-Photon Excitation. A**: Jablonski diagrams comparing one photon and two photon excitation in terms of energy levels. On the left, one photon of a long wavelength excites a molecule from the ground to the excited state. In a two photon system, as shown on the right, 2 photons, each approximately double the wavelength the single photon system provides sufficient energy to promote the same molecule to its excited state. **B:** The probability of 2P absorption increases with beam intensity, meaning the "excitation volume" (indicated by circles) is smaller in 2P microscopy, resulting in a less out of focus signal. Additionally, longer 2P excitation wavelengths are subject to less scattering than wavelengths in the visible spectrum used in single photon systems, meaning the focal place (indicated by the dashed line) can penetrate deeper in samples.

5.2 | Basics of Fluorescence Lifetime Imaging Microscopy

Figure 41 shows that fluorescence occurs when a molecule returns to the ground state from an excited state. This process is not 100% efficient, as a molecule in its excited state can also dissipate its energy through a number of non-radiative de-excitation mechanisms, including the transfer of energy to neighbouring molecules, known as quenching (Blacker et al., 2014). A high degree of non-radiative de-excitation increases the rate at which a molecule returns to the ground state from its excited state (Olympus, 2019). The length of time for this to occur is called the fluorescence life time decay. NADH has been observed to exhibit two distinct fluorescence lifetime decays; ~0.4 ns for free NADH, and ~2.0 ns for enzyme-bound NADH (Blacker and Duchen, 2016) (Figure 42). A shorter life time for free NADH is unsurprising given that the NADH molecule is free to move in solution and dissipate its energy to neighbouring molecules. The longer life time for bound NADH was considered to be a consequence of enzymes “shielding” NADH in binding sites and blocking it from potential quenching events, although now is now thought to also be as a result of enzyme binding physically reducing the conformational freedom of NADH, preventing another non-radiative de-excitation mechanism called internal conversion (Blacker et al., 2013).

Measuring the lifetime decay in a cell can therefore inform us as to the ratio of freely diffusing and enzyme-bound NADH, and thus provide more detailed information as to the metabolic state of the cell than measuring NADH fluorescence alone. To do this, 2 photon microscopy is combined with fluoresce lifetime imaging (FLIM), which essentially performs a series of single fluorescence lifetime measurements across a field of view to generate an image in which each pixel contains its own lifetime decay data (Suhling et al., 2015).

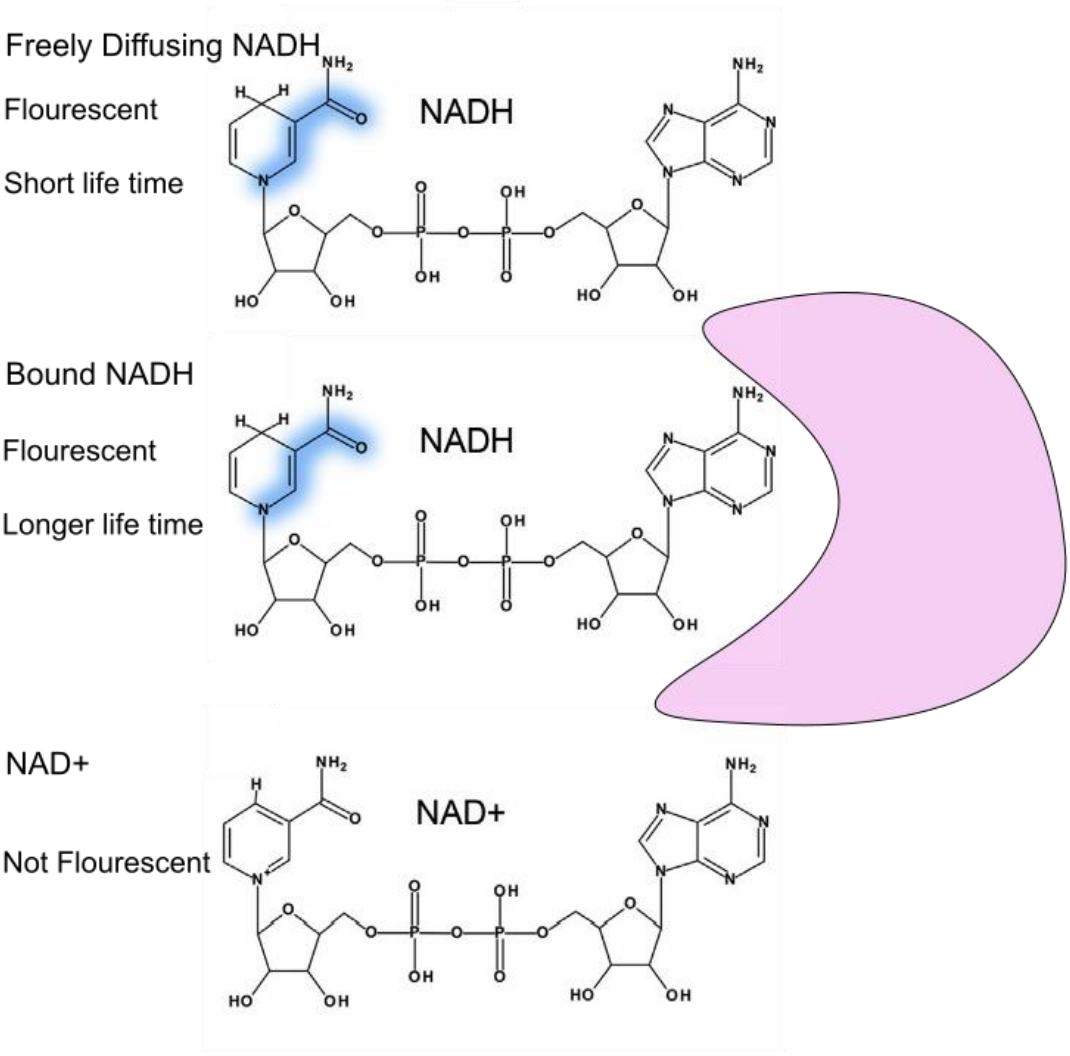

Figure 42 | Fluorescence and Lifetimes of NAD(P)H. NADH fluoresces (indicated by the blue aura) and has a short decay of ~0.4 ns when freely diffusing in solution. When bound to an enzyme, this decay increases to around ~2.0 ns. NAD+ is not fluorescent.

Although FLIM was conceived and developed in the early 1990's (Takatoku et al., 1993), the development of more powerful microscopes and photon counting techniques has meant 2P-FLIM has experienced a recent resurgence in popularity (Suhling et al., 2015). Most notable among these is time-correlated single-photon counting (TCSPC), which allows the detection of single photons with their arrival times from a sample with respect to a reference source to picosecond accuracies. By exciting the sample millions of times per second, TCSPC generates a probability distribution histogram of photon arrival times, which is the fluorescence

decay curve of the sample. Such a curve is shown in Figure 43. Because of its signal-to-noise ratio, wide dynamic range and single photon sensitivity, TCSPC is considered the gold standard of FLIM techniques (Suhling et al., 2015).

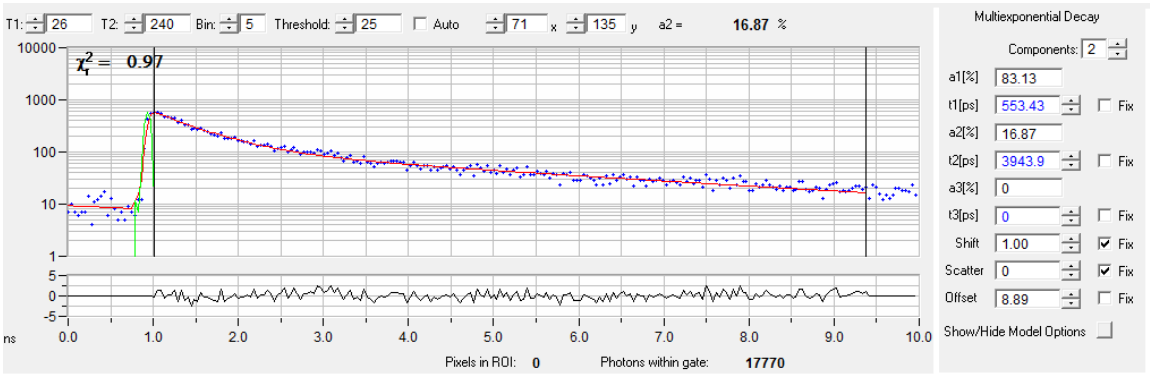

Figure 43 | The Lifetime Decay Curve of NAD(P)H. Image is a lifetime decay curve obtained from one pixel of an image of MCF7 cells using SPC image analysis software. Y axis: number of detected protons. X axis: time in nanoseconds. Vertical black line at the left hand side indicates the excitation pulse. To calculate lifetimes, SPCimage analysis software calculates multi-exponential best fit (red line) of detected photons (blue dots). The goodness of fit, measured by Pearson's chi-squared test, is shown in the top left. τ_1 and τ_2, on the right of the curve, are the calculated life time decays of free NADH and bound NADH respectively. α_1 and α_2 are the contributions of each lifetime to the overall decay.

In principle, as the spectral properties of NADH and NADPH are identical, there is an issue with resolving between the two species. This separation of NADH and NADPH remains a challenge in the field (Blacker et al., 2014). However, NADPH lifetime decay has been found to be insensitive to metabolic changes (Ghukasyan and Kao, 2009; Vishwasrao et al., 2005), which allows changes in lifetime decay to be primarily attributed to NADH, with minimal contribution from NADPH.

In this chapter, I use 2P-FLIM to observe the impact of acetate treatment on NAD(P)H metabolism in collaboration with Professor Stan Botchway at the Rutherford Appleton laboratory. The objectives in this chapter are twofold:

1. Measure the effect of acetate on NADH metabolism.
2. Improve and create a robust protocol for using FLIM to analyse drug interactions with cells.

In these experiments only MCF7 cells were used due to availability of cells at the Rutherford Appleton laboratory.

5.3 | The Effects of Acetate on NADH Lifetime Decay

The effect of acetate on NADH lifetime decay, as a measure of cellular and mitochondrial metabolism, was measured using 2P FLIM (Figures 44, 45 and 46).

DESIGNATION	PARAMETER	MEANING
T_1	T_{Free}	Lifetime of free NADH (in picoseconds)
T_2	T_{Bound}	Lifetime of bound NADH (in picoseconds)
α_1	α_{Free}	Contribution of free NADH to the overall decay curve (percentage)
α_2	α_{Bound}	Contribution of bound NADH to the overall decay curve (percentage)

Table 12 | Terms Used to Describe NADH Lifetime in 2P-FLIM. The symbols and parameters used in this study to describe the lifetime decay curve of NADH

Figure 44 shows a representative FLIM image of MCF7 cells treated with either DMSO (the negative control) or 10 mM acetate for 24 hours. As described in Section 5.2, each pixel of the image has its own calculated lifetime decay curve (similar to the example shown Figure 43). Using the SPC Image analysis software, a FLIM image can display a colour-coded heat map for any measured parameter, which in the case of this experiment are: the lifetime of free NADH (τ_1, or τ_{Free}), the lifetime of bound NADH (τ_2, or τ_{Bound}), the contribution of free NADH to the decay curve (α_1, or α_{Free}), and the contribution of bound NADH to the decay curve (α_2, or α_{Bound}) (see Table 12).

The images in Figure 44 are α_{Bound} encoded, where red pixels have a lower α_{Bound} value, and blue pixels have a higher α_{Bound} value. From these acquired images, two observations can be made: acetate did not appear to have a large effect on α_{Bound} and that the signal intensity is much higher in the mitochondria.

To draw more quantitative conclusions as to changes in NADH lifetime between treatments, I compared lifetime decay parameters between DMSO and acetate treated cells from pixels within the mitochondrial with pixels within the cytosol (Figure 45). In the mitochondria, treatment with 10 mM acetate caused a significant increase in the mean lifetime of free NAD(P)H, τ_{Free} compared to the untreated control (505.9 ± 12.26 picoseconds (ps) vs 475.1 ± 9.22 ps $p = 0.045$). The mean lifetime of bound NAD(P)H, τ_{Bound} in untreated cells was unaffected

compared to acetate-treated cells (2912 ± 57.98 ps vs 2881 ± 46.74 ps (p = 0.6817). The contribution of τ_{Bound} (also known as α_{Bound}) to the overall lifetime decay was unaffected by acetate treatment.

In cytosolic pixels, treatment with acetate had no effect on τ_{Free} compared to the untreated control. τ_{Bound} was again unaffected by acetate treatment, while α_{Bound} was significantly higher in acetate-treated cells (29.55 ± 0.868% vs 26.71 ± 0.605% p = 0.006).

In comparisons between mitochondrial and cytoplasmic values within the same treatments (Figure 46), τ_{Bound} was significantly higher in the mitochondria than the cytosol of control-treated cells. (2912 ± 57.98 ps vs 2708 ± 69.46 ps p = 0.027). When treated with acetate, there was no significant difference between mitochondrial and cytosolic τ_{Bound} values.

There was no significant difference in contribution of bound NADH (α_{Bound}) to the overall lifetime decay between mitochondria and the cytosol of control-treated cells. Treatment with 10 mM acetate caused a significant decrease in mitochondrial α_{Bound} compared to the cytosolic α_{Bound} (26.19 ± 0.64%, vs 29.55 ± 0.87 p = 0.002)

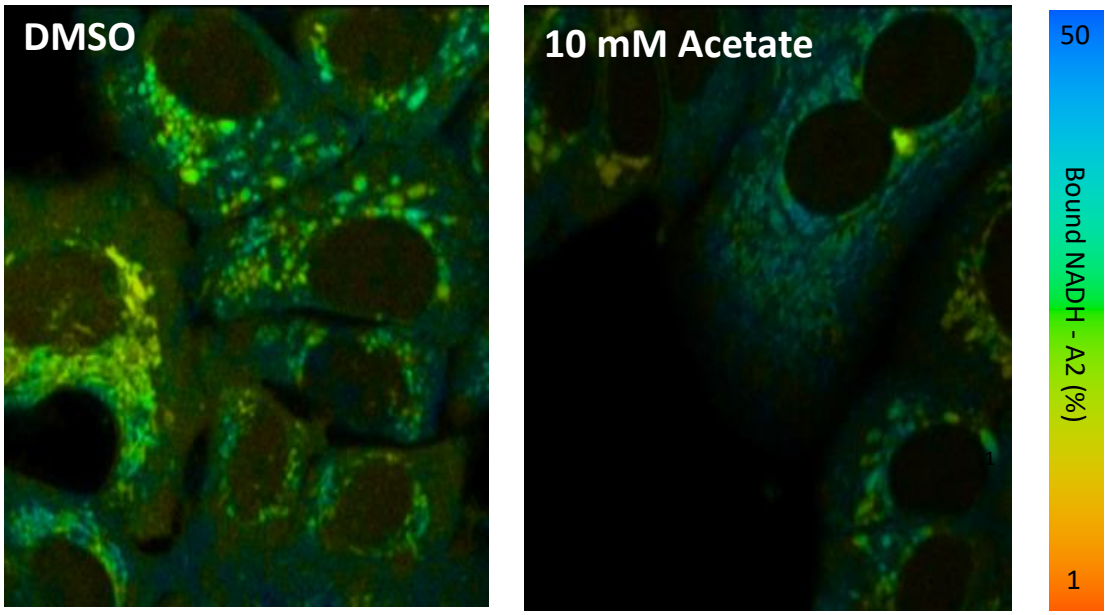

Figure 44 | The Effect of Acetate on NAD(P)H Lifetime Decay: 2P FLIM Images. Representative α_{Bound} encoded 2P FLIM images of MCF7 cells treated for 24 hours with DMSO (left) or 10 mM acetate (right). Images were encoded so that red pixels have a low α_{Bound} and blue pixels have high α_{Bound}

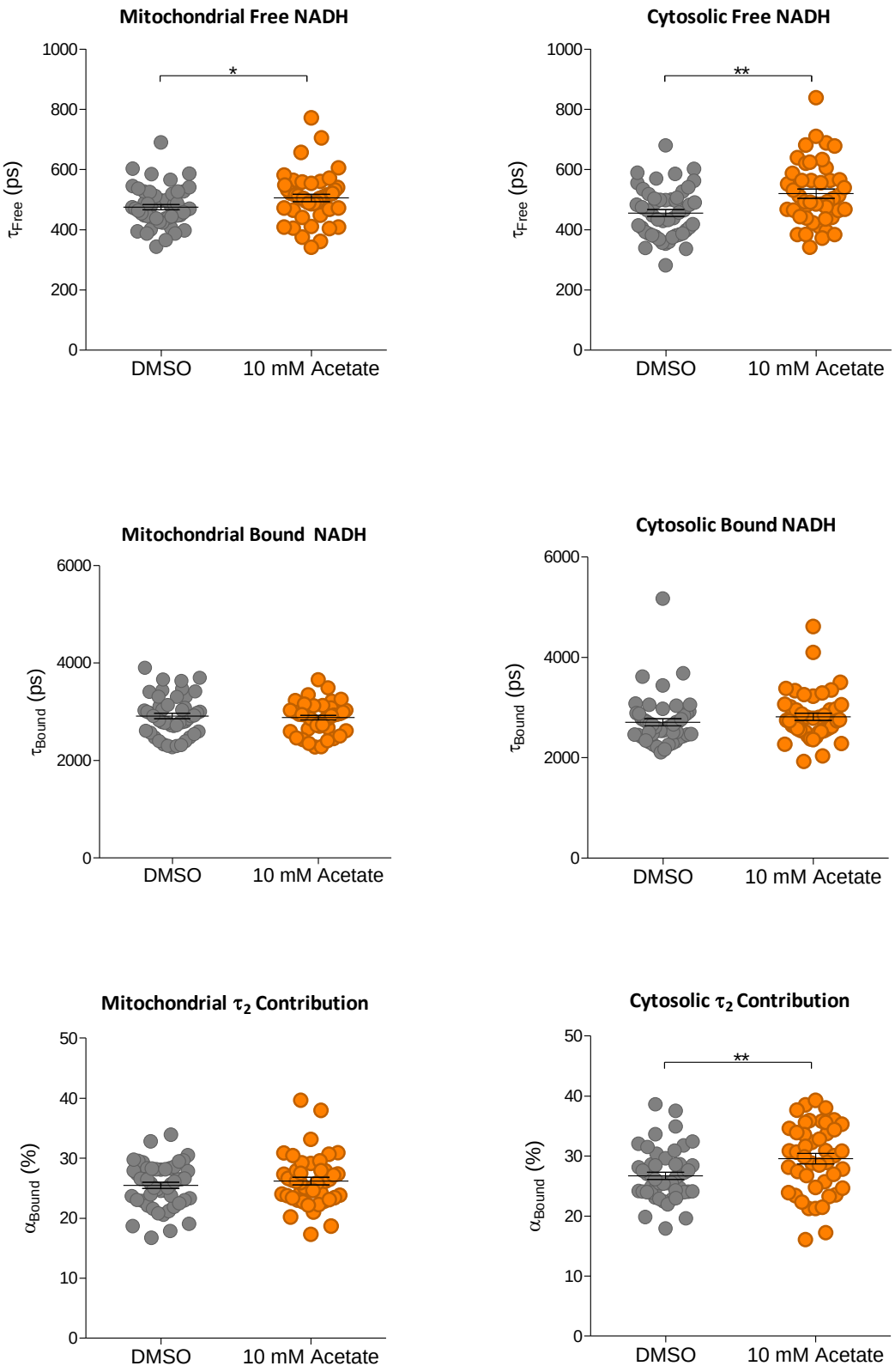

Figure 45 | **The Effect of Acetate on NAD(P)H Lifetime Decay**. **Top:** Lifetime of free NADH (τ_1) in the mitochondria and cytosol. Middle: Lifetimes of bound NADH (τ_2) in the mitochondria and cytosol. **Bottom:** contribution of Bound NADH (α_2) in the mitochondria and the cytosol. Data points indicate values from individual pixels ±SEM of n = 3 individual experiments. Significance compared to the untreated control indicated by * = p < 0.05, ** p <0.01. No asterisk means not statistically significant.

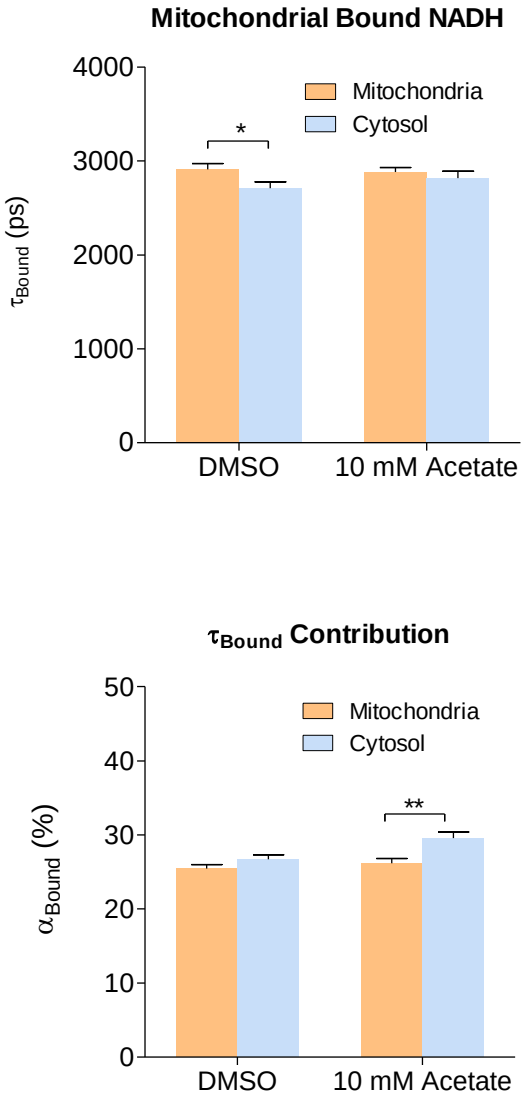

Figure 46 | The Effect of Acetate on NAD(P)H Lifetime Decay: Mitochondria and Cytosol Comparisons. Bars indicate average value ±SEM from *n* = 3 individual experiments. Differences between control and acetate treated values analysed with Unpaired Student's T-test. Significance compared to the untreated control indicated by * = $p < 0.05$, ** $p < 0.01$. No asterisk means not statistically significant.

5.4 | Discussion

5.4.1 | The Effects of Acetate on the Lifetime Decay of NAD(P)H

In this section, I set out to measure changes in metabolism caused by acetate by investigating changes in the fluorescence life time decay of NADH.

Data presented in Section 5.3 indicates that acetate treatment increases the decay lifetimes of free NADH (τ_{Free}) and the contribution of bound NAD(P)H to the lifetime decay curve (α_{Bound}) (Figure 45). The length of lifetime is related to the environment surrounding NADH. The significant increase in both mitochondrial and cytosolic τ_{Free} in acetate treated cells could therefore indicate an increase in the concentration of freely diffusing NADH [$NADH_{free}$]. However, the use of τ_{Free} is not widely reported in the literature, and could potentially be considered an artefact of the fitting process, since these shorter lifetimes are close to the resolution limit of the detection system (Blacker et al., 2014).

Of more interest to investigators is the lifetime of bound NADH (τ_{Bound}) and the contribution of τ_2 (α_{Bound}), variations in which can indicate changes in the concentration of enzyme-bound NADH, which in turn can indicate the cell's metabolic state. In acetate treated cells, τ_{Bound} in both mitochondrial and cytosolic pixels remained unchanged compared to the control. A decrease in τ_{Bound} has been associated with increased levels of glycolysis, as oxidative phosphorylation is a major site for NADH binding (Skala et al., 2009). Based on SeaHorse data from Section 3.5, in which acetate was observed to cause a decrease in OXPHOS after 24 hours, one may have predicted a decrease in τ_{Bound} in acetate-treated cells. Furthermore, α_{Bound} was found to be significantly increased in the cytosol, suggesting that treatment with acetate increases the ratio of cytosolic bound:free NADH. In the mitochondria, α_{Bound} was unchanged compared to the control, which again would seem to contradict earlier results indicating mitochondrial stress. However, there was a significant difference in α_{Bound} between mitochondrial and cytosolic pixels in acetate treated cells, which suggest that acetate does have an effect on NADH metabolism. One possible explanation for this is that in the face of decreased OXPHOS as a result of acetate-inducted oxidative stress, glycolysis

rates increase to ensure cell survival. In glycolysis, NAD+/NADH is bound by glycerldehyde 3-phosphate dehydrogenase, the enzyme that catalyses the conversion of glyceraldehyde 3-phosphate and 1,3-biphosphoglycerate (Sirover 1999). However, the lack of change in α_{Bound} in the mitochondria still contradicts what would be expected based on earlier work on acetate and metabolism. Further work will be needed to explore these observations.

An interesting finding came from observation of the acquired FLIM images (Figure 44): that the signal intensity was noticeably higher in mitochondrial pixels. Whilst from a biochemical point of view this may be unsurprising (as NAD^+ is converted to NADH in the TCA cycle within the mitochondrial matrix), it may present the opportunity to make morphological measurements of mitochondria in addition to acquisition of FLIM data. Without the need of a fluorescent probe, this has an advantage as a non-invasive measure of morphology, and circumvents caveats with traditional mitochondrial probes, such as membrane potential dependency (discussed in Section 3.14.5). However, similar resolution limitations still apply as they did with single photon confocal microscopy, and as in these experiments I used a format of 512x512 (to increase the acquisition time and to reduce laser exposure to cells), it was not possible to test whether NADH FLIM images could be used instead of conventional probes. Therefore, future work could include higher resolution FLIM acquisition to compare to conventional single photon confocal microscopy.

There are several weaknesses in this analysis which should be noted. First, DMSO was used as a negative control, whereas media had been used in other sections of this project. Whilst the working concentration used was very low (<0.01% volume/volume), future work should repeat the experiments using media as the control. Secondly, the data points gathered were from individual pixels from each obtained image. Whilst steps were taken to minimise subjectiveness, there was no way to ensure true randomness in selection. In addition, pixel to pixel variation could affect the data gathered. In future work, steps should be taken to reduce any unintentional bias, and to use a region-of-interest approach to analyse whole mitochondria, rather than single points. Unfortunately, this was not possible in this study as the resolution of the obtained images made it difficult to distinguish

mitochondrial boundaries. Finally, there are studies that suggest the rates of OXPHOS and glycolysis do not correlate with NAD(P)H lifetime decay as directly as initially proposed, and that the relationship is “considerably more nuanced” (Blacker et al., 2014; Guo et al., 2015). The use of known mitochondria-affecting drugs, such as oligomycin and FCCP, may improve the understanding of this relationship and provide greater insight to the results I have gathered thus far. Furthermore, the use of 2P-FLIM to investigate such metabolic effects, and the identification of issues and nuances of the technique is valuable for advancing such studies, which at present are sparse due to the limited availability of the instruments. Some current improvements which should be considered in future work include the use of a 4-component decay fit (1 component for free NAD(P)H and 3 for bound) to improve the resolution of data (Vishwasrao et al., 2005), or the phasor approach, described by Digman et al., which plots the raw FLIM data in a vector space, which they propose simplifies analysis by avoiding the computational difficulties of exponential fitting and providing a graphical, global view to acquired FLIM data (Digman et al., 2008).

6.0 | Final Conclusions

6.1 | A Proposed Mechanism for Acetate Priming

Priming the mitochondria of cancer cells for death presents a novel opportunity to increase the efficiency of new and existing anti-cancer drugs. Acetate, a SCFA produced in the gut as a by-product of fermentation, has been shown to possess anti-tumorigenic properties and so has potential as a priming agent. In this thesis I have further characterised the effect that treatment with acetate has on cancer cell lines, finding that acetate, whilst not inducing cell death alone, induces a state of oxidative stress, characterised by decreased mitochondrial function, increased levels of ROS and intracellular Ca^{2+}, changes in cell cycle state, changes in gene expression, and the morphology of mitochondria. I have also shown that after priming with acetate, cancer cells exhibited increased levels of apoptosis following treatment with cisplatin, compared to treatment with the drug alone. Importantly, this effect was not observed in the non-cancerous cells.

A suggested mechanism based on evidence gathered in this project for how acetate primes cancer cells for death is shown in Figure 47. I propose that through interactions with the g-coupled protein receptors FFAR2 and FFAR3 on the cell surface, acetate induces the release of Ca^{2+} from the endoplasmic reticulum. In turn, the increase in intracellular Ca^{2+} increases the rate of mitochondrial respiration. This drives the production of ROS, as a by-product of OXPHOS. Finally, the accumulation of ROS causes a state of oxidative stress - priming the cells for the death. There may also be secondary contributing mechanisms, such as the changes in gene expression, mediated by acetate's reported activity as a HDAC inhibitor, and the effects on the cell cycle – also linked to elevated ROS. The key to this hypothesis are the interactions with FFAR2 and FFAR3, and as such, future work should include knockdowns of the genes that express these receptors. Miletta et al. had shown that butyrate-induced increase in intracellular Ca^{2+} was muted by *FFAR2* and *FFAR3* knockdowns (Miletta et al., 2014), but as there is a lack of work studying acetate interactions, it would be important to

investigate whether the priming effect of acetate changes when the expression of the two receptors is altered. Overall, the proposed mechanism can be thought as “burning out” the mitochondria: by “pushing” mitochondrial function, acetate appears to render mitochondria more sensitive to additional stressors.

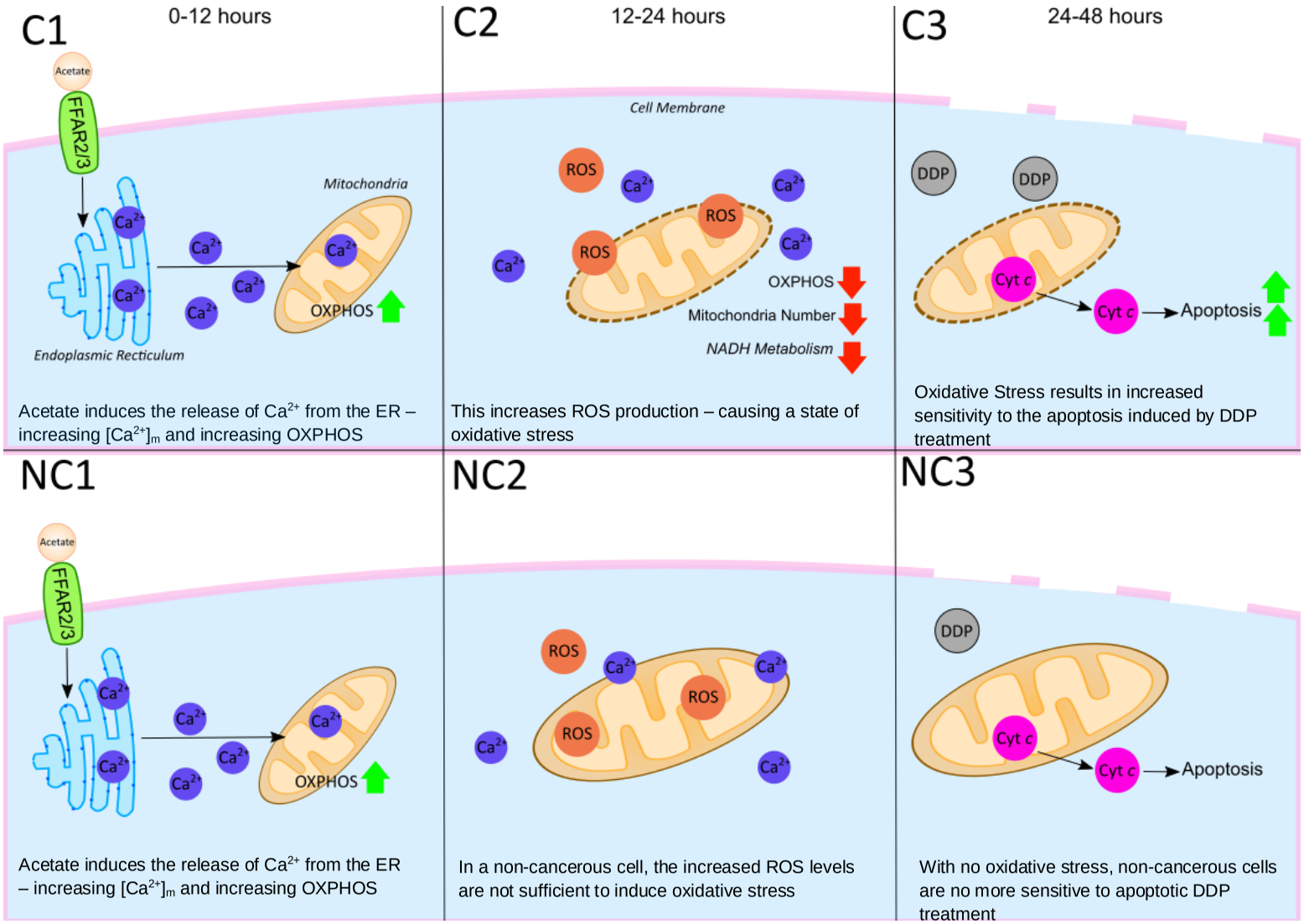

Figure 47 | A Proposed Mechanism for Priming. In cancer cells (C1-3) acetate primes the mitochondria cells for death, whilst the same effect is not observed in non-cancerous cells (NC1-3)

6.2 | Future Work

This thesis utilised a cell line model, which are invaluable for initial studies due to the relative ease of handling, infinite replication and homogeneity, all of which allow direct comparisons between experiments (Burdall et al., 2003). However, it is widely accepted that there are numerous disadvantages compared to the use of primary cell lines or animal models. These include genetic and phenotypic drift over the extended passage of cell lines (Kaur and Dufour, 2012), potential contamination (Olarerin-George and Hogenesch, 2015), cross-contamination, and the lack of some of the key characteristics of cancer, such as the development of the tumour environment and metastasis (Katt et al., 2016). Furthermore, the lack of cellular and molecular heterogeneity compared to a tumour means cell lines provide only a much-simplified model of cancer (Choi et al., 2014). It is therefore imperative that future work must include the use of more biologically relevant models, such as 3D cultures and *in vivo* models.

The proposed mechanism described in Section 6.1 effectively hinges on 2 key points: 1.) that the sensitivity of cells treated with acetate is a result of ROS-induced oxidative stress driven by Ca^{2+} interactions with the mitochondrial respiratory machinery, and 2.) the increase in Ca^{2+} is a result of acetate interactions with the free fatty acid receptors on the cell surface. To further test this mechanism, future work should include dissipating the ROS effect by use of a ROS scavenger or antioxidants (e.g. NAC), which interestingly has been shown to be effective in alleviating oxidative stress in a mouse model of sepsis (Hou et al., 2010). Furthermore, knockdowns of FFAR2 and FFAR3, which have been shown to inhibit butyrate induced Ca^{2+} release (Miletta et al., 2014), could be investigated to determine whether either treatment reduces the priming effect of acetate.

6.3 | Final Comments

The results gathered from this study point to a complex and multifaceted role of acetate in cancer cells, dependent on its source, cell type and treatment time. Nevertheless, I have shown that priming with acetate has the potential to improve the effectiveness of chemotherapy.

This thesis reveals for the first time a complex interaction between the SCFA acetate and the mitochondria and demonstrates that manipulating the function of mitochondria can result in cancer cell-specific sensitivity to death. The proposed mechanism of acetate – an initial increase in mitochondrial respiration followed by subsequent oxidative stress, is a novel approach to inducing chemosensitivity and may warrant investigation in other natural products. Through investigating the effect of acetate on NADH metabolism, I also demonstrate that 2P FLIM has potential to provide a non-invasive method to measure mitochondrial metabolism and morphology simultaneously. Finally, this thesis adds more evidence to the case for priming, demonstrating that this approach may be effective in improving the treatment of those prescribed with chemotherapy.

7.0 | References

Aglient, 2017. Seeding Adherent Cells in Agilent Seahorse XF24 Cell Culture Microplates [WWW Document]. URL https://www.agilent.com/cs/library/usermanuals/public/XFe24_DAY_BEFORE_CELL_SEEDING.pdf (accessed 1.28.19).

Altman, B.J., Dang, C. V., 2012. Normal and cancer cell metabolism: Lymphocytes and lymphoma. FEBS J. 279, 2598–2609. https://doi.org/10.1111/j.1742-4658.2012.08651.x

Alvaro, A., Solà, R., Rosales, R., Ribalta, J., Anguera, A., Masana, L., Vallvé, J.C., 2008. Gene expression analysis of a human enterocyte cell line reveals downregulation of cholesterol biosynthesis in response to short-chain fatty acids. IUBMB Life 60, 757–64. https://doi.org/10.1002/iub.110

American Cancer Society, 2016. What about chemo side effects? [WWW Document]. URL https://www.cancer.org/treatment/treatments-and-side-effects/treatment-types/chemotherapy/what-chemo-is-and-how-it-helps/chemo-side-effects.html (accessed 9.28.17).

Anand, P., Kunnumakara, A.B., Sundaram, C., Harikumar, K.B., Tharakan, S.T., Lai, O.S., Sung, B., Aggarwal, B.B., 2008. Cancer is a preventable disease that requires major lifestyle changes. Pharm. Res. 25, 2097–2116. https://doi.org/10.1007/s11095-008-9661-9

Anderson, S., Bankier, A.T., Barrell, B.G., de Bruijn, M.H., Coulson, A.R., Drouin, J., Eperon, I.C., Nierlich, D.P., Roe, B.A., Sanger, F., Schreier, P.H., Smith, A.J., Staden, R., Young, I.G., 1981. Sequence and organization of the human mitochondrial genome. Nature 290, 457–465. https://doi.org/10.1038/290457a0

Astakhova, L., Ngara, M., Babich, O., Prosekov, A., Asyakina, L., Dyshlyuk, L., Midtvedt, T., Zhou, X., Ernberg, I., Matskova, L., 2016. Short Chain Fatty Acids (SCFA) Reprogram gene expression in human malignant epithelial and lymphoid cells. PLoS One 11, 1–18. https://doi.org/10.1371/journal.pone.0154102

Auten, R.L., Davis, J.M., 2009. Oxygen toxicity and reactive oxygen species: the devil is in the details. Pediatr. Res. 66, 121–7. https://doi.org/10.1203/PDR.0b013e3181a9eafb

Baines, C.P., Kaiser, R.A., Sheiko, T., Craigen, W.J., Molkentin, J.D., 2007. Voltage-dependent anion channels are dispensable for mitochondrial-dependent cell death. Nat. Cell Biol. 9, 550–555. https://doi.org/10.1038/ncb1575

Baker, F., Denniston, M., Smith, T., West, M.M., 2005. Adult cancer survivors: How are they faring? Cancer 104, 2565–2576. https://doi.org/10.1002/cncr.21488

Bannister, A.J., Kouzarides, T., 2011. Regulation of chromatin by histone modifications. Cell Res. 21, 381–395. https://doi.org/10.1038/cr.2011.22

Barbi de Moura, M., Vincent, G., Fayewicz, S.L., Bateman, N.W., Hood, B.L., Sun, M., Suhan, J., Duensing, S., Yin, Y., Sander, C., Kirkwood, J.M., Becker, D., Conrads, T.P., Van Houten, B., Moschos, S.J., 2012. Mitochondrial respiration--an important therapeutic target in melanoma. PLoS One 7, e40690. https://doi.org/10.1371/journal.pone.0040690

Barneda-Zahonero, B., Parra, M., 2012. Histone deacetylases and cancer. Mol. Oncol. 6, 579–89. https://doi.org/10.1016/j.molonc.2012.07.003

Beckman, K.B., Ames, B.N., 1998. The free radical theory of aging matures. Physiol. Rev. 78, 547–581. https://doi.org/OSJC0001

Berridge, M.J., 1993. Inositol trisphosphate and calcium signalling. Nature 361, 315–25. https://doi.org/10.1038/361315a0

Berridge, M. V, Tan, A.S., 1993. Characterization of the cellular reduction of 3-(4,5-dimethylthiazol-2-yl)-2,5-diphenyltetrazolium bromide (MTT): subcellular localization, substrate dependence, and involvement of mitochondrial electron transport in MTT reduction. Arch. Biochem. Biophys. 303, 474–82. https://doi.org/10.1006/abbi.1993.1311

Bertram, J.S., 2000. The molecular biology of cancer. Mol. Aspects Med. 21, 167–223. https://doi.org/https://doi.org/10.1016/S0098-2997(00)00007-8

Bettum, I.J., Gorad, S.S., Barkovskaya, A., Pettersen, S., Moestue, S.A., Vasiliauskaite, K., Tenstad, E., Øyjord, T., Risa, Ø., Nygaard, V., Mælandsmo, G.M., Prasmickaite, L., 2015. Metabolic reprogramming supports the invasive phenotype in malignant melanoma. Cancer Lett. 366, 71–83. https://doi.org/10.1016/j.canlet.2015.06.006

Bianchi, K., Rimessi, A., Prandini, A., Szabadkai, G., Rizzuto, R., 2004. Calcium and mitochondria: Mechanisms and functions of a troubled relationship. Biochim. Biophys. Acta - Mol. Cell Res. 1742, 119–131. https://doi.org/10.1016/j.bbamcr.2004.09.015

Bingham, S.A., Day, N.E., Luben, R., Ferrari, P., Slimani, N., Norat, T., Clavel-chapelon, F., Kesse, E., Nieters, A., Boeing, H., Tjønneland, A., Overvad, K., Martinez, C., Dorronsoro, M., Gonzalez, C.A., Key, T.J., Trichopoulou, A., Naska, A., 2003. Dietary fibre in food and protection against colorectal cancer in the European Prospective Investigation into Cancer and Nutrition (EPIC): an observational study. Lancet 361, 1496–1501.

Birben, E., Sahiner, U.M., Sackesen, C., Erzurum, S., Kalayci, O., 2012. Oxidative stress and antioxidant defense. World Allergy Organ. J. 5, 9–19. https://doi.org/10.1097/WOX.0b013e3182439613

Blacker, T.S., Duchen, M.R., 2016. Investigating mitochondrial redox state using NADH and NADPH autofluorescence. Free Radic. Biol. Med. 100, 53–65. https://doi.org/10.1016/j.freeradbiomed.2016.08.010

Blacker, T.S., Mann, Z.F., Gale, J.E., Ziegler, M., Bain, A.J., Szabadkai, G., Duchen, M.R., 2014. Separating NADH and NADPH fluorescence in live cells and tissues using FLIM. Nat. Commun. 5, 1–9. https://doi.org/10.1038/ncomms4936

Blacker, T.S., Marsh, R.J., Duchen, M.R., Bain, A.J., 2013. Activated barrier crossing dynamics in the non-radiative decay of NADH and NADPH. Chem. Phys. 422, 184–194. https://doi.org/10.1016/j.chemphys.2013.02.019

Bloemen, J.G., Venema, K., van de Poll, M.C., Olde Damink, S.W., Buurman, W.A., Dejong, C.H., 2009. Short chain fatty acids exchange across the gut and liver in humans measured at surgery. Clin. Nutr. 28, 657–661. https://doi.org/10.1016/j.clnu.2009.05.011

Bookout, A.L., Cummins, C.L., Mangelsdorf, D.J., Pesola, J.M., Kramer, M.F., 2006. High-throughput real-time quantitative reverse transcription PCR. Curr. Protoc. Mol. Biol. Chapter 15, Unit 15.8. https://doi.org/10.1002/0471142727.mb1508s73

Brand, M.D., Nicholls, D.G., 2011. Assessing mitochondrial dysfunction in cells. Biochem. J. 437, 575.1-575. https://doi.org/10.1042/BJ4370575u

Brandon, M., Baldi, P., Wallace, D.C., 2006. Mitochondrial mutations in cancer. Oncogene 25, 4647–4662. https://doi.org/10.1038/sj.onc.1209607

Brattain, M.G., Fine, W.D., Khaled, F.M., Thompson, J., Brattain, D.E., 1981. Heterogeneity of malignant cells from a human colonic carcinoma. Cancer Res. 41, 1751–6.

Brody, L., Sahuri-Arisoylu, M., Parkinson, J., Parkes, H., So, P.-W., Hajji, N., Thomas, E.L., Frost, G., Miller, A., Bell, J., 2017. Cationic lipid-based nanoparticles mediate functional delivery of acetate to tumor cells in vivo leading to significant anticancer effects. Int. J. Nanomedicine Volume 12, 6677–6685. https://doi.org/10.2147/IJN.S135968

Brown, A.J., Goldsworthy, S.M., Barnes, A.A., Eilert, M.M., Tcheang, L., Daniels, D., Muir, A.I., Wigglesworth, M.J., Kinghorn, I., Fraser, N.J., Pike, N.B., Strum, J.C., Steplewski, K.M., Murdock, P.R., Holder, J.C., Marshall, F.H., Szekeres, P.G., Wilson, S., Ignar, D.M., Foord, S.M., Wise, A., Dowell, S.J., 2003. The orphan G protein-coupled receptors GPR41 and GPR43 are activated by propionate and other short chain carboxylic acids. J. Biol. Chem. 278, 11312–11319. https://doi.org/10.1074/jbc.M211609200

Burdall, S.E., Hanby, A.M., Lansdown, M.R.J., Speirs, V., 2003. Breast cancer cell lines: Friend or foe? Breast Cancer Res. 5, 89–95. https://doi.org/10.1186/bcr577

Burkitt, D.P., 1971. Epidemiology of cancer of the colon and rectum. Cancer 28, 3–13.

Cadenas, E., Davies, K.J., 2000. Mitochondrial free radical generation, oxidative stress, and aging. Free Radic. Biol. Med. 29, 222–30.

Camara, A.K.S., Zhou, Y.F., Wen, P.C., Tajkhorshid, E., Kwok, W.M., 2017. Mitochondrial VDAC1: A key gatekeeper as potential therapeutic target. Front. Physiol. 8, 1–18. https://doi.org/10.3389/fphys.2017.00460

Cancer Research UK, 2018. Cancer Incidence by Age [WWW Document]. URL http://www.cancerresearchuk.org/health-professional/cancer-statistics/incidence/age#heading-Zero (accessed 5.31.18).

Cancer Research UK, 2017. Treatment for cancer [WWW Document]. URL https://www.cancerresearchuk.org/about-cancer/cancer-in-general/treatment (accessed 9.10.18).

Caney, C., Bulmer, J., Singh, G., Lukka, H., Rainbow, A.J., 1999. Pre-exposure of human squamous carcinoma cells to low-doses of gamma-rays leads to an increased resistance to subsequent low-dose cisplatin treatment. Int. J. Radiat. Biol. 75, 963–972.

Carelle, N., Piotto, E., Bellanger, A., Germanaud, J., Thuillier, A., Khayat, D., 2002. Changing patient perceptions of the side effects of cancer chemotherapy. Cancer 95, 155–163. https://doi.org/10.1002/cncr.10630

Chambers, E.S., Viardot, A., Psichas, A., Morrison, D.J., Murphy, K.G., Zac-Varghese, S.E.K., MacDougall, K., Preston, T., Tedford, C., Finlayson, G.S., Blundell, J.E., Bell, J.D., Thomas, E.L., Mt-Isa, S., Ashby, D., Gibson, G.R., Kolida, S., Dhillo, W.S., Bloom, S.R., Morley, W., Clegg, S., Frost, G., 2015. Effects of targeted delivery of propionate to the human colon on appetite regulation, body weight maintenance and adiposity in overweight adults. Gut 64, 1744–1754. https://doi.org/10.1136/gutjnl-2014-307913

Chang, P. V., Hao, L., Offermanns, S., Medzhitov, R., 2014. The microbial metabolite butyrate regulates intestinal macrophage function via histone deacetylase inhibition. Proc. Natl. Acad. Sci. U. S. A. 111, 2247–52. https://doi.org/10.1073/pnas.1322269111

Chatterjee, A., Mambo, E., Sidransky, D., 2006. Mitochondrial DNA mutations in human cancer. Oncogene 25, 4663–74. https://doi.org/10.1038/sj.onc.1209604

Chen, G., Goeddel, D., 2002. TNF-R1 Signaling: A Beautiful Pathway. Science. 296. https://doi.org/10.1126/science.1071924

Chen, H.P., Zhao, Y.T., Zhao, T.C., 2015. Histone deacetylases and mechanisms of regulation of gene expression. Crit. Rev. Oncog. 20, 35–47.

Chevrollier, A., Loiseau, D., Reynier, P., Stepien, G., 2011. Adenine nucleotide translocase 2 is a key mitochondrial protein in cancer metabolism. Biochim. Biophys. Acta - Bioenerg. 1807, 562–567. https://doi.org/10.1016/j.bbabio.2010.10.008

Chipuk, J.E., Moldoveanu, T., Llambi, F., Parsons, M.J., Green, D.R., 2010. The BCL-2 Family Reunion. Mol. Cell 37, 299–310. https://doi.org/10.1016/j.molcel.2010.01.025

Choi, S.Y.C., Lin, D., Gout, P.W., Collins, C.C., Xu, Y., Wang, Y., 2014. Lessons from patient-derived xenografts for better in vitro modeling of human cancer. Adv. Drug Deliv. Rev. 79, 222–237. https://doi.org/10.1016/j.addr.2014.09.009

Choi, Y.M., Kim, H.K., Shim, W., Anwar, M.A., Kwon, J.W., Kwon, H.K., Kim, H.J., Jeong, H., Kim, H.M., Hwang, D., Kim, H.S., Choi, S., 2015. Mechanism of cisplatin-induced cytotoxicity is correlated to impaired metabolism due to mitochondrial ROS generation. PLoS One 10, 70271. https://doi.org/10.1371/journal.pone.0135083

Chonghaile, T., Sarosiek, K.A., Vo, T.-T.T., Ryan, J.A., Tammareddi, A., del Moore, V.G., Deng, J., Anderson, K.C., Richardson, P., Tai, Y.-T.T., Mitsiades, C.S., Matulonis, U.A., Drapkin, R., Stone, R., Deangelo, D.J., McConkey, D.J., Sallan, S.E., Silverman, L., Hirsch, M.S., Carrasco, D.R., Letai, A., 2011. Pretreatment mitochondrial priming correlates with clinical response to cytotoxic chemotherapy. Science. 334, 1129–1133. https://doi.org/10.1126/science.1206727

Clapham, D.E., 2007. Calcium Signaling. Cell 131, 1047–1058. https://doi.org/10.1016/j.cell.2007.11.028

Clark, W.H., 1991. Tumour progression and the nature of cancer. Br. J. Cancer 64, 631–644. https://doi.org/10.1038/bjc.1991.375

Coller, H.A., 2014. Is cancer a metabolic disease? Am. J. Pathol. 184, 4–17. https://doi.org/10.1016/j.ajpath.2013.07.035

Collins, K., Jacks, T., Pavletich, N.P., 1997. The cell cycle and cancer. Proc. Natl. Acad. Sci. U. S. A. 94, 2776–2778. https://doi.org/10.1073/pnas.94.7.2776

Comalada, M., Bailón, E., De Haro, O., Lara-Villoslada, F., Xaus, J., Zarzuelo, A., Gálvez, J., 2006. The effects of short-chain fatty acids on colon epithelial proliferation and survival depend on the cellular phenotype. J. Cancer Res. Clin. Oncol. 132, 487–497. https://doi.org/10.1007/s00432-006-0092-x

Comerford, S.A., Huang, Z., Du, X., Wang, Y., Cai, L., Witkiewicz, A.K., Walters, H., Tantawy, M.N., Fu, A., Manning, H.C., Horton, J.D., Hammer, R.E., Mcknight, S.L., Tu, B.P., 2014. Acetate dependence of tumors. Cell 159, 1591–1602. https://doi.org/10.1016/j.cell.2014.11.020

Contreras, L., Drago, I., Zampese, E., Pozzan, T., 2010. Mitochondria: the calcium connection. Biochim. Biophys. Acta (BBA)-Bioenergetics 1797, 607–618. https://doi.org/10.1016/j.bbabio.2010.05.005

Corrêa-Oliveira, R., Fachi, J.L., Vieira, A., Sato, F.T., Vinolo, M.A.R., 2016. Regulation of immune cell function by short-chain fatty acids. Clin. Transl. Immunol. 5, e73. https://doi.org/10.1038/cti.2016.17

Cosentino, K., García-sáez, A.J., 2014. Mitochondrial alterations in apoptosis. Chem. Phys. Lipids 181, 62–75. https://doi.org/10.1016/j.chemphyslip.2014.04.001

Courtnay, R., Ngo, D.C., Malik, N., Ververis, K., Tortorella, S.M., Karagiannis, T.C., 2015. Cancer metabolism and the Warburg effect: the role of HIF-1 and PI3K. Mol. Biol. Rep. https://doi.org/10.1007/s11033-015-3858-x

Cree, I.A., Charlton, P., 2017. Molecular chess ? Hallmarks of anti-cancer drug resistance. BMC Cancer 1–8. https://doi.org/10.1186/s12885-016-2999-1

Croce, C.M., 2008. Oncogenes and cancer. N. Engl. J. Med. 358, 502–11. https://doi.org/10.1056/NEJMra072367

Cummings, J.H., Pomare, E.W., Branch, W.J., Naylor, C.P., Macfarlane, G.T., 1987. Short chain fatty acids in human large intestine, portal, hepatic and venous blood. Gut 28, 1221–1227. https://doi.org/10.1136/gut.28.10.1221

da Costa, C.A., Checler, F., 2010. A novel parkin-mediated transcriptional function links p53 to familial Parkinson's disease. Cell Cycle 9, 16–7. https://doi.org/10.4161/cc.9.1.10420

Dai, J., Inscho, E.W., Yuan, L., Hill, S.M., 2002. Modulation of intracellular calcium and calmodulin by melatonin in MCF-7 human breast cancer cells. J. Pineal Res. 32, 112–119. https://doi.org/10.1034/j.1600-079x.2002.1844.x

Davidoff, F., Korn, E.D., 1963. The biosynthesis of fatty acids in the cellular slime mold, Dictyostelium discoideum. J. Biol. Chem. 238, 3210–5.

Davis, C., Naci, H., Gurpinar, E., Poplavska, E., Pinto, A., Aggarwal, A., 2017. Availability of evidence of benefits on overall survival and quality of life of cancer drugs approved by European Medicines Agency: retrospective cohort study of drug approvals 2009-13. BMJ 359, j4530. https://doi.org/10.1136/bmj.j4530

De Berardinis, R.J., Chandel, N.S., 2016. Fundamentals of cancer metabolism. Sci. Adv. 2. https://doi.org/10.1126/sciadv.1600200

de Jager, T.L., Cockrell, A.E., Du Plessis, S.S., 2017. Ultraviolet light induced generation of reactive oxygen species. Adv. Exp. Med. Biol. 996, 15–23. https://doi.org/10.1007/978-3-319-56017-5_2

den Besten, G., van Eunen, K., Groen, A.K., Venema, K., Reijngoud, D.-J., Bakker, B.M., 2013. The role of short-chain fatty acids in the interplay between diet, gut microbiota, and host energy metabolism. J. Lipid Res. 54, 2325–2340. https://doi.org/10.1194/jlr.R036012

Desbonnet, L., Clarke, G., Shanahan, F., Dinan, T.G., Cryan, J.F., 2014. Microbiota is essential for social development in the mouse. Mol. Psychiatry 19, 146–8. https://doi.org/10.1038/mp.2013.65

Diaspro, A., Bianchini, P., Vicidomini, G., Faretta, M., Ramoino, P., Usai, C., 2006. Multi-photon excitation microscopy. Biomed. Eng. Online 5, 1–14. https://doi.org/10.1186/1475-925X-5-36

Digman, M.A., Caiolfa, V.R., Zamai, M., Gratton, E., 2008. The phasor approach to fluorescence lifetime imaging analysis. Biophys. J. 94, 14–16. https://doi.org/10.1529/biophysj.107.120154

Dilruba, S., Kalayda, G. V, 2016. Platinum-based drugs: past, present and future. Cancer Chemother. Pharmacol. 77, 1103–24. https://doi.org/10.1007/s00280-016-2976-z

Ding, W.X., Yin, X.M., 2012. Mitophagy: Mechanisms, pathophysiological roles, and analysis. Biol. Chem. 393, 547–564. https://doi.org/10.1515/hsz-2012-0119

DiPaola, R.S., 2002. To arrest or not to G(2)-M Cell-cycle arrest : commentary re: A. K. Tyagi et al., Silibinin strongly synergizes human prostate carcinoma DU145 cells to doxorubicin-induced growth inhibition, G(2)-M arrest, and apoptosis. Clin. cancer res., 8: 3512-3519, 2. Clin. Cancer Res. 8, 3311–4.

Dolman, N.J., Chambers, K.M., Mandavilli, B., Batchelor, R.H., Janes, M.S., 2013. Tools and techniques to measure mitophagy using fluorescence microscopy. Autophagy 9, 1653–1662. https://doi.org/10.4161/auto.24001

Dranka, B.P., Benavides, G.A., Diers, A.R., Giordano, S., Blake, R., Reily, C., Zou, L., Chatham, J.C., Hill, B.G., Landar, A., Darley-usmar, V.M., 2011. Assessing bioenergetic function in response to oxidative stress by metabolic profiling. Free Radic Biol Med 51, 1621–1635. https://doi.org/10.1016/j.freeradbiomed.2011.08.005.Assessing

Duan, H., Heckman, C.A., Boxer, L.M., 2005. Histone deacetylase inhibitors down-regulate bcl-2 expression and induce apoptosis in t(14;18) lymphomas. Mol. Cell. Biol. 25, 1608–19. https://doi.org/10.1128/MCB.25.5.1608-1619.2005

Eisenberg, T., Schroeder, S., Andryushkova, A., Pendl, T., Küttner, V., Bhukel, A., Mariño, G., Pietrocola, F., Harger, A., Zimmermann, A., Moustafa, T., Sprenger, A., Jany, E., Büttner, S., Carmona-Gutierrez, D., Ruckenstuhl, C., Ring, J., Reichelt, W., Schimmel, K., Leeb, T., Moser, C., Schatz, S., Kamolz, L.-P., Magnes, C., Sinner, F., Sedej, S., Fröhlich, K.-U., Juhasz, G., Pieber, T.R., Dengjel, J., Sigrist, S.J., Kroemer, G., Madeo, F., 2014. Nucleocytosolic depletion of the energy metabolite acetyl-coenzyme a stimulates autophagy and prolongs lifespan. Cell Metab. 19, 431–44. https://doi.org/10.1016/j.cmet.2014.02.010

El-Senduny, F.F., Badria, F.A., El-Waseef, A.M., 2015. Approach for chemosensitization of cisplatin-resistant ovarian cancer by cucurbitacin B. Approach chemosensitization cisplatin-resistant ovarian cancer by cucurbitacin B. https://doi.org/10.1007/s13277-015-3773-8

Elliott, R.L., Jiang, X.P., Head, J.F., 2012. Mitochondria organelle transplantation: Introduction of normal epithelial mitochondria into human cancer cells inhibits proliferation and increases drug sensitivity. Breast Cancer Res. Treat. 136, 347–354. https://doi.org/10.1007/s10549-012-2283-2

Elmore, S., 2007. Apoptosis: a review of programmed cell death. Toxicol. Pathol. 35, 495–516. https://doi.org/10.1080/01926230701320337

Emenaker, N.J., Calaf, G.M., Cox, D., Basson, M.D., Qureshi, N., 2001. Short-chain fatty acids inhibit invasive human colon cancer by modulating uPA, TIMP-1, TIMP-2, mutant p53, Bcl-2, Bax, p21 and PCNA protein expression in an in vitro cell culture model. J. Nutr. 131, 3041S–6S. https://doi.org/10.1093/jn/131.11.3041S

Eruslanov, E., Kusmartsev, S., 2010. Identification of ROS using oxidized DCFDA and flow-cytometry, in: Armstrong, D. (Ed.), Advanced Protocols in Oxidative Stress II. Humana Press, Totowa, NJ, pp. 57–72. https://doi.org/10.1007/978-1-60761-411-1_4

Fadejeva, I., Olschewski, H., Hrzenjak, A., 2017. MicroRNAs as regulators of cisplatin-resistance in non-small cell lung carcinomas. Oncotarget 8, 115754–115773. https://doi.org/10.18632/oncotarget.22975

Feissner, R.F., Skalska, J., Gaum, W.E., Sheu, S.-S., 2009. Crosstalk signaling between mitochondrial Ca2+ and ROS. Front. Biosci. (Landmark Ed. 14, 1197–218. https://doi.org/10.2741/3303

Fernald, K., Kurokawa, M., 2013. Evading apoptosis in cancer. Trends Cell Biol. 23, 620–33. https://doi.org/10.1016/j.tcb.2013.07.006

Ferreira, C.G., Tolis, C., Giaccone, G., 1999. P53 and Chemosensitivity. Ann. Oncol. 10, 1011–1021. https://doi.org/10.1023/A:1008361818480

Fitzgerald, A.L., Osman, A.A., Xie, T.-X., Patel, A., Skinner, H., Sandulache, V., Myers, J.N., 2015. Reactive oxygen species and p21Waf1/Cip1 are both essential for p53-mediated senescence of head and neck cancer cells. Cell Death Dis. 6, e1678. https://doi.org/10.1038/cddis.2015.44

Flegal, K.M., Kit, B.K., Orpana, H., Graubard, B.I., 2013. Association of All-Cause Mortality With Overweight and Obesity Using Standard Body Mass Index Categories. JAMA 309, 71. https://doi.org/10.1001/jama.2012.113905

Fonteriz, R.I., de la Fuente, S., Moreno, A., Lobatón, C.D., Montero, M., Alvarez, J., 2010. Monitoring mitochondrial [Ca2+] dynamics with rhod-2, ratiometric pericam and aequorin. Cell Calcium 48, 61–69. https://doi.org/10.1016/j.ceca.2010.07.001

Frank, M., Duvezin-Caubet, S., Koob, S., Occhipinti, A., Jagasia, R., Petcherski, A., Ruonala, M.O., Priault, M., Salin, B., Reichert, A.S., 2012. Mitophagy is triggered by mild oxidative stress in a mitochondrial fission dependent manner. Biochim. Biophys. Acta - Mol. Cell Res. 1823, 2297–2310. https://doi.org/10.1016/j.bbamcr.2012.08.007

Frenkel, M., 2013. Refusing Treatment. Oncologist 18, 634–636. https://doi.org/10.1634/theoncologist.2012-0436

Fujino, T., Kondo, J., Ishikawa, M., Morikawa, K., Yamamoto, T.T., 2001. Acetyl-CoA synthetase 2, a mitochondrial matrix enzyme involved in the oxidation of acetate. J. Biol. Chem. 276, 11420–6. https://doi.org/10.1074/jbc.M008782200

Futreal, P. a. A., Coin, L., Marshall, M., Down, T., Hubbard, T., Wooster, R., Rahman, N., Stratton, M.R., 2004. A census of human cancer genes. Nat. Rev. Cancer 4, 177–83. https://doi.org/10.1038/nrc1299

Garrido, C., Galluzzi, L., Brunet, M., Puig, P.E., Didelot, C., Kroemer, G., 2006. Mechanisms of cytochrome c release from mitochondria. Cell Death Differ. 13, 1423–1433. https://doi.org/10.1038/sj.cdd.4401950

Gasparre, G., Hervouet, E., de Laplanche, E., Demont, J., Pennisi, L.F., Colombel, M., Mège-Lechevallier, F., Scoazec, J.Y., Bonora, E., Smeets, R., Smeitink, J., Lazar, V., Lespinasse, J., Giraud, S., Godinot, C., Romeo, G., Simonnet, H., 2008. Clonal expansion of mutated mitochondrial DNA is associated with tumor formation and complex I deficiency in the benign renal oncocytoma. Hum. Mol. Genet. 17, 986–995. https://doi.org/10.1093/hmg/ddm371

Gaumann, A.K.A., Kiefer, F., Alfer, J., Lang, S.A., Geissler, E.K., Breier, G., 2016. Receptor tyrosine kinase inhibitors: Are they real tumor killers? Int. J. Cancer. https://doi.org/10.1002/ijc.29499

Ge, H., Li, X., Weiszmann, J., Wang, P., Baribault, H., Chen, J.L., Tian, H., Li, Y., 2008. Activation of G protein-coupled receptor 43 in adipocytes leads to inhibition of lipolysis and suppression of plasma free fatty acids. Endocrinology 149, 4519–4526. https://doi.org/10.1210/en.2008-0059

Gee, K.R., Brown, K.A., Chen, W.N.U., Bishop-Stewart, J., Gray, D., Johnson, I., 2000. Chemical and physiological characterization of fluo-4 Ca2+-indicator dyes. Cell Calcium 27, 97–106. https://doi.org/10.1054/ceca.1999.0095

Geiszt, M., 2006. NADPH oxidases: New kids on the block. Cardiovasc. Res. 71, 289–299. https://doi.org/10.1016/j.cardiores.2006.05.004

Ghukasyan, V. V., Kao, F.J., 2009. Monitoring cellular metabolism with fluorescence lifetime of reduced nicotinamide adenine dinucleotide. J. Phys. Chem. C 113, 11532–11540. https://doi.org/10.1021/jp810931u

Giglio, P., Gilbert, M.R., 2010. Neurologic complications of cancer and its treatment. Curr. Oncol. Rep. 12, 50–59. https://doi.org/10.1007/s11912-009-0071-x

Gill, P.A., van Zelm, M.C., Muir, J.G., Gibson, P.R., 2018. Review article: short chain fatty acids as potential therapeutic agents in human gastrointestinal and inflammatory disorders. Aliment. Pharmacol. Ther. 48, 15–34. https://doi.org/10.1111/apt.14689

Giorgi, C., Baldassari, F., Bononi, A., Bonora, M., De Marchi, E., Marchi, S., Missiroli, S., Patergnani, S., Rimessi, A., Suski, J.M., Wieckowski, M.R., Pinton, P., 2012. Mitochondrial Ca2+and apoptosis. Cell Calcium 52, 36–43. https://doi.org/10.1016/j.ceca.2012.02.008

Giorgi, C., Bonora, M., Sorrentino, G., Missiroli, S., Poletti, F., Suski, J.M., Galindo Ramirez, F., Rizzuto, R., Di Virgilio, F., Zito, E., Pandolfi, P.P., Wieckowski, M.R., Mammano, F., Del Sal, G., Pinton, P., 2015. p53 at the endoplasmic reticulum regulates apoptosis in a Ca 2+ -dependent manner. Proc. Natl. Acad. Sci. 112, 1779–1784. https://doi.org/10.1073/pnas.1410723112

Gladyshev, V.N., 2014. The free radical theory of aging is dead. Long live the damage theory! Antioxid. Redox Signal. 20, 727–31. https://doi.org/10.1089/ars.2013.5228

Green, D.R., Llambi, F., 2015. Cell death signaling. Cold Spring Harb. Perspect. Biol. 7.

Griffiths, E.J., Rutter, G.A., 2009. Mitochondrial calcium as a key regulator of mitochondrial ATP production in mammalian cells. Biochim. Biophys. Acta - Bioenerg. 1787, 1324–1333. https://doi.org/10.1016/j.bbabio.2009.01.019

Guo, H.-W., Yu, J.-S., Hsu, S.-H., Wei, Y.-H., Lee, O.K., Dong, C.-Y., Wang, H.-W., 2015. Correlation of NADH fluorescence lifetime and oxidative phosphorylation metabolism in the osteogenic differentiation of human mesenchymal stem cell. J. Biomed. Opt. 20, 017004. https://doi.org/10.1117/1.JBO.20.1.017004

Guo, J., Wu, G., Bao, J., Hao, W., Lu, J., Chen, X., 2014. Cucurbitacin B induced ATM-mediated DNA damage causes G2/M cell cycle arrest in a ROS-dependent manner. PLoS One 9. https://doi.org/10.1371/journal.pone.0088140

Haanen, C., Vermes, I., 1996. Apoptosis: Programmed cell death in fetal development. Eur. J. Obstet. Gynecol. Reprod. Biol. 64, 129–133. https://doi.org/10.1016/0301-2115(95)02261-9

Hague, A., Elder, D.J.E., Hicks, D.J., Paraskeva, C., 1995. Apoptosis in colorectal tumour cells: Induction by the short chain fatty acids butyrate, propionate and acetate and by the bile salt deoxycholate. Int. J. Cancer 60, 400–406. https://doi.org/10.1002/ijc.2910600322

Hajnóczky, G., Robb-Gaspers, L.D., Seitz, M.B., Thomas, A.P., 1995. Decoding of cytosolic calcium oscillations in the mitochondria. Cell 82, 415–424. https://doi.org/10.1016/0092-8674(95)90430-1

Hanahan, D., Weinberg, R.A., 2011. Hallmarks of cancer: The next generation. Cell 144, 646–674. https://doi.org/10.1016/j.cell.2011.02.013

Hanahan, D., Weinberg, R.A., 2000. The Hallmarks of Cancer. Cell 100, 57–70. https://doi.org/10.1016/S0092-8674(00)81683-9

Hansen, T.H., Gøbel, R.J., Hansen, T., Pedersen, O., 2015. The gut microbiome in cardio-metabolic health. Genome Med. 7, 33. https://doi.org/10.1186/s13073-015-0157-z

Hatanaka, H., Takada, S., Tsukui, M., Choi, Y.L., Kurashina, K., Soda, M., Yamashita, Y., Haruta, H., Hamada, T., Tamada, K., Hosoya, Y., Sata, N., Nagai, H., Yasuda, Y., Sugano, K., Mano, H., 2010. Identification of transforming activity of free fatty acid receptor 2 by retroviral expression screening. Cancer Sci. 101, 60–64. https://doi.org/10.1111/j.1349-7006.2009.01355.x

Hawkins, B.J., Solt, L.A., Chowdhury, I., Kazi, A.S., Abid, M.R., Aird, W.C., May, M.J., Foskett, J.K., Madesh, M., 2007. G protein-coupled receptor Ca2+-linked mitochondrial reactive oxygen species are essential for endothelial/leukocyte adherence. Mol. Cell. Biol. 27, 7582–93. https://doi.org/10.1128/MCB.00493-07

He, J., Mao, C.-C., Reyes, A., Sembongi, H., Di Re, M., Granycome, C., Clippingdale, A.B., Fearnley, I.M., Harbour, M., Robinson, A.J., Reichelt, S., Spelbrink, J.N., Walker, J.E., Holt, I.J., 2007. The AAA+ protein ATAD3 has displacement loop binding properties and is involved in mitochondrial nucleoid organization. J. Cell Biol. 176, 141–6. https://doi.org/10.1083/jcb.200609158

Henley, A.B., 2015. Pretreating with Canabidiol (CBD) enhances chemotherapy: evidence for mitochondrial “priming.” Imperial College London.

Higuchi-Sanabria, R., Frankino, P.A., Paul, J.W., Tronnes, S.U., Dillin, A., 2018. A Futile Battle? Protein Quality Control and the Stress of Aging. Dev. Cell 44, 139–163. https://doi.org/10.1016/j.devcel.2017.12.020

Hinnebusch, B.F., Meng, S., Wu, J.T., Archer, S.Y., Hodin, R.A., 2002. The effects of short-chain fatty acids on human colon cancer cell phenotype are associated with histone hyperacetylation. J. Nutr. 132, 1012–1017. https://doi.org/10.1038/nrc3610

Ho, R.H., Chan, J.C.Y., Fan, H., Kioh, D.Y.Q., Lee, B.W., Chan, E.C.Y., 2017. In silico and in vitro interactions between short chain fatty acids and human histone deacetylases. Biochemistry 56, 4871–4878. https://doi.org/10.1021/acs.biochem.7b00508

Hoeijmakers, J.H.J., 2009. DNA Damage, Aging, and Cancer. N. Engl. J. Med. 1475–1485. https://doi.org/10.1056/NEJMra0804615

Holmstrom, K.M., Baird, L., Zhang, Y., Hargreaves, I., Chalasani, A., Land, J.M., Stanyer, L., Yamamoto, M., Dinkova-Kostova, A.T., Abramov, A.Y., 2013. Nrf2 impacts cellular bioenergetics by controlling substrate availability for mitochondrial respiration. Biol. Open 2, 761–770. https://doi.org/10.1242/bio.20134853

Holmström, K.M., Finkel, T., 2014. Cellular mechanisms and physiological consequences of redox-dependent signalling. Nat. Publ. Gr. 15, 411–421. https://doi.org/10.1038/nrm3801

Hou, L., Xie, K., Qin, M., Peng, D., Ma, S., Shang, L., Li, N., Li, S., Ji, G., Lu, Y., Xiong, L., 2010. Effects of reactive oxygen species scavenger on the protective action of 100% oxygen treatment

against sterile inflammation in mice. Shock 33, 646–54. https://doi.org/10.1097/SHK.0b013e3181c1b5d4

Housman, G., Byler, S., Heerboth, S., Lapinska, K., Longacre, M., Snyder, N., Sarkar, S., 2014. Drug resistance in cancer: an overview. Cancers (Basel). 6, 1769–92. https://doi.org/10.3390/cancers6031769

Hsu, P.P., Sabatini, D.M., 2008. Cancer cell metabolism: Warburg and beyond. Cell 134, 703–707. https://doi.org/10.1016/j.cell.2008.08.021

Ichimura, A., Hirasawa, A., Hara, T., Tsujimoto, G., 2009. Free fatty acid receptors act as nutrient sensors to regulate energy homeostasis. Prostaglandins Other Lipid Mediat. 89, 82–88. https://doi.org/10.1016/j.prostaglandins.2009.05.003

Invitrogen, 2011. Fluo-4, AM Protocol [WWW Document]. URL https://assets.thermofisher.com/TFS-Assets/LSG/manuals/mp01240.pdf (accessed 9.24.18).

Israel, B.A., Schaeffer, W.I., 1987. Cytoplasmic suppression of malignancy. In Vitro Cell. Dev. Biol. 23, 627–32.

Jackson, J.R., Gilmartin, A., Imburgia, C., Winkler, J.D., Marshall, L.A., Roshak, A., 2000. An indolocarbazole inhibitor of human checkpoint kinase (Chk1) abrogates cell cycle arrest caused by DNA damage. Cancer Res. 60, 566–572. https://doi.org/10.1158/0008-5472.can-09-2312

Jan, G., Belzacq, A.S., Haouzi, D., Rouault, A., Metivier, D., Kroemer, G., Brenner, C., 2002. Propionibacteria induce apoptosis of colorectal carcinoma cells via short-chain fatty acids acting on mitochondria. Cell Death Differ 9, 179–188. https://doi.org/10.1038/sj.cdd.4400935

Jastroch, M., Divakaruni, A.S., Mookerjee, S., Treberg, J.R., Brand, M.D., 2010. Mitochondrial proton and electron leaks. Essays Biochem. 47, 53–67. https://doi.org/10.1042/bse0470053

Jemal, A., Bray, F., Center, M.M., Ferlay, J., Ward, E., Forman, D., 2011. Global cancer statistics. CA. Cancer J. Clin. 61, 69–90. https://doi.org/10.3322/caac.20107

Jeyaraju, D. V., Cisbani, G., Pellegrini, L., 2009. Calcium regulation of mitochondria motility and morphology. Biochim. Biophys. Acta - Bioenerg. 1787, 1363–1373. https://doi.org/10.1016/j.bbabio.2008.12.005

Ji, M.M., Wang, L., Zhan, Q., Xue, W., Zhao, Y., Zhao, X., Xu, P.P., Shen, Y., Liu, H., Janin, A., Cheng, S., Zhao, W.L., 2015. Induction of autophagy by valproic acid enhanced lymphoma cell chemosensitivity through HDAC-independent and IP3-mediated PRKAA activation. Autophagy 11, 160–2171. https://doi.org/10.1080/15548627.2015.1082024

Jiang, W.G., Sanders, A.J., Katoh, M., Ungefroren, H., Gieseler, F., Prince, M., Thompson, S.K., Zollo, M., Spano, D., Dhawan, P., Sliva, D., Subbarayan, P.R., Sarkar, M., Honoki, K., Fujii, H., Georgakilas, A.G., Amedei, A., Niccolai, E., Amin, A., Ashraf, S.S., Ye, L., Helferich, W.G., Yang, X., Boosani, C.S., Guha, G., Ciriolo, M.R., Aquilano, K., Chen, S., Azmi, A.S., Keith, W.N., Bilsland, A., Bhakta, D., Halicka, D., Nowsheen, S., Pantano, F., Santini, D., 2015. Tissue invasion and metastasis: Molecular, biological and clinical perspectives. Semin. Cancer Biol. 35, S244–S275. https://doi.org/10.1016/j.semcancer.2015.03.008

Kaddour-Djebbar, I., Choudhary, V., Brooks, C., Ghazaly, T., Lakshmikanthan, V., Dong, Z., Kumar, M.V., 2010. Specific mitochondrial calcium overload induces mitochondrial fission in prostate cancer cells. Int. J. Oncol. 36, 1437–44. https://doi.org/10.3892/ijo

Kale, J., Osterlund, E.J., Andrews, D.W., 2018. BCL-2 family proteins: changing partners in the dance towards death. Cell Death Differ. 25, 65–80. https://doi.org/10.1038/cdd.2017.186

Kalyanaraman, B., Darley-Usmar, V., Davies, K., Dennery, P., Forman, H., Grisham, M., Mann, G., Moore, K., Roberts II, L., Ischiropoulos, H., 2012. Measuring reactive oxygen and nitrogen species with fluorescent probes: challenges and limitations. Free Radic Biol Med. 52, 1–6. https://doi.org/10.1016/j.freeradbiomed.2011.09.030.Measuring

Katt, M.E., Placone, A.L., Wong, A.D., Xu, Z.S., Searson, P.C., 2016. In Vitro Tumor Models: Advantages, Disadvantages, Variables, and Selecting the Right Platform. Front. Bioeng. Biotechnol. 4. https://doi.org/10.3389/fbioe.2016.00012

Kaur, G., Dufour, J.M., 2012. Cell lines: Valuable tools or useless artifacts. Spermatogenesis 2, 1–5. https://doi.org/10.4161/spmg.19885

Keenan, M.M., Chi, J.-T., 2015. Alternative fuels for cancer cells. Cancer J. 21, 49–55. https://doi.org/10.1097/PPO.0000000000000104

Kelly, J.R., Borre, Y., Aidy, S. El, Deane, J., Patterson, E., Kennedy, P.J., Beers, S., Scott, K., Moloney, G., Scott, L., Ross, P., Stanton, C., Clarke, G., Cryan, J.F., Dinan, T.G., 2016. P.4.001 Transferring the blues: depression-associated gut microbiota induces neurobehavioural changes in the rat. Eur. Neuropsychopharmacol. 26, S85–S86. https://doi.org/10.1016/S0924-977X(16)70091-5

Keston, A.S., Brandt, R., 1965. The fluorometric analysis of ultramicro quantities of hydrogen peroxide. Anal. Biochem. 11, 1–5.

Kim, E.H., Koh, E.H., Park, J.-Y., Lee, K.-U., 2010. Adenine nucleotide translocator as a regulator of mitochondrial function: implication in the pathogenesis of metabolic syndrome. Korean Diabetes J. 34, 146–53. https://doi.org/10.4093/kdj.2010.34.3.146

Kirat, D., Kato, S., 2006. Monocarboxylate transporter 1 (MCT1) mediates transport of short-chain fatty acids in bovine caecum. Exp. Physiol. 91, 835–844. https://doi.org/10.1113/expphysiol.2006.033837

Kirches, E., 2017. MtDNA As a cancer marker: a finally closed chapter? Curr. Genomics 18, 255–267. https://doi.org/10.2174/1389202918666170105093635

Kirichok, Krapivinsky, Clapham, Kirichok, Y., Krapivinsky, G., Clapham, D.E., 2004. The Mitochondrial Calcium Uniporter is a Highly Selective Ion Channel. Nature 427, 360–364. https://doi.org/10.1038/nature02246

Kowaltowski, A.J., Naia-da-Silva, E.S., Castilho, R.F., Vercesi, A.E., 1998. Ca2+-stimulated mitochondrial reactive oxygen species generation and permeability transition are inhibited by dibucaine or Mg2+. Arch. Biochem. Biophys. 359, 77–81. https://doi.org/10.1006/abbi.1998.0870

Krishan, A., 1975. Rapid flow cytofluorometric analysis of mammalian cell cycle by propidium iodide staining. J. Cell Biol. 66, 188–93.

Kroemer, G., Galluzzi, L., Brenner, C., 2007. Mitochondrial membrane permeabilization in cell death. Physiol. Rev. 87, 99–163. https://doi.org/10.1152/physrev.00013.2006

Kruiswijk, F., Labuschagne, C.F., Vousden, K.H., 2015. P53 in survival, death and metabolic health: A lifeguard with a licence to kill. Nat. Rev. Mol. Cell Biol. 16, 393–405. https://doi.org/10.1038/nrm4007

Kumar, D., Basu, S., Parija, L., Rout, D., Manna, S., Dandapat, J., Debata, P.R., 2016. Curcumin and Ellagic acid synergistically induce ROS generation, DNA damage, p53 accumulation and apoptosis in

HeLa cervical carcinoma cells. Biomed. Pharmacother. 81, 31–37. https://doi.org/10.1016/j.biopha.2016.03.037

Kuo, M.H., Allis, C.D., 1998. Roles of histone acetyltransferases and deacetylases in gene regulation. BioEssays 20, 615–626. https://doi.org/10.1002/(SICI)1521-1878(199808)20:8<615::AID-BIES4>3.0.CO;2-H

Kwong, J.Q., Molkentin, J.D., 2015. Physiological and pathological roles of the mitochondrial permeability transition pore in the heart. Cell Metab. 21, 206–214. https://doi.org/10.1016/j.cmet.2014.12.001

Lakhter, A.J., Hamilton, J., Konger, R.L., Brustovetsky, N., Broxmeyer, H.E., Naidu, S.R., 2016. Glucose-independent acetate metabolism promotes melanoma cell survival and tumor growth. J. Biol. Chem. 291, 21869–21879. https://doi.org/10.1074/jbc.M115.712166

Lambeth, J.D., 2004. NOX enzymes and the biology of reactive oxygen. Nat. Rev. Immunol. 4, 181–9. https://doi.org/10.1038/nri1312

Larraufie, P., Martin-Gallausiaux, C., Lapaque, N., Dore, J., Gribble, F.M., Reimann, F., Blottiere, H.M., 2018. SCFAs strongly stimulate PYY production in human enteroendocrine cells. Sci. Rep. 8, 1–9. https://doi.org/10.1038/s41598-017-18259-0

Layden, B.T., Angueira, A.R., Brodsky, M., Durai, V., Jr, W.L.L., 2012. Short chain fatty acids and their receptors: new metabolic targets. Transl. Res. 161, 131–140. https://doi.org/10.1016/j.trsl.2012.10.007

LeBel, C.P., Ischiropoulos, H., Bondy, S.C., 1992. Evaluation of the probe 2',7'-dichlorofluorescin as an indicator of reactive oxygen species formation and oxidative stress. Chem. Res. Toxicol. 5, 227–31. https://doi.org/10.1021/tx00026a012

Lee, H.C., Wei, Y.H., 2005. Mitochondrial biogenesis and mitochondrial DNA maintenance of mammalian cells under oxidative stress. Int. J. Biochem. Cell Biol. 37, 822–834. https://doi.org/10.1016/j.biocel.2004.09.010

Lee, W.T.Y., John, J.S., 2015. The control of mitochondrial DNA replication during development and tumorigenesis. Ann. N. Y. Acad. Sci. 1, 95–106. https://doi.org/10.1111/nyas.12873

Lee, Y., Jeong, S., Karbowski, M., Smith, C.L., Youle, R.J., 2004. Roles of the Mammalian Mitochondrial Fission and Fusion Mediators Fis1, Drp1, and Opa1 in Apoptosis. Mol. Biol. Cell 15, 5001–5011. https://doi.org/10.1091/mbc.e04-04-0294

Lemasters, J.J., Holmuhamedov, E.L., Czerny, C., Zhong, Z., Maldonado, E.N., 2012. Regulation of mitochondrial function by voltage dependent anion channels in ethanol metabolism and the Warburg effect. Biochim. Biophys. Acta - Biomembr. 1818, 1536–1544. https://doi.org/10.1016/j.bbamem.2011.11.034

Lemasters, J.J., Theruvath, T.P., Zhong, Z., Nieminen, A.L., 2009. Mitochondrial calcium and the permeability transition in cell death. Biochim. Biophys. Acta - Bioenerg. 1787, 1395–1401. https://doi.org/10.1016/j.bbabio.2009.06.009

Levine, B., Klionsky, D.J., 2004. Development by self-digestion: Molecular mechanisms and biological functions of autophagy. Dev. Cell. https://doi.org/10.1016/S1534-5807(04)00099-1

Li, Y., Qin, Y., Yang, C., Zhang, H., Li, Y., Wu, B., Huang, J., Zhou, X., Huang, B., Yang, K., Wu, G., 2017. Cardamonin induces ROS-mediated G2/M phase arrest and apoptosis through inhibition of NF-

κB pathway in nasopharyngeal carcinoma. Cell Death Dis. 8, e3024. https://doi.org/10.1038/cddis.2017.407

Lim, J.-H., Lee, Y.-M., Chun, Y.-S., Park, J.-W., 2008. Reactive oxygen species-mediated cyclin D1 degradation mediates tumor growth retardation in hypoxia, independently of p21cip1 and hypoxia-inducible factor. Cancer Sci. 99, 1798–805. https://doi.org/10.1111/j.1349-7006.2008.00892.x

Lin, H. V., Frassetto, A., Kowalik, E.J., Nawrocki, A.R., Lu, M.M., Kosinski, J.R., Hubert, J.A., Szeto, D., Yao, X., Forrest, G., Marsh, D.J., 2012. Butyrate and propionate protect against diet-induced obesity and regulate gut hormones via free fatty acid receptor 3-independent mechanisms. PLoS One 7, 1–9. https://doi.org/10.1371/journal.pone.0035240

Lin, X., Okuda, T., Holzer, A., Howell, S.B., 2002. The copper transporter CTR1 regulates cisplatin uptake in Saccharomyces cerevisiae. Mol. Pharmacol. 62, 1154–1159. https://doi.org/10.1124/mol.62.5.1154

Liu, Y., Bi, T., Dai, W., Wang, G., Qian, L., Shen, G., Gao, Q., 2016. Lupeol enhances inhibitory effect of 5-fluorouracil on human gastric carcinoma cells. Naunyn. Schmiedebergs. Arch. Pharmacol. https://doi.org/10.1007/s00210-016-1221-y

Liu, Y., Gao, L., Xue, Q., Li, Z., Wang, L., Chen, R., Liu, M., Wen, Y., Guan, M., Li, Y., Wang, S., 2011. Voltage-dependent anion channel involved in the mitochondrial calcium cycle of cell lines carrying the mitochondrial DNA A4263G mutation. Biochem. Biophys. Res. Commun. 404, 364–369. https://doi.org/10.1016/j.bbrc.2010.11.124

Liu, Z., Butow, R.A., 2006. Mitochondrial Retrograde Signaling. Annu. Rev. Genet. 40, 159–185. https://doi.org/10.1146/annurev.genet.40.110405.090613

Livestrong, American Cancer Society, 2010. The Global Economic Cost of Cancer [WWW Document]. Am. Cancer Soc. Tech. Rep. URL http://www.cancer.org/acs/groups/content/@internationalaffairs/documents/document/acspc-026203.pdf (accessed 8.10.16).

Lomeli, N., Di, K., Czerniawski, J., Guzowski, J.F., Bota, D.A., 2017. Cisplatin-induced mitochondrial dysfunction is associated with impaired cognitive function in rats. Free Radic. Biol. Med. 102, 274–286. https://doi.org/10.1016/j.freeradbiomed.2016.11.046

Lorusso, D., Bria, E., Costantini, A., Di Maio, M., Rosti, G., Mancuso, A., 2017. Patients' perception of chemotherapy side effects: Expectations, doctor-patient communication and impact on quality of life - An Italian survey. Eur. J. Cancer Care (Engl). 26, e12618. https://doi.org/10.1111/ecc.12618

Louis, P., Hold, G.L., Flint, H.J., 2014. The gut microbiota, bacterial metabolites and colorectal cancer. Nat. Rev. Microbiol. 12, 661–672. https://doi.org/10.1038/nrmicro3344

Louis S Goodman; Maxwell M Wintrobe; William Dameshek; Morton J Goodman; Alfred Gilman; Margaret T McLennan, 1946. Nitrogen mustard therapy; use of methyl-bis (beta-chloroethyl) amine hydrochloride and tris (beta-chloroethyl) amine. J. Am. Med. Assoc. https://doi.org/10.1001/jama.1946.02870380008004

Luong, A., Hannah, V.C., Brown, M.S., Goldstein, J.L., 2000. Molecular characterization of human acetyl-CoA synthetase, an enzyme regulated by sterol regulatory element-binding proteins. J. Biol. Chem. 275, 26458–26466. https://doi.org/10.1074/jbc.M004160200

Marchi, S., Pinton, P., 2014. The mitochondrial calcium uniporter complex: Molecular components, structure and physiopathological implications. J. Physiol. 592, 829–839. https://doi.org/10.1113/jphysiol.2013.268235

Mardinoglu, A., Shoaie, S., Bergentall, M., Ghaffari, P., Zhang, C., Larsson, E., Bäckhed, F., Nielsen, J., 2015. The gut microbiota modulates host amino acid and glutathione metabolism in mice. Mol. Syst. Biol. 11, 834. https://doi.org/10.15252/msb.20156487

Marques, C., Oliveira, C.S.F., Alves, S., Chaves, S.R., Coutinho, O.P., Côrte-Real, M., Preto, a, 2013. Acetate-induced apoptosis in colorectal carcinoma cells involves lysosomal membrane permeabilization and cathepsin D release. Cell Death Dis. 4, e507. https://doi.org/10.1038/cddis.2013.29

Martinou, J.C., Youle, R.J., 2011. Mitochondria in Apoptosis: Bcl-2 Family Members and Mitochondrial Dynamics. Dev. Cell 21, 92–101. https://doi.org/10.1016/j.devcel.2011.06.017

Marullo, R., Werner, E., Degtyareva, N., Moore, B., Altavilla, G., Ramalingam, S.S., Doetsch, P.W., 2013. Cisplatin induces a mitochondrial-ROS response that contributes to cytotoxicity depending on mitochondrial redox status and bioenergetic functions. PLoS One 8, e81162. https://doi.org/10.1371/journal.pone.0081162

Marusyk, A., Polyak, K., 2011. Tumor heterogeneity: causes and consequences. Biochim Biophys Acta 1805, 1–28. https://doi.org/10.1016/j.bbcan.2009.11.002.Tumor

Maruyama, T., Yamamoto, S., Qiu, J., Ueda, Y., Suzuki, T., Nojima, M., Shima, H., 2012. Apoptosis of bladder cancer by sodium butyrate and cisplatin. J. Infect. Chemother. 18, 288–295. https://doi.org/10.1007/s10156-011-0322-2

Maschek, G., Savaraj, N., Priebe, W., Braunschweiger, P., Hamilton, K., Tidmarsh, G., De Young, L., Lampidis, T., 2004. 2-deoxy-D-glucose increases the efficacy of adriamycin and paclitaxel in human osteosarcoma and non-small cell lung cancers in vivo. Cancer Res. 64, 31–34.

Maslowski, K.M., Vieira, A.T., Ng, A., Kranich, J., Sierro, F., Di Yu, Schilter, H.C., Rolph, M.S., MacKay, F., Artis, D., Xavier, R.J., Teixeira, M.M., MacKay, C.R., 2009. Regulation of inflammatory responses by gut microbiota and chemoattractant receptor GPR43. Nature 461, 1282–1286. https://doi.org/10.1038/nature08530

Mathew, R., Karantza-Wadsworth, V., White, E., 2007. Role of autophagy in cancer. Nat Rev Cancer 7, 961–967. https://doi.org/nrc2254 [pii]\r10.1038/nrc2254

Matthews, G.M., Howarth, G.S., Butler, R.N., 2007. Short-chain fatty acid modulation of apoptosis in the Kato III human gastric carcinoma cell line. Cancer Biol. Ther. 6, 1051–1057. https://doi.org/10.4161/cbt.6.7.4318

Mauro-lizcano, M., Esteban-martínez, L., Seco, E., Serrano-puebla, A., Figueiredo-pereira, C., Vieira, H.L. a, Boya, P., 2015. Autophagy New method to assess mitophagy flux by flow cytometry New method to assess mitophagy flux by flow cytometry. Autophagy 37–41. https://doi.org/10.1080/15548627.2015.1034403

McIlwain, D.R., Berger, T., Mak, T.W., 2015. Caspase Functions in Cell Death and Disease: Figure 1. Cold Spring Harb. Perspect. Biol. 7, a026716. https://doi.org/10.1101/cshperspect.a026716

Meeusen, S., DeVay, R., Block, J., Cassidy-Stone, A., Wayson, S., McCaffery, J.M., Nunnari, J., 2006. Mitochondrial inner-membrane fusion and crista maintenance requires the dynamin-related GTPase Mgm1. Cell 127, 383–95. https://doi.org/10.1016/j.cell.2006.09.021

Merlo, L.M.F., Pepper, J.W., Reid, B.J., Maley, C.C., 2006. Cancer as an evolutionary and ecological process. Nat. Rev. Cancer 6, 924–935. https://doi.org/10.1038/nrc2013

Miletta, M.C., Petkovic, V., Eblé, A., Ammann, R.A., Flück, C.E., Mullis, P.E., 2014. Butyrate increases intracellular calcium levels and enhances growth hormone release from rat anterior pituitary cells via the G-protein-coupled receptors GPR41 and 43. PLoS One 9. https://doi.org/10.1371/journal.pone.0107388

Miyamoto, J., Hasegawa, S., Kasubuchi, M., Ichimura, A., Nakajima, A., Kimura, I., 2016. Nutritional signaling via free fatty acid receptors. Int. J. Mol. Sci. 17, 1–12. https://doi.org/10.3390/ijms17040450

Miyauchi, S., Gopal, E., Fei, Y.-J., Ganapathy, V., 2004. Functional identification of SLC5A8, a tumor suppressor down-regulated in colon cancer, as a Na(+)-coupled transporter for short-chain fatty acids. J. Biol. Chem. 279, 13293–6. https://doi.org/10.1074/jbc.C400059200

Mizushima, N., Komatsu, M., 2011. Autophagy: Renovation of cells and tissues. Cell 147, 728–741. https://doi.org/10.1016/j.cell.2011.10.026

Morrison, D.J., Preston, T., 2016. Formation of short chain fatty acids by the gut microbiota and their impact on human metabolism. Gut Microbes 7, 189–200. https://doi.org/10.1080/19490976.2015.1134082

Mosmann, T., 1983. Rapid colorimetric assay for cellular growth and survival: Application to proliferation and cytotoxicity assays. J. Immunol. Methods 65, 55–63. https://doi.org/10.1016/0022-1759(83)90303-4

Narendra, D., Tanaka, A., Suen, D.F., Youle, R.J., 2009. Parkin-induced mitophagy in the pathogenesis of Parkinson disease. Autophagy 5, 706–708. https://doi.org/10.4161/auto.5.5.8505

National Cancer Institute, 2018. Cancer Statistics [WWW Document]. URL https://www.cancer.gov/about-cancer/understanding/statistics (accessed 9.26.18).

National Cancer Institute, 2015. What is Cancer? [WWW Document]. Natl. Cancer Inst. URL https://www.cancer.gov/about-cancer/understanding/what-is-cancer (accessed 1.7.19).

Nelson, D., Cox, M., 2008. Principles of Biochemistry, 5th ed.

Ng, S., De Clercq, I., Van Aken, O., Law, S.R., Ivanova, A., Willems, P., Giraud, E., Van Breusegem, F., Whelan, J., 2014. Anterograde and retrograde regulation of nuclear genes encoding mitochondrial proteins during growth, development, and stress. Mol. Plant 7, 1075–1093. https://doi.org/10.1093/mp/ssu037

NHS, 2017. Chemotherapy [WWW Document]. URL https://www.nhs.uk/conditions/chemotherapy/ (accessed 9.10.18).

Ni Chonghaile, T., Sarosiek, K.A., Vo, T.-T., Ryan, J.A., Tammareddi, A., Moore, V.D.G., Deng, J., Anderson, K.C., Richardson, P., Tai, Y.-T., Mitsiades, C.S., Matulonis, U.A., Drapkin, R., Stone, R., Deangelo, D.J., McConkey, D.J., Sallan, S.E., Silverman, L., Hirsch, M.S., Carrasco, D.R., Letai, A., 2011. Pretreatment mitochondrial priming correlates with clinical response to cytotoxic chemotherapy. Science 334, 1129–33. https://doi.org/10.1126/science.1206727

Nikolaev, A., McLaughlin, T., O'Leary, D.D.M., Tessier-Lavigne, M., 2009. APP binds DR6 to trigger axon pruning and neuron death via distinct caspases. Nature 457, 981–989. https://doi.org/10.1038/nature07767

Noje, C., Walker, M., Kublin, J.G., Zunt, J.R., 2009. Hemorrhagic and ischemic stroke in children with cancer. Pedatric Neurol. 42, 115–125. https://doi.org/10.1086/498510.Parasitic

Olarerin-George, A.O., Hogenesch, J.B., 2015. Assessing the prevalence of mycoplasma contamination in cell culture via a survey of NCBI's RNA-seq Archive. Nucleic Acids Res. 43, 2535–2542. https://doi.org/10.1093/nar/gkv136

Oliveira, C.S.F., Pereira, H., Alves, S., Castro, L., Baltazar, F., Chaves, S.R., Preto, A., Côrte-Real, M., 2015. Cathepsin D protects colorectal cancer cells from acetate-induced apoptosis through autophagy-independent degradation of damaged mitochondria. Cell Death Dis. 6, e1788. https://doi.org/10.1038/cddis.2015.157

Olympus, 2019. Basic Concepts in Fluorescence [WWW Document]. URL https://www.olympus-lifescience.com/en/microscope-resource/primer/techniques/fluorescence/fluorescenceintro/ (accessed 1.28.19).

Orrenius, S., Gogvadze, V., Zhivotovsky, B., 2015. Calcium and mitochondria in the regulation of cell death. Biochem. Biophys. Res. Commun. 460, 72–81. https://doi.org/10.1016/j.bbrc.2015.01.137

Ouyang, L., Shi, Z., Zhao, S., Wang, F.T., Zhou, T.T., Liu, B., Bao, J.K., 2012. Programmed cell death pathways in cancer: A review of apoptosis, autophagy and programmed necrosis. Cell Prolif. 45, 487–498. https://doi.org/10.1111/j.1365-2184.2012.00845.x

Ozaki, T., Nakagawara, A., 2011. Role of p53 in cell death and human cancers. Cancers (Basel). 3, 994–1013. https://doi.org/10.3390/cancers3010994

Pacher, P., Hajnóczky, G., 2001. Propagation of the apoptotic signal by mitochondrial waves. EMBO J. 20, 4107–4121. https://doi.org/10.1093/emboj/20.15.4107

Pan, X., Liu, J., Nguyen, T., Liu, C., Sun, J., Teng, Y., Fergusson, M.M., Rovira, I.I., Allen, M., Springer, D.A., Aponte, A.M., Gucek, M., Balaban, R.S., Murphy, E., Finkel, T., 2013. The Physiological Role of Mitochondrial Calcium Revealed by Mice Lacking the Mitochondrial Calcium Uniporter. Nat. Cell Biol. 15, 1464–1472. https://doi.org/10.1038/ncb2868

Pandey, M., Sarita, G.P., Devi, N., Thomas, B.C., Hussain, B.M., Krishnan, R., 2006. Distress, anxiety, and depression in cancer patients undergoing chemotherapy. World J. Surg. Oncol. 4, 68. https://doi.org/10.1186/1477-7819-4-68

Pandey, S.K., Yadav, S., Temre, M.K., Singh, S.M., 2018. Tracking acetate through a journey of living world: Evolution as alternative cellular fuel with potential for application in cancer therapeutics. Life Sci. 215, 86–95. https://doi.org/S0024320518307094

Panieri, E., Santoro, M.M., 2016. ROS homeostasis and metabolism: a dangerous liason in cancer cells. Cell Death Dis. 7, e2253. https://doi.org/10.1038/cddis.2016.105

Pavlova, N.N., Thompson, C.B., 2016. The emerging hallmarks of cancer metabolism. Cell Metab. 23, 27–47. https://doi.org/10.1016/j.cmet.2015.12.006

Peng, T.I., Jou, M.J., 2010. Oxidative stress caused by mitochondrial calcium overload. Ann. N. Y. Acad. Sci. 1201, 183–188. https://doi.org/10.1111/j.1749-6632.2010.05634.x

Peng, Y., Croce, C.M., 2016. The role of MicroRNAs in human cancer. Signal Transduct. Target. Ther. 1, 15004. https://doi.org/10.1038/sigtrans.2015.4

Perego, S., Sansoni, V., Banfi, G., Lombardi, G., 2018. Sodium butyrate has anti-proliferative, pro-differentiating, and immunomodulatory effects in osteosarcoma cells and counteracts the TNFα-induced low-grade inflammation. Int. J. Immunopathol. Pharmacol. 31, 039463201775224. https://doi.org/10.1177/0394632017752240

Perry, S.W., Norman, J.P., Barbieri, J., Brown, E.B., Gelbard, H.A., 2011. Mitochondrial membrane potential probes and the proton gradient: a practical usage guide. Biotechniques 50, 98–115. https://doi.org/10.2144/000113610

Pietrocola, F., Galluzzi, L., Bravo-San Pedro, J.M., Madeo, F., Kroemer, G., 2015. Acetyl coenzyme A: a central metabolite and second messenger. Cell Metab. 21, 805–21. https://doi.org/10.1016/j.cmet.2015.05.014

Portt, L., Norman, G., Clapp, C., Greenwood, M., Greenwood, M.T., 2011. Anti-apoptosis and cell survival: A review. Biochim. Biophys. Acta - Mol. Cell Res. 1813, 238–259. https://doi.org/10.1016/j.bbamcr.2010.10.010

Poteet, E., Choudhury, G.R., Winters, A., Li, W., Ryou, M.G., Liu, R., Tang, L., Ghorpade, A., Wen, Y., Yuan, F., Keir, S.T., Yan, H., Bigner, D.D., Simpkins, J.W., Yang, S.H., 2013. Reversing the Warburg effect as a treatment for glioblastoma. J. Biol. Chem. 288, 9153–9164. https://doi.org/10.1074/jbc.M112.440354

Poyton, R., McEwen, J., 1996. Crosstalk between nuclear and mitochondrial genomes. Annu. Rev. Biochem.

Priyadarshini, M., Villa, S.R., Fuller, M., Wicksteed, B., Mackay, C.R., Alquier, T., Poitout, V., Mancebo, H., Mirmira, R.G., Gilchrist, A., Layden, B.T., 2015. An acetate-specific GPCR, FFAR2, regulates insulin secretion. Mol. Endocrinol. 29, 1055–66. https://doi.org/10.1210/me.2015-1007

Proietti, S., Cucina, A., Minini, M., Bizzarri, M., 2017. Melatonin, mitochondria, and the cancer cell. Cell. Mol. Life Sci. https://doi.org/10.1007/s00018-017-2612-z

Qiang, M., 2013. Role of nrf2 in oxidative stress and toxicity. Annu. Rev. Pharmacol. Toxicol. 401–426. https://doi.org/10.1146/annurev-pharmtox-011112-140320.Role

Reczek, C.R., Chandel, N.S., 2018. ROS promotes cancer cell survival through calcium Signaling. Cancer Cell 33, 949–951. https://doi.org/10.1016/j.ccell.2018.05.010

Reed, J.C., 2011. Priming cancer cells for death. Science. 334, 1075–1076. https://doi.org/10.1126/science.1215568

Reznik, E., Miller, M.L., Şenbabaoğlu, Y., Riaz, N., Sarungbam, J., Tickoo, S.K., Al-Ahmadie, H.A., Lee, W., Seshan, V.E., Hakimi, A.A., Sander, C., 2016. Mitochondrial DNA copy number variation across human cancers. Elife 5, 1–20. https://doi.org/10.7554/eLife.10769

Rimmerman, N., Ben-Hail, D., Porat, Z., Juknat, A., Kozela, E., Daniels, M.P., Connelly, P.S., Leishman, E., Bradshaw, H.B., Shoshan-Barmatz, V., Vogel, Z., 2013. Direct modulation of the outer mitochondrial membrane channel, voltage-dependent anion channel 1 (VDAC1) by cannabidiol: A novel mechanism for cannabinoid-induced cell death. Cell Death Dis. 4, e949-11. https://doi.org/10.1038/cddis.2013.471

Riss TL, Moravec RA, Niles AL, et al, 2013. Cell Viability Assays, Assay Guidence Manual.

Rizzuto, R., Marchi, S., Bonora, M., Aguiiari, P., Bononi, A., Stefani, D., Giorgi, C., Leo, S., Rimessi, A., Siviero, R., Zecchini, E., Pinton, P., 2010. Ca2+ transfer from the ER to mitochondria: When, how and why. Biochim. Biophys. Acta 1787, 1342–1351. https://doi.org/10.1016/j.bbabio.2009.03.015.Ca

Robb, K.A., Simon, A.E., Miles, A., Wardle, J., 2014. Public perceptions of cancer: a qualitative study of the balance of positive and negative beliefs. BMJ Open 4, e005434. https://doi.org/10.1136/bmjopen-2014-005434

Robinson, K.M., Janes, M.S., Beckman, J.S., 2008. The selective detection of mitochondrial superoxide by live cell imaging. Nat. Protoc. 3, 941–947. https://doi.org/10.1038/nprot.2008.56

Roland, K.P., Jakobi, J.M., Jones, G.R., 2011. Does yoga engender fitness in older adults? A critical review. J. Aging Phys. Act. 19, 62–79. https://doi.org/10.1007/978-3-319-55330-6

Rostovtseva, T.K., Tan, W., Colombini, M., 2005. On the role of VDAC in apoptosis: Fact and fiction. J. Bioenerg. Biomembr. 37, 129–142. https://doi.org/10.1007/s10863-005-6566-8

Sablina, A.A., Budanov, A. V, Ilyinskaya, G. V, Larissa, S., Kravchenko, J.E., Chumakov, P.M., 2009. The antioxidant function of the p53 tumor suppressor 11, 1306–1313. https://doi.org/10.1038/nm1320.The

Sahuri Arisoylu, M., Bell, J., 2016. Effect of short-chain fatty acid acetate on colon cancer. FASEB J. 30.

Sanchez, T., Wang, T., Pedro, M.V., Zhang, M., Esencan, E., Sakkas, D., Needleman, D., Seli, E., 2018. Metabolic imaging with the use of fluorescence lifetime imaging microscopy (FLIM) accurately detects mitochondrial dysfunction in mouse oocytes. Fertil. Steril. 110, 1387–1397. https://doi.org/10.1016/j.fertnstert.2018.07.022

Sareen, D., Darjatmoko, S.R., Albert, D.M., Polans, A.S., 2007. Mitochondria, calcium, and calpain are key mediators of resveratrol-induced apoptosis in breast cancer. Mol. Pharmacol. 72, 1466–75. https://doi.org/10.1124/mol.107.039040

Sarsour, E.H., Kumar, M.G., Chaudhuri, L., Kalen, A.L., Goswami, P.C., 2009. Redox control of the cell cycle in health and disease. Antioxid. Redox Signal. 11, 2985–3011. https://doi.org/10.1089/ars.2009.2513

Schug, Z.T., Peck, B., Jones, D.T., Zhang, Q., Grosskurth, S., Alam, I.S., Goodwin, L.M., Smethurst, E., Mason, S., Blyth, K., McGarry, L., James, D., Shanks, E., Kalna, G., Saunders, R.E., Jiang, M., Howell, M., Lassailly, F., Thin, M.Z., Spencer-Dene, B., Stamp, G., van den Broek, N.J.F., Mackay, G., Bulusu, V., Kamphorst, J.J., Tardito, S., Strachan, D., Harris, A.L., Aboagye, E.O., Critchlow, S.E., Wakelam, M.J.O., Schulze, A., Gottlieb, E., 2015. Acetyl-CoA synthetase 2 promotes acetate utilization and maintains cancer cell growth under metabolic stress. Cancer Cell 27, 57–71. https://doi.org/10.1016/j.ccell.2014.12.002

Schug, Z.T., Voorde, J. Vande, Gottlieb, E., 2016. The metabolic fate of acetate in cancer. Nat. Rev. Cancer. https://doi.org/10.1038/nrc.2016.87

Schumacker, P.T., 2006. Reactive oxygen species in cancer cells: Live by the sword, die by the sword. Cancer Cell 10, 175–176. https://doi.org/10.1016/j.ccr.2006.08.015

Schutte, B., Nuydens, R., Geerts, H., Ramaekers, F., 1998. Annexin V binding assay as a tool to measure apoptosis in differentiated neuronal cells. J. Neurosci. Methods 86, 63–69. https://doi.org/10.1016/S0165-0270(98)00147-2

Schwartz, G.K., Shah, M.A., 2005. Targeting the cell cycle: a new approach to cancer therapy. J. Clin. Oncol. 23, 9408–21. https://doi.org/10.1200/JCO.2005.01.5594

Senft, D., Ronai, Z.A., 2016. Regulators of mitochondrial dynamics in cancer. Curr. Opin. Cell Biol. 39, 43–52. https://doi.org/10.1016/j.ceb.2016.02.001

Seyfried, T.N., Flores, R.E., Poff, A.M., D'Agostino, D.P., 2014. Cancer as a metabolic disease: Implications for novel therapeutics. Carcinogenesis 35, 515–527. https://doi.org/10.1093/carcin/bgt480

Shalini, S., Dorstyn, L., Dawar, S., Kumar, S., 2014. Old, new and emerging functions of caspases. Cell Death Differ. 22, 526–539. https://doi.org/10.1038/cdd.2014.216

Shankar, S., Lanza, E., 1991. Dietary fiber and cancer prevention. Hematol. Oncol. Clin. North Am. 5, 25–41.

Sharaf El Dein, O., Gallerne, C., Brenner, C., Lemaire, C., 2012. Increased expression of VDAC1 sensitizes carcinoma cells to apoptosis induced by DNA cross-linking agents. Biochem. Pharmacol. 83, 1172–1182. https://doi.org/10.1016/j.bcp.2012.01.017

Sharma, H., Sen, S., Singh, N., 2005. Molecular pathways in the chemosensitization of cisplatin by quercetin in human head and neck cancer. Cancer Biol. Ther. 4, 949–55. https://doi.org/10.4161/cbt.4.9.1908

Sherr, C.J., 2004. Principles of tumor suppression. Cell 116, 235–46. https://doi.org/10.1016/S0092-8674(03)01075-4

Shi, R., Guberman, M., Kirshenbaum, L.A., 2017. Mitochondrial quality control: The role of mitophagy in aging. Trends Cardiovasc. Med. https://doi.org/10.1016/j.tcm.2017.11.008

Shokolenko, I., Venediktova, N., Bochkareva, A., Wilson, G.I., Alexeyev, M.F., 2009. Oxidative stress induces degradation of mitochondrial DNA. Nucleic Acids Res. 37, 2539–2548. https://doi.org/10.1093/nar/gkp100

Shore, G.C., 2009. Apoptosis: it's BAK to VDAC. EMBO Rep. 10, 1311–1313. https://doi.org/10.1038/embor.2009.249

Shoshan-Barmatz, V., Ben-Hail, D., Admoni, L., Krelin, Y., Tripathi, S.S., 2015. The mitochondrial voltage-dependent anion channel 1 in tumor cells. Biochim. Biophys. Acta - Biomembr. 1848, 2547–2475. https://doi.org/10.1016/j.bbamem.2014.10.040

Shoshan-Barmatz, V., De Pinto, V., Zweckstetter, M., Raviv, Z., Keinan, N., Arbel, N., 2010. VDAC, a multi-functional mitochondrial protein regulating cell life and death. Mol. Aspects Med. 31, 227–285. https://doi.org/10.1016/j.mam.2010.03.002

Siddik, Z.H., 2003. Cisplatin: mode of cytotoxic action and molecular basis of resistance. Oncogene 22, 7265–7279. https://doi.org/10.1038/sj.onc.1206933

Sirover, M.A., Sirover, M.A., 1999. New insights into an old protein: the functional diversity of mammalian glyceraldehyde-3-phosphate dehydrogenase. Biochim. Biophys. Acta 1432, 159–184. https://doi.org/10.1016/S0167-4838(99)00119-3

Sivalingam, K.S., Paramasivan, P., Weng, C.F., Viswanadha, V. padma, 2017. Neferine potentiates the antitumor effect of cisplatin in human lung adenocarcinoma cells via a mitochondria-mediated apoptosis pathway † Sivalingam Kalai Selvi. J. Cell. Biochem. 118, 2865–2876. https://doi.org/10.1002/jcb.25937

Skala, M.C., Riching, K.M., Bird, D.K., Gendron-Fitzpatrick, A., Eickhoff, J., Eliceiri, K.W., Keely, P.J., Ramanujam, N., 2009. In vivo multiphoton fluorescence lifetime imaging of protein-bound and free nicotinamide adenine dinucleotide in normal and precancerous epithelia. J. Biomed. Opt. 12, 024014. https://doi.org/10.1117/1.2717503

Smirnova, E., Griparic, L., Shurland, D.L., van der Bliek, A.M., 2001. Dynamin-related protein Drp1 is required for mitochondrial division in mammalian cells. Mol. Biol. Cell 12, 2245–56. https://doi.org/10.1091/mbc.12.8.2245

Smith, P.M., Howitt, M.R., Panikov, N., Michaud, M., Gallini, C.A., Bohlooly-Y, M., Glickman, J.N., Garrett, W.S., 2013. The microbial metabolites, short-chain fatty acids, regulate colonic Treg cell homeostasis. Science. 341, 569–73. https://doi.org/10.1126/science.1241165

Soliman, M.L., Rosenberger, T.A., 2011. Acetate supplementation increases brain histone acetylation and inhibits histone deacetylase activity and expression. Mol. Cell. Biochem. 352, 173–180. https://doi.org/10.1007/s11010-011-0751-3

Sompakdee, V., Prawan, A., Senggunprai, L., Kukongviriyapan, U., Samathiwat, P., Wandee, J., Kukongviriyapan, V., 2018. Suppression of Nrf2 confers chemosensitizing effect through enhanced oxidant-mediated mitochondrial dysfunction. Biomed. Pharmacother. 101, 627–634. https://doi.org/10.1016/j.biopha.2018.02.112

Sosa, V., Moliné, T., Somoza, R., Paciucci, R., Kondoh, H., LLeonart, M.E., 2013. Oxidative stress and cancer: An overview. Ageing Res. Rev. 12, 376–390. https://doi.org/10.1016/j.arr.2012.10.004

Soto, A.M., Sonnenschein, C., 2004. The somatic mutation theory of cancer: growing problems with the paradigm? Bioessays 26, 1097–107. https://doi.org/10.1002/bies.20087

Soule, H.D., Maloney, T.M., Wolman, S.R., Peterson, W.D., Brenz, R., McGrath, C.M., Russo, J., Pauley, R.J., Jones, R.F., Brooks, S.C., 1990. Isolation and characterization of a spontaneously immortalized human breast epithelial cell line, MCF-10. Cancer Res. 50, 6075–86.

Soule, H.D., Vazguez, J., Long, A., Albert, S., Brennan, M., 1973. A human cell line from a pleural effusion derived from a breast carcinoma. J. Natl. Cancer Inst. 51, 1409–16. https://doi.org/10.1093/jnci/51.5.1409

Stine, Z.E., Walton, Z.E., Altman, B.J., Hsieh, A.L., Dang, C. V., 2015. MYC, metabolism, and cancer. Cancer Discov. 5, 1024–1039. https://doi.org/10.1158/2159-8290.CD-15-0507

Suen, D.-F., Norris, K.L., Youle, R.J., 2008. Mitochondrial dynamics and apoptosis. Genes Dev. 22, 1577–1590. https://doi.org/10.1101/gad.1658508

Suh, D.H., Kim, M.-K., Kim, H.S., Chung, H.H., Song, Y.S., 2013. Mitochondrial permeability transition pore as a selective target for anti-cancer therapy. Front. Oncol. 3, 1–11. https://doi.org/10.3389/fonc.2013.00041

Suhling, K., Hirvonen, L.M., Levitt, J.A., Chung, P.H., Tregidgo, C., Le Marois, A., Rusakov, D.A., Zheng, K., Ameer-Beg, S., Poland, S., Coelho, S., Henderson, R., Krstajic, N., 2015. Fluorescence lifetime imaging (FLIM): Basic concepts and some recent developments. Med. Photonics 27, 3–40. https://doi.org/10.1016/j.medpho.2014.12.001

Sullivan, L.B., Chandel, N.S., 2014. Mitochondrial reactive oxygen species and cancer. Cancer Metab. 2, 17. https://doi.org/10.1186/2049-3002-2-17

Svoboda, K., Yasuda, R., 2006. Principles of two-photon excitation microscopy and its applications to neuroscience. Neuron 50, 823–39. https://doi.org/10.1016/j.neuron.2006.05.019

Szabadkai, G., Simoni, A.M., Bianchi, K., De Stefani, D., Leo, S., Wieckowski, M.R., Rizzuto, R., 2006. Mitochondrial dynamics and Ca2+signaling. Biochim. Biophys. Acta - Mol. Cell Res. 1763, 442–449. https://doi.org/10.1016/j.bbamcr.2006.04.002

Tailor, D., Hahm, E.-R., Kale, R.K., Singh, S. V., Singh, R.P., 2014. Sodium butyrate induces DRP1-mediated mitochondrial fusion and apoptosis in human colorectal cancer cells. Mitochondrion 16, 55–64. https://doi.org/10.1016/j.mito.2013.10.004

Takahashi, N., Chen, H.-Y., Harris, I.S., Stover, D.G., Selfors, L.M., Bronson, R.T., Deraedt, T., Cichowski, K., Welm, A.L., Mori, Y., Mills, G.B., Brugge, J.S., 2018. Cancer cells co-opt the neuronal redox-Sensing channel TRPA1 to promote oxidative-stress tolerance. Cancer Cell 33, 985–1003.e7. https://doi.org/10.1016/j.ccell.2018.05.001

Takatoku, O., Yasushi, S., Akihiro, K., 1993. Fluorescence lifetime imaging microscopy (flimscopy). Biophys. J. 64, 676–685.

Tal, M.C., Sasai, M., Lee, H.K., Yordy, B., Shadel, G.S., Iwasaki, A., 2009. Absence of autophagy results in reactive oxygen species-dependent amplification of RLR signaling. Proc. Natl. Acad. Sci. 106, 2770–2775. https://doi.org/10.1073/pnas.0807694106

Tan, A.S., Baty, J.W., Dong, L.F., Bezawork-Geleta, A., Endaya, B., Goodwin, J., Bajzikova, M., Kovarova, J., Peterka, M., Yan, B., Pesdar, E.A., Sobol, M., Filimonenko, A., Stuart, S., Vondrusova, M., Kluckova, K., Sachaphibulkij, K., Rohlena, J., Hozak, P., Truksa, J., Eccles, D., Haupt, L.M., Griffiths, L.R., Neuzil, J., Berridge, M. V., 2015. Mitochondrial genome acquisition restores respiratory function and tumorigenic potential of cancer cells without mitochondrial DNA. Cell Metab. 21, 81–94. https://doi.org/10.1016/j.cmet.2014.12.003

Tang, K.H., Tang, Y.J., Blankenship, R.E., 2011. Carbon metabolic pathways in phototrophic bacteria and their broader evolutionary implications. Front. Microbiol. 2, 1–23. https://doi.org/10.3389/fmicb.2011.00165

Tang, Y., Chen, Y., Jiang, H., Nie, D., 2010. Short-chain fatty acids induced autophagy serves as an adaptive strategy for retarding mitochondria-mediated apoptotic cell death. Cell Death Differ. 18, 602–618. https://doi.org/10.1038/cdd.2010.117

Tang, Y., Chen, Y., Jiang, H., Robbins, G.T., Nie, D., 2011. G-protein-coupled receptor for short-chain fatty acids suppresses colon cancer. Int. J. Cancer 128, 847–856. https://doi.org/10.1002/ijc.25638

Taylor, R.W., Turnbull, D.M., 2005. Mitochondrial DNA mutations in human disease. Nat. Rev. Genet. 6, 389–402. https://doi.org/10.1038/nrg1606

Thomas, D., Tovey, S.C., Collins, T.J., Bootman, M.D., Berridge, M.J., Lipp, P., 2000. A comparison of fluorescent Ca2+ indicator properties and their use in measuring elementary and global Ca2+ signals. Cell Calcium 28, 213–223. https://doi.org/10.1054/ceca.2000.0152

Thummuri, D., Jeengar, M.K., Shrivastava, S., Areti, A., Yerra, V.G., Yamjala, S., Komirishetty, P., Naidu, V.G.M., Kumar, A., Sistla, R., 2014. Boswellia ovalifoliolata abrogates ROS mediated NF-κB activation, causes apoptosis and chemosensitization in Triple Negative Breast Cancer cells. Environ. Toxicol. Pharmacol. 38, 58–70. https://doi.org/10.1016/j.etap.2014.05.002

Tolhurst, G., Heffron, H., Lam, Y.S., Parker, H.E., Habib, A.M., Diakogiannaki, E., Cameron, J., Grosse, J., Reimann, F., Gribble, F.M., 2012. Short-chain fatty acids stimulate glucagon-like peptide-1 secretion via the G-protein-coupled receptor FFAR2. Diabetes 61, 364–371. https://doi.org/10.2337/db11-1019

Trock, B., Lanza, E., Greenwald, P., 1990. Dietary fiber, vegetables, and colon cancer: critical review and meta-analyses of the epidemiologic evidence. J. Natl. Cancer Inst. 82, 650–61.

Tyagi, A.K., Singh, R.P., Agarwal, C., Chan, D.C.F., Agarwal, R., 2002. Silibinin strongly synergizes human prostate carcinoma DU145 cells to doxorubicin-induced growth inhibition, G2-M arrest, and apoptosis. Clin. Cancer Res. 8, 3512–3519. https://doi.org/10.1186/1471-2407-12-117

Valenti, D., Bari, L. De, Arcangela, G., Rossi, L., Mutti, L., Moro, L., Anna, R., 2013. Biochimica et Biophysica Acta Negative modulation of mitochondrial oxidative phosphorylation by epigallocatechin-3

gallate leads to growth arrest and apoptosis in human malignant pleural mesothelioma cells. BBA - Mol. Basis Dis. 1832, 2085–2096. https://doi.org/10.1016/j.bbadis.2013.07.014

Van Raamsdonk, J.M., Hekimi, S., 2009. Deletion of the mitochondrial superoxide dismutase sod-2 extends lifespan in Caenorhabditis elegans. PLoS Genet. 5, e1000361. https://doi.org/10.1371/journal.pgen.1000361

Van Remmen, H., Ikeno, Y., Hamilton, M., Pahlavani, M., Wolf, N., Thorpe, S.R., Alderson, N.L., Baynes, J.W., Epstein, C.J., Huang, T.-T., Nelson, J., Strong, R., Richardson, A., 2003. Life-long reduction in MnSOD activity results in increased DNA damage and higher incidence of cancer but does not accelerate aging. Physiol. Genomics 16, 29–37. https://doi.org/10.1152/physiolgenomics.00122.2003

Vergen, J., Hecht, C., Zholudeva, L. V, Marquardt, M.M., Hallworth, R., Nichols, M.G., 2012. Metabolic imaging using two-photon excited NADH intensity and fluorescence lifetime imaging. Microsc. Microanal. 18, 761–70. https://doi.org/10.1017/S1431927612000529

Vermeulen, K., Berneman, Z.N., Van Bockstaele, D.R., 2003. Cell cycle and apoptosis. Cell Prolif. https://doi.org/10.1046/j.1365-2184.2003.00267.x

Vishwasrao, H.D., Heikal, A.A., Kasischke, K.A., Webb, W.W., 2005. Conformational dependence of intracellular NADH on metabolic state revealed by associated fluorescence anisotropy. J. Biol. Chem. 280, 25119–25126. https://doi.org/10.1074/jbc.M502475200

Vorobiof, D.A., 2016. Recent advances in the medical treatment of breast cancer. F1000Research 5, 2786. https://doi.org/10.12688/f1000research.9619.1

Vowinckel, J., Hartl, J., Butler, R., Ralser, M., 2015. MitoLoc: A method for the simultaneous quantification of mitochondrial network morphology and membrane potential in single cells. Mitochondrion 24, 77–86. https://doi.org/10.1016/j.mito.2015.07.001

Wajant, H., 2002. The Fas signaling pathway: more than a paradigm. Science. 296, 1635–1636. https://doi.org/10.1126/science.1071553

Walkington, L., Newsham, A., Deverede, L., Mehran, A., Hall, P., Perren, T., Dodwell, D., Thomas, J., Glaser, A., Hall, G., 2012. Patterns of breast cancer recurrence and associated health care costs of 1000 patients: a longitudinal study. 8th NCRI Cancer Conf.

Wallace, D.C., 2015. Mitochondria and cancer. Nat. Rev. Cancer 12, 685–698. https://doi.org/10.1038/nrc3365.Mitochondria

Wang, H., Zhang, T., Sun, W., Wang, Z., Zuo, D., Zhou, Z., Li, S., Xu, J., Yin, F., Hua, Y., Cai, Z., 2016. Erianin induces G2/M-phase arrest, apoptosis, and autophagy via the ROS/JNK signaling pathway in human osteosarcoma cells in vitro and in vivo. Cell Death Dis. 7. https://doi.org/10.1038/cddis.2016.138

Wang, L., Luo, H.-S., Xia, H., 2009. Sodium butyrate induces human colon carcinoma HT-29 cell apoptosis through a mitochondrial pathway. J. Int. Med. Res. 37, 803–11.

Wang, P., Henning, S.M., Heber, D., 2010. Limitations of MTT and MTS-based assays for measurement of antiproliferative activity of green tea polyphenols. PLoS One 5, e10202. https://doi.org/10.1371/journal.pone.0010202

Warburg, O., 1956. On the origin of cancer cells. Science. 123, 309–14.

Weisthal, S., Keinan, N., Ben-Hail, D., Arif, T., Shoshan-Barmatz, V., 2014. Ca2+-mediated regulation of VDAC1 expression levels is associated with cell death induction. Biochim. Biophys. Acta - Mol. Cell Res. 1843, 2270–2281. https://doi.org/10.1016/j.bbamcr.2014.03.021

Wong, J.M.W., de Souza, R., Kendall, C.W.C., Emam, A., Jenkins, D.J. a, 2006. Colonic health: fermentation and short chain fatty acids. J. Clin. Gastroenterol. 40, 235–243. https://doi.org/10.1097/00004836-200603000-00015

Wong, R., Steenbergen, C., Murphy, E., 2012. Mitochondrial permeability transition pore and calcium handling. Methods Mol. Biol. 810, 235–42. https://doi.org/10.1007/978-1-61779-382-0_15

Woods, L.C., Berbusse, G.W., Naylor, K., 2016. Microtubules Are essential for mitochondrial dynamics-fission, fusion, and motility-in Dictyostelium discoideum. Front. Cell Dev. Biol. 4, 19. https://doi.org/10.3389/fcell.2016.00019

World Health Organization, 2018. Cancer [WWW Document]. URL http://www.who.int/news-room/fact-sheets/detail/cancer (accessed 5.31.18).

World Health Organization, 2017. Cancer Fact sheet [WWW Document]. URL http://www.who.int/mediacentre/factsheets/fs297/en/ (accessed 9.25.17).

Wu, C., Ho, Y., Tsai, C., Wang, Y., Tseng, H., Wei, P., Lee, C., Liu, R., Lin, S., 2009. In vitro and in vivo study of phloretin-induced apoptosis in human liver cancer cells involving inhibition of type II glucose transporter. Int. J. Cancer 124, 2210–2219. https://doi.org/10.1002/ijc.24189

Wu, S., Zhang, T., Du, J., 2016. Ursolic acid sensitizes cisplatin-resistant HepG2/DDP cells to cisplatin via inhibiting Nrf2/ARE pathway. Drug Des. Devel. Ther. 10, 3471–3481. https://doi.org/10.2147/DDDT.S110505

Xiao, B., Deng, X., Zhou, W., Tan, E.-K., 2016. Flow cytometry-based assessment of mitophagy using MitoTracker. Front. Cell. Neurosci. 10, 76. https://doi.org/10.3389/fncel.2016.00076

Xu, X., Chen, D., Ye, B., Zhong, F., Chen, G., 2015. Curcumin induces the apoptosis of non-small cell lung cancer cells through a calcium signaling pathway. Int. J. Mol. Med. 35, 1610–1616. https://doi.org/10.3892/ijmm.2015.2167

Xu, Y., Her, C., 2015. Inhibition of topoisomerase (DNA) I (TOP1): DNA damage repair and anticancer therapy. Biomolecules 5, 1652–70. https://doi.org/10.3390/biom5031652

Yadav, N., Kumar, S., Marlowe, T., Chaudhary, A.K., Kumar, R., Wang, J., O'Malley, J., Boland, P.M., Jayanthi, S., Kumar, T.K.S., Yadava, N., Chandra, D., 2015. Oxidative phosphorylation-dependent regulation of cancer cell apoptosis in response to anticancer agents. Cell Death Dis. 6, e1969. https://doi.org/10.1038/cddis.2015.305

Yamamoto, T., Suzuki, T., Kobayashi, A., Wakabayashi, J., Maher, J., Motohashi, H., Yamamoto, M., 2008. Physiological Significance of Reactive Cysteine Residues of Keap1 in Determining Nrf2 Activity. Mol. Cell. Biol. 28, 2758–2770. https://doi.org/10.1128/MCB.01704-07

Yang, D., Qu, J., Qu, X., Cao, Y., Xu, L., Hou, K., Feng, W., Liu, Y., 2015. Gossypol sensitizes the antitumor activity of 5-FU through down-regulation of thymidylate synthase in human colon carcinoma cells. Cancer Chemother. Pharmacol. 76, 575–586. https://doi.org/10.1007/s00280-015-2749-0

Yonekawa, T., Thorburn, A., 2013. Autophagy and cell death. Essays Biochem. 55, 105–17. https://doi.org/10.1042/bse0550105

Yonezawa, T., Kobayashi, Y., Obara, Y., 2007. Short-chain fatty acids induce acute phosphorylation of the p38 mitogen-activated protein kinase/heat shock protein 27 pathway via GPR43 in the MCF-7 human breast cancer cell line. Cell. Signal. 19, 185–193. https://doi.org/10.1016/j.cellsig.2006.06.004

Yoon, Y., Krueger, E.W., Oswald, B.J., McNiven, M.A., 2003. The mitochondrial protein hFis1 regulates mitochondrial fission in mammalian cells through an interaction with the dynamin-like protein DLP1. Mol. Cell. Biol. 23, 5409–20. https://doi.org/10.1128/MCB.23.15.5409

Youle, R.J., van der Bliek, A.M., 2012. Mitochondrial fission, fusion, and stress. Science. 337, 1062–5. https://doi.org/10.1126/science.1219855

Yun, J., Mullarky, E., Lu, C., Bosch, K.N., Kavalier, A., Rivera, K., Roper, J., Chio, I.I.C., Giannopoulou, E.G., Rago, C., Muley, A., Asara, J.M., Paik, J., Elemento, O., Chen, Z., Pappin, D.J., Dow, L.E., Papadopoulos, N., Gross, S.S., Cantley, L.C., 2015. Vitamin C selectively kills KRAS and BRAF mutant colorectal cancer cells by targeting GAPDH. Science. 350, 1391–1396. https://doi.org/10.1126/science.aaa5004

Yun, M., Bang, S.-H., Kim, J.W., Park, J.Y., Kim, K.S., Lee, J.D., 2009. The importance of acetyl coenzyme A synthetase for 11C-acetate uptake and cell survival in hepatocellular carcinoma. J. Nucl. Med. 50, 1222–8. https://doi.org/10.2967/jnumed.109.062703

Zamzami, N., Kroemer, G., 2003. Apoptosis: mitochondrial membrane permeabilization--the (w)hole story? Curr. Biol. 13, R71-3. https://doi.org/10.1016/S0960-9822(02)01433-1

Zhang, D., Chen, G., Manwani, D., Mortha, A., Xu, C., Faith, J.J., Burk, R.D., Kunisaki, Y., Jang, J.-E., Scheiermann, C., Merad, M., Frenette, P.S., 2015. Neutrophil ageing is regulated by the microbiome. Nature 525, 528–32. https://doi.org/10.1038/nature15367

Zhang, J., Wang, X., Vikash, V., Ye, Q., Wu, D., Liu, Y., Dong, W., 2016. ROS and ROS-mediated cellular signaling. Oxid. Med. Cell. Longev. 2016, 4350965. https://doi.org/10.1155/2016/4350965

Zhang, J., Yi, M., Zha, L., Chen, S., Li, Z., Li, C., Gong, M., Deng, H., Chu, X., Chen, J., Zhang, Z., Mao, L., Sun, S., 2016. Sodium butyrate induces endoplasmic reticulum stress and autophagy in colorectal cells: implications for apoptosis. PLoS One 11, e0147218. https://doi.org/10.1371/journal.pone.0147218

Zhang, Z., Singh, R., Aschner, M., 2016. Methods for the Detection of Autophagy in Mammalian Cells. Curr. Protoc. Toxicol. 69, 20.12.1-20.12.26. https://doi.org/10.1002/cptx.11

Zheng, M., Wang, Q., Teng, Y., Wang, X., Wang, F., Chen, T., Samaj, J., Lin, J., Logan, D.C., 2010. The speed of mitochondrial movement is regulated by the cytoskeleton and myosin in Picea wilsonii pollen tubes. Planta 231, 779–91. https://doi.org/10.1007/s00425-009-1086-0

Zi, F., Zi, H., Li, Y., He, J., Shi, Q., Cai, Z., 2018. Metformin and cancer: An existing drug for cancer prevention and therapy (review). Oncol. Lett. 15, 683–690. https://doi.org/10.3892/ol.2017.7412

Zimmerman, M.A., Singh, N., Martin, P.M., Thangaraju, M., Ganapathy, V., Waller, J.L., Shi, H., Robertson, K.D., Munn, D.H., Liu, K., 2012. Butyrate suppresses colonic inflammation through HDAC1-dependent Fas upregulation and Fas-mediated apoptosis of T cells. AJP Gastrointest. Liver Physiol. 302, G1405–G1415. https://doi.org/10.1152/ajpgi.00543.2011

Zong, W.-X., Rabinowitz, J.D., White, E., 2016. Mitochondria and cancer. Mol. Cell 61, 667–676. https://doi.org/10.1016/j.molcel.2016.02.011

Zorova, L.D., Popkov, V.A., Plotnikov, E.Y., Silachev, D.N., Pevzner, I.B., Jankauskas, S.S., Babenko, V.A., Zorov, S.D., Balakireva, A. V., Juhaszova, M., Sollott, S.J., Zorov, D.B., 2018.

Mitochondrial membrane potential. Anal. Biochem. 552, 50–59. https://doi.org/10.1016/j.ab.2017.07.009

Zou, J., Zhu, L., Jiang, X., Wang, Y., Wang, Y., Wang, X., Chen, B., 2018. Curcumin increases breast cancer cell sensitivity to cisplatin by decreasing FEN1 expression. Oncotarget 9, 11268–11278. https://doi.org/10.18632/oncotarget.24109

Zou, Z., Chang, H., Li, H., Wang, S., 2017. Induction of reactive oxygen species: an emerging approach for cancer therapy. Apoptosis 22, 1321–1335. https://doi.org/10.1007/s10495-017-1424-9

Zu, X.L., Guppy, M., 2004. Cancer metabolism: Facts, fantasy, and fiction. Biochem. Biophys. Res. Commun. 313, 459–465. https://doi.org/10.1016/j.bbrc.2003.11.136